Aus dem Institut für Klinische Neurowissenschaften und Medizinische Psychologie

Direktor: Univ.-Prof. Dr. med. Alfons Schnitzler

Verlangsamung kortikaler oszillatorischer Aktivität bei Hepatischer Enzephalopathie

Habilitationsschrift

zur Erlangung der Venia Legendi für das Fach

Klinische Neurowissenschaften und Medizinische Psychologie

an der Hohen Medizinischen Fakultät der Heinrich-Heine-Universität Düsseldorf

Vorgelegt von

Dr. rer. nat. Markus Butz

Düsseldorf 2015

Eidesstattliche Erklärung

Hiermit versichere ich an Eides statt, dass ich die vorliegende Habilitationsschrift ohne unerlaubte Hilfe angefertigt und das benutzte Schrifttum vollständig erwähnt habe.

Zudem versichere ich, dass die Habilitationsschrift noch von keiner anderen Fakultät abgelehnt worden ist.

Bei den wissenschaftlichen Untersuchungen, die Gegenstand dieser schriftlichen Habilitationsleistung sind, wurden ethische Grundsätze und die jeweils gültigen Empfehlungen zur Sicherung guter wissenschaftlicher Praxis beachtet.

Düsseldorf, den 27. März 2015

Dr. rer. nat. Markus Butz

Zusammenfassung

Die oszillatorische Aktivität des menschlichen Gehirns wird als ein entscheidender Mechanismus für die funktionelle Interaktion innerhalb und zwischen verschiedenen Hirnarealen betrachtet und kann mithilfe der Magnetenzephalographie (MEG) nicht-invasiv untersucht werden. Für verschiedene neurologische und psychiatrische Erkrankungen wie den *Morbus Parkinson* und die Schizophrenie konnte bereits gezeigt werden, dass es zu charakteristischen Veränderungen der oszillatorischen Aktivität im Krankheitsverlauf kommt, die eng mit der jeweiligen Symptomatik assoziiert sind.

Die in dieser Arbeit zusammengefassten Studien untersuchen oszillatorische Aktivität im Rahmen der Hepatischen Enzephalopathie (HE), einer Hirnleistungseinschränkung aufgrund einer mangelnden Leberfunktion bei Patienten mit Leberzirrhose.

Als charakteristische Veränderungen der oszillatorischen Aktivität bei HE konnte eine globale Verlangsamung über zerebrale Subsysteme und Frequenzbereiche hinweg beschrieben werden. Im *Alpha*-Band (8-12 Hz) zeigte sich neben einer Verlangsamung der Spontanaktivität im okzipitalen Kortex eine Verlangsamung der stimulusassoziierten, oszillatorischen Aktivität im primären somatosensorischen Kortex nach elektrischer Stimulation des *Nervus medianus*. Für das *Beta*-Band (15-30 Hz) konnte beschrieben werden, dass die funktionelle Interaktion im motorischen System verlangsamt ist und dass es pathophysiologische Gemeinsamkeiten bei der Entstehung der sogenannten *Mini-Asterixis* und der *Asterixis* gibt. Auch im *Gamma*-Band (30-100 Hz) wurde eine Verlangsamung der oszillatorischen Aktivität im visuellen Kortex im Rahmen von Aufmerksamkeitsaufgaben demonstriert. Die sogenannte Kritische Flimmerfrequenz (*Critical Flicker Frequency*, CFF) diente dabei als Maß für die Schwere der HE und korrelierte eng mit den in dieser Arbeit beschriebenen Veränderungen der oszillatorischen Aktivität.

Insgesamt unterstützen die hier zusammengefassten Ergebnisse die Annahme, dass die Verlangsamung kortikaler oszillatorischer Aktivität ein zentrales Phänomen bei HE ist, das in verschiedenen Frequenzbändern und Subsystemen des Gehirns beobachtet werden kann. Somit kann im Rahmen der HE exemplarisch untersucht werden, wie sich oszillatorische Aktivität bei sich graduell verschlechternder Hirnleistung verändert und mit der Symptomatik zusammenhängt. Zudem unterstützen diese Befunde, dass die CFF ein aussagekräftiger klinischer Parameter ist, um die verminderte Leistungsfähigkeit des Gehirns bei HE-Patienten zu quantifizieren.

In dieser Habilitationsschrift zusammengefasste Originalarbeiten:

1.) Brenner M, **Butz M[c],** May ES, Kahlbrock N, Kircheis G, Häussinger D, Schnitzler A, *"Patients with manifest hepatic encephalopathy reveal impaired thermal perception",* Acta Neurol Scand 2015 Sep;132(3):156-63.

2.) May ES, **Butz M[c]**, Kahlbrock N, Brenner M, Hoogenboom N, Kircheis G, Häussinger D, Schnitzler A, "*Hepatic encephalopathy is associated with slowed and delayed stimulus-associated somatosensory alpha activity*", Clin Neurophysiol 2014 Dez, 125(12): 2427–2435.

3.) **Butz M[c]**, Timmermann L, Gross J, Pollok B, Südmeyer M, Kircheis G, Häussinger D, Schnitzler A, *„Cortical activation associated with asterixis in hepatic encephalopathy",* Acta Neurol Scand 2014 Okt;130(4):260-7.

4.) May ES*, **Butz M*,[c]**, Kahlbrock N, Hoogenboom N, Brenner M, Schnitzler A, "*Pre- and post-stimulus alpha activity shows differential modulation with spatial attention during the processing of pain",* Neuroimage 2012 Sep;62(3):1965-74.

5.) Kahlbrock N, **Butz M[c]**, May ES, Brenner M, Kircheis G, Häussinger D, Schnitzler A, "*Lowered frequency and impaired modulation of gamma band oscillations in a bimodal attention task are associated with reduced critical flicker frequency*", Neuroimage 2012 Mai 15;61(1):216-27.

6.) Kahlbrock N*,[c], **Butz M***, May ES, Schnitzler A, "*Sustained gamma band synchronization in early visual areas reflects the level of selective attention."* Neuroimage 2012 Jan 2;59(1):673-81.

7.) **Butz M*,[c]**, Timmermann L*, Braun M, Groiss SJ, Wojtecki L, Ostrowski S, Krause H, Pollok B, Gross J, Südmeyer M, Kircheis G, Häussinger D, Schnitzler A, "*Motor impairment in Liver Cirrhosis without and with Minimal Hepatic Encephalopathy*", Acta Neurol Scand 2010 Jul;122(1):27-35.

8.) Timmermann L*,[c], **Butz M*,** Gross J, Ploner M, Südmeyer M, Kircheis G, Häussinger D, Schnitzler A[c], *"Pathological Oscillatory Processing of the human motor and visual system in hepatic encephalopathy",* Clin Neurophysiol 2008 Feb;119(2):265-72.

***** Die beiden ersten Autoren haben einen gleichwertigen Beitrag zur Arbeit geliefert

[c] Korrespondierender Autor

Inhaltsverzeichnis

Abkürzungsverzeichnis

Abb.	*Abbildung*
BOLD	*Blood oxygen level dependent*
bp	*band-pass*
CFF	*Critical flicker frequency*
dcSQUID	*direct current superconducting quantum interference device*
EDC	*Extensor digitorum communis*
EEG	*Elektroenzephalographie*
EMG	*Elektromyography*
FDI	*Flexor digitorum interosseus I.*
FDL	*Flexor digitorum longus*
fMRT	*funktionelle Magnetresonanztomographie*
DFNS	*Deutschen Forschungsverbund Neuropathischer Schmerz*
GABA	*γ-Aminobuttersäure*
HE	*Hepatische Enzephalopathie*
Hz	*Hertz*
MEG	*Magnetenzephalographie*
mHE	*Minimale Hepatische Enzephalopathie*
M1	*Primärer motorischer Kortex*
PHES	*Psychometric Hepatic Encephalopathy Score*
QST	*Quantitative Sensorische Testung*
SHE	*Subklinische Hepatische Enzephalopathie*
SQUID	*Superconducting quantum interference device*
S1	*Primärer somatosensorischer Kortex*
TSL	*Thermal sensory limen*

1. Einleitung

Die modernen Neurowissenschaften konnten innerhalb der letzten drei Jahrzehnte mithilfe der sogenannten bildgebenden Verfahren unser Verständnis des menschlichen Gehirns wesentlich voranbringen. Dieses sehr dynamische Forschungsfeld versucht zu ergründen, wie die vielen Milliarden Nervenzellen des Gehirns es schaffen, ihre Interaktion immer wieder neu zu optimieren und anzupassen, um die sich ergebenden diversen Aufgaben zu lösen.

Als wesentliches Organisationsprinzip hat sich dabei die Synchronisation der Aktivität von Nervenzellen herausgestellt. Dabei führt eine gleichzeitige Aktivität von einer Vielzahl von Neuronen zu an der Schädeloberfläche detektierbaren Signalen, der sogenannten oszillatorischen Aktivität (Buzsaki, 2006; Singer, 1999; Varela et al., 2001). Kortikale oszillatorische Aktivität beschreibt periodisch auftretende Aktivitätsschwankungen großer Neuronenpopulationen, die in verschiedene Frequenzbänder unterteilt werden können (Hansen et al., 2010; Schomer und Lopes da Silva, 2011).

Mittlerweile gibt es eine Vielzahl von Studien, die zeigen konnten, dass kortikale oszillatorische Aktivität eine wesentliche Rolle bei der dynamischen Anpassung des Gehirns an die sich verändernden Anforderungen der Umwelt spielt. Zudem konnte beschrieben werden, dass ebendiese oszillatorische Aktivität im Rahmen von neurologischen und neuropsychiatrischen Erkrankungen verändert und mit der der jeweiligen Symptomatik assoziiert ist (Schnitzler und Gross, 2005b; Uhlhaas und Singer, 2006).

In der vorliegenden Habilitationsschrift geht es um die Veränderungen von oszillatorischer Aktivität im Rahmen der Hepatischen Enzephalopathie (HE), einer Erkrankung, die häufig als Komplikation bei Patienten mit Leberzirrhose auftritt. Dabei schließt die vielfältigen Symptomatik der HE neben kognitiven Defiziten auch Beeinträchtigungen der Vigilanz sowie motorische Symptome ein (Häussinger und Blei, 2007).

Die hier zusammengefassten Befunde zeigen, dass es im Rahmen der HE in Abhängigkeit von der Schwere der Symptomatik zu einer umfassenden, d.h. globalen Verlangsamung der oszillatorischen Aktivität in unterschiedlichen Frequenzbändern und parallel zur Schwere der HE kommt.

2. Stand der Forschung

2.1 Oszillatorische Aktivität

Oszillatorische Aktivität ist in den letzten Jahrzehnten zunehmend in den Blickpunkt der Neurowissenschaften gerückt (Buzsaki, 2006; Buzsaki und Draguhn, 2004; Singer, 1999; Varela et al., 2001). Wenn genügend große Populationen von Neuronen im gleichen Rhythmus, d.h. synchron aktiv sind, werden diese Aktivitätsschwankungen an der Schädeloberfläche mithilfe der Magnetenzephalographie (MEG) (Hansen et al., 2010) bzw. mithilfe der Elektroenzephalographie (EEG) (Schomer und Lopes da Silva, 2011) messbar.

Die wohl bekannteste und auch stärkste oszillatorische Aktivität, die vom menschlichen Gehirn im Wachzustand abgeleitet werden kann, ist die sogenannte *Alpha*-Band-Aktivität im Frequenzbereich von 8-12 Hz. Diese wird zuweilen auch als Berger-Rhythmus bezeichnet, da der deutsche Neurologe Hans Berger diese erstmalig 1929 in Jena beschrieb (Abb. 1; Berger, 1929).

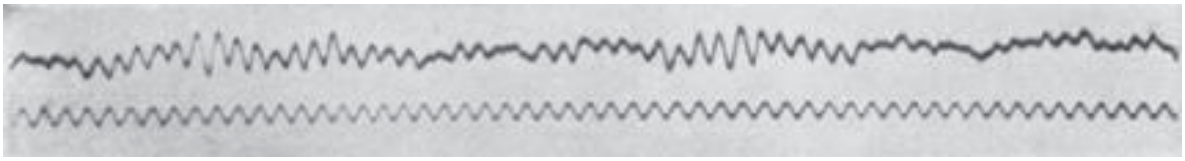

Abb. 1: Abbildung aus der Erstbeschreibung oszillatorischer Hirnaktivität im *Alpha*-Band durch Hans Berger (aus Berger, 1929). Die obere Spur zeigt 5,5 s Hirnaktivität von Bergers 15-jährigem Sohn Klaus. Die untere Linie dient der Darstellung der Zeit anhand einer 10 Hz Sinusschwingung.

Wenn oszillatorische Aktivität nicht nur in einem Hirnareal lokal auftritt, sondern zwei Hirnareale in einem festen zeitlichen Verhältnis die gleiche oszillatorische Aktivität zeigen, lässt sich eine oszillatorische Kopplung beschreiben z.B. mithilfe des mathematischen Maßes der Kohärenz. Eine solche oszillatorische Kopplung kann man inhaltlich als funktionelle Interaktion interpretieren, d.h. man geht davon aus, dass diese Areale an der gleichen Aufgabe bzw. Symptomatik beteiligt sind (Schnitzler und Gross, 2005b). Zudem kann durch Berechnung der Kohärenz auch eine funktionelle Interaktion zwischen neuronaler und peripherer Aktivität, wie z.B. der Muskelaktivität, beschrieben werden (Gross et al., 2000).

Derzeit wird oszillatorische Aktivität als ein wichtiger Mechanismus für die funktionelle Interaktion zwischen verschiedenen Hirnarealen und somit als Grundlage für Netzwerkinteraktionen angesehen (Schnitzler und Gross, 2005b; Varela et al., 2001). Aber nicht nur diese wichtige Rolle der oszillatorischen Aktivität im gesunden

Gehirn ist von Interesse. Von hoher Relevanz ist auch die Frage, inwieweit es im Rahmen von neurologischen bzw. psychiatrischen Erkrankungen zu Veränderungen von oszillatorischer Aktivität kommt und inwieweit die Aufklärung dieser Veränderungen helfen kann, die Pathophysiologie dieser Erkrankungen besser zu verstehen. Als Beispiele seien neben der HE der *Morbus Parkinson*, Schizophrenie und Epilepsie genannt (Schnitzler und Gross, 2005b; Uhlhaas und Singer, 2006).

Frequenzbänder

Sowohl in der klinischen Routine als auch in der wissenschaftlichen Forschung unterteilt man oszillatorische Aktivität in verschiedene Frequenzbänder: Das *Delta*- (1-3 Hz), *Theta*- (3-7 Hz), *Alpha*- (8-12 Hz), *Beta*- (13-30 Hz) und *Gamma*-Band (30-100 Hz). Dabei können den einzelnen Frequenzbändern spezifische Funktionen zugeordnet werden bzw. sind diese mit bestimmten Symptomen assoziiert. Auf die drei Frequenzbänder, die für die in dieser Arbeit vorgestellten Studien am wichtigsten sind, soll im folgendem näher eingegangen werden.

***Alpha*-Band (8-12 Hz):** *Alpha*-Aktivität findet sich in den primären Kortizes aller sensorischen Modalitäten und wird durch externe Stimuli, Bewegung und sogar allein durch die Vorstellung einer Bewegung unterdrückt. Die funktionelle Rolle der stärksten oszillatorischen Aktivität des menschlichen Gehirns ist noch nicht gänzlich verstanden. Man geht aber davon aus, dass eine Amplitudenverringerung im *Alpha*-Band eine Aktivierung der entsprechenden Areale repräsentiert (Neuper und Pfurtscheller, 2001; Pfurtscheller et al., 1996). Dies wird unterstützt durch Befunde, die zeigen konnten, dass guten perzeptuellen Detektions- und Diskriminationsleistungen eine verminderte *Alpha*-Aktivität vorausgeht (Ergenoglu et al., 2004; Hanslmayr et al., 2007; Romei et al., 2010; van Dijk et al., 2008) und dass die Erregbarkeit eines kortikalen Areals erhöht ist, wenn dessen Aktivität im *Alpha*-Band niedrig ist (Romei et al., 2008; Sauseng et al., 2009).

Während dem *Alpha*-Band ursprünglich eher eine passive Rolle zugeschrieben wurde, d.h. angenommen wurde, dass die *Alpha*-Band-Aktivität eher einen „kortikalen Leerlauf-Zustand“ widerspiegelt (Pfurtscheller et al., 1996), gehen neuere Vorstellungen davon aus, dass eine erhöhte *Alpha*-Band-Aktivität eine aktive Inhibition dieser Areale repräsentiert, d.h. eine „Herunterregulierung“ i.S. einer Steuerung des Informationsflusses (*gating*). Dieses Modell wird als die sogenannte *alpha-inhibition*-Hypothese bezeichnet (Foxe und Snyder, 2011; Jensen und

Mazaheri, 2010; Klimesch et al., 2007) und durch eine Vielzahl von Arbeiten in jüngster Zeit gestützt (z.B. Anderson und Ding, 2011; Haegens et al., 2011; May et al., 2012).

***Beta*-Band (15-30 Hz):** Auch wenn eine einheitliche Sicht auf die funktionelle Bedeutung der *Beta*-Band-Aktivität bislang fehlt, so ist doch klar, dass diese nicht nur bei kognitiven Prozessen eine Rolle spielt sondern insbesondere auch im motorischen System und bei Erkrankungen des motorischen Systems, z.B. im Rahmen von Bewegungsstörungen wie dem *Morbus Parkinson*. So wird angenommen, dass die Aktivität im *Beta*-Band der Aufrechterhaltung des gegenwärtigen sensomotorischen bzw. kognitiven Status dient (Engel und Fries, 2010).
Bei Gesunden kann eine Kopplung zwischen den Muskeln und dem Motorkortex im *Beta*-Band bei einer isometrischen Kontraktion der Unterarmmuskulatur beobachtet werden (Gross et al., 2000; Schnitzler et al., 2000). Im klinischen Kontext hingegen ist für den *Morbus Parkinson* bekannt, dass die oszillatorische Kopplung sowohl zwischen den Muskeln und dem Gehirn als auch zwischen kortikalen bzw. subkortikalen Arealen verändert ist und eine erhöhte Aktivität im *Beta*-Band von entscheidender Bedeutung zu seien scheint (Hammond et al., 2007; Hirschmann et al., 2013a; Hirschmann et al., 2013b; Little und Brown, 2014; Oswal et al., 2013; Timmermann et al., 2003b).

***Gamma*-Band (30-100 Hz):** Die oszillatorische Aktivität im *Gamma*-Band wird mit unterschiedlichsten Hirnfunktionen in Verbindung gebracht (Fries, 2009), z.B. mit dem *visual feature binding* (Gray et al., 1989), der visuo-motorischen Kontrolle (Roelfsema et al., 1997), dem Arbeitsgedächtnis (Tallon-Baudry et al., 1998), dem assoziativem Lernen (Miltner et al., 1999) und der Aufmerksamkeit (Fries et al., 2001). Insbesondere bezüglich der Rolle von *Gamma*-Band-Aktivität im Rahmen von Aufmerksamkeitsprozessen liefern zahlreiche Studien Evidenz für die Annahme, dass die aufmerksamkeitsassoziierte Modulation von sensorischer Information mit der kortikalen Aktivität im *Gamma*-Band zusammenhängt (Fries et al., 2001; Hoogenboom et al., 2010; Hoogenboom et al., 2006; Kaiser et al., 2006; Lachaux et al., 2005). Zudem konnte gezeigt werden, dass es im Rahmen von Aufmerksamkeitsveränderungen auch zu einer Änderung induzierter *Gamma*-Band-Aktivität kommt (Gruber et al., 1999; Siegel et al., 2008; Tallon-Baudry et al., 2005; Vidal et al., 2006; Wyart und Tallon-Baudry, 2008). Aber nicht nur bei Gesunden,

sondern auch bei verschiedenen Erkrankungen ist die *Gamma*-Band-Aktivität von Bedeutung. Als Beispiel sei hier Schizophrenie erwähnt, wo bei den betroffenen Patienten eine beeinträchtigte neuronale Synchronisation beobachtet werden kann, die sowohl in einer verminderten Amplitude in diesem Frequenzbereich zum Ausdruck kommt als auch in einer frequenzspezifischen reduzierten Kopplung zwischen verschiedenen Hirnarealen (Uhlhaas und Singer, 2006).

Magnetenzephalographie (MEG)

Die Messung von oszillatorischer Aktivität des menschlichen Gehirns erfordert Methoden mit einer sehr hohen zeitlichen Auflösung. Neben der EEG erfüllt die MEG diese Voraussetzung (Ahonen et al., 1993; Cohen, 1968, 1972; Hämäläinen et al., 1993; Hansen et al., 2010; Hari, 2011; Schnitzler und Gross, 2005a). Dabei werden nicht-invasiv winzige magnetische Felder (~10^{-13} T) gemessen, die aus der elektrischen Aktivität der Neurone resultieren.

In modernen Ganzkopf-MEG-Systemen wird mithilfe mehrerer hundert sogenannter *superconducting quantum interference devices* (SQUID-Sensoren) die neuromagnetische Hirnaktivität von der gesamten Schädeloberfläche abgeleitet (Abb. 2) (Ahonen et al., 1993; Hansen et al., 2010). Die dabei verwendeten direct current (dc)SQUID-Sensoren werden mit flüssigem Helium auf 4 K, d.h. -269 °C, heruntergekühlt und erreichen somit den supraleitenden Zustand, der eine Messung solch kleinster Magnetfelder erst ermöglicht (Hämäläinen et al., 1993).

Theoretische Überlegungen gehen davon aus, dass primär exitatorische und inhibitorische postsynaptische Potentiale, von Pyramidenzellen, die tangential zur Schädeloberfläche verlaufen, der mit dem MEG messbaren Aktivität zugrunde liegen (Hari, 2011).

Abbildung 2: Ganzkopf-MEG-System an der Heinrich-Heine-Universität Düsseldorf (Firma Elekta Oy, Helsinki, Finnland). Mithilfe von 306 dcSQUID-Sensoren kann die neuromagnetische Aktivität von der gesamten Schädeloberfläche abgeleitet werden (Foto: Pressestelle des UKD).

Der große Vorteil der MEG ist, dass die sich sehr schnell verändernde neuronale Aktivität direkt abgeleitet wird. Dies ist zugleich auch der wesentlichen Unterschied gegenüber anderen bildgebenden Verfahren wie den vaskulär basierten Verfahren bei denen z.B. bei der funktionellen Magnetresonanztomographie (fMRT) ein zeitlich verzögertes Stoffwechselkorrelat der neuronalen Aktivität, das sogenannten BOLD-Signal (*blood oxygen level dependent*) (Ogawa et al., 1990), gemessen wird.
Zudem erlaubt die MEG eine relativ hohe räumliche Auflösung von wenigen Millimetern im kortikalen Bereich und eine referenzfreie Signalaufzeichnung - die wesentlichen Vorteile im Vergleich zur deutlich weiter verbreiteten EEG. Dies liegt darin begründet, dass bei der EEG die gemessenen elektrischen Felder durch Schädel und Gewebe verzehrt werden (Hari, 2011), die bei der MEG gemessenen magnetischen Felder hingegen nicht. Um solche winzigen magnetischen Felder gut quantifizieren zu können, ist allerdings eine Abschirmung von störenden magnetischen Feldern wie dem Erdmagnetfeld (~10^{-5} T) oder der Netzspannung notwendig. Dies kann mit Hilfe einer sogenannten magnetischen Abschirmkammer erreicht werden (Ahonen et al., 1993). Somit erlaubt die Kombination aus hochsensitiven Sensoren und effektiver Abschirmung die Quantifizierung neuromagnetischer Hirnaktivität im Sub-Millisekundenbereich.

2.2 Hepatische Enzephalopathie (HE)

Die Hepatische Enzephalopathie (HE) ist eine häufige Komplikation bei Patienten mit Leberzirrhose. Dabei führt die Leberzirrhose zu einer verminderten Leberfunktion, insbesondere einer verminderten Entgiftungsfunktion. Dadurch reichern sich Neurotoxine wie Ammoniak im Blut an und gelangen auch ins Gehirn, sofern sie die Blut-Hirn-Schranke passieren können.

Pathophysiologie

Auch wenn die Pathophysiologie der HE noch nicht vollständig verstanden ist (Häussinger und Blei, 2007; Häussinger und Sies, 2013), gibt es doch aktuell vorherrschende Vorstellungen zur Krankheitsentstehung (siehe Abb. 3).
Weitestgehend Einigkeit besteht darin, dass insbesondere das Ammoniak als Neurotoxin entscheidend ist (Butterworth, 2000). Es wird davon ausgegangen, dass ein erhöhter Ammoniakblutspiegel mittelbar zu einem erhöhten Ammoniakspiegel im

Gehirn führt, der wiederum ein geringgradiges Gliaödem durch Anschwellen der Astrozyten verursacht (Felipo, 2013; Häussinger, 2004; Häussinger und Blei, 2007; Häussinger et al., 2000; Prakash und Mullen, 2010).

Zusätzlich zu den Neurotoxinen wie Ammoniak tragen aber auch noch weitere Faktoren zu einem Anschwellen der Astrozyten bei, so etwa Hyponatriämie, inflammatorische Zytokine und gegebenenfalls Benzodiazepine. Zusammen lösen diese Faktoren oxidative bzw. nitrosative Stressantworten aus. Diese Stressreaktion und das Anschwellen der Astrozyten begünstigen sich gegenseitig, so dass eine sich selbst verstärkende Wechselwirkung eintritt.

Nach aktueller Sicht geht man davon aus, dass die ausgelösten Prozesse letztendlich zu einer gestörten glioneuronalen Kommunikation und einer veränderten synaptischen Plastizität führen, was als Ursache für die Veränderung auf der systemischen Ebene wie der Veränderungen der oszillatorischen Aktivität (rot umrahmt in Abb. 3) gesehen wird und die breite HE Symptomatik erklären könnte.

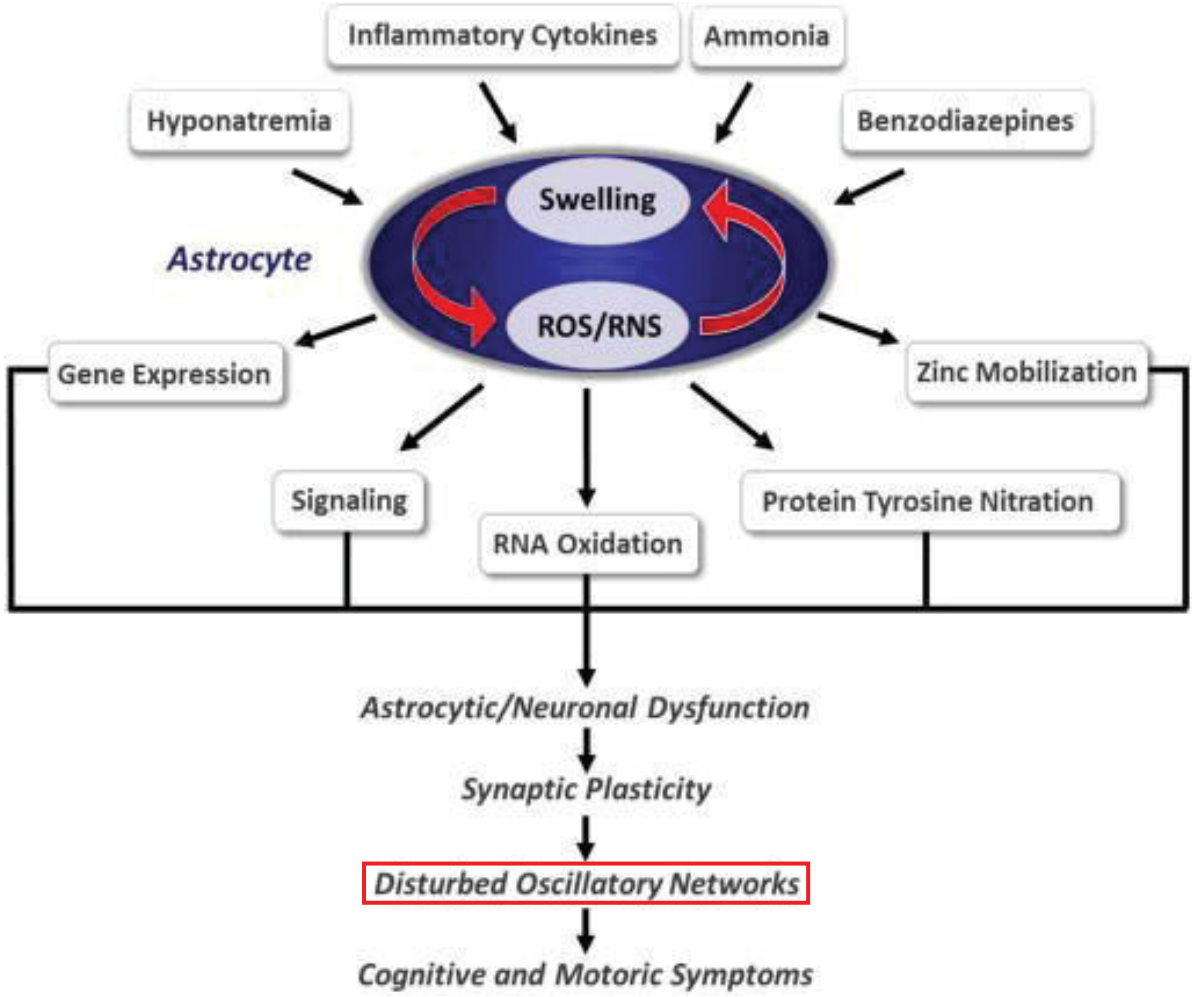

Abbildung 3: Pathophysiologisches Model der HE (adaptiert aus Häussinger und Sies, 2013).

Epidemiologie

Zur Epidemiologie der HE liegen nur wenige verlässliche Daten vor. Dies ist u.a. wohl darin begründet, dass bis dato die Diagnose der HE uneinheitlich erfolgt und die Symptome schleichend eintreten. Dies führt dazu, dass zum einen die Diagnose erschwert ist und zum anderen der diagnostizierende Arzt lediglich eine relativ subjektive Bewertung vornimmt. Die Angaben zur Prävalenz der HE schwanken zwischen 20 % und 80 % der Patienten mit Leberzirrhose (Kircheis et al., 2007). In Deutschland geht man von einer Größenordnung von 300.000 – 400.000 Patienten mit Leberzirrhose aus. Etwa 20.000 Patienten pro Jahr versterben in Folge der Leberzirrhose (Schölmerich, 2010).

Symptomatik

Die HE ist durch eine Vielzahl von Symptomen geprägt, wie zum Beispiel leichten Persönlichkeitsveränderungen, Aufmerksamkeitsdefiziten, veränderten Schlaf-Wach-Rhythmen bzw. Schlafstörungen und motorischen Symptomen. Bei den motorischen Symptomen sind neben der Ataxie insbesondere die tremorartigen *Mini-Asterixis* bzw. die *Asterixis*, auch *flapping tremor* genannt, von Bedeutung (Adams und Foley, 1949; Butz et al., 2014b; Shahani und Young, 1976). Mit zunehmender Schwere werden die betroffenen Patienten somnolent bzw. lethargisch, schließlich kommt es zum Hepatischen Koma (*Coma hepaticum*), das für die Patienten meist letal verläuft (Butterworth, 2000).

Diagnostik und Graduierung

In der derzeitigen klinischen Praxis erfolgt die Diagnose und Graduierung der HE anhand der klinischen Symptomatik (Häussinger, 2004; Häussinger und Blei, 2007).
Als Goldstandard hat sich hierbei die Graduierung anhand der sogenannten *West-Haven-Kriterien* etabliert (Ferenci et al., 2002). Dabei wird die klinisch manifeste HE in vier Stadien unterteilt, die von geringfügigen Bewusstseinsstörungen bis zum Hepatischen Koma reichen (siehe Tabelle 1).
Da die ersten beiden Stadien fließend ineinander übergehen, wurde vorgeschlagen diese als *‚low-grade HE‘* zusammenzufassen und von den stärker betroffenen Patienten (HE 2-4) mit einer *‚high-grade HE‘* abzugrenzen (Häussinger et al., 2006). Die *‚low-grade HE‘* schließt auch die Patienten mit einer sogenannten minimalen HE (mHE), die früher auch als subklinische HE bezeichnet wurde, mit ein. Obwohl diese Patienten unter einer Leberzirrhose leiden, können durch eine detaillierte neuro-

psychometrischer Testung Beeinträchtigungen erfasst werden, da keine klinischen Anzeichen einer HE bestehen. Ein Problem ist aber, dass die mHE nicht einheitlich definiert ist und die unterschiedlichen klinischen Zentren unterschiedliche Verfahren zur Diagnose heranziehen. Weit verbreitet sind *Paper-Pencil-Tests* (Wettstein et al., 2003) bzw. der speziell für die HE entwickelte PHES (*Psychometric Hepatic Encephalopathy Score*) (Weissenborn et al., 2001), wobei eine geringe Spezifität und Sensitivität deren Aussagekraft limitieren (Wettstein et al., 2003).

HE-Grad	Symptome
0	- Patienten mit Leberzirrhose aber ohne Anzeichen einer Hepatischen Enzephalopathie
mHE	- Minimale HE beschreibt Patienten, die klinisch unauffällig sind, aber bei detaillierter neuropsychometrischer Testung Beeinträchtigungen zeigen
1	- Geringfügige Bewusstseinsminderung - Euphorie oder Angst - Verkürzte Aufmerksamkeitsdauer - Verminderte Additions-Rechenleistung
2	- Lethargie oder Apathie - Minimale zeitliche und örtliche Desorientierung - Subtile Persönlichkeitsänderung - Unangebrachtes Benehmen - Verminderte Subtraktions-Rechenleistung
3	- Somnolenz bis Semistupor, noch Reaktion auf verbale Stimuli - Verwirrung - Starke Desorientierung
4	- Koma; keine Reaktion auf verbale Reize

Tabelle 1: Klinischen Graduierung der HE. Die etablierten *West-Haven*-Kriterien umfassen vier Grade klinisch manifester HE (Ferenci u. a., 2002); deutsche Übersetzung nach Wettstein u. a., 2003. Zudem können noch HE 0- und mHE-Patienten definiert werden (grau unterlegt), die aber nicht zu der engeren klinischen Einteilung zählen.

Durch Kircheis et al. wurde die sogenannte Kritische Flimmerfrequenz (*critical flicker frequency (CFF*)) als zusätzlicher Parameter zur Graduierung der HE vorgeschlagen *(*Kircheis et al., 2002). Dabei konzentrieren sich die Testpersonen auf einen flimmernden roten Punkt in einem Tubus, der zuerst mit 60 Hz flimmert und als konstantes Licht wahrgenommen wird. Dann verlangsamt sich die Frequenz kontinuierlich und bei einer bestimmten Frequenz erkennt die Testperson, dass es sich um ein flimmerndes und nicht um ein kontinuierliches Licht handelt. Diese Frequenz wird als CFF bezeichnet. Bei Patienten mit HE konnte gezeigt werden, dass die CFF sich mit der Schwere der HE verlangsamt und sowohl eine Graduierung als auch eine Verlaufskontrolle der HE erlaubt. Andere Gruppen replizierten

diese Ergebnisse und eine *cut-off* Frequenz von 39 Hz bzw. 38 Hz konnte definiert werden, die eine Unterscheidung von klinisch manifesten HE-Patienten von gesunden Probanden erlaubt (Kircheis et al., 2014; Kircheis et al., 2002; Romero-Gomez et al., 2007; Sharma et al., 2007). Zudem bestätigt eine Metaanalyse die Vorteile der CFF (Torlot et al., 2013).

Diese Ergebnisse unterstützen die Annahme, dass die CFF ein geeigneter und wichtiger klinischer Parameter für die Diagnosestellung und die Verlaufskontrolle bei der HE ist und sprechen für eine zukünftige weitere Verbreitung in der klinischen Praxis. Die Verwendung der CFF allein oder in Kombination mit neuropsychometrischen Verfahren könnte ein sinnvoller und wichtiger Schritt sein, die HE mehr als ein Kontinuum zu sehen bzw. abzubilden anstelle der derzeitigen Einteilung in starre und relativ unspezifische klinische Grade (Bajaj et al., 2009).

Während bei den Untersuchungen in dieser Arbeit ausschließlich die HE gemeint ist, die aufgrund einer Leberzirrhose auftritt (*Typ C*), muss der Vollständigkeit halber auch erwähnt werden, dass eine HE auch durch ein akutes Leberversagen (*Typ A*) sowie durch einen portosystemischen Shunt (*Typ B*) hervorgerufen werden kann. Zudem unterscheidet man neben der mHE auch noch die sogenannte persistierende HE und die episodische HE (Wettstein et al., 2003). Bei der episodischen HE kommt es aufgrund begünstigender Faktoren wie z.B. gastrointestinale Blutungen oder Infektionen zur Ausbildung der HE-Symptomatik (Ferenci et al., 2002; Wettstein et al., 2003). Von einer persistierenden HE spricht man, wenn die HE in wiederholten Episoden auftritt und es zu einer andauernden Veränderungen des mentalen Zustands kommt (Ferenci et al., 2002; Wettstein et al., 2003).

Therapie

Die Therapie der HE zielt primär auf die Behandlung der auslösenden Faktoren ab (Prakash und Mullen, 2010; Wettstein und Häussinger, 2003). Insbesondere gastrointestinale Blutungen und Infektionen spielen dabei eine Rolle (Häussinger und Blei, 2007). Zudem ist es von hoher praktischer Relevanz, auf eine verminderte Produktion und Absorption von stickstoffhaltigen Verbindungen aus dem Darm durch eine geeignete Diät, eine Laktulose-Gabe und in manchen Fällen auch den Einsatz von Antibiotika hinzuwirken (Bass et al., 2010; Galhenage et al., 2006; Mullen, 2006). Allerdings ist nicht für alle diese Therapien die Wirksamkeit in placebokontrollierten Studien belegt worden. Eine solche kann aber aufgrund der langjährigen klinischen Erfahrung dennoch als gesichert gelten (Häussinger, 2004).

Bisherige Neurophysiologische Befunde zur HE

In den letzten Jahrzehnten haben sich bereits einige Arbeiten mit den Veränderungen der neurophysiologischen Hirnaktivität bei HE beschäftigt und Veränderungen der Spontanaktivität, evozierter Potentiale sowie oszillatorischer Aktivität gezeigt (siehe Übersichtsarbeiten von Amodio und Gatta, 2005; Butz et al., 2013; Schnitzler et al., 2006; Timmermann et al., 2005).

Bereits in den ersten Beschreibungen durch Foley und andere (Foley et al., 1950; Parsons-Smith et al., 1957) wurden markante Veränderungen der EEG Aktivitäten beobachtet und eine nicht näher quantifizierte Verlangsamung der EEG Aktivität beschrieben (Davies et al., 1991; Senzolo et al., 2005). Die Spontanaktivität wird zudem auch diagnostisch genutzt, um die Graduierung der HE bzw. die Diagnose der mHE zu unterstützen (Guerit et al., 2009). Die bereits bekannten Veränderungen der Spontanaktivität zeichnen sich durch eine Verlangsamung der dominanten Frequenz der Spontanaktivität sowie ein verstärktes Auftreten von oszillatorischer Aktivität im *Theta*-Band (3-7 Hz) aus (Davies et al., 1991; Kullmann et al., 2001; Senzolo et al., 2005; van der Rijt et al., 1984). Dieser Effekt verstärkt sich mit fortschreitender Schwere der HE und es kommt zu den sogenannten triphasischen Wellen, d.h. zwei negativen Wellen, der eine positive Welle folgt (Bickford und Butt, 1955; Pang et al., 2011). Diese triphasischen Wellen sind charakteristisch für metabolisch induzierte Enzephalopathien. Man geht davon aus, dass diese Folge einer veränderten thalamo-kortikalen Interaktion sind (Davies et al., 1990; Pang et al., 2011). Zudem gibt es erste Befunde, die einen Zusammenhang zwischen veränderter EEG-Aktivität und Beeinträchtigungen bei Verhaltensmaßen wie etwa dem PHES zeigen (Amodio et al., 2008; Olesen et al., 2011). Und auch zu den Blutwerten wie Ammoniak konnte ein Zusammenhang beobachtet werden (Montagnese et al., 2011; Senzolo et al., 2005). Nicht zu vernachlässigen ist zudem die prognostische Bedeutung der EEG-Spektralanalyse. Diese erlaubt eine Voraussage über das Auftreten von klinisch manifester HE und einer frühen Sterblichkeit (Amodio et al., 2001; Saxena et al., 2002).

Untersuchungen zu evozierten Antworten zeigten ebenso vielfältige Veränderungen im Rahmen der HE (siehe Übersichtsarbeiten von Amodio und Gatta, 2005; Montagnese et al., 2004). Insgesamt ergeben sich Hinweise auf verzögerte evozierte Antworten bzw. Verzerrungen der Antworten u.a. auch Abschwächung bis hin zum Ausbleiben von Antworten sowohl bei visueller Stimulation als auch bei auditorischer

und sensorischer Stimulation (Montagnese et al., 2004). So konnte zum Beispiel für somatosensorisch evozierte Potenziale in mehreren Arbeiten eine verzögerte Latenz der maximalen Amplitude sowie eine zunehmende Deformation des evozierten Potenzials mit zunehmender Schwere der HE gezeigt werden (Blauenfeldt et al., 2010; Yang et al., 1985).

Zu Veränderungen von oszillatorischer Aktivität gibt es neben den obengenannten Arbeiten zur Spontanaktivität erst wenige Vorarbeiten primär aus dem motorischen System (Timmermann et al., 2003a; Timmermann et al., 2002). Diese werden im Detail in den Abschnitten zu den eigenen Arbeiten näher behandelt.

Was bislang allerdings fehlt, sind systematische Arbeiten zum Zusammenhang zwischen Ausprägung der HE und den Veränderungen der oszillatorischen Aktivität. Dies gilt insbesondere für die leicht betroffenen HE-Patienten (mHE) und für stimulusassoziierte oszillatorische Aktivität, d.h. Studien, die die Rolle von oszillatorischer Aktivität bei der Verarbeitung von visuellen und somatosensorischen Reizen untersuchen. Solche Arbeiten sind von großer Wichtigkeit, da sie zum einen helfen können, die Pathophysiologie der HE besser zu verstehen und zum anderen auch dazu beitragen können, den Zusammenhang zwischen oszillatorischer Aktivität und Verhalten generell näher zu beleuchten.

Des Weiteren lagen bisher nur wenige bzw. keine Arbeiten vor, die den Zusammenhang zwischen der CFF, der Leistungsfähigkeit bei motorischen und kognitiven Aufgaben und den Veränderungen auf neurophysiologischer Ebene untersucht haben.

Die hier zusammengefassten Arbeiten liefern neue und weitergehende Antworten auf diese bislang wenig untersuchten Fragen.

3. Eigene Arbeiten

Die Grundhypothese, die in den hier zusammengefassten eigenen Arbeiten verfolgt wird, ist, dass es im Rahmen der Hepatischen Enzephalopathie zu einer globalen Verlangsamung oszillatorischer Aktivität kommt.

Global heißt in diesem Zusammenhang, dass eine Verlangsamung sowohl in verschiedenen Frequenzbändern als auch in verschiedenen zerebralen Subsystemen beobachtet werden kann. Dementsprechend untersuchen die hier vorgestellten Arbeiten die verschiedenen Frequenzbänder, sprich *Alpha-, Beta-* und *Gamma*-Band, und Subsysteme, d.h. das motorische System, das sensorische System und das visuelle System.

Für die Aktivität im *Alpha*-Band konnte gezeigt werden, dass es sowohl zu einer Verlangsamung der Spontanaktivität kommt als auch zu einer Verlangsamung von stimulusassoziierter Aktivität im primären somatosensorischen Kortex. Zudem konnten auch Veränderungen auf der Verhaltensebene bei der Verarbeitung sensorischer Reize beschrieben werden.

Ebenso kommt es im *Beta*-Band zu Veränderungen, die sich in einer verlangsamten kortiko-muskulären Kopplung bei HE-Patienten manifestiert. Auch hier werden die neurophysiologischen Befunde durch Verhaltensdaten gestützt, die eine Verlangsamung der schnellstmöglichen Geschwindigkeit bei Fingerbewegungen belegen.

Für das *Gamma*-Band zeigte sich, dass es auch in diesem Frequenzbereich zu einer Verlangsamung kommt, die durch eine Verschlechterung der Performanz, d.h. verlängerten Reaktionszeiten sowie erhöhten Fehlerraten, begleitet wird.

Für alle vorliegenden Arbeiten gilt, dass die CFF als klinischer Parameter eng mit den neurophysiologischen Veränderungen und Verhaltensdaten korreliert.

Insgesamt unterstützen die hier zusammengefassten Arbeiten somit die Annahme, dass die globale Verlangsamung der oszillatorischen Aktivität ein zentrales pathophysiologisches Phänomen bei HE darstellt.

3.1 Alpha-Band

Spontanaktivität

Von der Grundhypothese ausgehend, dass es im Rahmen der HE zu einer Verlangsamung oszillatorischer Aktivität über verschiedene Frequenzbänder und kortikale Subsysteme hinweg kommt, ist die *Alpha*-Band-Aktivität als stärkste spontane oszillatorische Aktivität des menschlichen Gehirns von großem Interesse. In einer Studie, die insgesamt 50 Probanden einschloss, wurde untersucht, wie sich im Rahmen der HE die Spontanaktivität verändert und inwieweit diese Veränderungen mit der CFF korrelieren (Butz et al., 2014a).

Die untersuchte Population bestand aus 5 Gruppen à 10 Probanden unterschiedlicher Ausprägung der Schwere der HE, d.h. Patienten mit minimaler HE, HE 1 und HE 2 sowie Patienten, die trotz Vorliegens einer Leberzirrhose keine Anzeichen einer HE zeigten (HE 0) und gesunden, im Hinblick auf Alter und Geschlecht parallelisierten Kontrollprobanden. Die Spontanaktivität wurde mithilfe des MEG erfasst und die Frequenz der stärksten Spontanaktivität (*Dominant Frequency*) im Bereich des okzipitalen Kortex im Frequenzbereich von 5-16 Hz, d.h. dem eigentlich Bereich der *Alpha*-Band Aktivität erweitert um +/- 3Hz, bestimmt. Zudem wurde die individuelle CFF erhoben.

Es zeigte sich, dass die klinisch manifest betroffenen HE-Patienten eine signifikant verlangsamte Spontanaktivität aufwiesen und dass die Frequenz der stärksten Spontanaktivität mit der CFF korrelierte ($R = 0.50$, $p < 0.01$) (Abb. 4).

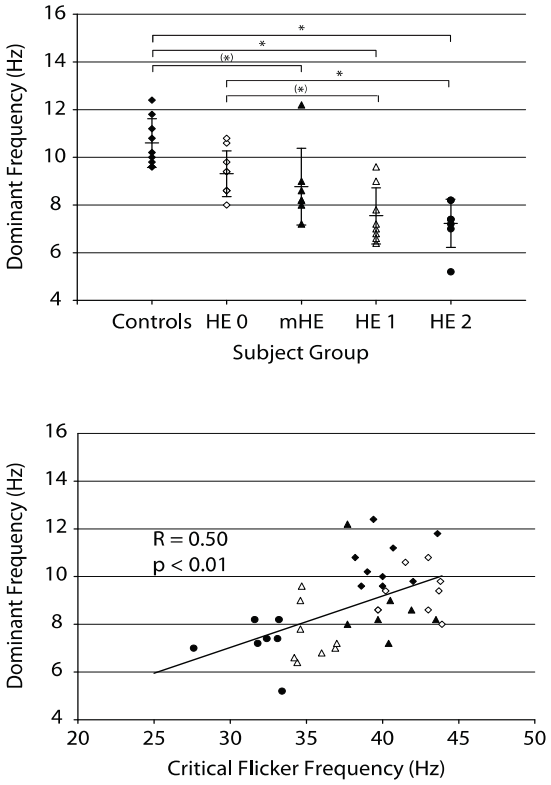

Abbildung 4: Ozillatorische Spontanaktivität bei HE. ***Oben:*** Stärkste Spontanaktivität (*Dominant Frequency*) im Frequenzbereich von 5-16 Hz der fünf untersuchten Gruppen. Die manifest betroffenen Patienten (HE 1, HE 2) zeigen eine signifikant verlangsamte Spontanaktivität im Vergleich mit gesunden Kontrollprobanden. ***Unten:*** Korrelation zwischen der Spontanaktivität und der CFF als Maß für die klinische Schwere der HE. Es zeigt sich, dass es mit einer sich verlangsamenden CFF auch zu einer verlangsamten Spontanaktivität kommt (aus Butz et al., 2014a).

Dieser Befund belegt eindrücklich, dass das reine Verhaltensmaß der CFF anscheinend aussagekräftige Hinweise auf die oszillatorische Hirnaktivität zulässt, die als klinisch etabliertes Maß die Schwere der Betroffenheit beschreibt.

Somatosensorisches System

Im somatosensorischen System ist oszillatorische Aktivität im *Alpha*-Band von Bedeutung, da z.B. die Verarbeitung einfacher somatosensorischer Reize bei Gesunden mit einer Modulation von *Alpha*-Band-Aktivität verbunden ist. Nach einer initialen Suppression kommt es zum sogenannten *rebound*, einer Zunahme der oszillatorischen Aktivität, die noch über das Ausgansniveau hinausgeht (Della Penna et al., 2004; Nikouline et al., 2000; Salenius et al., 1997). Bei der HE kommt es zu einer Verlängerung der Antworten sowie einer Deformation oder sogar einem Verlust von Komponenten der somatosensorisch evozierten Potentiale (Blauenfeldt et al., 2010; Chu und Yang, 1987; Davies et al., 1991; Yang et al., 1985).

Was bis dato allerdings fehlte, waren Studien zur oszillatorischen Aktivität und dessen Veränderungen im Rahmen der HE bei somatosensorischer Stimulation.

Um dies zu untersuchen, wurden 21 Patienten mit Leberzirrhose und unterschiedlicher Schwere der HE (HE 0, mHE, HE 1) und 7 gesunde altersgleiche Kontrollen im Rahmen einer eigenen Arbeit untersucht (May et al., 2014).

Bei allen Probanden wurde der *Nervus medianus* der rechten Hand elektrisch stimuliert während die neuromagnetische Aktivität simultan abgeleitet wurde. Im Rahmen der Auswertung wurde die oszillatorische Aktivität im kontralateralen primären somatosensorischen Kortex (S1) analysiert.

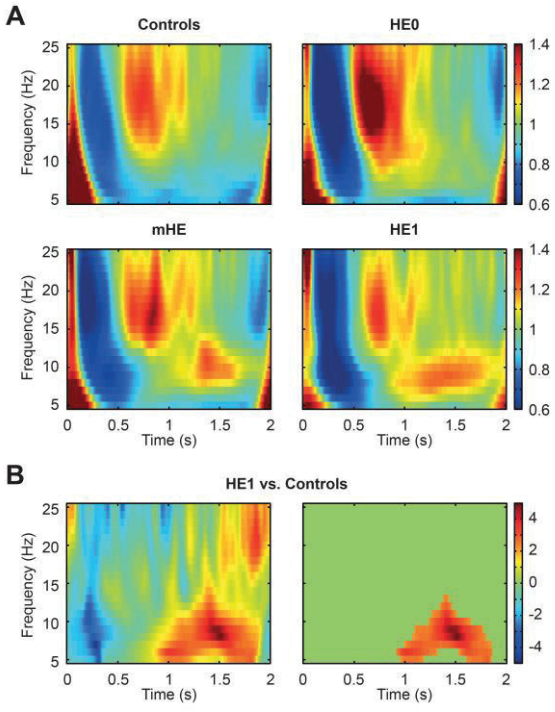

Abbildung 5: Zeit-Frequenz-Spektren der oszillatorischen Aktivität bei Stimulation des *Nervus medianus*. ***A:*** Zeit-Frequenz-Spektren der oszillatorischen Aktivität im S1 nach elektrischer Stimulation des rechten *Nervus medianus* (Zeitpunkt 0 s). Farblich dargestellt ist die Veränderung zur Baseline. ***B:*** Differenzplot sowie Darstellung der signifikant unterschiedlichen Frequenz- und Zeitbereiche im Vergleich Gesunde vs. HE 1-Patienten (aus May et al., 2014).

Während das zuvor beschriebene Aktivierungsmuster weitgehend auch bei den HE-Patienten zu beobachten war, konnte mit zunehmender Schwere der HE eine Verlangsamung der stimulusassoziierten *Alpha*-Band-Aktivität sowie ein verzögerter *rebound* gezeigt werden (Abb. 5). Beide Veränderungen korrelierten zudem mit der CFF (Abb. 6).

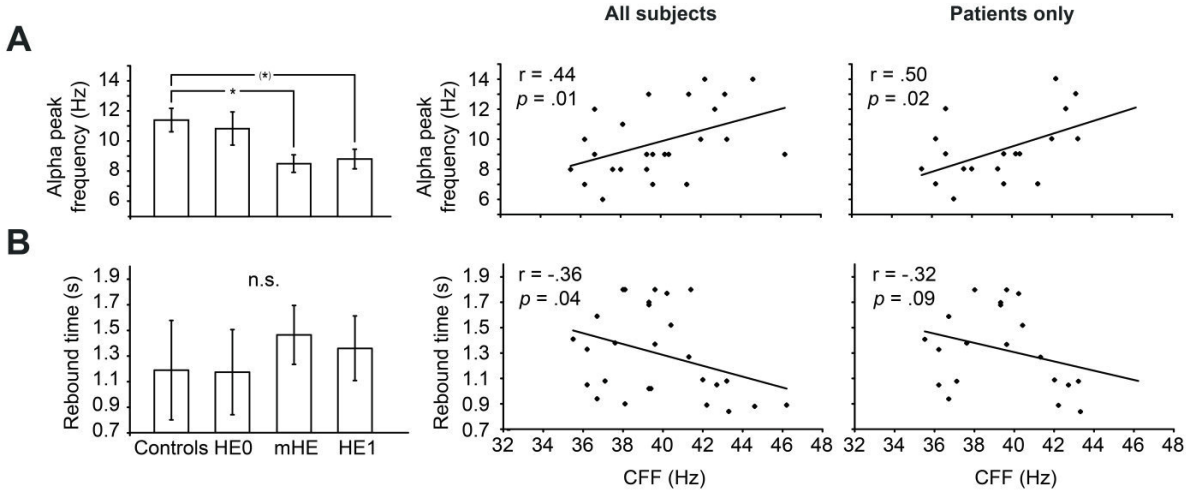

Abbildung 6: Frequenz und Zeit bis zum *rebound* der stimulusassoziierten *Alpha*-Band-Aktivität. ***A:*** Gruppenunterschiede in der stärksten Frequenz im *Alpha*-Band im S1. Es zeigt sich eine Verlangsamung über alle Probanden hinweg. Diese Verlangsamung der stärksten *Alpha*-Band-Aktivität korreliert mit der CFF und besteht auch bei ausschließlicher Betrachtung der Patienten. ***B:*** Gruppenunterschiede in der Zeit bis zum *rebound* der *Alpha*-Band-Aktivität im S1. Auch die Zeit bis zum *rebound* korreliert mit der CFF für alle Probanden. Bei ausschließlicher Betrachtung der HE-Patienten zeigt sich ein Trend zu einer Verlangsamung (aus May et al., 2014).

Behaviorale Evidenz: Quantitative Sensorische Testung bei HE

Die Ergebnisse zu Veränderungen der neurophysiologischen Aktivität im somatosensorischen Kortex werden interessanterweise auch durch eigene Verhaltensdaten gestützt, die eine z.T. beeinträchtigte sensorische Performanz bei HE zeigen (Brenner et al., 2015). Hierbei wurde bei 42 HE-Patienten (12 HE 0, 12 mHE, 12 HE 1, 6 HE 2) sowie 12 gesunden altersgleichen Probanden die Somatosensorik umfassend mithilfe der sogenannten Quantitativen Sensorischen Testung (QST) erfasst. Bei der QST handelt es sich um ein standardisiertes Protokoll, das vom Deutschen Forschungsverbund Neuropathischer Schmerz (DFNS) entwickelt wurde, um das sensorische Empfinden und insbesondere die Schmerzwahrnehmung quantifizieren zu können (Rolke et al., 2006).

Neben der QST wurden die Patienten umfassend klinisch charakterisiert, was eine neuropsychometrische Testung, die Erhebung der individuellen CFF sowie eine Einteilung entsprechend der *West-Haven*-Kriterien einschloss. Im Ergebnis zeigte sich, dass HE-Patienten keine Zeichen erhöhter Wahrnehmungs- bzw. Schmerz-

schwellen für Druck und Vibrationsreize aufwiesen. Bei der thermischen Testung allerdings bemerkten HE 2-Patienten Kälte erst bei niedrigeren Temperaturen. Zudem zeigten HE 2-Patienten im Vergleich zu den vier anderen untersuchten Gruppen eine erhöhte Wahrnehmungsschwelle (*thermal sensory limen, TSL*) in Bezug auf Temperaturunterschiede (Abb. 7).

Diese Veränderungen in der Temperaturwahrnehmung korrelierten negativ mit den CFF-Werten der Probanden, d.h. je niedriger die CFF war, umso stärker beeinträchtigt war auch die Temperaturwahrnehmung.

Mithilfe einer partiellen Korrelation unter Berücksichtigung der neuropsychometrischen Testergebnisse konnten die beobachteten Effekte auf eine Beeinträchtigung der Aufmerksamkeit der Patienten zurückgeführt werden. Daher und darüber hinaus aufgrund der Anamnese der Patienten sowie der durchgeführten Neurographie kann eine periphere Ursache wie z.B. eine Neuropathie, wie man es für Patienten mit Leberzirrhose auch vermuten könnte, als eher unwahrscheinlich angesehen werden. Unbeantwortet blieb aber, warum gerade die thermischen Tests betroffen sind und das Störungsbild nicht sehr viel breiter auftritt, wie es eigentlich erwartet war.

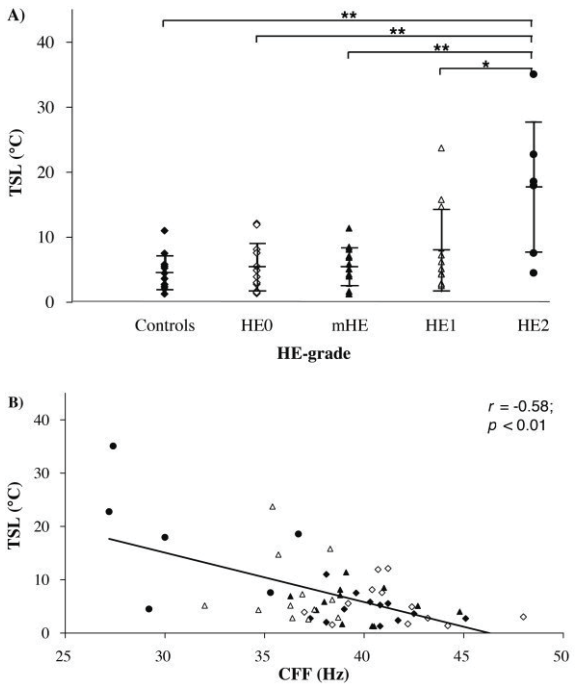

Abbildung 7: Temperaturwahrnehmung bei HE. ***A*** Gruppenunterschiede bei der Detektion von Temperaturunterschiede (*thermal sensory limen*, TSL). Schwer betroffenen Patienten (HE 2) zeigen eine deutlich beeinträchtigte Wahrnehmung. ***B:*** Negative Korrelation zwischen der CFF und der TSL: Je niedriger die CFF, desto größer die TSL (aus Brenner et al., 2015).

Die mit diesen Verhaltensdaten parallel auftretenden Veränderungen der oszillatorischen Aktivität im S1 könnten erste Hinweise auf möglichen Mechanismen geben, die zu diesen Einschränkungen führen. So könnte man z.B. vermuten, dass der beobachtete verzögerte *rebound* mit der verschlechterten Sensorik verbunden seien könnte. Diese hypothetisch denkbaren Zusammenhänge müssen aber erst in zukünftigen Studien eingehender untersucht werden.

3.2 Beta-Band

Im Rahmen der HE treten sehr markante motorische Symptome auf (Burkhard et al., 2003; Butterworth, 2000; Häussinger und Blei, 2007; Spahr et al., 2000). Bei den schwer betroffenen Patienten ist die grobschlägige *Asterixis*, auch *flapping tremor* genannt, das prominenteste motorische Symptom (Adams und Foley, 1949; Young und Shahani, 1986). Dabei kommt es zu einem wiederholten Ausbleiben der Muskelaktivität für einen Zeitraum von jeweils 50-200 ms, die zu der auffälligen Symptomatik des „Flügelschlagens" führt (Shibasaki, 1995; Ugawa et al., 1989; Young und Shahani, 1986). Aber bereits im ersten klinisch manifesten Stadium (HE 1) kann es neben der Ataxie auch zu einem feinschlägigem Zittern kommen, der sogenannten *Mini-Asterixis* oder auch *„metabolic tremor"*. Dieser setzt beim Vorhalten der Arme nach etwa 2-30 s ein und tritt in einem Frequenzbereich von 6-12 Hz auf (Leavitt und Tyler, 1964). Für beide Phänomene wurde ein gemeinsamer pathophysiologischer Mechanismus vermutet, der aber bislang nicht gezeigt werden konnte (Leavitt und Tyler, 1964).

Oszillatorische Kopplung im motorischen System bei HE

Bei gesunden Probanden kommt es beim Vorhalten der Arme, d.h. bei isometrischer Kontraktion, zu einer oszillatorischen Kopplung der Muskeln mit dem kontralateralen primären Motorkortex (M1) im *Beta*-Band, d.h. in einem Frequenzbereich von ~20 Hz (Gross et al., 2000). In früheren Arbeiten konnte an einer Gruppe von 12 Patienten mit Leberzirrhose gezeigt werden, dass der kontralaterale primäre Motorkortex an der Entstehung der *Mini-Asterixis* im Rahmen der HE beteiligt ist und es zu einer Verlangsamung der zuvor bei Gesunden beschriebenen Kopplung kommt (Timmermann et al., 2002). In einer darauf aufbauenden Arbeit wurden diese Daten weitergehend analysiert und es konnte gezeigt werden, dass die beobachtete Verlangsamung nicht nur zwischen Muskel und M1 auftritt, sondern auch in der Interaktion zwischen M1 und Thalamus (Timmermann et al., 2003a).

In einer sich anschließenden eigenen Arbeit wurde untersucht, ob sich diese Ergebnisse auch in einer größeren Patientenkohorte replizieren lassen und inwieweit es zudem einen Zusammenhang mit der bekannten Verlangsamung der CFF gibt (Timmermann et al., 2008).

Bei 32 Patienten mit Leberzirrhose und unterschiedlich starker Ausprägung der HE wurde mithilfe der MEG die neuromagnetische Aktivität während einer isometrischen Halteaufgabe untersucht, d.h. simultan die Aktivität des Gehirns und der beteiligten

Muskeln abgeleitet. Dadurch konnte der M1 als Quelle der stärksten Kopplung zum Muskel lokalisiert und die entsprechende Kopplungsfrequenz bestimmt werden.

Diese Studie zeigte, dass sich nicht nur die CFF (Abb. 8 A), sondern parallel auch die Frequenz der kortiko-muskulären Kopplung mit der Schwere der HE verlangsamt. Bei Patienten mit Leberzirrhose aber ohne Anzeichen einer HE (HE 0) trat die kortiko-muskuläre Kopplung im physiologischen Bereich auf, d.h. im *Beta*-Band. Die leicht betroffenen Patienten (SHE, HE 1) hingegen zeigten bereits eine Kopplung in niedrigeren Frequenzbereichen ~15 Hz. Die stark betroffenen Patienten (HE 2) waren sogar noch stärker verlangsamt und lagen bei ~11 Hz (Abb. 8 B). Damit konnten die Ergebnisse der vorhergehenden Arbeiten repliziert werden und darüber hinaus zeigte sich, dass die Verlangsamung der kortiko-muskulären Kopplung mit der Verlangsamung der CFF korrelierte (Abb. 8 C).

Somit lieferten diese Ergebnisse initiale Evidenz dafür, dass die Verlangsamung oszillatorischer Aktivität parallel in verschiedenen Subsystemen des Gehirns auftritt - hier die Verarbeitung eines oszillierenden Stimulus im visuellen System und oszillatorische Kopplungen im motorischen System - und folglich ein wichtiges pathophysiologisches Phänomen bei HE sein könnte.

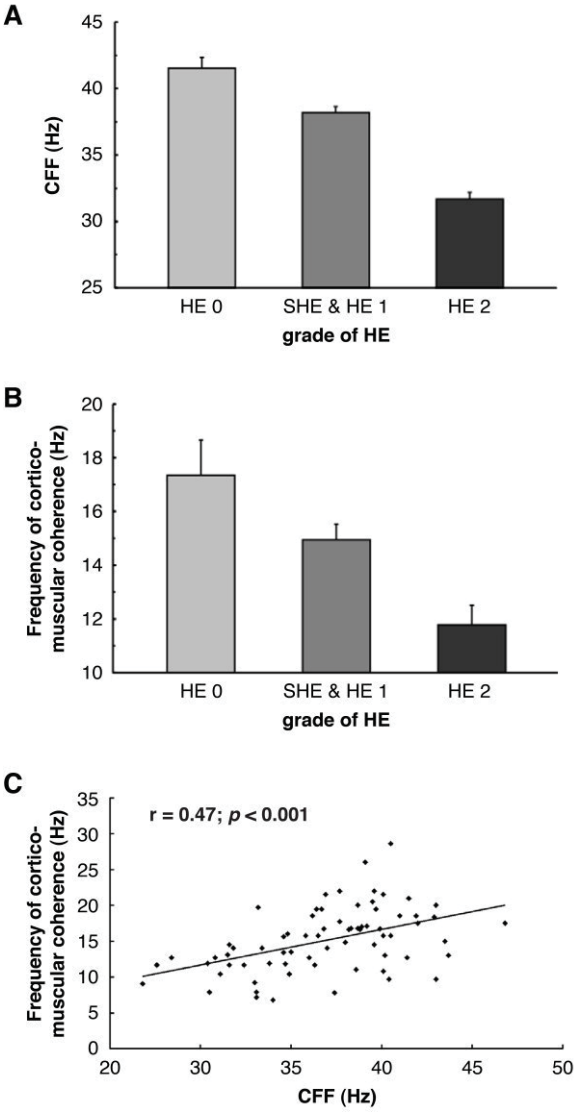

Abbildung 8: CFF und kortiko-muskuläre Kopplung bei HE. ***A*** Die CFF nimmt mit der Schwere der Betroffenheit ab (SHE = subklinische HE, dies entspricht der minimalen HE); ***B:*** Die Frequenz der kortiko-muskulären Kohärenz nimmt eben-so mit der Schwere der Betroffenheit ab; **C:** Beide Parameter, CFF und Kohärenz, korrelieren (aus Butz et al., 2013; adaptiert aus Timmermann et al., 2008).

Mini-Asterixis und Asterixis

Eine weitere eigene Studie widmete sich der Frage, welche kortikalen Areale an der Entstehung der *Asterixis* beteiligt sind und inwieweit die Pathophysiologie von *Asterixis* und *Mini-Asterixis* Gemeinsamkeiten aufweist (Butz et al., 2014b).

Neuromagnetische Aktivität von 9 Patienten mit manifester HE (HE 2 und HE 3), die *Asterixis* zeigten, wurde mithilfe der MEG gemessen. Simultan wurde die Muskelaktivität (EMG) der Unterarmmuskulatur abgeleitet sowie die Handposition mit einem Ultraschallpositionsbestimmungssystem (Zebris Medical GmbH, Isny) erfasst. Anhand dieser Daten wurden die Zeiten des Auftretens der *Asterixis* bestimmt (siehe Abb. 9). Diese wurden gemittelt und ein Dipolmodell errechnet, das das Auftreten der neuromagnetischen Aktivität abbildet, die mit dem *Asterixis* verbundenen ist.

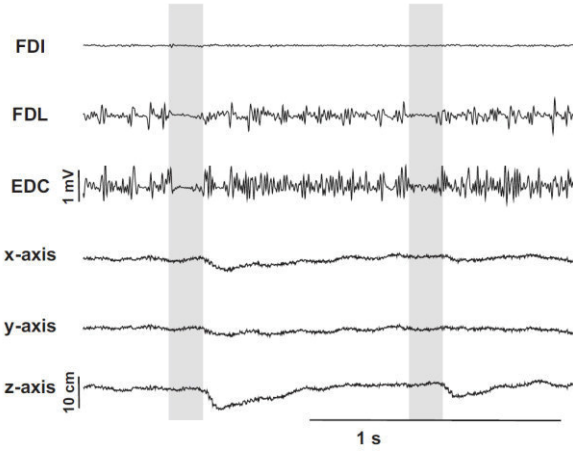

Abbildung 9: Beispiel eines Patienten mit *Mini-Asterixis* und *Asterixis*. Die oberen drei Spuren zeigen die Muskelaktivität der an der *Asterixis* beteiligten Arm- bzw. Handmuskeln. Die unteren drei Spuren bilden die Handposition in den drei Raumebenen ab. Bei der Muskelaktivität ist das periodische Auftreten der „Tremoraktivität" der *Mini-Asterixis* zu erkennen, die im Rahmen des abgebildeten Zeitraums zweimal völlig ausbleibt (grau unterlegt). Dies sind die beiden *Asterixis*-Ereignisse, die sich auch in der Position der Hand in den drei untersten Spuren widerspiegeln (aus Butz et al., 2014b).

Zudem wurde die Quelle der stärksten kortiko-muskulären Kohärenz in der Frequenz der individuellen Frequenz der *Mini-Asterixis* lokalisiert.

Für die Quelle der stärksten kortiko-muskulären Kohärenz konnte erwartungsgemäß der kontralaterale M1 lokalisiert und damit die Ergebnisse der vorherigen Arbeiten repliziert werden (siehe Abb. 10 B). Darüber hinaus zeigte sich, dass auch die mit der *Asterixis* assoziierte Aktivität, d.h. der entsprechende Dipol, im gleichen Areal zu finden war (siehe Abb. 10 A).

Diese Befunde lieferten somit Hinweise darauf, dass sowohl an der *Asterixis* als auch an der *Mini-Asterixis* der kontralaterale M1 beteiligt ist, was eine gemeinsame Pathophysiologie wahrscheinlich macht. Eine mögliche Interpretation ist, dass der *Asterixis* eine ausgeprägte Form der *Mini-Asterixis* darstellt und der Entstehungsmechanismus auf den gleichen Grundprinzipien beruht.

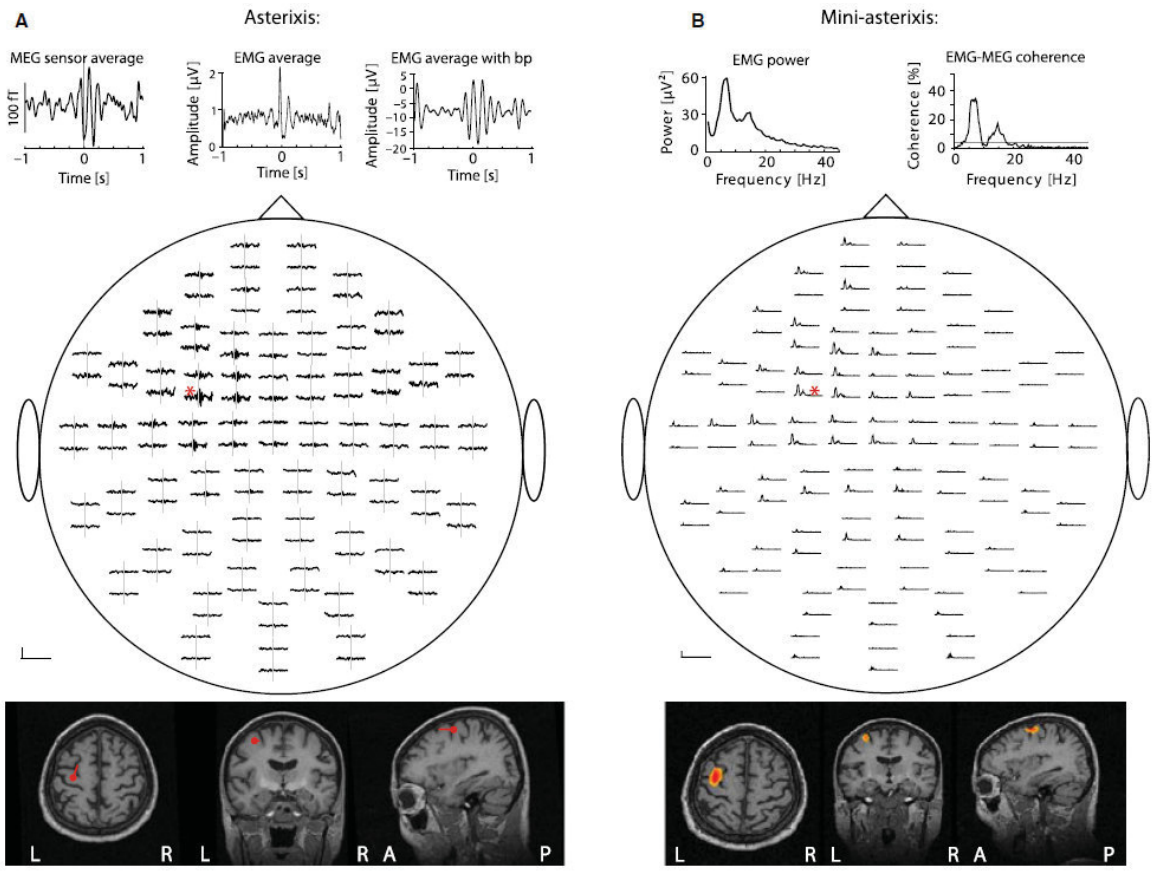

Abbildung 10: Beispiel eines HE-Patienten mit *Mini-Asterixis* und *Asterixis*. **A:** Über die einzelnen *Asterixis*-Ereignisse gemittelte Aktivität. Der Zeitpunkt 0 s markiert den Anfang der Pause im EMG. Die gemittelte Aktivität entstammt primär dem kontralateralen M1. Unten ist die Position des berechneten Dipols zu sehen (bp = band-pass). **B:** Die stärkste kortiko-muskuläre Kohärenz bei Patienten mit *Mini-Asterixis* tritt in der individuellen Frequenz der *Mini-Asterixis* auf. Bei der Lokalisation der Kohärenz lässt sich auch hier der kontralaterale M1 als Quelle der stärksten Kohärenz lokalisieren (aus Butz et al., 2014b).

Behaviorale Evidenz: Schnellste Fingerbewegungen, Tremor und Ataxie bei HE

Die Ergebnisse zu Veränderungen der neurophysiologischen Aktivität im motorischen System werden ebenfalls durch eigene Verhaltensdaten gestützt (Butz et al., 2010). Bei vier Probandengruppen (11 Kontrollen, 8 HE 0-, 8 mHE- und 8 HE 1-Patienten) wurden unterschiedliche Bewegungsparameter erfasst. Dies geschah zum einen anhand von etablierten klinischen Bewertungsskalen zur klinischen Beurteilung des Tremors und der Ataxie (*Fahn Tremor Scale, International Ataxia Rating Scale*) und zum anderen im Rahmen einer Bewegungsanalyse mithilfe eines Ultraschallpositionsbestimmungssystems bei der schnellstmöglich alternierende Fingerbewegungen durchgeführt werden sollten (Zebris Medical GmbH, Isny).

Für Ataxie und Tremor konnte eine Zunahme der Schwere mit der Schwere der HE gezeigt werden, d.h. die manifesten HE-Patienten wurden jeweils als stärker betroffen beurteilt. Zudem zeigte sich, dass auch die individuelle Bewertung eng mit

der CFF korrelierte, d.h. je niedriger die CFF desto ausgeprägter war die Symptomatik (siehe Abb. 11).

Bei der Bewegungsanalyse zeigte sich, dass die maximale Frequenz, mit der die Patienten die Fingerbewegungen ausführen konnten, bei allen Patientengruppen verlangsamt war. Dies galt sogar bereits für die Gruppe der HE 0-Patienten und damit Patienten, die ansonsten unauffällig waren. Sowohl die Amplitude als auch die Frequenz der alternierenden Fingerbewegungen korrelierten signifikant mit der CFF.

Diese Ergebnisse zeigten erstmalig, dass es bereits bei Patienten mit Leberzirrhose aber ohne Anzeichen einer HE zu messbaren Einschränkungen der motorischen Leistungsfähigkeit kommt. Zudem unterstützen diese Befunde, dass mit zunehmender Schwere der HE die motorische Leistungsfähigkeit graduell abnimmt. Somit könnte die Quantifizierung der motorischen Leistungsfähigkeit potenziell die klinische Diagnose bzw. Graduierung der HE unterstützen.

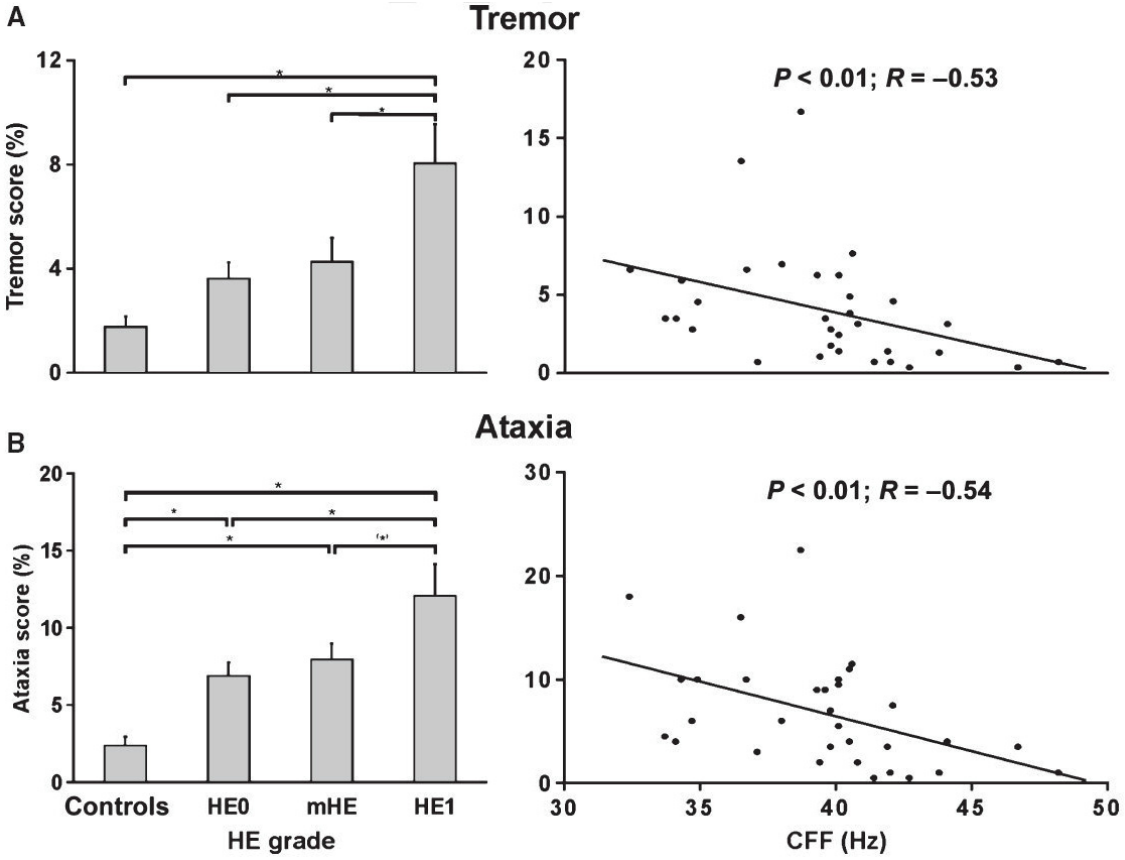

Abbildung 11: Beurteilung der Schwere von Tremor und Ataxie bei HE Patienten anhand klinischer Bewertungsskalen. **A:** Der Tremor der HE 1-Patienten wurde als gravierender beurteilt als bei allen drei Vergleichsgruppen. Zudem korrelierte die Beurteilung mit der CFF. **B:** Die Ataxie bei den gesunden, altersgleichen Kontrollprobanden war weniger ausgeprägt als bei den drei Vergleichsgruppen. Des Weiteren zeigte sich auch bei hier eine Korrelation der klinischen Bewertung mit der CFF (aus Butz et al., 2010).

3.3 Gamma-Band

Da die *Gamma*-Band-Aktivität mit Aufmerksamkeitsprozessen in Verbindung gebracht wird und die Beeinträchtigung der Aufmerksamkeit eines der zentralen Symptome der HE ist, stellt sich die Frage, inwieweit auch Veränderungen oszillatorischer Aktivität in diesem Frequenzbereich bei HE-Patienten zu beobachten sind.
In vielen Studien wurde ein enger Zusammenhang zwischen Aufmerksamkeit und oszillatorischer Aktivität sowohl im *Alpha*- als auch im *Gamma*-Band gezeigt. In den zwei im Folgenden vorgestellten, eigenen Arbeiten wurde ebenfalls dieser Zusammenhang eingehender untersucht. Auf eine dieser Arbeiten aufbauend konnte dann überzeugend nachgewiesen werden, dass es im Rahmen der HE zu einer Verlangsamung der *Gamma*-Band-Aktivität kommt.

Aufmerksamkeitsassoziierte oszillatorische Aktivität

Für verschiedene Sinnesmodalitäten konnte gezeigt werden, dass oszillatorische *Alpha*-Band-Aktivität bereits in Erwartung eines Stimulus moduliert wird, so z.B. für den visuellen Kortex (Thut et al., 2006), den auditorischen Kortex (Thorpe et al., 2012) und den primären somatosensorischen Kortex (S1) (Anderson und Ding, 2011; Haegens et al., 2011; Jones et al., 2010). Die dabei auftretende Lateralisierung oszillatorischer Aktivität wurde als *gating* Mechanismus interpretiert (Foxe und Snyder, 2011), d.h. die sensorische Information wird gesteuert. Zudem ist bekannt, dass Schmerz oszillatorische Aktivität in mehreren Frequenzbändern beeinflusst (Hauck et al., 2007, 2008; Ploner et al., 2006a, b). Was allerdings nicht bekannt war, ist, ob der für taktile Reize zuvor beschriebene *gating* Mechanismus auch bei Schmerzreizen zu beobachten ist.
Um diese Frage zu beantworten, wurde in einer eigenen Arbeit ein räumliches Aufmerksamkeitsparadigma entwickelt, bei dem 15 Probanden Schmerzreize auf einer Hand beachten, Schmerzreize auf der anderen Hand aber ignorieren sollten (May et al., 2012). Es zeigte sich, dass Schmerzreize mit einer bilateralen Suppression der *Alpha*-Aktivität einhergingen und dies sowohl für beachtete als auch für nicht-beachtete Reize galt. Die Verschiebung der räumlichen Aufmerksamkeit führte hierbei im Einklang mit vorherigen Ergebnisse zu taktilen Reizen zu einer antizipatorischen Lateralisierung der *Alpha*-Band-Aktivität, d.h. vor dem Stimulus kam es im kontralateralen S1 zu einer Abnahme der *Alpha*-Band-Aktivität. Nach den Schmerzreizen hingegen zeigte sich kontralateral zur beachteten Hand eine stärkere

Verringerung der *Alpha*-Band-Aktivität. Und dies war unabhängig davon, welche der beiden Hände stimuliert wurde (Abb. 11).

Diese Ergebnisse zeigen damit, dass auch für die Verarbeitung von Schmerzreizen angenommen werden kann, dass die Aktivität im *Alpha*-Band eine *gating*-Funktion hat.

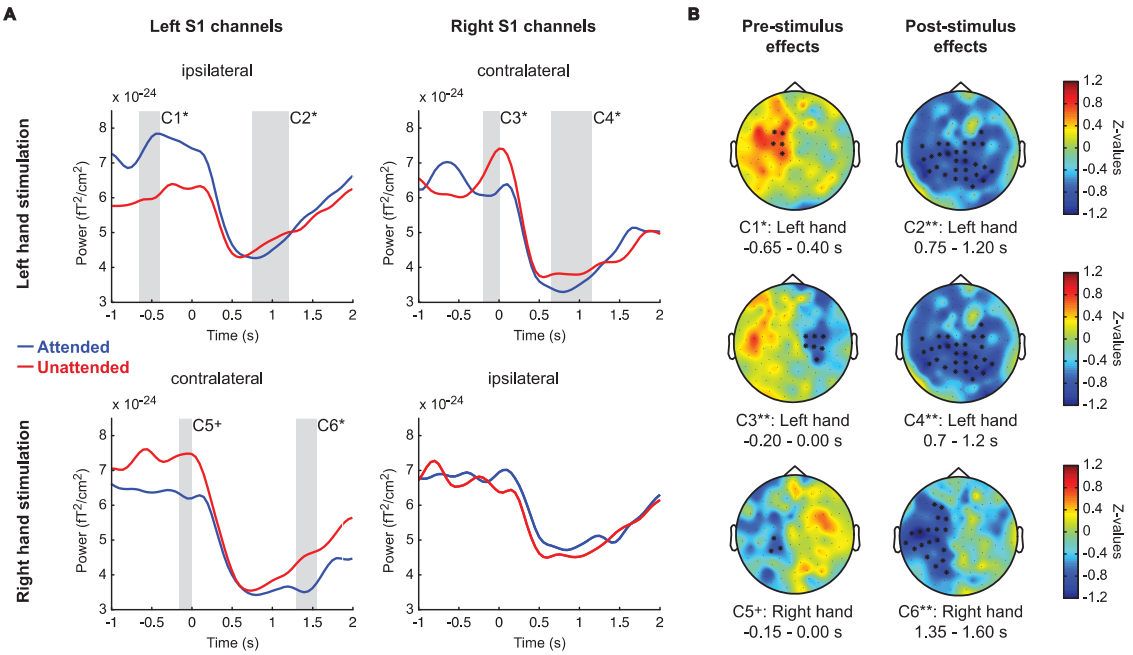

Abbildung 11: Effekte der räumlichen Aufmerksamkeit auf die neuromagnetische Aktivität bei Schmerzreizen. **A:** Über die Gruppe gemittelter Zeitverlauf der *Alpha*-Band-Aktivität über dem linken bzw. rechten primären somatosensorischen Kortex (S1) bei Schmerzstimulation der linken (oben) bzw. rechten Hand (unten). Der Zeitpunkt 0 s markiert den Laserreiz und die grau unterlegten Zeitabschnitte signifikante Unterschiede zwischen beachteten (blau) und nicht-beachteten Reizen (rot). **B:** Topographische Darstellung der Unterschiede beim Vergleich beachtete vs. nicht-beachtete Stimuli im *Alpha*-Band zu den Zeiten entsprechend der Benennung in A (C1-C6). Positive Werte zeigen eine gesteigerte Aktivität bei Aufmerksamkeit an (rot), negative Werte eine verminderte Aktivität bei Aufmerksamkeit (blau) (aus May et al., 2012).

In einer weiteren, eigenen MEG-Studie wurde in einem bimodalen Paradigma untersucht, inwieweit oszillatorische Aktivität in den primären Kortizes durch Aufmerksamkeitsverschiebung moduliert werden kann (Kahlbrock et al., 2012b). Dazu mussten die 16 untersuchten Probanden sich auf einen visuellen Reiz, einen auditorischen Reiz oder diese beiden Reize gleichzeitig konzentrieren und bei einer Veränderung eines Reizes bzw. eines der beiden Reize so schnell wie möglich reagieren. Als visueller Reiz diente ein etablierter Stimulus, von dem bekannt ist, dass dieser starke *Gamma*-Band-Aktivität im visuellen Kortex hervorruft (Hoogenboom et al., 2006).

Auf Verhaltensebene konnten drei verschiedene Aufmerksamkeitsniveaus in Bezug auf den visuellen Stimulus beschrieben werden: Hoch bei alleiniger Aufmerksamkeit auf den visuellen Stimulus, mittel bei Aufmerksamkeit auf beide Reize, d.h. geteilter Aufmerksamkeit, und niedrig bei alleiniger Aufmerksamkeit auf den auditorischen Reiz. Die Analyse der MEG-Daten zeigte, dass in allen drei Konditionen *Gamma*-Band-Aktivität zu beobachten war und dass deren Intensität mit dem Grad der Aufmerksamkeit zunimmt. Somit spiegelte die Amplitude der *Gamma*-Band-Aktivität die Verhaltensdaten wider (Abb. 12).

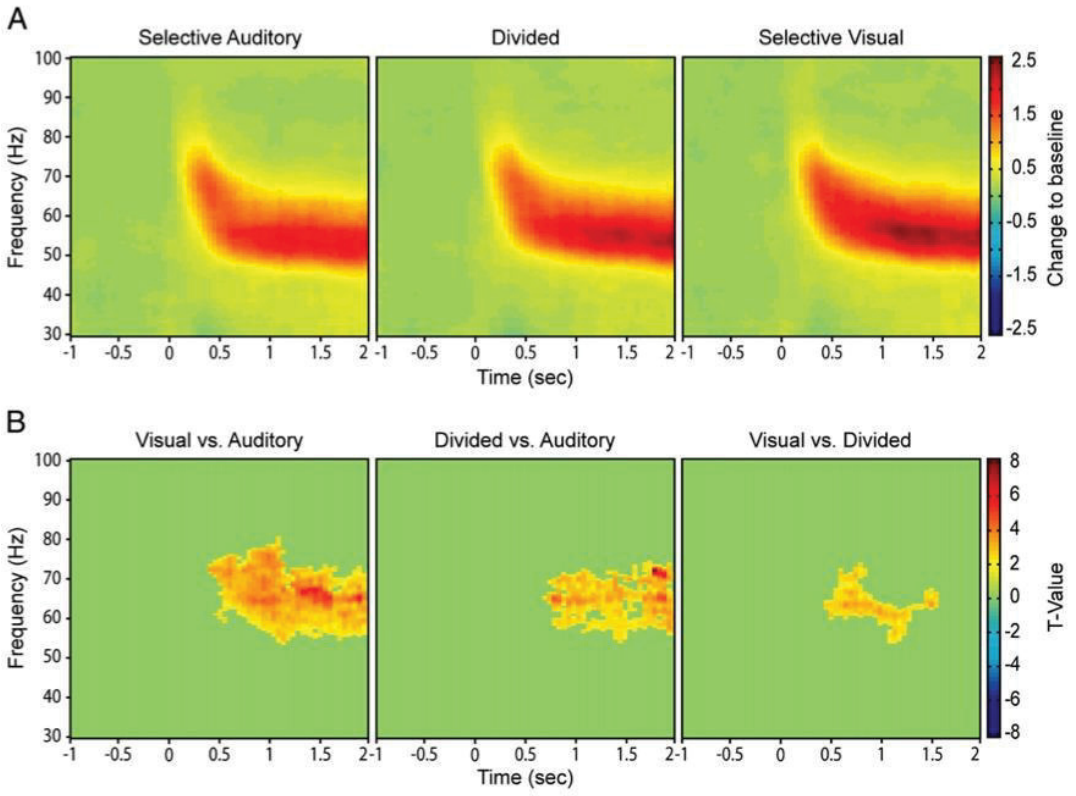

Abbildung 12: Zeit-Frequenz-Spektren der Aktivität im primären visuellen Kortex. **A:** Gezeigt ist die Aktivität im Vergleich zur Baseline-Aktivität für die drei verschiedenen Konditionen, die mit unterschiedlich ausgeprägter visueller Aufmerksamkeit assoziiert sind (selective auditory = niedrig, divided = mittel, selective visual = hoch). In allen drei Bedingungen ist *Gamma*-Band-Aktivität zu sehen, die um bis zu 250 % stärker ist als vor Beginn der Präsentation des Stimulus (0 s). **B:** Statistischer Vergleich der drei Konditionen anhand einer sogenannten *cluster*-Analyse, die in der FieldTrip-Analysesoftware (Oostenveld et al., 2011) implementiert ist. Die *Gamma*-Band-Aktivität war am stärksten in der rein visuellen Kondition, gefolgt von der Kondition mit der geteilten Aufmerksamkeit. In der Bedingung mit alleiniger Aufmerksamkeitsausrichtung auf den auditorischen Reiz war die schwächste *Gamma*-Band-Aktivität im Bereich des visuellen Kortex zu beobachten (aus Kahlbrock et al., 2012b).

Diese Ergebnisse legen einen direkten Zusammenhang zwischen Aufmerksamkeit und *Gamma*-Band-Aktivität in primären visuellen Arealen nahe. Damit ergänzen und erweitern diese Befunde vorherige Arbeiten und unterstreichen den Zusammenhang zwischen oszillatorischer Aktivität und Aufmerksamkeitsprozessen.

Modulation im Rahmen der Hepatischen Enzephalopathie

In einer auf dieser Studie aufbauenden eigenen Arbeit wurde das bimodale Paradigma vereinfacht, um es auch auf HE-Patienten anwenden zu können (Kahlbrock et al., 2012a). Die Hypothese dieser Studie war, dass die im Rahmen der HE auftretenden Aufmerksamkeitsbeeinträchtigungen ein neurophysiologisches Korrelat in Form einer Verlangsamung der *Gamma*-Band-Aktivität haben könnte.

Bei 34 Probanden (8 mHE, 8 HE 0, 8 HE 1, 10 gesunde Kontrollen) wurde die neuromagnetische Aktivität mithilfe der MEG getestet. Die Patienten wurden zudem klinisch und neuropsychometrisch untersucht, was die Erfassung der individuellen CFF beinhaltete. Die Auswertung der MEG-Daten konzentrierte sich auf den visuellen Kortex.

Erwartungsgemäß konnte bei alle Probanden ausgeprägte *Gamma*-Band-Aktivität beobachtet werden (Abb. 13). Die Frequenz der individuell stärksten Aktivität wurde bestimmt. Es zeigte sich, dass die Frequenz der *Gamma*-Band-Aktivität mit zunehmender Schwere der HE abnahm und mit der CFF korrelierte. Zudem korrelierte die CFF auch mit den Verhaltensmassen des Paradigmas, d.h. Reaktionszeit und Fehlerhäufigkeit. Ferner konnte nur bei den Probanden, die eine CFF im physiologischen Bereich zeigten (>39 Hz), eine Modulation der Amplitude der *Gamma*-Band-Aktivität durch Aufmerksamkeit festgestellt werden, bei Probanden mit einer CFF >39 Hz hingegen nicht.

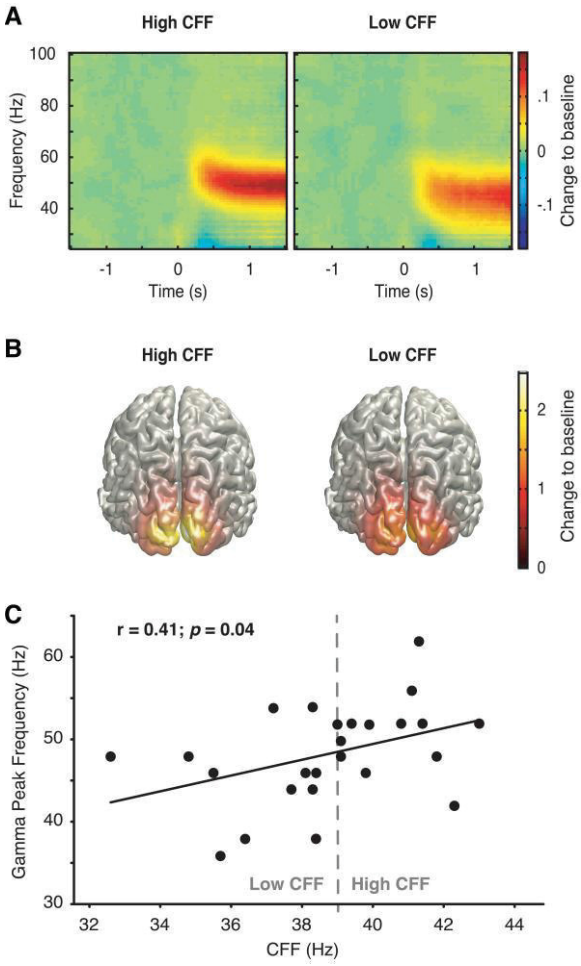

Abbildung 13: *Gamma*-Band-Aktivität im primären visuellen Kortex. ***A*** Sowohl Probanden mit einer CFF im physiologischen Bereich (>39 Hz), als auch im HE-Bereich (<39 Hz) zeigen *Gamma*-Band-Aktivität; ***B:*** Diese kann im primären visuellen Kortex lokalisiert werden; **C:** Die Frequenz der stärksten *Gamma*-Band-Aktivität korreliert mit der CFF, d.h. mit zunehmender Schwere der HE nimmt die Frequenz der *Gamma*-Band-Aktivität ab. (aus Butz et al., 2013; adaptiert aus Kahlbrock et al., 2012a).

Die gezeigte Korrelation zwischen verlangsamter Aktivität im *Gamma*-Band und beeinträchtigter Performanz auf der Verhaltenseben legen einen Zusammenhang zwischen beiden nahe, d.h. die beobachtete Veränderungen könnten das neurophysiologische Korrelat der beobachteten Verhaltensbeeinträchtigung sein. Dies wird zudem durch die enge Korrelation mit der CFF als Parameter für die Schwere der HE unterstützt.

4. Gesamtdiskussion & Ausblick

Die in dieser Arbeit zusammengefassten Studien zeigen, dass im Rahmen der HE die oszillatorische Aktivität sowohl in verschiedenen Frequenzbändern als auch in verschiedenen Subsystemen des Gehirns verlangsamt ist.

So konnte für die *Alpha*-Band-Aktivität (8-12 Hz) eine verlangsamte Spontanaktivität im okzipitalen Kortex gezeigt werden und eine Verlangsamung der stimulus-assoziierten *Alpha*-Band-Aktivität im S1. Ebenso konnten eine Verlangsamung im *Beta*-Band (15-30 Hz) im Rahmen der kortiko-muskulären Kopplungen beschrieben werden sowie eine Verlangsamung der Bewegungsgeschwindigkeit bei Fingerbewegungen. Auch für die höherfrequente Aktivität des *Gamma*-Bandes (30-100 Hz) wurde eine Verlangsamung im primären visuellen Kortex im Rahmen von Aufmerksamkeitsaufgaben demonstriert. Dabei korreliert die CFF eng mit den beschriebenen neurophysiologischen Verlangsamungen und den gezeigten Verhaltensdaten, was die Bedeutung der CFF als wichtigen klinischen Parameter zur Quantifizierung der HE unterstützt.

Die Quintessenz der zusammengefassten Arbeiten lautet, dass die Verlangsamung kortikaler oszillatorischer Aktivität ein zentrales Phänomen bei HE ist, das global auftritt und verschiedene Frequenzbänder und Subsysteme des Gehirns betrifft.

Die potenziellen Mechanismen, die dieser Verlangsamung zugrunde liegen, die wissenschaftliche und klinische Relevanz der Befunde sowie ein Ausblick, welchen Fragen sich zukünftige Untersuchungen widmen sollten, werden im Folgenden diskutiert.

Potenzielle Mechanismen der Verlangsamung der oszillatorischen Aktivität

Auch wenn die Pathophysiologie der HE noch nicht vollständig verstanden ist, so kristallisierten sich doch wichtige Mechanismen in jüngerer Vergangenheit heraus. Die derzeitigen Vorstellungen gehen davon aus, dass es bei der HE zu einem Zusammenspiel einer Vielzahl von pathophysiologischen Mechanismen kommt (Görg et al., 2013; Häussinger und Sies, 2013). Dabei spielen unter anderem Entzündungsprozesse (Coltart et al., 2013) und genetische Faktoren (Romero-Gomez et al., 2010) eine Rolle. Insbesondere wird aber auch der Akkumulation von Neurotoxinen wie z.B. Ammoniak eine entscheidende Rolle zugesprochen, da diese zu einem osmotischen Anschwellen der Astrozyten führen und damit zu deren Minder- bzw. Fehlfunktion. Durch das Auftreten dieses geringgradigen, zerebralen Ödems kommt es zu

oxidativem bzw. nitrosativem Stress (Görg et al., 2013; Lachmann et al., 2013), was in der Folge eine Beeinträchtigung der glio-neuronalen Kommunikation bzw. der neuronalen Funktionen nach sich zieht (Häussinger und Görg, 2010).

Als Resultat werden Veränderungen der synaptischen Plastizität (Wen et al., 2013) und der oszillatorischen Aktivität und Synchronisation angenommen, die dann zu den vielfältigen Symptomen der HE führen. Allerdings ist bislang nicht verstanden, wie diese einzelnen Prozesse im Detail zusammenhängen bzw. sich beeinflussen und die beschriebenen Veränderungen oszillatorischer Aktivität herbeiführen (siehe Übersichtsartikel von Butz et al., 2013).

Im Hinblick auf die Reizweiterleitung im Gehirn sind bereits Veränderungen für mehrere Neurotransmitter für HE beschrieben worden, insbesondere γ-Aminobuttersäure (GABA), Glutamin, Dopamin und Serotonin (Häussinger und Blei, 2007). Von anderen neurologischen Erkrankungen ist bereits bekannt, dass Veränderungen im Neurotransmitterhaushalt und Veränderungen der oszillatorischen Aktivität gemeinsam auftreten; der *Morbus Parkinson* (Brown, 2003; Hammond et al., 2007; Weinberger und Dostrovsky, 2011) und die Schizophrenie seien als Beispiele genannt (Gonzalez-Burgos et al., 2010; Uhlhaas und Singer, 2006). Ausgehend von diesem Wissen scheint auch ein enger Zusammenhang dieser Phänomene bei der HE als sehr wahrscheinlich. Insbesondere das Beispiel der durch GABA-vermittelten Reizleitung bzw. des GABAergen Tonus wurde intensiv als pathogenetischer Faktor der HE diskutiert (Ahboucha, 2011; Cauli et al., 2009; Jones et al., 1984), wobei aber die zugrundeliegenden Mechanismen bislang nicht geklärt sind (Sergeeva, 2013). Dabei wird GABA eine wichtige Funktion bei der Entstehung von oszillatorischer Aktivität zugewiesen, z.B. durch die GABAerge Verschaltung der Interneurone bei der Entstehung der *Alpha*-Band-Aktivität (Lorincz et al., 2009). Zudem konnte in MEG-Arbeiten ein Zusammenhang zwischen *Gamma*-Band-Aktivität und GABA-Konzentrationen in sensomotorischen (Gaetz et al., 2011) und visuellen (Muthukumaraswamy et al., 2009) Arealen demonstriert werden. Diese Ergebnisse für den visuellen Kortex konnten allerdings in neueren Arbeiten nicht repliziert werden (Cousijn et al., 2014). Trotz dieser noch widersprüchlichen Datenlage kann die GABAerge Reizweiterleitung als teilweise beteiligt an der Verlangsamung oszillatorischer Aktivität vermutet werden - zumindest in Bezug auf die beschrieben Verlangsamung Stimulus induzierter visueller *Gamma*-Band-Aktivität (Kahlbrock et

al., 2012a). Weitere Studien sind aber nötig, um einen eventuellen Zusammenhang weitergehend zu belegen.

Ein weiterer wichtiger pathophysiologischer Faktor in der Entstehung der HE ist das geringgradige, zerebrale Ödem, dass relativ eng mit dem erhöhten Blutammoniakspiegel bei Leberzirrhose zusammen hängt (Häussinger und Schliess, 2008). MRT-Studien lieferten Befunde, die für einen erhöhten zerebralen Wassergehalt bei HE-Patienten sprechen (Neeb et al., 2006; Shah et al., 2008). Dieses Ergebnis wurde bis dato allerdings noch nicht repliziert und der Zusammenhang von erhöhtem zerebralen Wassergehalt und verlangsamter oszillatorischer Aktivität ist unklar. Neuere Studien am Tiermodell konnten zeigen, dass auch die Astrozyten an der Entstehung oszillatorischer Aktivität beteiligt sind (Lee et al., 2014). Eine Veränderung der oszillatorischen Aktivität bei HE vermittelt durch die im Rahmen des zerebralen Ödems angeschwollenen Astrozyten ist somit vorstellbar.

Wissenschaftliche Relevanz

Die Veränderung von oszillatorischer Aktivität wurde in vorherigen Studien bereits für eine Vielzahl von neurologischen bzw. psychiatrischen Erkrankungen gezeigt (Hammond et al., 2007; Oswal et al., 2013; Schnitzler und Gross, 2005b; Uhlhaas und Singer, 2006). Bei diesen Erkrankungen treten die Veränderungen jedoch in spezifischen Frequenzbändern bzw. zerebralen Subsystemen auf. So wurden z.B. beim *Morbus Parkinson* primär Veränderungen im motorischen System und im *Beta*-Band bzw. der individuellen Tremorfrequenz beschrieben (Hammond et al., 2007; Hirschmann et al., 2013a; Hirschmann et al., 2013b; Oswal et al., 2013; Schnitzler und Gross, 2005b; Timmermann et al., 2003b). Auch für die als zweites Beispiel genannte Schizophrenie wurden Veränderungen im *Beta*-Band beschrieben. Bei dieser Erkrankung scheinen aber Veränderungen der Aktivität im *Gamma*-Band eine spezifische und herausragende Rolle zu spielen (Uhlhaas und Singer, 2006). Im Gegensatz dazu zeigen die hier zusammengefassten Arbeiten, dass es bei der HE zu einer globalen Verlangsamung kommt, die alle untersuchten Frequenzbänder und Subsysteme des Gehirns einschließt. Diese Verlangsamung findet in enger Parallelität zur Entwicklung der Schwere der HE statt, was mithilfe der CFF gezeigt werden konnte.

Auch wenn die genauen Mechanismen der beschriebenen Verlangsamung noch nicht geklärt sind, so ist ein Unterschied zu anderen pathophysiologischen Veränderungen der oszillatorischen Aktivität offensichtlich. Da die HE eine sich graduell

verschlechternde Erkrankung ist, kann die HE als Modell für die Veränderungen von oszillatorischer Aktivität dienen und dadurch gleichzeitig helfen, den Zusammenhang zwischen oszillatorischer Aktivität und daraus resultierenden Verhaltensänderungen bzw. damit assoziierten Symptomen besser zu verstehen. Dabei reicht das ‚Modell HE' von einer nahezu nicht beeinträchtigten Leistungsfähigkeit bei HE 0- und mHE-Patienten über Patienten mit deutlichen Einschränkungen (HE 1 und HE 2) bis hin zu sehr schwer betroffenen lethargischen und sogar komatösen Patienten. Somit kann unter Berücksichtigung der CFF sehr kleinschrittig verfolgt werden, wie sich die neurophysiologische Aktivität im Verlauf der Verschlechterung der Hirnleistung verändert.

Zugleich kann die HE auch mittelbar helfen, die Funktion von oszillatorischer Aktivität bei Gesunden zu verstehen. So lassen sich Rückschlüsse von den zusammen auftretenden neurophysiologischen Veränderungen und dem beeinträchtigten Verhaltensdaten ziehen. Als Beispiel seien die hier gezeigten Veränderungen im *Gamma*-Band genannt. Für das *Gamma*-Band wird eine zentrale Funktion bei Aufmerksamkeitsprozessen vermutet und ebendiese sind bei HE-Patienten gestört. Somit kann die beobachte Verlangsamung im Rahmen der HE als Evidenz für die Richtigkeit dieser Annahme gesehen werden.

Klinische Relevanz

Die klinische Graduierung der HE ist eine wissenschaftlich und klinisch stark diskutierte Frage. Während es unstrittig ist, dass die recht grobe Klassifikation der HE in vier Stadien nur eine unzureichende Einteilung darstellt (Bajaj et al., 2009; Häussinger et al., 2006; Kircheis et al., 2007), werden eine Reihe weiterer Parameter diskutiert. Zu deren Vorteilen, Nachteilen und klinischen Nutzen gibt es aber noch keinen tragfähigen wissenschaftlichen Konsens. Die hier zusammengefassten Arbeiten argumentieren sowohl jede für sich als auch in ihrer Gesamtheit für die CFF als Parameter zur klinischen Graduierung. So zeigte sich durchweg eine enge Korrelation zwischen der CFF und sowohl den neurophysiologischen Ergebnissen als auch den Verhaltensdaten. Während die Einteilung entsprechend der *West-Haven*-Kriterien zum Teil keine aussagekräftigen Schlüsse zuließ, zeigte die CFF einen Zusammenhang mit der HE. Dies liegt sehr wahrscheinlich an der deutlich feineren Graduierung der HE durch die CFF. Bei der derzeitigen Einteilung in Hz/10 in einem Frequenzbereich von ~25-45 Hz ergibt sich eine bis zu 200-schrittige Einteilung für Patienten mit Leberzirrhose ohne HE bis zu Patienten mit einer ausgeprägten HE 2.

Eine solche sehr viel feinere Einteilung als die übliche Einteilung in lediglich vier bzw. zwei grobe klinische Grade scheint sehr viel angemessener für die HE zu sein. Zudem sprechen die vorgestellten Daten dafür, dass sich mithilfe der CFF auch der Verlauf der HE nachverfolgen lässt, was deren klinischen Nutzen zusätzlich betont bzw. erhöht.

Aus der vorliegenden Arbeit ergibt sich aber auch, dass neben der CFF noch andere Parameter eine sinnvolle Ergänzung der klinischen Beurteilung von HE-Patienten sein können. So kann dies zum einen die dominante Frequenz der Spontanaktivität sein als auch die Erfassung der Bewegungsgeschwindigkeit im Rahmen von schnellsten Fingerbewegungen. Ungeachtet dessen sind weitere Studien nötig, um die Aussagekraft unterschiedlicher Parameter bzw. Kombination von Parametern genauer anhand eines größeren Kollektivs zu evaluieren bzw. zu etablieren.

Zukünftige Untersuchungen

Die hier beschriebenen Arbeiten erweitern wesentlich den bisherigen Kenntnisstand zur oszillatorischen Aktivität bei HE. Zugleich werfen die dargestellten Ergebnisse aber auch neue Fragen auf. Während in den hier zusammengefassten Arbeiten bereits eine sehr umfassende Verlangsamung kortikaler oszillatorischer Aktivität demonstriert werden konnte, muss noch untersucht werden, inwieweit die beobachtete Verlangsamung auch für noch weitere Frequenzbänder und zerebrale Subsysteme gilt, um die postulierte Hypothese einer globalen Verlangsamung weitergehend zu überprüfen.

So wäre z.B. eine naheliegende Fragestellung, inwieweit es auch im auditorischen System zu einer Verlangsamung kommt. Aufgrund der hier gezeigten Ergebnisse kann man z.B. auf der Verhaltensebene eine Beeinträchtigung in Form einer ‚*critical auditory flicker frequency*' erwarten. D.h. dass HE-Patienten in Abhängigkeit von der Schwere der Betroffenheit einen unterbrochenen konstanten Ton bzw. eine Tonreihenfolge erst später als nicht kontinuierlich detektieren können als dies weniger betroffene Patienten oder gesunde Probanden können. Einhergehend damit lässt sich auch eine veränderte oszillatorische Aktivität bei auditorischer Stimulation bei HE-Patienten erwarten.

Genauso ist auch im somatosensorischen System eine beeinträchtigte Verarbeitung kurz aufeinander folgender sensorischer Reize im Sinne einer ‚*critical sensory flicker frequency*' vorstellbar, insbesondere aufgrund des hier beschriebenen verzögerten *rebounds* bei somatosensorischer Stimulation bei HE-Patienten.

Desgleichen stehen bei den verschiedenen Frequenzbändern noch Untersuchungen aus. So ist eine Frage, inwieweit die oszillatorische Aktivität im *Theta*-Band (3-7 Hz) bzw. im *Delta*-Band (1-3 Hz) pathologische Veränderungen aufweist. Zudem fehlen Arbeiten zu den sogenannten hochfrequenten Oszillationen (>100 Hz).
Eine weitere wichtige Fragestellung ist, inwieweit die hier beschriebene Verlangsamung bei anderen neurologischen Erkrankungen zu beobachten ist. In erster Linie würde man eine ähnliche globale Verlangsamung bei anderen Hirnleistungseinschränkungen aufgrund metabolischer Erkrankungen erwarten, so z.B. bei Nierenversagen (Pang et al., 2011).
Eine weitere Forschungsfrage ist die nach dem kausalem Zusammenhang zwischen den beobachten neurophysiologischen Veränderungen und anderen für die HE beschriebenen pathologischen Veränderungen. Hierbei sind insbesondere der veränderte Neurotransmitterhaushalt wie z.B. der veränderte GABA Haushalt, der erhöhte Ammoniakspiegel im Blut und Gehirn bzw. das beschriebene geringgradige zerebrale Ödem von Interesse. Diesen Fragestellungen widmen sich z.T. aktuelle Studien an unserem Institut, so dass in naher Zukunft mit entsprechenden Ergebnissen gerechnet werden darf.

Fazit

Die in dieser Habilitationsschrift zusammengefassten Arbeiten zur kortikalen oszillatorischen Aktivität bei HE konnten einen engen Zusammenhang zwischen der Schwere der HE und der Verlangsamung der kortikalen oszillatorischen Aktivität über Frequenzbänder und zerebrale Subsysteme hinweg zeigen.
In Anbetracht der vielfältigen kognitiven, somatosensorischen und motorischen Symptome bei HE kann diese globale Verlangsamung der oszillatorische Aktivität als zentrales Phänomen im Rahmen der HE gesehen werden, für das eine entscheidende Rolle bei der Entstehung dieser Symptome angenommen werden kann. Oder vereinfacht gesagt, die HE zeichnet sich durch ein global „*verlangsamtes Gehirn*“ aus.

5. Literaturverzeichnis

Adams, R.D., Foley, J.M., 1949. *The neurological changes in the more common types of severe liver disease.* Trans Am Neurol Assoc 74, 217-219.

Ahboucha, S., 2011. *Neurosteroids and hepatic encephalopathy: an update on possible pathophysiologic mechanisms.* Curr Mol Pharmacol 4, 1-13.

Ahonen, A.I., Hämäläinen, M.S., Kajola, M.J., Knuutila, J.E.T., Laine, P.P., Lounasmaa, O.V., Parkkonen, L.T., Simola, J.T., Tesche, C.D., 1993. *122-channel squid instrument for investigating the magnetic signals from the human brain* Physica Scripta T49, 198-205.

Amodio, P., Campagna, F., Olianas, S., Iannizzi, P., Mapelli, D., Penzo, M., Angeli, P., Gatta, A., 2008. *Detection of minimal hepatic encephalopathy: normalization and optimization of the Psychometric Hepatic Encephalopathy Score. A neuropsychological and quantified EEG study.* J Hepatol 49, 346-353.

Amodio, P., Del Piccolo, F., Petteno, E., Mapelli, D., Angeli, P., Iemmolo, R., Muraca, M., Musto, C., Gerunda, G., Rizzo, C., Merkel, C., Gatta, A., 2001. *Prevalence and prognostic value of quantified electroencephalogram (EEG) alterations in cirrhotic patients.* J Hepatol 35, 37-45.

Amodio, P., Gatta, A., 2005. *Neurophysiological investigation of hepatic encephalopathy.* Metab Brain Dis 20, 369-379.

Anderson, K.L., Ding, M., 2011. *Attentional modulation of the somatosensory mu rhythm.* Neuroscience 180, 165-180.

Bajaj, J.S., Wade, J.B., Sanyal, A.J., 2009. *Spectrum of neurocognitive impairment in cirrhosis: Implications for the assessment of hepatic encephalopathy.* Hepatology 50, 2014-2021.

Bass, N.M., Mullen, K.D., Sanyal, A., Poordad, F., Neff, G., Leevy, C.B., Sigal, S., Sheikh, M.Y., Beavers, K., Frederick, T., Teperman, L., Hillebrand, D., Huang, S., Merchant, K., Shaw, A., Bortey, E., Forbes, W.P., 2010. *Rifaximin treatment in hepatic encephalopathy.* N Engl J Med 362, 1071-1081.

Berger, H., 1929. *Über das Elektrenkephalogramm des Menschen.* Archive für Psychiatre und Nervenkrankheiten 87, 527-570.

Bickford, R.G., Butt, H.R., 1955. *Hepatic coma: the electroencephalographic pattern.* J Clin Invest 34, 790-799.

Blauenfeldt, R.A., Olesen, S.S., Hansen, J.B., Graversen, C., Drewes, A.M., 2010. *Abnormal brain processing in hepatic encephalopathy: evidence of cerebral reorganization?* Eur J Gastroenterol Hepatol 22, 1323-1330.

Brenner, M., Butz, M., May, E.S., Kahlbrock, N., Kircheis, G., Häussinger, D., Schnitzler, A., 2015. *Patients with manifest hepatic encephalopathy reveal impaired thermal perception.* Acta Neurol Scand (in press).

Brown, P., 2003. *Oscillatory nature of human basal ganglia activity: relationship to the pathophysiology of Parkinson's disease.* Mov Disord 18, 357-363.

Burkhard, P.R., Delavelle, J., Du Pasquier, R., Spahr, L., 2003. *Chronic parkinsonism associated with cirrhosis: a distinct subset of acquired hepatocerebral degeneration.* Arch Neurol 60, 521-528.

Butterworth, R.F., 2000. *Complications of cirrhosis III. Hepatic encephalopathy.* J Hepatol 32, 171-180.

Butz, M., May, E.S., Gross, J., Timmermann, L., Pollok, B., Kircheis, G., Häussinger, D., Schnitzler, A., 2014a. *The critical flicker frequency reflects the dominant frequency of spontaneous oscillatory brain activity in hepatic encephalopathy.* Clin Neurophysiol 125, S92.

Butz, M., May, E.S., Häussinger, D., Schnitzler, A., 2013. *The slowed brain: cortical oscillatory activity in hepatic encephalopathy.* Arch Biochem Biophys 536, 197-203.

Butz, M., Timmermann, L., Braun, M., Groiss, S.J., Wojtecki, L., Ostrowski, S., Krause, H., Pollok, B., Gross, J., Südmeyer, M., Kircheis, G., Häussinger, D., Schnitzler, A., 2010. *Motor impairment in liver cirrhosis without and with minimal hepatic encephalopathy.* Acta Neurol Scand 122, 27-35.

Butz, M., Timmermann, L., Gross, J., Pollok, B., Südmeyer, M., Kircheis, G., Häussinger, D., Schnitzler, A., 2014b. *Cortical activation associated with asterixis in manifest hepatic encephalopathy.* Acta Neurol Scand 130, 260-267.

Buzsaki, G., 2006. *Rhythms of the Brain*. Oxford University Press, Oxford.

Buzsaki, G., Draguhn, A., 2004. *Neuronal oscillations in cortical networks.* Science 304, 1926-1929.

Cauli, O., Rodrigo, R., Llansola, M., Montoliu, C., Monfort, P., Piedrafita, B., El Mlili, N., Boix, J., Agusti, A., Felipo, V., 2009. *Glutamatergic and gabaergic neurotransmission and neuronal circuits in hepatic encephalopathy.* Metab Brain Dis 24, 69-80.

Chu, N.S., Yang, S.S., 1987. *Somatosensory and brainstem auditory evoked potentials in alcoholic liver disease with and without encephalopathy.* Alcohol 4, 225-230.

Cohen, D., 1968. *Magnetoencephalography: evidence of magnetic fields produced by alpha-rhythm currents.* Science 161, 784-786.

Cohen, D., 1972. *Magnetoencephalography: detection of the brain's electrical activity with a superconducting magnetometer.* Science 175, 664-666.

Coltart, I., Tranah, T.H., Shawcross, D.L., 2013. *Inflammation and hepatic encephalopathy.* Arch Biochem Biophys 536, 189-196.

Cousijn, H., Haegens, S., Wallis, G., Near, J., Stokes, M.G., Harrison, P.J., Nobre, A.C., 2014. *Resting GABA and glutamate concentrations do not predict visual gamma frequency or amplitude.* Proc Natl Acad Sci U S A 111, 9301-9306.

Davies, M.G., Rowan, M.J., Feely, J., 1990. *Flash visual evoked responses in the early encephalopathy of chronic liver disease.* Scand J Gastroenterol 25, 1205-1214.

Davies, M.G., Rowan, M.J., Feely, J., 1991. *EEG and event related potentials in hepatic encephalopathy.* Metab Brain Dis 6, 175-186.

Della Penna, S., Torquati, K., Pizzella, V., Babiloni, C., Franciotti, R., Rossini, P.M., Romani, G.L., 2004. *Temporal dynamics of alpha and beta rhythms in human SI and SII after galvanic median nerve stimulation. A MEG study.* Neuroimage 22, 1438-1446.

Engel, A.K., Fries, P., 2010. *Beta-band oscillations--signalling the status quo?* Curr Opin Neurobiol 20, 156-165.

Ergenoglu, T., Demiralp, T., Bayraktaroglu, Z., Ergen, M., Beydagi, H., Uresin, Y., 2004. *Alpha rhythm of the EEG modulates visual detection performance in humans.* Brain Res Cogn Brain Res 20, 376-383.

Felipo, V., 2013. *Hepatic encephalopathy: effects of liver failure on brain function.* Nat Rev Neurosci 14, 851-858.

Ferenci, P., Lockwood, A., Mullen, K., Tarter, R., Weissenborn, K., Blei, A.T., 2002. *Hepatic encephalopathy--definition, nomenclature, diagnosis, and quantification: final report of the working party at the 11th World Congresses of Gastroenterology, Vienna, 1998.* Hepatology 35, 716-721.

Foley, J.M., Watson, C.W., Adams, R.D., 1950. *Significance of the electroencephalographic changes in hepatic coma.* Trans Am Neurol Assoc 51, 161-165.

Foxe, J.J., Snyder, A.C., 2011. *The Role of Alpha-Band Brain Oscillations as a Sensory Suppression Mechanism during Selective Attention.* Front Psychol 2, 154.

Fries, P., 2009. *Neuronal gamma-band synchronization as a fundamental process in cortical computation.* Annu Rev Neurosci 32, 209-224.

Fries, P., Reynolds, J.H., Rorie, A.E., Desimone, R., 2001. *Modulation of oscillatory neuronal synchronization by selective visual attention.* Science 291, 1560-1563.

Gaetz, W., Edgar, J.C., Wang, D.J., Roberts, T.P., 2011. *Relating MEG measured motor cortical oscillations to resting gamma-aminobutyric acid (GABA) concentration.* Neuroimage 55, 616-621.

Galhenage, S., Almeida, J., Yu, J., Kurtovic, J., Segal, I., Riordan, S.M., 2006. *Modulation of intestinal flora for the treatmentb of hepatic encephalopathy.* In: Häussinger, D., Kircheis, G., Schliess, F. (Hrsg.), Hepatic encephalopathy and nitrogen Metabolism. Springer, Dordrecht, Niederlande, S. 539-550.

Gonzalez-Burgos, G., Hashimoto, T., Lewis, D.A., 2010. *Alterations of cortical GABA neurons and network oscillations in schizophrenia.* Curr Psychiatry Rep 12, 335-344.

Görg, B., Schliess, F., Häussinger, D., 2013. *Osmotic and oxidative/nitrosative stress in ammonia toxicity and hepatic encephalopathy.* Arch Biochem Biophys 536, 158-163.

Gray, C.M., Konig, P., Engel, A.K., Singer, W., 1989. *Oscillatory responses in cat visual cortex exhibit inter-columnar synchronization which reflects global stimulus properties.* Nature 338, 334-337.

Gross, J., Tass, P.A., Salenius, S., Hari, R., Freund, H.J., Schnitzler, A., 2000. *Cortico-muscular synchronization during isometric muscle contraction in humans as revealed by magnetoencephalography.* J Physiol 527 Pt 3, 623-631.

Gruber, T., Muller, M.M., Keil, A., Elbert, T., 1999. *Selective visual-spatial attention alters induced gamma band responses in the human EEG.* Clin Neurophysiol 110, 2074-2085.

Guerit, J.M., Amantini, A., Fischer, C., Kaplan, P.W., Mecarelli, O., Schnitzler, A., Ubiali, E., Amodio, P., 2009. *Neurophysiological investigations of hepatic encephalopathy: ISHEN practice guidelines.* Liver Int 29, 789-796.

Haegens, S., Handel, B.F., Jensen, O., 2011. *Top-down controlled alpha band activity in somatosensory areas determines behavioral performance in a discrimination task.* J Neurosci 31, 5197-5204.

Hämäläinen, M., Hari, R., Ilmoniemi, R.J., Knuutila, J., Lounasmaa, O.V., 1993. *Magnetoencephalography - Theory, Instrumentation, and Application to Noninvasive Studies of the Working Human Brain.* Rev Mod Phys 65, 413-497.

Hammond, C., Bergman, H., Brown, P., 2007. *Pathological synchronization in Parkinson's disease: networks, models and treatments.* Trends Neurosci 30, 357-364.

Hansen, P.C., Kringelbach, M.L., Salmelin, R. (Hrsg.), 2010. *MEG: An Introduction to Methods* 1ed. Oxford University Press, USA, New York.

Hanslmayr, S., Aslan, A., Staudigl, T., Klimesch, W., Herrmann, C.S., Bauml, K.H., 2007. *Prestimulus oscillations predict visual perception performance between and within subjects.* Neuroimage 37, 1465-1473.

Hari, R., 2011. *Magnetoencephalography: Methods and Applications.* In: Schomer, D.L., Lopes da Silva, F.H. (Hrsg.), Niedermeyer's electroencephalography: basic principles, clinical applications, and related fields. Lippincott Williams & Wilkins, Philadelphia, PA, USA, S. 865-900.

Hauck, M., Lorenz, J., Engel, A.K., 2007. *Attention to painful stimulation enhances gamma-band activity and synchronization in human sensorimotor cortex.* J Neurosci 27, 9270-9277.

Hauck, M., Lorenz, J., Engel, A.K., 2008. *Role of synchronized oscillatory brain activity for human pain perception.* Rev Neurosci 19, 441-450.

Häussinger, D., 2004. *[Hepatic encephalopathy: clinical aspects and pathogenesis].* Dtsch Med Wochenschr 129 Suppl 2, S66-67.

Häussinger, D., Blei, A.T., 2007. *Hepatic Encephalopathy.* In: Rodes, J., Benhamou, J.-P., Blei, A.T., Reichen, J., Rizzetto, M. (Hrsg.), The Textbook of Hepatology: From Basic Science to Clinical Practise. Wiley-Blackwell, Oxford, S. 728–760.

Häussinger, D., Cordoba, J., Kircheis, G., Vilstrup, H., Fleig, W.E., Jones, E.A., Schliess, F., Blei, A.T., 2006. *Definition and assessment of low-grade hepatic encephalopathy.* In: Häussinger, D., Kircheis, G., Schliess, F. (Hrsg.), Hepatic encephalopathy and nitrogen Metabolism. Springer, Dordrecht, Niederlande, S. 423-432.

Häussinger, D., Görg, B., 2010. *Interaction of oxidative stress, astrocyte swelling and cerebral ammonia toxicity.* Curr Opin Clin Nutr Metab Care 13, 87-92.

Häussinger, D., Kircheis, G., Fischer, R., Schliess, F., vom Dahl, S., 2000. *Hepatic encephalopathy in chronic liver disease: a clinical manifestation of astrocyte swelling and low-grade cerebral edema?* J Hepatol 32, 1035-1038.

Häussinger, D., Schliess, F., 2008. *Pathogenetic mechanisms of hepatic encephalopathy.* Gut 57, 1156-1165.

Häussinger, D., Sies, H., 2013. *Hepatic encephalopathy: clinical aspects and pathogenetic concept.* Arch Biochem Biophys 536, 97-100.

Hirschmann, J., Hartmann, C.J., Butz, M., Hoogenboom, N., Ozkurt, T.E., Elben, S., Vesper, J., Wojtecki, L., Schnitzler, A., 2013a. *A direct relationship between oscillatory subthalamic nucleus-cortex coupling and rest tremor in Parkinson's disease.* Brain 136, 3659-3670.

Hirschmann, J., Özkurt, T.E., Butz, M., Homburger, M., Elben, S., Hartmann, C.J., Vesper, J., Wojtecki, L., Schnitzler, A., 2013b. *Differential modulation of STN-cortical and cortico-muscular coherence by movement and levodopa in Parkinson's disease.* Neuroimage 68, 203-213.

Hoogenboom, N., Schoffelen, J.M., Oostenveld, R., Fries, P., 2010. *Visually induced gamma-band activity predicts speed of change detection in humans.* Neuroimage 51, 1162-1167.

Hoogenboom, N., Schoffelen, J.M., Oostenveld, R., Parkes, L.M., Fries, P., 2006. *Localizing human visual gamma-band activity in frequency, time and space.* Neuroimage 29, 764-773.

Jensen, O., Mazaheri, A., 2010. *Shaping functional architecture by oscillatory alpha activity: gating by inhibition.* Front Hum Neurosci 4, 186.

Jones, E.A., Schafer, D.F., Ferenci, P., Pappas, S.C., 1984. *The GABA hypothesis of the pathogenesis of hepatic encephalopathy: current status.* Yale J Biol Med 57, 301-316.

Jones, S.R., Kerr, C.E., Wan, Q., Pritchett, D.L., Hamalainen, M., Moore, C.I., 2010. *Cued spatial attention drives functionally relevant modulation of the mu rhythm in primary somatosensory cortex.* J Neurosci 30, 13760-13765.

Kahlbrock, N., Butz, M., May, E.S., Brenner, M., Kircheis, G., Häussinger, D., Schnitzler, A., 2012a. *Lowered frequency and impaired modulation of gamma band oscillations in a bimodal attention task are associated with reduced critical flicker frequency.* Neuroimage 61, 216-227.

Kahlbrock, N., Butz, M., May, E.S., Schnitzler, A., 2012b. *Sustained gamma band synchronization in early visual areas reflects the level of selective attention.* Neuroimage 59, 673-681.

Kaiser, J., Hertrich, I., Ackermann, H., Lutzenberger, W., 2006. *Gamma-band activity over early sensory areas predicts detection of changes in audiovisual speech stimuli.* Neuroimage 30, 1376-1382.

Kircheis, G., Fleig, W.E., Gortelmeyer, R., Grafe, S., Häussinger, D., 2007. *Assessment of low-grade hepatic encephalopathy: a critical analysis.* J Hepatol 47, 642-650.

Kircheis, G., Hilger, N., Häussinger, D., 2014. *Value of critical flicker frequency and psychometric hepatic encephalopathy score in diagnosis of low-grade hepatic encephalopathy.* Gastroenterology 146, 961-969.

Kircheis, G., Wettstein, M., Timmermann, L., Schnitzler, A., Häussinger, D., 2002. *Critical flicker frequency for quantification of low-grade hepatic encephalopathy.* Hepatology 35, 357-366.

Klimesch, W., Sauseng, P., Hanslmayr, S., 2007. *EEG alpha oscillations: the inhibition-timing hypothesis.* Brain Res Rev 53, 63-88.

Kullmann, F., Hollerbach, S., Lock, G., Holstege, A., Dierks, T., Scholmerich, J., 2001. *Brain electrical activity mapping of EEG for the diagnosis of (sub)clinical hepatic encephalopathy in chronic liver disease.* Eur J Gastroenterol Hepatol 13, 513-522.

Lachaux, J.P., George, N., Tallon-Baudry, C., Martinerie, J., Hugueville, L., Minotti, L., Kahane, P., Renault, B., 2005. *The many faces of the gamma band response to complex visual stimuli.* Neuroimage 25, 491-501.

Lachmann, V., Görg, B., Bidmon, H.J., Keitel, V., Häussinger, D., 2013. *Precipitants of hepatic encephalopathy induce rapid astrocyte swelling in an oxidative stress dependent manner.* Arch Biochem Biophys 536, 143-151.

Leavitt, S., Tyler, H.R., 1964. *Studies in Asterixis.* Arch Neurol 10, 360-368.

Lee, H.S., Ghetti, A., Pinto-Duarte, A., Wang, X., Dziewczapolski, G., Galimi, F., Huitron-Resendiz, S., Pina-Crespo, J.C., Roberts, A.J., Verma, I.M., Sejnowski, T.J., Heinemann, S.F., 2014. *Astrocytes contribute to gamma oscillations and recognition memory.* Proc Natl Acad Sci U S A 111, E3343-3352.

Little, S., Brown, P., 2014. *The functional role of beta oscillations in Parkinson's disease.* Parkinsonism Relat Disord 20 Suppl 1, S44-48.

Lorincz, M.L., Kekesi, K.A., Juhasz, G., Crunelli, V., Hughes, S.W., 2009. *Temporal framing of thalamic relay-mode firing by phasic inhibition during the alpha rhythm.* Neuron 63, 683-696.

May, E.S., Butz, M., Kahlbrock, N., Brenner, M., Hoogenboom, N., Kircheis, G., Häussinger, D., Schnitzler, A., 2014. *Hepatic encephalopathy is associated with slowed and delayed stimulus-associated somatosensory alpha activity.* Clin Neurophysiol 125, 2427-2435.

May, E.S., Butz, M., Kahlbrock, N., Hoogenboom, N., Brenner, M., Schnitzler, A., 2012. *Pre- and post-stimulus alpha activity shows differential modulation with spatial attention during the processing of pain.* Neuroimage 62, 1965-1974.

Miltner, W.H., Braun, C., Arnold, M., Witte, H., Taub, E., 1999. *Coherence of gamma-band EEG activity as a basis for associative learning.* Nature 397, 434-436.

Montagnese, S., Amodio, P., Morgan, M.Y., 2004. *Methods for diagnosing hepatic encephalopathy in patients with cirrhosis: a multidimensional approach.* Metab Brain Dis 19, 281-312.

Montagnese, S., Biancardi, A., Schiff, S., Carraro, P., Carla, V., Mannaioni, G., Moroni, F., Tono, N., Angeli, P., Gatta, A., Amodio, P., 2011. *Different biochemical correlates for different neuropsychiatric abnormalities in patients with cirrhosis.* Hepatology 53, 558-566.

Mullen, K., 2006. *Evidence-based medicine and hepatic encephalopathy treatment.* In: Häussinger, D., Kircheis, G., Schliess, F. (Hrsg.), Hepatic encephalopathy and nitrogen Metabolism. Springer, Dordrecht, Niederlande, S. 505-512.

Muthukumaraswamy, S.D., Edden, R.A., Jones, D.K., Swettenham, J.B., Singh, K.D., 2009. *Resting GABA concentration predicts peak gamma frequency and fMRI amplitude in response to visual stimulation in humans.* Proc Natl Acad Sci U S A 106, 8356-8361.

Neeb, H., Zilles, K., Shah, N.J., 2006. *A new method for fast quantitative mapping of absolute water content in vivo.* Neuroimage 31, 1156-1168.

Neuper, C., Pfurtscheller, G., 2001. *Event-related dynamics of cortical rhythms: frequency-specific features and functional correlates.* Int J Psychophysiol 43, 41-58.

Nikouline, V.V., Linkenkaer-Hansen, K., Wikstrom, H., Kesaniemi, M., Antonova, E.V., Ilmoniemi, R.J., Huttunen, J., 2000. *Dynamics of mu-rhythm suppression caused by median nerve stimulation: a magnetoencephalographic study in human subjects.* Neurosci Lett 294, 163-166.

Ogawa, S., Lee, T.M., Kay, A.R., Tank, D.W., 1990. *Brain magnetic resonance imaging with contrast dependent on blood oxygenation.* Proc Natl Acad Sci U S A 87, 9868-9872.

Olesen, S.S., Graversen, C., Hansen, T.M., Blauenfeldt, R.A., Hansen, J.B., Steimle, K., Drewes, A.M., 2011. *Spectral and dynamic electroencephalogram abnormalities are correlated to psychometric test performance in hepatic encephalopathy.* Scand J Gastroenterol 46, 988-996.

Oostenveld, R., Fries, P., Maris, E., Schoffelen, J.M., 2011. *FieldTrip: Open source software for advanced analysis of MEG, EEG, and invasive electrophysiological data.* Comput Intell Neurosci 2011, 156869.

Oswal, A., Brown, P., Litvak, V., 2013. *Synchronized neural oscillations and the pathophysiology of Parkinson's disease.* Curr Opin Neurol 26, 662-670.

Pang, T., Selvitelli, M., Schomer, D.L., Lopes da Silva, F.H., 2011. *Metabolic Disorders and EEG.* In: Schomer, D.L., Lopes da Silva, F.H. (Hrsg.), Niedermeyer's electroencephalography: basic

principles, clinical applications, and related fields. Lippincott Williams & Wilkins, Philadelphia, PA, USA, S. 395-411.

Parsons-Smith, B.G., Summerskill, W.H., Dawson, A.M., Sherlock, S., 1957. *The electroencephalograph in liver disease.* Lancet 273, 867-871.

Pfurtscheller, G., Stancak, A., Jr., Neuper, C., 1996. *Event-related synchronization (ERS) in the alpha band--an electrophysiological correlate of cortical idling: a review.* Int J Psychophysiol 24, 39-46.

Ploner, M., Gross, J., Timmermann, L., Pollok, B., Schnitzler, A., 2006a. *Oscillatory activity reflects the excitability of the human somatosensory system.* Neuroimage 32, 1231-1236.

Ploner, M., Gross, J., Timmermann, L., Pollok, B., Schnitzler, A., 2006b. *Pain suppresses spontaneous brain rhythms.* Cereb Cortex 16, 537-540.

Prakash, R., Mullen, K.D., 2010. *Mechanisms, diagnosis and management of hepatic encephalopathy.* Nat Rev Gastroenterol Hepatol 7, 515-525.

Roelfsema, P.R., Engel, A.K., Konig, P., Singer, W., 1997. *Visuomotor integration is associated with zero time-lag synchronization among cortical areas.* Nature 385, 157-161.

Rolke, R., Baron, R., Maier, C., Tolle, T.R., Treede, R.D., Beyer, A., Binder, A., Birbaumer, N., Birklein, F., Botefur, I.C., Braune, S., Flor, H., Huge, V., Klug, R., Landwehrmeyer, G.B., Magerl, W., Maihofner, C., Rolko, C., Schaub, C., Scherens, A., Sprenger, T., Valet, M., Wasserka, B., 2006. *Quantitative sensory testing in the German Research Network on Neuropathic Pain (DFNS): standardized protocol and reference values.* Pain 123, 231-243.

Romei, V., Brodbeck, V., Michel, C., Amedi, A., Pascual-Leone, A., Thut, G., 2008. *Spontaneous fluctuations in posterior alpha-band EEG activity reflect variability in excitability of human visual areas.* Cereb Cortex 18, 2010-2018.

Romei, V., Gross, J., Thut, G., 2010. *On the role of prestimulus alpha rhythms over occipito-parietal areas in visual input regulation: correlation or causation?* J Neurosci 30, 8692-8697.

Romero-Gomez, M., Cordoba, J., Jover, R., del Olmo, J.A., Ramirez, M., Rey, R., de Madaria, E., Montoliu, C., Nunez, D., Flavia, M., Company, L., Rodrigo, J.M., Felipo, V., 2007. *Value of the critical flicker frequency in patients with minimal hepatic encephalopathy.* Hepatology 45, 879-885.

Romero-Gomez, M., Jover, M., Del Campo, J.A., Royo, J.L., Hoyas, E., Galan, J.J., Montoliu, C., Baccaro, E., Guevara, M., Cordoba, J., Soriano, G., Navarro, J.M., Martinez-Sierra, C., Grande, L., Galindo, A., Mira, E., Manes, S., Ruiz, A., 2010. *Variations in the promoter region of the glutaminase gene and the development of hepatic encephalopathy in patients with cirrhosis: a cohort study.* Ann Intern Med 153, 281-288.

Salenius, S., Schnitzler, A., Salmelin, R., Jousmaki, V., Hari, R., 1997. *Modulation of human cortical rolandic rhythms during natural sensorimotor tasks.* Neuroimage 5, 221-228.

Sauseng, P., Klimesch, W., Gerloff, C., Hummel, F.C., 2009. *Spontaneous locally restricted EEG alpha activity determines cortical excitability in the motor cortex.* Neuropsychologia 47, 284-288.

Saxena, N., Bhatia, M., Joshi, Y.K., Garg, P.K., Dwivedi, S.N., Tandon, R.K., 2002. *Electrophysiological and neuropsychological tests for the diagnosis of subclinical hepatic encephalopathy and prediction of overt encephalopathy.* Liver 22, 190-197.

Schnitzler, A., Butz, M., Gross, J., Kircheis, G., Häussinger, D., Timmermann, L., 2006. *Altered neural oscillations and synchronization: a pathophysiological hallmark of hepatic encephalopathy.* In: Häussinger, D., Kircheis, G., Schliess, F. (Hrsg.), Hepatic encephalopathy and nitrogen Metabolism. Springer, Dordrecht, Niederlande, S. 245-254.

Schnitzler, A., Gross, J., 2005a. *Magnetenzephalographie (MEG).* In: Walter, H. (Hrsg.), *Funktionelle Bildgebung in Psychatrie und Psychotherapie - Methodische Grundlagen und klinische Anwendungen*. Schattauer, Stuttgart, Deutschland, S. 151-161.

Schnitzler, A., Gross, J., 2005b. *Normal and pathological oscillatory communication in the brain.* Nat Rev Neurosci 6, 285-296.

Schnitzler, A., Gross, J., Timmermann, L., 2000. *Synchronised oscillations of the human sensorimotor cortex.* Acta Neurobiol Exp (Wars) 60, 271-287.

Schölmerich, J., 2010. *Leberzirrhose.* In: Riemann, J.F., Fischbach, W., Galle, P.R., Mössner, J. (Hrsg.), *Gastroenterologie - Das Referenzwerk für Klinik und Praxis.* Thieme, Stuttgart, Deutschland, S. 1422-1486.

Schomer, D.L., Lopes da Silva, F.H. (Hrsg.), 2011. *Niedermeyer's electroencephalography: basic principles, clinical applications, and related fields*, 6th ed. Lippincott Williams & Wilkins, Philadelphia, PA, USA.

Senzolo, M., Amodio, P., D'Aloiso, M.C., Fagiuoli, S., Del Piccolo, F., Canova, D., Masier, A., Bassanello, M., Zanus, G., Burra, P., 2005. *Neuropsychological and neurophysiological evaluation in cirrhotic patients with minimal hepatic encephalopathy undergoing liver transplantation.* Transplant Proc 37, 1104-1107.

Sergeeva, O.A., 2013. *GABAergic transmission in hepatic encephalopathy.* Arch Biochem Biophys 536, 122-130.

Shah, N.J., Neeb, H., Kircheis, G., Engels, P., Häussinger, D., Zilles, K., 2008. *Quantitative cerebral water content mapping in hepatic encephalopathy.* Neuroimage 41, 706-717.

Shahani, B.T., Young, R.R., 1976. *Asterixis - a disorder of the neural mechanisms underlying sustained muscle contraction.* In: Shahani, M. (Hrsg.), The motor system: neurophyiology and musle mechanisms. Elsevier, Amsterdam, S. 301-306.

Sharma, P., Sharma, B.C., Puri, V., Sarin, S.K., 2007. *Critical flicker frequency: Diagnostic tool for minimal hepatic encephalopathy.* J Hepatol 47, 67-73.

Shibasaki, H., 1995. *Pathophysiology of negative myoclonus and asterixis.* Adv Neurol 67, 199-209.

Siegel, M., Donner, T.H., Oostenveld, R., Fries, P., Engel, A.K., 2008. *Neuronal synchronization along the dorsal visual pathway reflects the focus of spatial attention.* Neuron 60, 709-719.

Singer, W., 1999. *Neuronal synchrony: a versatile code for the definition of relations?* Neuron 24, 49-65, 111-125.

Spahr, L., Vingerhoets, F., Lazeyras, F., Delavelle, J., DuPasquier, R., Giostra, E., Mentha, G., Terrier, F., Hadengue, A., 2000. *Magnetic resonance imaging and proton spectroscopic alterations correlate with parkinsonian signs in patients with cirrhosis.* Gastroenterology 119, 774-781.

Tallon-Baudry, C., Bertrand, O., Henaff, M.A., Isnard, J., Fischer, C., 2005. *Attention modulates gamma-band oscillations differently in the human lateral occipital cortex and fusiform gyrus.* Cereb Cortex 15, 654-662.

Tallon-Baudry, C., Bertrand, O., Peronnet, F., Pernier, J., 1998. *Induced gamma-band activity during the delay of a visual short-term memory task in humans.* J Neurosci 18, 4244-4254.

Thorpe, S., D'Zmura, M., Srinivasan, R., 2012. *Lateralization of frequency-specific networks for covert spatial attention to auditory stimuli.* Brain Topogr 25, 39-54.

Thut, G., Nietzel, A., Brandt, S.A., Pascual-Leone, A., 2006. *Alpha-band electroencephalographic activity over occipital cortex indexes visuospatial attention bias and predicts visual target detection.* J Neurosci 26, 9494-9502.

Timmermann, L., Butz, M., Gross, J., Kircheis, G., Häussinger, D., Schnitzler, A., 2005. *Neural synchronization in hepatic encephalopathy.* Metab Brain Dis 20, 337-346.

Timmermann, L., Butz, M., Gross, J., Ploner, M., Südmeyer, M., Kircheis, G., Häussinger, D., Schnitzler, A., 2008. *Impaired cerebral oscillatory processing in hepatic encephalopathy.* Clin Neurophysiol 119, 265-272.

Timmermann, L., Gross, J., Butz, M., Kircheis, G., Häussinger, D., Schnitzler, A., 2003a. *Mini-asterixis in hepatic encephalopathy induced by pathologic thalamo-motor-cortical coupling.* Neurology 61, 689-692.

Timmermann, L., Gross, J., Dirks, M., Volkmann, J., Freund, H.J., Schnitzler, A., 2003b. *The cerebral oscillatory network of parkinsonian resting tremor.* Brain 126, 199-212.

Timmermann, L., Gross, J., Kircheis, G., Häussinger, D., Schnitzler, A., 2002. *Cortical origin of mini-asterixis in hepatic encephalopathy.* Neurology 58, 295-298.

Torlot, F.J., McPhail, M.J., Taylor-Robinson, S.D., 2013. *Meta-analysis: the diagnostic accuracy of critical flicker frequency in minimal hepatic encephalopathy.* Aliment Pharmacol Ther 37, 527-536.

Ugawa, Y., Shimpo, T., Mannen, T., 1989. *Physiological analysis of asterixis: silent period locked averaging.* J Neurol Neurosurg Psychiatry 52, 89-93.

Uhlhaas, P.J., Singer, W., 2006. *Neural synchrony in brain disorders: relevance for cognitive dysfunctions and pathophysiology.* Neuron 52, 155-168.

van der Rijt, C.C., Schalm, S.W., De Groot, G.H., De Vlieger, M., 1984. *Objective measurement of hepatic encephalopathy by means of automated EEG analysis.* Electroencephalogr Clin Neurophysiol 57, 423-426.

van Dijk, H., Schoffelen, J.M., Oostenveld, R., Jensen, O., 2008. *Prestimulus oscillatory activity in the alpha band predicts visual discrimination ability.* J Neurosci 28, 1816-1823.

Varela, F., Lachaux, J.P., Rodriguez, E., Martinerie, J., 2001. *The brainweb: phase synchronization and large-scale integration.* Nat Rev Neurosci 2, 229-239.

Vidal, J.R., Chaumon, M., O'Regan, J.K., Tallon-Baudry, C., 2006. *Visual grouping and the focusing of attention induce gamma-band oscillations at different frequencies in human magnetoencephalogram signals.* J Cogn Neurosci 18, 1850-1862.

Weinberger, M., Dostrovsky, J.O., 2011. *A basis for the pathological oscillations in basal ganglia: the crucial role of dopamine.* Neuroreport 22, 151-156.

Weissenborn, K., Ennen, J.C., Schomerus, H., Ruckert, N., Hecker, H., 2001. *Neuropsychological characterization of hepatic encephalopathy.* J Hepatol 34, 768-773.

Wen, S., Schroeter, A., Klöcker, N., 2013. *Synaptic plasticity in hepatic encephalopathy - a molecular perspective.* Arch Biochem Biophys 536, 183-188.

Wettstein, M., Häussinger, D., 2003. *[Hepatic encephalopathy--therapy].* Dtsch Med Wochenschr 128, 2658-2660.

Wettstein, M., Kircheis, G., Häussinger, D., 2003. *[Hepatic encephalopathy--diagnostics].* Dtsch Med Wochenschr 128, 2654-2657.

Wyart, V., Tallon-Baudry, C., 2008. *Neural dissociation between visual awareness and spatial attention.* J Neurosci 28, 2667-2679.

Yang, S.S., Chu, N.S., Liaw, Y.F., 1985. *Somatosensory evoked potentials in hepatic encephalopathy.* Gastroenterology 89, 625-630.

Young, R.R., Shahani, B.T., 1986. *Asterixis: one type of negative myoclonus.* Adv Neurol 43, 137-156.

6. Danksagung

An dieser Stelle möchte ich zunächst meinem langjährigen wissenschaftlichen Mentor Prof. Dr. Alfons Schnitzler danken. Seine ansteckende Begeisterung für die Wissenschaft waren für mich Vorbild und steter Ansporn. Daraus entwickelte sich eine gemeinsame Leidenschaft für die Magnetenzephalographie und die damit verbundenen Möglichkeiten, klinische Fragestellung zu untersuchen, um neurologische Krankheitsbilder besser zu verstehen. Sein Anspruch Wissenschaftler der unterschiedlichen Disziplinen in diesem Bemühen zu vereinen, ist von essentieller Bedeutung für den Erfolg in diesem Forschungsfeld und damit auch für diese Arbeit. Seine fortdauernde Unterstützung meiner Arbeit war und ist eine der wichtigsten Grundlagen.

Auch danken möchte ich den Kooperationspartnern aus der Klinik für Gastroenterologie unter Leitung von Prof. Dr. Dieter Häussinger. Die enge Zusammenarbeit machte viele der Studien dieser Arbeit erst möglich und hier seien stellvertretend Dr. Gerald Kircheis und Herr Diethelm Plate genannt.

Dr. Nina Kahlbrock, Dr. Elisabeth May und Frau Meike Brenner danke ich für die vertrauensvolle und freundschaftliche Zusammenarbeit bei vielen der hier genannten Studien.

Ebenso danken möchte ich allen ehemaligen und jetzigen Kollegen aus der Arbeitsgruppe bzw. dem Institut. Wichtige Wegbegleiter seit meinen wissenschaftlichen Anfangstagen sind Prof. Dr. Joachim Groß, PD Dr. Bettina Pollok und Prof. Dr. Lars Timmermann. Alle drei waren durch ihren Enthusiasmus und ihre Hilfsbereitschaft eine wichtige Stütze.

Auch PD Dr. Martin Südmeyer, Dr. Katja Biermann-Ruben, Dr. Holger Krause und Dr. Lars Wojtecki bin ich durch lange und gute Zusammenarbeit verbunden.

Nicht zuletzt möchte ich meine jetzigen Kollegen nennen und insbesondere diejenigen, die mit mir zusammen in den laufenden Projekten zum Parkinson und der tiefen Hirnstimulation arbeiten: Dr. Jan Hirschmann, Herr Omid Abassi und Frau Lena Storzer.

Abgesehen von diesen vielen beruflichen Verbindungen gilt großer Dank meiner Familie, die mich immer unterstützt hat: Meine Eltern Sita und Dr. iur. Horst Butz, mein Bruder PD Dr. med. Thomas Butz mit seiner Frau Vanessa und ihren drei Töchtern sowie meine Schwiegerfamilie im fernen Shanghai.

Der größte Dank gilt meiner Frau Lan Wang sowie unseren beiden Söhnen Johannes Chongyi Xu und Lukas Anlan Xu!

7. Anhang mit Originalarbeiten

1.)

Brenner M, **Butz M[c],** May ES, Kahlbrock N, Kircheis G, Häussinger D, Schnitzler A, *"Patients with manifest hepatic encephalopathy reveal impaired thermal perception",* Acta Neurol Scand 2015, doi: 10.1111/ane.12376.

Impact-Faktor: 2.4

***** Die beiden ersten Autoren haben einen gleichwertigen Beitrag zur Arbeit geliefert

[c] Korrespondierender Autor

Acta Neurologica Scandinavica

Acta Neurol Scand 2015: 132: 156–163 DOI: 10.1111/ane.12376

ACTA NEUROLOGICA SCANDINAVICA

Patients with manifest hepatic encephalopathy can reveal impaired thermal perception

Brenner M, Butz M, May ES, Kahlbrock N, Kircheis G, Häussinger D, Schnitzler A. Patients with manifest hepatic encephalopathy can reveal impaired thermal perception.
Acta Neurol Scand 2015: 132: 156–163.

Objectives – Previous evoked potential studies indicated central impairments of somatosensory function in patients suffering from hepatic encephalopathy (HE). The aim of this study was to quantify the somatosensory perception in patients with minimal and overt HE. *Materials and Methods* – Forty-two patients with liver cirrhosis and HE up to grade 2 and 12 age-matched healthy controls underwent a comprehensive graduation of HE including the *West Haven criteria*, the critical flicker frequency (CFF), and neuropsychometric testing. Quantitative sensory testing, standardized by the *German Research Network on Neuropathic Pain*, was performed on both hands. *Results* – Pain and mechanical detection thresholds were unchanged in HE. Tests of thermal processing revealed that patients with HE of grade 2 perceive cold at lower temperatures (cold detection threshold) and need a higher temperature difference to distinguish between warm and cold (thermal sensory limen). These impairments correlated with the CFF. A correction for attention deficits by performing partial correlations using neuropsychometric test results canceled these correlations. *Conclusions* – The present findings demonstrate an impairment of temperature perception in HE. The extent of this impairment correlates with HE severity as quantified by the CFF. The attenuation of the correlations after correction for attention deficits suggests a strong role of attention deficits for the impaired thermal perception. Thus, it provides initial evidence for a central impairment of thermal processing in HE due to alterations in high-level processes rather than due to peripheral neuropathic processes, which are a frequent complication in patients with liver cirrhosis.

M. Brenner[1,2], M. Butz[1], E. S. May[1], N. Kahlbrock[1], G. Kircheis[3], D. Häussinger[3], A. Schnitzler[1,2]

[1]Medical Faculty, Institute of Clinical Neuroscience and Medical Psychology, Heinrich-Heine University Düsseldorf, Düsseldorf, Germany; [2]Department of Neurology, Medical Faculty, Heinrich-Heine University Düsseldorf, Düsseldorf, Germany; [3]Department of Gastroenterology, Hepatology and Infectious Disease, Medical Faculty, Heinrich-Heine University Düsseldorf, Düsseldorf, Germany

Key words: attention; critical flicker frequency; liver cirrhosis; minimal hepatic encephalopathy; pain; quantitative sensory testing; somatosensory system; *West Haven criteria*

M. Butz, Medical Faculty, Institute of Clinical Neuroscience and Medical Psychology, Heinrich-Heine University Düsseldorf, Universitätsstraße 1, D-40225 Düsseldorf, Germany
Tel.: +49 81 18415
Fax: +49 81 13015
e-mail: Markus.Butz@hhu.de

Accepted for publication December 16, 2014

Introduction

Hepatic encephalopathy (HE) is a severe and frequent complication of liver cirrhosis (1), which is characterized by a variety of vigilance, motor, and neuropsychological dysfunctions (1, 2). Clinically, HE manifests in the form of a lack of attention, alertness, and cognitive and psychomotor dysfunctions (2) escalating to lethargy, somnolence, and hepatic coma (3). Patients with so-called minimal HE (mHE) do not show clinically overt signs of HE but mild motor and cognitive impairments, which can be revealed by detailed neuropsychometric testing (1, 3, 4). As mHE is not captured by the *West Haven criteria* (4), Kircheis and colleagues proposed the critical flicker frequency (CFF) as parameter for the quantification of low-grade HE (5). To this end, a red light is presented flickering with a frequency of 60 Hz perceived as a constant light. During decrease of the frequency, the CFF is defined as the frequency at which the light is perceived as flickering light for the first time. The CFF decreases with increasing HE severity and enables a fine-scaled assessment of HE severity (6–8). A cutoff frequency of 39 Hz was defined separating

with high diagnostic specifity overt HE patients from healthy controls and patients with cirrhosis but without HE (5, 6, 9).

Previous work using neurophysiological methods indicated impairments of both central and peripheral parts of the somatosensory system in patients with liver cirrhosis and HE. A central impairment was indicated by evoked potential studies of somatosensory processing. Thus, a sequential prolongation of peak and interpeak latencies in combination with a deformation or loss of components of somatosensory evoked potentials could be demonstrated as well as alterations of oscillatory activity with increasing HE severity (10–13). Sensory nerve conduction studies, however, revealed a sensorimotor peripheral neuropathy in >70% of cirrhotic patients (14–16). Moreover, in psychophysiological studies, a reduction of thermal detection thresholds was found in >90% of patients with liver cirrhosis (14, 15), but, importantly, the specific influence of HE was not addressed.

Taken together, evidence exists for somatosensory impairments associated with liver cirrhosis and HE. However, a systematic characterization and quantification of somatosensory perception on a behavioral level in HE is still lacking. To this end, somatosensory perception was quantified in a cohort of patients with HE in different states of disease severity.

Material and methods

Patients

Forty-two patients with liver cirrhosis (for etiologies see Table 1) and 12 age-matched healthy controls underwent a clinical assessment and standard venous blood examination including ammonia levels. These were determined using an enzymatic and photometric test device (Cobas c 701 system Roche/Hitachi, Mannheim, Germany) with catalysis of the glutamate dehydrogenase classifying values above 94 μg/dl as pathological. Cirrhosis was verified by FibroScan or histology. In addition, all patients underwent ultrasound in their normal clinical routine, and no anatomic portosystemic shunt was diagnosed in any of the patients under study. The presence of transjugular intrahepatic portosystemic stent shunt (TIPSS) is depicted in Table 2. Liver function was assessed according to the *Child–Pugh score* (17). By self-report, one patient with mHE and two controls were left handed, the others right handed.

The classification of low-grade HE (5) included the CFF and the results of selected neuropsychometric tests of the Vienna test system (Dr. Schuhfried GmbH, Mödling, Österreich). Participants were classified into five groups: (i) HE0, that is, patients with liver cirrhosis but no signs of HE ($n = 12$); (ii) mHE, that is, patients without clinical signs of HE but with deficits in at least two neuropsychometric tests ($n = 12$); (iii) HE1 ($n = 12$) and (iv) HE2 ($n = 6$) with clinically overt HE, graded according to the *West Haven criteria*; and (v) healthy, age-matched controls ($n = 12$) (see Table 2 for details).

Exclusion criteria were neurological or psychiatric diseases other than HE, spontaneous bacterial peritonitis or gastrointestinal hemorrhage during 1 week before testing, HIV infection, decompensated heart, respiratory or renal failure, decompensated diabetes mellitus, drug abuse, color blindness, current pain medication, and acute or chronic pain conditions. Participants with a history of alcohol addiction had to have remained abstinent for ≥4 weeks. Carpal tunnel syndrome and large fiber neuropathy, that is, sensory neuropathy of A-beta-fibers, were ruled out clinically and by bilateral sensory nerve conduction measures. All patients were interviewed for clinical symptoms of small fiber neuropathy like numbness, tingling, burning, or shooting pain (18) and excluded, if present.

All examinations were completed within 1 day except for three severely affected patients, who

Table 1 Etiologies of cirrhosis as assessed by individual patients' medical history

Group	Hepatitis B	Hepatitis C	Alcoholic steatohepatitis	Non-alcoholic steatohepatitis	Nutritive toxic	Primary sclerosing cholangitis	Primary biliary cirrhosis	Overlap syndrome
HE0 ($n = 12$)	1	7	2	1	0	0	1	0
mHE ($n = 12$)	0	3	3	1	4	1	1	0
HE1 ($n = 12$)	1	5	1	2	0	1	0	2
HE2 ($n = 6$)	0	1	4	0	0	0	1	0
Total ($n = 42$)	2	16	10	4	4	2	3	2

HE, hepatic encephalopathy.
Please note that one patient from the mHE group suffered from both hepatitis C and alcoholic steatohepatitis. Thus, the number of etiologies differs from the number of patients in the mHE group (overlap syndrome, overlap syndrome between primary biliary cirrhosis and autoimmune hepatitis).

Table 2 Clinical data of the different groups under study given as mean values ± standard deviation

Group	*n*	Age (years)	Sex (m/f)	Ammonia (μg/dl)	FibroScan (kPa)	TIPSS (*n*)	CPG A (*n*)	CPG B (*n*)	CPG C (*n*)	CFF (Hz)	Vienna reaction test (ms)	Cognitrone (s)
Control	12	64.7 ± 9.4	7/5	29.6 ± 16.8	5.1 ± 1.7	0	–	–	–	40.4 ± 2.1	500.0 ± 123.2	3.1 ± 0.7
HE0	12	57.9 ± 9.1	8/4	84.5 ± 46.6	37.1 ± 25.5	1	10	2	0	41.5 ± 2.8	490.3 ± 74.9	3.2 ± 0.7
mHE	12	64.7 ± 9.8	6/6	64.3 ± 24.9	40.0 ± 20.5	4	11	1	0	39.7 ± 2.2	574.4 ± 124.5	3.6 ± 0.7
HE1	12	64.2 ± 8.3	6/6	85.3 ± 58.3	45.4 ± 23.6	2	2	6	4	36.5 ± 1.9	667.5 ± 213.4	5.1 ± 1.9
HE2	6	68.0 ± 4.9	3/3	121.3 ± 83.9	39.5 ± 25.3	1	2	2	2	31.0 ± 3.7	1080.6 ± 395.6	10.5 ± 6.4
Total	54	–	30/24	–	–	8	25	11	6	–	–	–

f, female; m, male; *n*, number of participants; CPG A, *Child–Pugh* Group A; CPG B, *Child–Pugh* Group B; CPG C, *Child–Pugh* Group C; TIPSS, transjugular intrahepatic portosystemic stent shunt; CFF, critical flicker frequency; HE, hepatic encephalopathy

Liver cirrhosis was verified by FibroScan, a special ultrasound device measuring liver stiffness, which is related to the histological extent of cirrhosis. Values above 13 kPa indicate the existence of liver cirrhosis. Liver function was estimated according to *Child–Pugh score* (17). As ammonia is understood to be a key factor in the pathogenesis of HE, venous blood ammonia levels were examined. From the administered subtests of the Vienna test system, results of the Vienna reaction test and the Cognitrone subtest are shown.

were studied on two subsequent days. All participants gave written informed consent prior to the study. The study was approved by the local ethics committee and performed in accordance with the Declaration of Helsinki (19).

Critical flicker frequency and neuropsychometric testing

The CFF and a neuropsychological test battery were assessed using the Schuhfried Test System (Dr. Schuhfried GmbH) (5). Each participant performed five computerized test, namely *Cognitrone*, *reaction test*, *visual pursuit test*, *tachistoscopic traffic perception test*, and *motor performance series*. As described by Kircheis et al. (5), for diagnosis of mHE, ≥2 of the psychometric test had to be abnormal in patients showing no signs of clinical manifest HE.

Quantitative sensory testing

Quantitative sensory testing was performed in accordance with the standards of the *German Research Network on Neuropathic Pain* described in detail by Rolke et al. (20). The QST protocol includes 13 parameters. Thermal testing comprises (i) cold and (ii) warm detection thresholds (CDT, WDT), (iii) paradoxical heat sensations (PHS), that is, perception of heat after a cold stimulus during (iv) alternating warm and cold stimulation (thermal sensory limen; TSL), (v) cold, and (vi) heat pain thresholds (CPT, HPT). Mechanical testing consists of (vii) mechanical detection thresholds for touch (MDT) and (viii) vibration (vibration detection threshold; VDT), (ix) mechanical pain thresholds for pinprick (MPT) and (x) blunt pressure (pressure pain threshold; PPT), (xi) mechanical pain sensitivity (MPS), (xii) dynamic mechanical allodynia (ALL), and (xiii) the wind-up ratio (WUR). QST was performed bilaterally in the innervation areas of the *median* and *radial nerves*.

The order of testing of the right and left hand was balanced between participants in all groups.

Importantly, thermal testing was based on reaction time measures in response to temperature changes. A thermode was used for temperature application, and temperature was increased or decreased at a rate of 1°C /s. Detection and pain thresholds were indicated by the participant by a button press and were thus affected by the individual reaction time, which is known to be prolonged with worsening HE severity (5). Therefore, thermal tests were corrected for potential delays. To this end, individual reaction time as assessed by the Vienna reaction test was taken into consideration using the following formula: $(\mathrm{ThTe})°\mathrm{C} = (\mathrm{ThTe_{raw}})°\mathrm{C} - (\mathrm{RT})\mathrm{s} \times 1°\mathrm{C/s}$
[ThTe: result of thermal testing corrected by reaction time; $\mathrm{ThTe_{raw}}$: raw data of thermal testing; RT: median reaction time (Vienna reaction test, individual result)]. The TSL measures the detection of temperature differences and is quantified as the mean of the differences of three warm and cold thresholds. As the reaction time influences the results of the TSL twice, the following formula was used: $(\mathrm{TSL})°\mathrm{C} = (\mathrm{TSL_{raw}})°\mathrm{C} - 2 \times (\mathrm{RT})\mathrm{s} \times 1°\mathrm{C/s}$.

Statistics

Statistical analyses were performed using the SPSS software (IBM, Munich, Germany). *Z*-scores were calculated according to Rolke and colleagues (20): $z = (\mathrm{value_{patient}} - \mathrm{mean_{control}})/\mathrm{standard\ deviation_{control}}$. Results of the control group were used for normalization and group comparisons. Mean group values ± standard deviation of the raw data and mean group values of *z*-scores were calculated. For group

comparisons, unifactorial analyses of variance (ANOVA) were computed for all QST subtests, the CFF, and age. *Post-hoc* tests were performed using the *Scheffé* test, testing differences between HE groups. QST subtests showing significant group effects were retested for differences between groups based on the *Child–Pugh score*. Pearson's correlation coefficients were calculated between all QST subtests and the CFF. Using *Bonferroni–Holm* correction (21), alpha levels of correlations coefficients were corrected for the number of comparisons, that is, 22. Significant correlations were recalculated correcting for attention deficits using partial correlations. Partial correlation measures the degree of association between two variables (here: CFF and CDT/TSL), with the effect of a controlling variable (here: attention) removed. Attention was operationalized using results of the *Cognitrone* subtest. This subtest is specifically designed to quantify sustained attention. Participants check abstract figures for congruency as fast and precisely as possible. 200 tasks of different complexity are presented so that the working speed has to be adapted continuously. One result is a measure of working speed, which is determined by the mean time taken to correctly reject incongruent figures (22). This was used for the correction of attention deficits. Again, Bonferroni–Holm correction was applied to all alpha levels correcting for the number of comparisons, that is, four. Finally, the CFF and QST subtests showing significant differences between HE groups or significant correlations with the CFF were retested for correlations with the plasma ammonia level.

Results

Clinical assessment

No significant age differences were found between the five groups under study ($P = 0.20$). Blood tests of control participants lay within normal range. Blood results of cirrhotic patients were in line with the individual state of liver cirrhosis. Results of the assessment of liver function using the *Child–Pugh score* and venous blood ammonia levels for the different patient groups are given in Table 2.

Tallying previous reports (5–7), a main effect of group was found for the CFF (ANOVA: $P < 0.01$). The CFF was lower in patients with HE2 compared to all other groups (*Scheffé*: HE2 vs HE0: $P < 0.01$; HE2 vs mHE: $P < 0.01$; HE2 vs HE1: $P < 0.01$; HE2 vs controls: $P < 0.01$; for mean CFF values ± standard deviation please see Table 2). In addition, the CFF of patients with HE1 was lower than that from HE0 and control group. For the comparison with the mHE group a trend was observed (*Scheffé*: HE1 vs HE0: $P < 0.01$; HE1 vs mHE: $P = 0.06$; HE1 vs controls: $P = 0.01$). No significant differences were found between HE0, mHE patients, and controls. Correlation analysis between the CFF and the plasma ammonia level showed a trend for a negative correlation, suggesting that a lower CFF was paralleled by an increased ammonia level ($r = -0.27$, $P = 0.051$).

The results of the Vienna reaction test were normally distributed. Mean reaction times are depicted in Table 2. Again, a main effect of group was found (ANOVA: $P < 0.01$). *Post hoc* tests revealed longer reaction times in patients with HE2 compared to all other groups (*Scheffé*: HE2 vs HE0: $P < 0.01$; HE2 vs mHE: $P < 0.01$; HE2 vs HE1: $P < 0.01$; HE2 vs controls: $P < 0.01$).

Quantitative sensory testing

Mean group raw values, standard deviations, and ranges of the QST subtests are depicted in Table 3. Mean group *z*-scores for the right hand are illustrated in Fig. 1. Please note that *z*-scores could not be calculated for PHSs and allodynia (ALL), as the standard deviation in both subtests was zero for the control group. Importantly, all mean group values of the control group lay within the 95% confidence interval of the QST norm data for both male and female participants (20).

Neither group comparisons nor correlations with the CFF revealed effects for WDT, CPT, HPT. MDT for touch and vibration, MPT for pinprick and pressure, MPS, or the WUR. PHS and ALL were observed in very few patients only, disallowing the calculation of group comparisons and correlations. In detail, PHS were found in one patient with HE0, one with mHE, two with HE1, and three with HE2. ALL was observed in one patient with mHE and one with HE2.

For the CDT, ANOVA revealed group differences on both hands (right hand: $P < 0.01$; left hand $P = 0.01$). *Post hoc* tests showed that patients with HE2 had a lower CDT than HE0 and mHE patients and controls on the right hand (Fig. 2A; *Scheffé*: HE2 vs HE0: $P < 0.01$; HE2 vs mHE: $P = 0.02$; HE2 vs HE1: $P = 0.06$; HE2 vs controls: $P < 0.01$) and than patients with HE0 and the control group on the left hand (HE2 vs HE0: $P < 0.05$; HE2 vs mHE: $P = 0.27$; HE2 vs HE1: $P = 0.10$; HE2 vs controls: $P = 0.02$; not depicted). Furthermore, positive correlations

Table 3 Mean values, standard deviation, ranges, and results of ANOVA for the QST tests for the right (re) and left (le) hand

QST parameter		Controls	HE0	mHE	HE1	HE2
Cold detection threshold (°C; $n = 54$) ($P \leq 0.01$)	**ri**	**−1.3 ± 1.0 (−3.85 to 0.02)**	**−1.1 ± 0.8 (−3.14 to 0.29)**	**−2.0 ± 1.5 (−5.01 to 0.20)**	**−2.6 ± 3.8 (−14.96 to 0.58)**	**−6.8 ± 4.7 (−12.94 to 0.86)**
	le	**−1.0 ± 0.8 (−3.22 to 0.15)**	**−1.5 ± 2.3 (−8.31 to 0.38)**	**−2.7 ± 3.9 (−14.51 to 0.30)**	**−1.9 ± 1.9 (−6.92 to 0.04)**	**−5.8 ± 3.3 (−11.96 to 1.36)**
Warm detection threshold (°C; $n = 54$)	ri	3.1 ± 2.3 (0.47 to 9.49)	3.0 ± 2.1 (0.62 to 8.68)	3.9 ± 2.7 (0.77 to 10.15)	4.3 ± 2.6 (1.24 to 10.74)	6.0 ± 3.1 (2.70 to 11.83)
	le	2.8 ± 1.5 (0.64 to 6.66)	2.7 ± 1.4 (0.91 to 5.13)	2.7 ± 2.7 (0.80 to 10.71)	3.3 ± 1.8 (1.64 to 7.12)	5.7 ± 3.9 (1.96 to 13.40)
Thermal sensory limen (°C; $n = 54$) ($P \leq 0.01$)	**ri**	**4.5 ± 2.6 (1.92 to 11.60)**	**5.4 ± 3.6 (1.85 to 12.51)**	**5.5 ± 3.0 (1.93 to 12.11)**	**7.9 ± 6.3 (3.14 to 24.25)**	**17.7 ± 10.0 (5.16 to 36.34)**
	le	**4.5 ± 2.3 (2.44 to 11.69)**	**5.0 ± 2.7 (2.32 to 11.91)**	**5.1 ± 4.9 (2.06 to 20.21)**	**6.8 ± 4.0 (2.67 to 17.50)**	**16.5 ± 9.6 (4.30 to 31.81)**
Cold pain threshold (°C; $n = 54$)	ri	7.3 ± 7.7 (−4.45 to 23.46)	8.8 ± 11.2 (−4.54 to 26.99)	14.3 ± 7.7 (1.06 to 26.32)	10.0 ± 11.7 (−3.92 to 27.85)	10.3 ± 14.9 (−4.23 to 30.34)
	le	2.8 ± 9.3 (−4.35 to 27.26)	10.7 ± 11.9 (−4.50 to 28.96)	17.1 ± 9.6 (2.04 to 29.53)	11.0 ± 13.4 (−4.57 to 31.27)	10.8 ± 14.2 (−4.23 to 30.14)
Heat pain threshold (°C; $n = 54$)	ri	42.6 ± 4.0 (35.17 to 48.38)	44.6 ± 3.6 (37.94 to 49.07)	43.6 ± 3.4 (36.43 to 48.21)	44.5 ± 4.6 (35.65 to 48.65)	43.7 ± 4.5 (36.36 to 48.43)
	le	41.5 ± 4.0 (35.14 to 49.58)	43.8 ± 3.2 (36.11 to 47.87)	41.7 ± 4.1 (35.40 to 47.37)	44.0 ± 3.7 (38.48 to 49.44)	43.8 ± 4.6 (34.76 to 48.37)
Mechanical detection threshold (mN; $n = 52$)	ri	1.3 ± 0.8 (0.18 to 3.03)	1.9 ± 2.0 (0.20 to 3.73)	1.6 ± 0.9 (0.35 to 3.25)	0.9 ± 0.5 (0.22 to 1.87)	2.5 ± 1.1 (0.81 to 4.00)
	le	1.0 ± 0.8 (0.29 to 3.25)	1.4 ± 1.6 (0.23 to 5.66)	1.3 ± 1.5 (0.23 to 6.06)	1.1 ± 0.8 (0.18 to 2.46)	2.7 ± 2.4 (0.35 to 6.50)
Mechanical pain threshold (mN; $n = 53$)	ri	56.5 ± 34.0 (11.31 to 103.97)	72.9 ± 59.7 (14.93 to 207.94)	46.0 ± 33.8 (5.66 to 137.19)	44.2 ± 34.4 (5.66 to 119.43)	86.2 ± 65.6 (12.13 to 181.02)
	le	46.6 ± 46.6 (13.93 to 157.59)	127.3 ± 151.2 (13.93 to 512.00)	63.4 ± 53.3 (5.66 to 168.90)	32.6 ± 26.8 (9.19 to 111.43)	123.1 ± 148.0 (17.15 to 415.87)
Mechanical pain sensitivity ($n = 51$)	ri	1.5 ± 2.0(0.01 to 6.17)	5.1 ± 7.3 (0.00 to 21.22)	2.4 ± 3.5 (0.00 to 11.65)	1.7 ± 1.9 (0.00 to 7.29)	3.7 ± 4.4 (0.09 to 11.17)
	le	1.4 ± 1.8 (0.04 to 5.24)	4.7 ± 6.8 (0.00 to 18.44)	2.1 ± 3.3 (0.00 to 12.26)	2.3 ± 4.1 (0.04 to 15.11)	2.9 ± 2.1 (0.28 to 6.23)
Wind-up ratio ($n = 45$)	ri	4.6 ± 7.5 (1.25 to 28.00)	1.5 ± 0.3 (1.00 to 2.00)	2.0 ± 0.6 (1.14 to 3.31)	3.5 ± 2.4 (1.56 to 9.00)	2.1 ± 0.9 (1.20 to 3.04)
	le	2.3 ± 0.7 (1.05 to 3.25)	1.7 ± 0.5 (1.05 to 3.00)	2.0 ± 0.9 (1.17 to 4.30)	2.3 ± 0.6 (1.00 to 3.20)	1.3 ± 0.3 (1.00 to 1.75)
Vibration detection threshold (/8; $n = 53$)	ri	7.1 ± 0.8 (5.17 to 8.00)	6.9 ± 0.6 (6.00 to 8.00)	6.8 ± 0.6 (5.83 to 8.00)	7.1 ± 0.9 (5.33 to 8.00)	6.8 ± 0.3 (6.33 to 7.17)
	le	7.0 ± 0.8 (5.50 to 8.00)	6.9 ± 0.4 (6.33 to 8.00)	6.8 ± 0.6 (6.00 to 8.00)	7.0 ± 0.8 (6.00 to 8.00)	6.9 ± 0.2 (6.67 to 7.17)
Pressure pain threshold (kPa; $n = 53$)	ri	614.8 ± 213.8 (363 to 1079)	549.8 ± 163.9 (330 to 909)	522.0 ± 163.0 (317 to 824)	618.6 ± 205.1 (196 to 1102)	593.8 ± 129.2 (422 to 814)
	le	622.7 ± 213.4 (330 to 1079)	553.9 ± 166.0 (340 to 818)	507.1 ± 110.4 (281 to 693)	570.3 ± 162.7 (425 to 863)	582.8 ± 175.5 (412 to 860)

HE, hepatic encephalopathy; QST, quantitative sensory testing.

Data of thermal testing were corrected by individual reaction times. Tests showing significant effects in the ANOVA are highlighted in bold and corresponding *P*-values are given. Both the cold detection threshold (CDT) and the thermal sensory limen (TSL) showed a mean effect of group. For the CDT, *post hoc* tests revealed a lower threshold for patients with HE2 compared to HE0, mHE patients, and controls on the right hand and to patients with HE0 and controls on the left hand. For the TSL, patients with HE2 showed a higher threshold than all other groups on both hands.

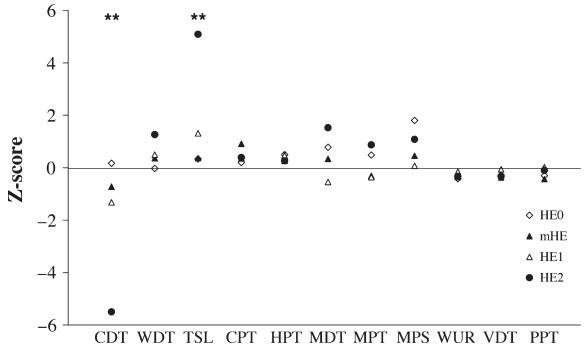

Figure 1. *Z*-score sensory profiles of the right hand data of the QST subtests for the four patient groups normalized to the results of the control group. For the cold detection threshold (CDT) and the thermal sensory limen (TSL), patients with HE2 differ from the control group. WDT, warm detection threshold; CPT, cold pain threshold; HPT, heat pain threshold; MDT, mechanical detection threshold; MPT, mechanical pain threshold; MPS, mechanical pain sensitivity; WUR, wind-up ratio; VDT, vibration detection threshold; PPT, pressure pain threshold; HE, hepatic encephalopathy; QST, quantitative sensory testing.

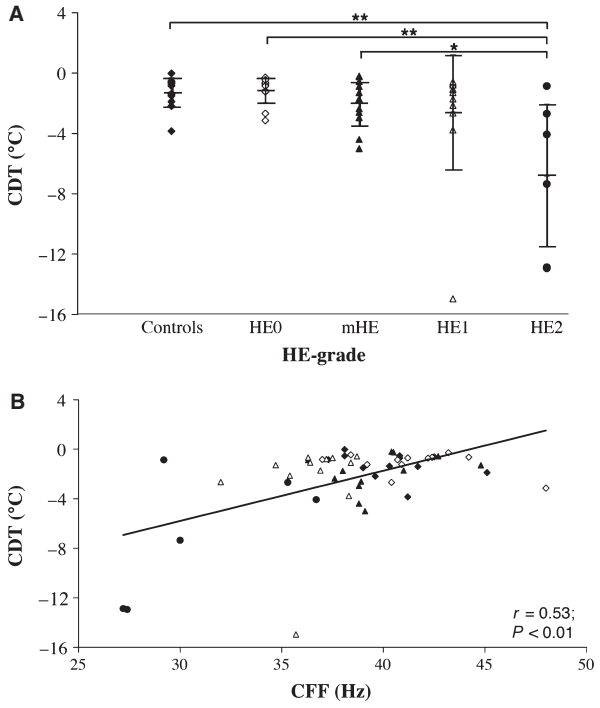

Figure 2. (A) Group effects of the cold detection threshold (CDT) for the right hand. ANOVA revealed a main effect of group ($P < 0.01$). *Post hoc* tests showed lower thresholds for patients with HE2 than for HE0, mHE patients, and controls (**$P < 0.01$; *$P < 0.05$). Thus, patients with HE2 detect cold at lower temperatures. (B) Correlation between the critical flicker frequency (CFF) and the CDT for the right hand. The correlation suggests that the perception of cold worsens with HE severity (symbols according to 2A). HE, hepatic encephalopathy.

between the CDT and the CFF were found for both sides (right hand: $r = 0.53$, $P < 0.01$, Fig. 2B; left hand: $r = 0.41$, $P = 0.04$, not depicted). No correlation was observed between the CDT and the plasma ammonia level.

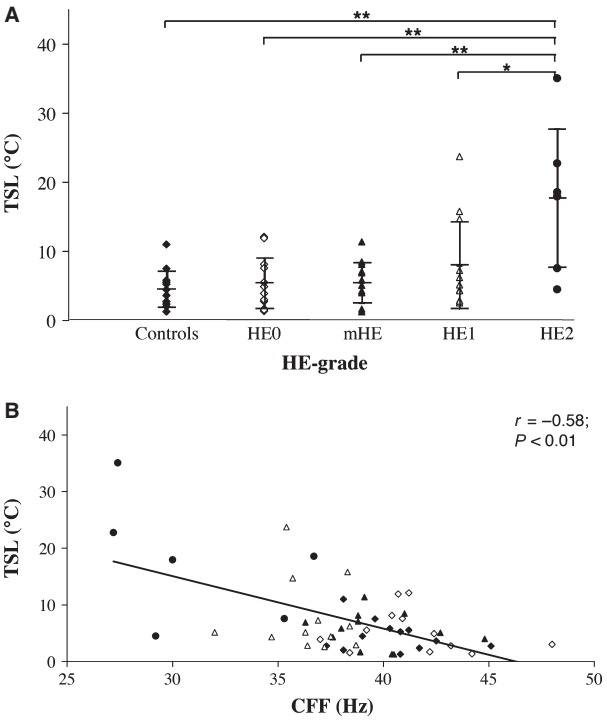

Figure 3. (A) Group differences of the thermal sensory limen (TSL) for the right hand. Group comparisons revealed a main effect (ANOVA: $P < 0.01$); *post hoc* tests showed higher thresholds for patients with HE2 than for all other groups (**$P < 0.01$; *$P < 0.05$). Hence, patients with HE2 need a higher temperature difference to distinguish between warm and cold. (B) Negative correlation between the critical flicker frequency (CFF) and the TSL for the right hand. The correlation indicates that the perception of temperature changes deteriorates with increasing HE severity (symbols according to 3A). HE, hepatic encephalopathy.

For the TSL, main effects of group were observed for both hands (both hands: $P < 0.01$). *Post hoc* tests revealed higher thresholds in patients with HE2 compared to all other groups on both sides (*Scheffé*: right hand: HE2 vs HE0: $P < 0.01$; HE2 vs mHE: $P < 0.01$; HE2 vs HE1: $P = 0.02$; HE2 vs controls: $P < 0.01$, Fig. 3A; left hand: *Scheffé*: HE2 vs HE0: $P < 0.01$; HE2 vs mHE: $P < 0.01$; HE2 vs HE1: $P < 0.01$; HE2 vs controls: $P < 0.01$, not depicted). Moreover, negative correlations were found between the TSL and the CFF (right hand: $r = -0.58$, $P < 0.01$, Fig. 3B; left hand: $r = -0.50$; $P < 0.01$, not depicted). Plasma ammonia levels correlated with the TSL for the right hand ($r = 0.45$, $P < 0.01$) only.

Performing partial correlations, neither the correlations between the CFF and the CDT (right hand: $r = 0.17$, $P = 0.24$; left hand: $r = 0.25$; $P = 0.08$) nor the correlations between the CFF and the TSL (right hand: $r = -0.23$, $P = 0.11$; left hand: $r = -0.31$, $P = 0.12$) remained significant.

Testing for effects between groups according to the *Child–Pugh score* (17) did not reveal effects, neither for the CDT nor the TLS.

Discussion

The aim of the present study was to systematically quantify somatosensory perception in HE. The three main findings are as follows: (i) pain thresholds and MDTs are unchanged in HE, but (ii) the CDT is decreased, and (iii) the TSL is increased in patients with severe HE. The extent of these impairments correlates with the CFF, indicating that the deterioration of thermal perception parallels HE severity.

Specific parts of the somatosensory perception are impaired in HE

While pain and mechanical stimuli remain unchanged, the present results provide first time evidence for an impaired detection of cold and temperature changes in HE. For both tests, it was found that thermal perception worsens with HE severity as quantified by the CFF. However, group effects were shown for patients with HE2 only, suggesting that the observed alterations mainly emerge in advanced stages of the disease.

An interesting question is why of the thermal QST parameters specifically the CDT and the TSL are altered in HE. The preservation of thermal pain detection might be due to the alerting effect of pain (23), evoking a higher state of arousal. In addition, one might speculate that the unchanged warm detection threshold can be explained by fewer warm than cold points on the back of the hand. This has been suggested to make the measure of warm detection less precise than that of cold detection (24). Although the reasons for these specific impairments still need to be resolved in detail, the current findings indicate that the processing of thermal stimuli is more prone to be affected by the pathology of HE than that of pain and mechanical stimuli. Nevertheless, it is desirable to replicate the present results in a larger patient cohort.

Deficits of thermal perception: Central or peripheral impairment?

The potential coexistence of central and peripheral impairments in patients with HE limits the interpretability of the QST results. Both central alterations due to HE and peripheral neuropathy, which is known to be a frequent complication of liver cirrhosis (14–16), might lead to similar alterations of sensory perception.

The comparisons of the different groups under study revealed a deficit of the perception of cold and temperature changes for patients with HE2 only. Nevertheless, correlations with the CFF suggest that the impairment of thermal processing parallels HE severity. To account for confounding effects of attentional dysfunction, a key symptom of HE, partial correlations correcting for effects of attentional deficits were performed. This correction canceled the originally observed correlations with the CFF, indicating that a dysfunction of sustained attention crucially affects the thermal perception of patients with HE. This finding and previous evoked potential studies (10–13) strongly advocate a central impairment.

However, earlier work also identified a peripheral neuropathy as a frequent complication in patients suffering from liver cirrhosis (14–16). Sensory neuropathies impair sensory perception and may lead to corresponding alterations of sensory testing. In the present study, a sensory neuropathy of A-beta-fibers was ruled out by nerve conduction studies. The perception of cold and warmth, however, is mediated by A-delta- and C-fibers, respectively, that is, small nerve fibers. The clinical gold standard for the diagnosis of a small fiber neuropathy is nerve or skin biopsies (18, 24). Due to their invasive character and resulting ethical concerns, these interventions were not performed in the present study. Thus, the presence of a small fiber neuropathy cannot be entirely ruled out. Importantly, participants were questioned and did not report any symptoms of small fiber neuropathy (18). Nevertheless, peripheral nerve pathologies in patients with liver cirrhosis can be asymptomatic (14, 15). In addition, systematic testing revealed that an isolated neuropathy of small nerve fibers causes deficits of thermal perception partly in line with the ones observed here, comprising impairments of the CDT and the TSL (18, 24). In contrast to the present findings in patients with HE, elevated warm detection thresholds were reported additionally (18). Furthermore, an impairment of pain perception could also be expected in the case of small fiber neuropathy as A-delta- and C-fibers also mediate nociception. Again, such a deficit was not observed in the patients studied here arguing against a small fiber neuropathy as cause of the observed deficits in thermal perception, although to the best of our knowledge, this assumption has never been proven by systematic studies. Moreover, CDT and TSL did not depend on liver disease severity as quantified by the *Child–Pugh score*. Assuming that the observed dysfunction of thermal perception is caused by small fiber neuropathy, which is frequent in patients with a

decompensated cirrhosis (14–16), the deficits should have paralleled the severity of liver cirrhosis.

Taken together, both central and peripheral impairments in HE might lead to similar alterations of the QST profile and even add together. However, our results suggest that a central attentional impairment seems more likely to cause the observed deficits in somatosensory processing. Future work on bigger sample sizes is needed to confirm the present findings and to further disentangle the effects of the two factors.

Acknowledgements

The authors thank all participants, patients, and healthy controls, who kindly took part in this study. We are very grateful for the work of Diethelm Plate (Department of Gastroenterology, Hepatology and Infectious Diseases of the University of Düsseldorf) and his unfailing support in patient recruitment and data collection. We thank PD Dr. Bettina Pollok (Institute of Clinical Neuroscience and Medical Psychology, Heinrich-Heine University Düsseldorf) for helpful comments on the data analysis and expert statistical advice.

Conflict of interest and sources of funding statement

G.K. and D.H. belong to a group of patent holders for a bedside device for determination of critical flicker frequency. The authors have no further conflict of interest. This study was supported by the German Research Foundation (SFB 575 and SFB 974). M.Br. was supported by the Integrated Graduate School 575, M.Bu. by a Marie Curie Fellowship of the EU (FP7-PEOPLE-2009-IEF-253965), and N.K. by the German National Academic Foundation. E.M. and N.K. were supported by travel grants from the Integrated Graduate School 575, the Boehringer Ingelheim Foundation (B.I.F.) and the German Academic Exchange Service (DAAD).

References

1. Häussinger D, Blei AT. Hepatic encephalopathy. In: Rodes J, Benhamou J-P, Blei AT, eds. The Textbook of Hepatology: From Basic Science to Clinical Practise. Oxford: Wiley-Blackwell, 2007;pp. 728–760.
2. Weissenborn K, Giewekemeyer K, Heidenreich S, Bokemeyer M, Berding G, Ahl B. Attention, memory, and cognitive function in hepatic encephalopathy. Metab Brain Dis 2005;**20**:359–67.
3. Butterworth RF. Complications of cirrhosis III. Hepatic encephalopathy. J Hepatol 2000;**32**(1 Suppl):171–80.
4. Ferenci P, Lockwood A, Mullen K, Tarter R, Weissenborn K, Blei AT. Hepatic encephalopathy–definition, nomenclature, diagnosis, and quantification: final report of the working party at the 11th World Congresses of Gastroenterology, Vienna, 1998. Hepatology 2002;**35**:716–21.
5. Kircheis G, Wettstein M, Timmermann L, Schnitzler A, Häussinger D. Critical flicker frequency for quantification of low-grade hepatic encephalopathy. Hepatology 2002;**35**:357–66.
6. Sharma P, Sharma BC, Puri V, Sarin SK. Critical flicker frequency: diagnostic tool for minimal hepatic encephalopathy. J Hepatol 2007;**47**:67–73.
7. Romero-Gómez M, Córdoba J, Jover R et al. Value of the critical flicker frequency in patients with minimal hepatic encephalopathy. Hepatology 2007;**45**:879–85.
8. Biecker E, Hausdörfer I, Grünhage F, Strunk H, Sauerbruch T. Critical flicker frequency as a marker of hepatic encephalopathy in patients before and after transjugular intrahepatic portosystemic shunt. Digestion 2011;**83**:24–31.
9. Kircheis G, Hilger N, Häussinger D. Value of critical flicker frequency and psychometric hepatic encephalopathy score in diagnosis of low-grade hepatic encephalopathy. Gastroenterology 2014;**146**:961–9.
10. Blauenfeldt RA, Olesen SS, Hansen JB, Graversen C, Drewes AM. Abnormal brain processing in hepatic encephalopathy: evidence of cerebral reorganization? Eur J Gastroenterol Hepatol 2010;**22**:1323–30.
11. Chu NS, Yang SS, Liaw YF. Evoked potentials in liver diseases. J Gastroenterol Hepatol 1997;**10**:S288–93.
12. Butz M, May ES, Häussinger D, Schnitzler A. The slowed brain: cortical oscillatory activity in hepatic encephalopathy. Arch Biochem Biophys 2013;**536**:197–203.
13. May ES, Butz M, Kahlbrock N et al. Hepatic encephalopathy is associated with slowed and delayed stimulus-associated somatosensory alpha activity. Clin Neurophysiol 2014;**126**:2427–35.
14. Ng K, Lin CS-Y, Murray NMF, Burroughs AK, Bostock H. Conduction and excitability properties of peripheral nerves in end-stage liver disease. Muscle Nerve 2007;**35**:730–8.
15. Chaudhry V, Corse AM, O'Brian R, Cornblath DR, Klein AS, Thuluvath PJ. Autonomic and peripheral (sensorimotor) neuropathy in chronic liver disease: a clinical and electrophysiologic study. Hepatology 1999;**29**:1698–703.
16. Höckerstedt K, Kajaste S, Muuronen A, Raininko R, Seppäläinen AM, Hillbom M. Encephalopathy and neuropathy in end-stage liver disease before and after liver transplantation. J Hepatol 1992;**16**:31–7.
17. Pugh RNH, Murray-Lyon IM, Dawson JL, Pietroni MC, Williams R. Transection of the oesophagus for bleeding oesophageal varices. Br J Surg 1973;**60**:646–9.
18. Scott K, Simmons Z, Kothari MJ. A comparison of quantitative sensory testing with skin biopsy in small fiber neuropathy. J Clin Neuromuscul Dis 2003;**4**:129–32.
19. World Medical Association. Human Experimentation: code of Ethics of the World Medical Association (Declaration of Helsinki). Can Med Assoc J 1964;**91**:619.
20. Rolke R, Baron R, Maier C et al. Quantitative sensory testing in the German Research Network on Neuropathic Pain (DFNS): standardized protocol and reference values. Pain 2006;**123**:231–43.
21. Holm S. A simple sequentially rejective multiple test procedure. Scand J Stat 1979;**6**:65–70.
22. Schuhfried G. Wiener Test System (WINWTS), Mödling. Österreich: Dr. Schuhfried GmbH, 1999.
23. Ploner M, Gross J, Timmermann L, Pollok B, Schnitzler A. Pain suppresses spontaneous brain rhythms. Cereb Cortex 2006;**16**:537–40.
24. Løseth S, Lindal S, Stålberg E, Mellgren SI. Intraepidermal nerve fibre density, quantitative sensory testing and nerve conduction studies in a patient material with symptoms and signs of sensory polyneuropathy. Eur J Neurol 2006;**13**:105–11.

2.)

May ES, **Butz M**[c], Kahlbrock N, Brenner M, Hoogenboom N, Kircheis G, Häussinger D, Schnitzler A,

"*Hepatic encephalopathy is associated with slowed and delayed stimulus-associated somatosensory alpha activity*",

Clin Neurophysiol 2014 Dez, 125(12): 2427–2435.

Impact-Faktor: 3.0

Clinical Neurophysiology 125 (2014) 2427–2435

Contents lists available at ScienceDirect

Clinical Neurophysiology

journal homepage: www.elsevier.com/locate/clinph

Hepatic encephalopathy is associated with slowed and delayed stimulus-associated somatosensory alpha activity

Elisabeth S. May [a], Markus Butz [a,b,*], Nina Kahlbrock [a], Meike Brenner [a], Nienke Hoogenboom [a], Gerald Kircheis [c], Dieter Häussinger [c], Alfons Schnitzler [a]

[a] Heinrich-Heine-University Düsseldorf, Medical Faculty, Institute of Clinical Neuroscience and Medical Psychology, Universitätsstraße 1, D-40225 Düsseldorf, Germany
[b] Sobell Department of Motor Neuroscience and Movement Disorders, UCL Institute of Neurology, Queen Square, London, WC1N 3BG, United Kingdom
[c] Heinrich-Heine-University Düsseldorf, Medical Faculty, Department of Gastroenterology, Hepatology and Infectious Diseases, Universitätsstraße 1, D-40225 Düsseldorf, Germany

ARTICLE INFO

Article history:
Accepted 19 March 2014
Available online 26 March 2014

Keywords:
Critical flicker frequency (CFF)
Cirrhosis
Liver
Magnetoencephalography (MEG)
Oscillations
Slowing

HIGHLIGHTS

- This study for the first time investigated alterations of oscillatory brain activity within the somatosensory system in hepatic encephalopathy (HE).
- The frequency of somatosensory alpha activity was slowed and its stimulation-induced rebound delayed with increasing HE severity.
- These findings provide further evidence for a global slowing of brain activity in HE and a deficit of somatosensory stimulus processing.

ABSTRACT

Objective: Hepatic encephalopathy (HE) is associated with motor symptoms and attentional deficits, which are related to pathologically slowed oscillatory brain activity. Here, potential alterations of oscillatory activity in the somatosensory system were investigated.
Methods: 21 patients with liver cirrhosis and varying HE severity and 7 control subjects received electrical stimulation of the right median nerve while brain activity was recorded using magnetoencephalography (MEG). Oscillatory activity within the contralateral primary somatosensory cortex (S1) and its stimulus-induced modulation were analyzed as a function of disease severity.
Results: Median nerve stimuli evoked an early broadband power increase followed by suppression and then rebound of S1 alpha and beta activity. Increasing HE severity as quantified by the critical flicker frequency (CFF) was associated with a slowing of the alpha peak frequency and a delay of the alpha rebound.
Conclusion: The present results provide the first evidence for a slowing of oscillatory activity in the somatosensory system in HE in combination with a previously unknown deficit of S1 in adjusting activation levels back to baseline.
Significance: These findings advance the understanding of the manifold symptoms of HE by strengthening the theory that disease related slowing of oscillatory brain activity also affects the somatosensory system.

1. Introduction

Hepatic encephalopathy (HE) is a frequent, neuropsychiatric complication of acute and chronic liver diseases comprising a range of different symptoms of varying severity, including vigilance, cognitive, and motor deficits (Butterworth, 2000; Ferenci et al., 2002; Häussinger & Blei, 2007; Prakash and Mullen, 2010). In the extreme, HE can lead to coma and death, but even in its mildest forms without overt clinical symptoms, HE impairs many aspects of daily life functioning (Groeneweg et al., 1998). Its pathophysiological mechanisms, however, are not yet fully understood.

HE has been associated with slowed and pathologically synchronized oscillatory brain activity. Magneto- and

* Corresponding author at: Sobell Department of Motor Neuroscience and Movement Disorders, UCL Institute of Neurology, Queen Square, London, WC1N 3BG, United Kingdom. Tel.: +44 20 3448 8756; fax: +44 20 72789836.
E-mail address: m.butz@ucl.ac.uk (M. Butz).

http://dx.doi.org/10.1016/j.clinph.2014.03.018
1388-2457/

electroencephalography studies (M/EEG) demonstrated a slowing of the peak frequency of spontaneous brain activity (e.g. Kullmann et al., 2001; Montagnese et al., 2007; Amodio et al., 2009) and a stronger but slowed thalamo-cortico-muscular coupling was associated with the tremor-like motor symptoms of HE (Timmermann et al., 2002, 2003, 2008). In addition, a slowing and impaired attentional modulation of stimulus-induced visual activity in the gamma band was shown (Kahlbrock et al., 2012). Importantly, studies using the critical flicker frequency (CFF) as a behavioral oscillatory marker of HE severity (Kircheis et al., 2002; Romero-Gómez et al., 2007; Sharma et al., 2007; Prakash and Mullen, 2010) revealed a correlation between the slowing of oscillatory brain activity and the CFF (Timmermann et al., 2008; Kahlbrock et al., 2012). Hence, slowed oscillatory activity in the brain is thought to be a key pathophysiological mechanism underlying the different clinical symptoms in HE (Timmermann et al., 2005, 2008). Yet, it is not clear to what extent these pathophysiological alterations affect different sub-systems of the brain.

A predominant feature of the somatosensory system is oscillatory alpha activity (8 to 12 Hz), which is thought to reflect the degree of engagement/disengagement of a cortical region (Pfurtscheller et al., 1996; Jensen and Mazaheri, 2010; Foxe and Snyder, 2011). In early somatosensory cortices, the processing of simple somatosensory stimuli is associated with a characteristic modulation of alpha activity: It is initially suppressed, indicating cortical activation, and subsequently rebounds to and often briefly above baseline levels (Salenius et al., 1997; Nikouline et al., 2000; Della Penna et al., 2004). This well-known and reliable response of alpha activity to simple somatosensory stimulation represents a useful measure of oscillatory processing in the somatosensory system.

In HE, the study of somatosensory evoked potentials has already allowed the first insights into somatosensory processing. A prolongation of peak and inter peak latencies in combination with a deformation or loss of somatosensory evoked components was demonstrated, indicating altered and delayed processing of simple somatosensory stimuli (Yang et al., 1985; Chu and Yang, 1987; Davies et al., 1991; Blauenfeldt et al., 2010). However, oscillatory activity and in particular oscillatory alpha activity has not yet been studied in this context.

The objective of the present work was to investigate potential alterations of oscillatory activity in primary somatosensory areas in association with stimulation of the median nerve in HE using MEG. Our findings provide evidence for a slowing of somatosensory alpha activity and a delayed stimulus-associated alpha rebound. Thereby, they extend the notion of slowed oscillatory brain activity as a key phenomenon in HE to the somatosensory system and advance the understanding of the disease.

2. Methods

2.1. Subjects and clinical evaluation

21 patients with liver cirrhosis and 7 healthy controls underwent a clinical assessment and standard blood examination including venous ammonia levels. Single subject characteristics are given in Table 1. Liver cirrhosis was verified by sonography or fibroscan (>13 kPa). The etiology of liver cirrhosis was assessed by examining each patient's medical history. Liver function was estimated according to the Child Pugh score (Pugh et al., 1973).

For the assessment of HE severity, we chose a twofold approach: We used both (i) the well-established *West-Haven*-Criteria (Ferenci et al., 2002) and (ii) the critical flicker frequency (CFF), which was suggested as a new and more fine-graded measure of HE (Kircheis et al., 2002).

Table 1
Participant data. Data are summarized using mean values ± standard deviation (Controls = healthy control subjects, HE0 = cirrhotic patients showing no signs of hepatic encephalopathy (HE), mHE = minimal HE, HE1 = HE grade 1, M = male, F = female, CFF = critical flicker frequency, ALC = alcoholic, PSC = primary sclerosing cholangitis, HCV = hepatitis C virus, CRYP = cryptogenic, PBC = primary biliary cirrhosis).

Group	Subj. No.	Age (y)	Sex	CFF (Hz)	Etiology of cirrhosis	Child Pugh score
Controls	1	52	M	44.6	–	–
	2	58	F	41.4	–	–
	3	61	F	39.4	–	–
	4	74	M	38.1	–	–
	5	67	M	46.2	–	–
	6	48	M	39.3	–	–
	7	69	M	38.1	–	–
	n = 7	**61.3 ± 9.4**		**41.0 ± 3.2**		
HE0	8	50	M	43.2	ALC	A
	9	44	F	43.3	PSC	A
	10	70	F	42.2	HCV	A
	11	76	F	39.6	CRYP	B
	12	62	F	39.6	PBC	A
	13	54	M	42.7	HCV	A
	n= 6	**59.3 ± 12.2**		**41.8 ± 1.7**		
mHE	14	67	F	40.2	HCV	A
	15	63	M	39.3	ALC	A
	16	52	M	39.3	HCV	A
	17	62	M	40.4	CRYP	A
	18	56	M	42.0	HCV	A
	19	77	M	-	HCV	A
	20	53	F	41.3	ALC	B
	21	43	F	37.1	ALC	C
	n = 8	**59.1 ± 10.4**		**39.9 ± 1.6**		
HE1	22	57	M	38.0	ALC	B
	23	58	M	36.7	HCV	C
	24	45	M	36.2	PSC	B
	25	61	M	35.5	HCV	C
	26	70	M	37.6	ALC	A
	27	63	M	36.7	ALC	A
	28	47	M	36.2	ALC	B
	n = 7	**57.3 ± 8.8**		**36.7 ± 0.9**		

For the grading according to the *West-Haven*-Criteria, patients were classified into three clinical groups of HE severity on the basis of computer psychometric test results and mental state as defined in Ferenci et al. (2002). A detailed description can be found elsewhere (Kircheis et al., 2002; Timmermann et al., 2003). A battery of 5 computerized neuropsychological tests from the Vienna Test System (Dr. Schuhfried GmbH, Mödling, Austria) (Vienna test system, WINWTS, Version 4.50, 1999) with 22 evaluable neurophysiological parameters directed to cognition, emotion, and behavior was used. Test results were considered abnormal, when they were outside 1 standard deviation from the mean of a large age-matched control population (Vienna test system, WINWTS, Version 4.50, 1999). The grading included an estimate of the clinical degree of consciousness by an expert clinical doctor. Patients without evidence for manifest HE according to their mental state were defined as having *HE0* when $\leqslant 1$ of the computer psychometric test results were abnormal (n = 6) and as having *mHE* (minimal HE) when $\geqslant 2$ were abnormal (n = 8). Patients were classified as having *HE1* when their mental state showed symptoms of manifest HE in line with grade 1 according to the *West-Haven*-Criteria (n = 7). The fourth group comprised age-matched, healthy control subjects, i.e. *controls* (n = 7).

For the grading using the CFF, CFF was determined as previously described (Kircheis et al., 2002). One participant (subject 19) had reduced eyesight of only 25% in one eye, not allowing for a valid CFF measurement. The CFF of this subject was therefore not used for further analysis.

Exclusion criteria were neurological and psychiatric diseases other than HE, psychoactive drug use, a history of severe HE (HE3 or HE4), acute gastrointestinal hemorrhage or spontaneous bacterial peritonitis during the last 7 days, diabetes of a severity requiring medical treatment, and significant other non-hepatic diseases. Patients with a history of alcohol abuse had to have remained abstinent for at least 4 weeks, which was confirmed by blood alcohol level and carbohydrate deficient transferrin (CDT). To control for impairments of peripheral nerve function, sensory neuropathy of the median and radial nerves was ruled out clinically and by bilateral sensory nerve conduction measures. In addition, structural magnetic resonance images (MRIs) obtained for co-registration with MEG data (see Section 2.2) were visually inspected for obvious brain atrophy or other brain tissue alterations. If present, the subject was not included in the study.

The study was approved by the local ethics committee (study No. 2895) of the Düsseldorf University Hospital and conducted in accordance with the Declaration of Helsinki. All subjects participated in the study after having given their written informed consent.

2.2. Paradigm and MEG recording

While subjects sat in a comfortable chair within a magnetically and acoustically shielded room, non-painful 0.3 ms pulses of electric current were applied to the right median nerve at the wrist. Stimulation intensity was individually adjusted to be slightly above motor threshold and to elicit a small thumb twitch (mean amplitude ± SD: 4.3 ± 1.3 mA). A total of 300 stimuli were administered with a constant inter-stimulus interval of 2 s. Subjects passively perceived the stimuli with open eyes and no other task. Simultaneously, neuromagnetic brain activity was measured with a 306-channel MEG system (Elekta Oy, Helsinki, Finland). Individual high-resolution standard T1-weighted structural MRIs were obtained with a 3 T Siemens Magnetom MRI scanner (Munich/Erlangen, Germany) for later co-registration of MEG and MRI data. For three participants (subjects 11, 27, and 28), no MRI could be obtained. Instead, the template MRI of the SPM2 Matlab toolbox (Litvak et al., 2011) was used.

2.3. MEG data analysis

Data were analyzed using Matlab 7.1 (Mathworks, Natick, MA, USA), the open-source Matlab toolbox FieldTrip (Oostenveld et al., 2011), and IBM SPSS Statistics 20 (IBM Corporation, Somers, USA).

2.3.1. Preprocessing

MEG data were divided into non-overlapping epochs of interest surrounding each median nerve stimulus using data of the 204 planar gradiometers only. For each epoch, power line noise was removed. After visual inspection, epochs and sensors with high variance (containing e.g. muscle artifacts or sensor jumps) were removed from the data.

2.3.2. Virtual sensor analysis

Analysis of oscillatory brain activity was performed in source space using a linearly constrained minimum variance (LCMV) beamformer (Van Veen et al., 1997) in two steps. First, the strongest source of evoked responses to median nerve stimulation was localized for each individual. Second, this source was used as a virtual sensor location and single-trial time courses within the source were estimated. The obtained source waveforms were then used for the subsequent analysis.

To determine the source of evoked responses to median nerve stimulation, covariance matrices across all MEG sensors were calculated from the average across all trials after filtering the preprocessed data between 3 and 50 Hz. This was done separately for a pre-stimulus baseline (−0.5 to −0.3 s) and a post-stimulus interval (0 to 0.2 s) including strongest stimulus-evoked responses. From these covariance matrices, neural activity during both intervals was localized. The leadfield matrix was computed for grid points in a realistically shaped single-shell volume conduction model, derived from the individual structural MRIs (Nolte, 2003). To this end, a regular 3D 5-mm grid in the Montreal Neurological Institute (MNI) template brain was created, and each subject's structural MRI was linearly warped onto this template. The inverse of this warp was applied to the template grid, resulting in individual grids based on the individual subject's volume conduction model. For each grid point, the ratio of post-stimulus to pre-stimulus activity was computed. The grid point showing the highest activity-ratio in response to median nerve stimulation was selected as the virtual sensor location. The brain areas closest to the virtual sensor location were identified using the AFNI atlas (http://afni.nimh.nih.gov/afni).

Subsequently, single trial source waveforms at the individual virtual sensor location were reconstructed for each subject. To this end, covariance matrices were computed for the averaged, non-overlapping trials from −1 to 1 s with respect to stimulus onset after filtering (3 to 50 Hz) and baseline-correction (−0.5 to −0.3 s). From these covariance matrices, a spatial filter was created. Single trial sensor data of ±2.5 s length were projected through this filter to obtain the source waveforms.

2.3.3. Time–frequency analysis

Time–frequency representations (TFRs) of power were estimated using the fast Fourier transform (FFT). For each trial, an adaptive time window of 4 cycles length was shifted in 10 ms time steps across the complete source waveform of each trial. After applying a Hanning taper, power was estimated for frequencies between 1 and 25 Hz in steps of 1 Hz. Then, TFRs were averaged across trials for each subject. Subsequent analysis focused on the time interval from 0 to 2 s, comprising the time period from the onset of the stimulus to the onset of the subsequent stimulus, i.e. one complete stimulus cycle. To normalize for inter-individual differences, power values were expressed relative to the mean power

across the complete time interval. As a control analysis for potential effects in higher frequencies, a corresponding analysis was performed for frequencies up to 100 Hz.

2.3.4. Alpha peak frequencies

To obtain estimates of the individual peak frequency of somatosensory alpha activity, segments of data from 0 to 2 s were extracted from the source waveforms and multiplied with a Hanning taper prior to applying a fast Fourier transform (FFT). Power spectra were computed between 1 and 25 Hz and the frequency between 6 and 14 Hz with the highest power was determined for each subject.

To confirm that the determined alpha peak frequencies were not mainly driven by early stimulus-evoked activity, alpha peak frequency determination was repeated on a time interval from 0.7 to 2 s.

2.3.5. Time of maximal alpha rebound

To quantify the time of the maximal rebound of alpha activity to or above baseline levels after its initial stimulus-induced suppression, the time course of alpha activity was estimated for each subject. Power obtained from TFRs was averaged across a 4 Hz frequency band encompassing the individual alpha peak frequency ±2 Hz. Then, the time point of alpha rebound defined as the maximum alpha power during the period of 0.7 to 1.8 s after stimulus onset was extracted. The time window was chosen to start after the initial alpha suppression and end 0.2 s prior to the subsequent stimulus to avoid an intermixture of alpha activity estimates with stimulus-induced alpha increases from the next stimulus.

2.4. Statistics

Differences between TFRs from the four subject groups (controls, HE0, mHE, and HE1) were examined by statistical group comparisons. For every comparison, independent sample *t*-tests were calculated for each time–frequency point between 5 and 25 Hz. Statistical inference was based on a non-parametric cluster-based randomization test (Nichols and Holmes, 2002; Maris and Oostenveld, 2007). This approach corrects for multiple comparisons due to a multitude of time and frequency points and reveals time–frequency clusters showing significant differences between two groups.

Differences of stimulation intensities for median nerve stimulation, alpha peak frequencies, and the time of alpha rebound between the different subject groups were analyzed using analysis of variance (ANOVA). Post-hoc tests were performed using one-sided independent samples *t*-tests, applying Bonferroni–Holm correction (13) to all *p*-values to correct for multiple comparisons. To test for relationships between stimulation intensities, blood levels of ammonia, the alpha peak frequency, the time of alpha rebound, the CFF, and Child Pugh ranks (four ranks: healthy liver function, Child Pugh score A, B, or C), partial one-sided Pearson's correlation coefficients were calculated, correcting for effects of age. Lastly, we compared the alpha peak frequency and the time of alpha rebound between patients with alcohol-induced cirrhosis and cirrhosis of other origin using independent samples *t*-tests.

3. Results

Stimulation intensities used for median nerve stimulation (Table 2) were not significantly different between the four groups ($F_{(3,24)} = 2.97$, $p = 0.052$). In addition, no significant correlation with the CFF was found ($r = 0.33$, $p = 0.052$), indicating that individually adjusted stimulation intensities did not depend on HE disease severity.

3.1. Localization of evoked responses for virtual sensor analysis

For each subject, the strongest source of evoked responses during the first 0.2 s after median nerve stimulation was localized for placement of a virtual sensor. Localizations were consistent with the primary somatosensory cortex (S1) contralateral to the stimulated hand. Individual coordinates of the virtual sensor locations and the labels of the closest brain areas are given in Table 2. The average localization of evoked responses across all 28 subjects is illustrated in Fig. 1.

3.2. Time–frequency analysis

In all four groups under study, median nerve stimuli elicited an early broadband power increase reflecting the evoked response, followed by a suppression of activity in alpha and beta frequency bands and a rebound to or above baseline levels (Fig. 2A). Cluster-based randomization statistics revealed a cluster of increased alpha activity from 5 to 13 Hz and 0.9 to 1.9 s for the comparison between HE1 patients and healthy controls (Fig. 2B, $p < 0.01$), in line with a stronger and/or delayed rebound of alpha activity in patients with overt symptoms of HE. No other group differences were observed, so that the further analyses were focused on oscillatory activity in the alpha band.

Importantly, a control time–frequency analysis for frequencies up to 100 Hz did not reveal additional stimulus-induced modulations in higher frequencies. Cluster-based randomization statistics confirmed the significant cluster of increased alpha activity for HE1 patients compared to healthy controls for this broader frequency range ($p = 0.04$; data not shown).

3.3. Alpha peak frequencies

To examine a possible slowing of S1 alpha activity, individual alpha peak frequencies were determined (Table 2). An ANOVA revealed a significant effect of the subject group (Fig. 3A, left panel; $F_{(3,24)} = 3.83$, $p = 0.02$). Post-hoc tests showed lower alpha peak frequencies for mHE patients compared to controls ($p = 0.03$), but no other significant comparisons (HE1 patients vs. controls: $p = 0.06$, all other comparisons: $p > 0.1$). Correlations between the CFF and the alpha peak frequency revealed a positive relationship between the two measures, across all subjects (Fig. 3A, middle panel; $r = 0.44$, $p = 0.01$) as well as for patients only (Fig. 3A, right panel; $r = 0.50$, $p = 0.02$). Thus, the individual alpha peak frequency was slowed with increasing HE severity.

To confirm that the obtained alpha peak frequencies were not mainly driven by early stimulus-induced alpha activity increases, alpha peak frequency analysis was repeated based on the time interval from 0.7 to 2 s covering the alpha rebound. Again, the same pattern of results was found (ANOVA: $F_{(3,24)} = 3.33$, $p = 0.04$, post hoc test controls vs. mHE: $p < 0.05$, post hoc test controls vs. HE1: $p = 0.06$, all other post hoc tests $p > 0.1$; correlation CFF vs. alpha peak frequency: all subjects: $r = 0.38$, $p = 0.03$, patients only: $r = 0.49$, $p = 0.02$). For subsequent analyses, peak frequencies determined from the complete period were used.

Relationships between the alpha peak frequency and the blood level of ammonia were not significant, for either all subjects ($r = -0.26$, $p = 0.098$) or for patients only ($r = -0.06$, $p > 0.1$). However, the slowing of the alpha peak frequency was related to increasing overall liver dysfunction as measured by the Child Pugh score, both for all subjects ($r = -0.55$, $p < 0.01$) and for patients only ($r = -0.44$, $p = 0.03$). Importantly, alpha peak frequencies were found not to be different between patients with alcohol-induced cirrhosis and patients with cirrhosis of other origin ($p = 0.32$).

Table 2
MEG-related data. Data are summarized using mean values ± standard deviation (Controls = healthy control subjects, HE0 = cirrhotic patients showing no signs of hepatic encephalopathy (HE), mHE = minimal HE, HE1 = HE grade 1, MNI = Montreal Neurological Institute, BA = Brodmann Area).

Group	Subj. No.	Stimulation intensity (mA)	Alpha peak frequency (Hz)	Time of maximal alpha rebound (s)	Virtual sensor location			
					MNI coordinates			Closest label(s)
					x	*y*	*z*	
Controls	1	3.2	14	0.9	−3.7	1.9	8.5	Postcentral gyrus, BA 3
	2	4.5	13	1.8	−3.7	−0.3	8.5	Postcentral gyrus, BA 3
	3	5.0	13	1.0	−3.2	−0.0	8.6	Precentral gyrus
	4	7.0	11	1.8	−3.8	−0.6	9.3	Postcentral gyrus, BA 3
	5	7.5	9	0.9	−4.6	0.3	8.9	Postcentral gyrus
	6	4.0	9	1.0	−3.3	0.2	9.0	Precentral gyrus
	7	3.0	11	0.9	−4.5	−0.2	8.8	Postcentral gyrus
	n = 7	**4.9 ± 1.8**	**11.4 ± 2.0**	**1.2 ± 0.4**				
HE0	8	4.5	13	1.1	−3.9	0.9	8.9	Postcentral gyrus, BA 3
	9	3.2	10	0.8	−4.3	−0.5	8.1	Postcentral gyrus
	10	3.4	14	0.9	−4.5	0.3	9.4	Precentral gyrus
	11	2.7	9	1.8	−5.0	0.2	8.8	Precentral gyrus
	12	3.2	7	1.4	−3.7	−0.9	7.8	Postcentral gyrus
	13	3.5	12	1.1	−3.5	−0.6	9.7	No label found
	n = 6	**3.4 ± 0.6**	**10.8 ± 2.6**	**1.2 ± 0.4**				
mHE	14	5.0	9	1.8	−4.3	−0.4	8.1	Postcentral gyrus
	15	4.6	8	1.7	−4.3	−0.9	6.9	Inferior parietal lobule
	16	5.0	8	1.7	−3.9	0.1	7.6	Postcentral gyrus, BA 3
	17	4.5	9	1.5	−5.0	1.3	8.7	Postcentral gyrus
	18	5.5	10	1.1	−3.6	−0.4	9.6	Postcentral gyrus, BA 3/1
	19	4.4	11	1.6	−4.2	0.5	9.0	Precentral gyrus
	20	6.5	7	1.3	−3.8	0.5	8.3	Postcentral gyrus, BA 3
	21	3.4	6	1.1	−3.8	0.3	8.9	Postcentral gyrus, BA 3
	n = 8	**4.9 ± 0.9**	**8.5 ± 1.6**	**1.5 ± 0.3**				
HE1	22	4.0	8	1.8	−4.7	−0.0	8.3	Postcentral gyrus
	23	5.0	9	1.6	−3.9	−0.5	10.6	Precentral gyrus
	24	3.0	10	1.1	−4.8	0.0	9.3	Postcentral gyrus
	25	4.0	8	1.4	−4.4	0.1	8.4	Postcentral gyrus
	26	4.6	8	1.4	−4.4	0.8	8.5	Precentral gyrus
	27	3.4	12	0.9	−4.0	−1.3	7.1	BA 13
	28	2.0	7	1.3	−4.4	−0.6	8.5	Precentral gyrus
	n = 7	**3.7 ± 1.0**	**8.9 ± 1.7**	**1.4 ± 0.3**				

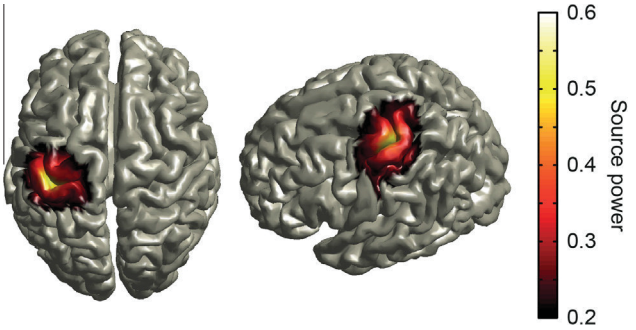

Fig. 1. Localization of evoked responses for virtual sensor analysis. Locations for the virtual sensor analysis were obtained from analysis of evoked responses to median nerve stimuli and were consistent with the primary somatosensory cortex contralateral to the stimulated hand. For visualization, individual maps of stimulus-evoked power increases were normalized by setting their maximum value to 1 and averaged across all subjects. This resulted in an average power increase with dimension-less values (color-coded). Values below 0.2 are masked. For each subject, the point of the individual maximum of the power increase was used as virtual sensor location. (For interpretation of the references to colour in this figure legend, the reader is referred to the web version of this article.)

3.4. Time of maximal alpha rebound

To investigate a possible delay of the alpha rebound in HE, the time point of maximal alpha power in individually adjusted frequency bands during the rebound period was determined (Table 2). An ANOVA did not reveal significant differences between the four groups (Fig. 3B, left panel; $F_{(3,24)} = 1.21$, $p > 0.1$). The time of alpha rebound inversely correlated with the CFF across all subjects (Fig. 3B, middle panel; $r = -0.36$, $p = 0.04$), but not for patients only (Fig. 3B, right panel; $r = -0.32$, $p = 0.09$). Thus, a later time of alpha rebound was associated with increasing disease severity as quantified by the CFF when considering all subjects.

Further analyses revealed a positive relation between the time of alpha rebound and the blood ammonia level across all subjects ($r = 0.36$, $p = 0.03$), but not for patients only ($r = 0.34$, $p = 0.07$). Increasing overall liver dysfunction as measured by the Child Pugh scores showed a significant relationship with the time of alpha rebound for all subjects ($r = 0.35$, $p = 0.04$), but not for patients only ($r = 0.31$, $p = 0.095$). The time of alpha rebound did not differ between patients with alcohol-induced cirrhosis and patients with cirrhosis of other origin ($p = 0.71$).

4. Discussion

The aim of the current study was to investigate potential pathological alterations of oscillatory brain activity associated with the processing of somatosensory stimuli in HE. Our results provide the first evidence for a slowing of alpha activity in S1 in combination with a delayed stimulus-induced modulation as a function of HE disease severity as quantified by the CFF.

4.1. Altered oscillatory alpha activity in HE

The overall occurrence and stimulus-induced modulation of S1 alpha activity in HE is in good accordance with previous findings in

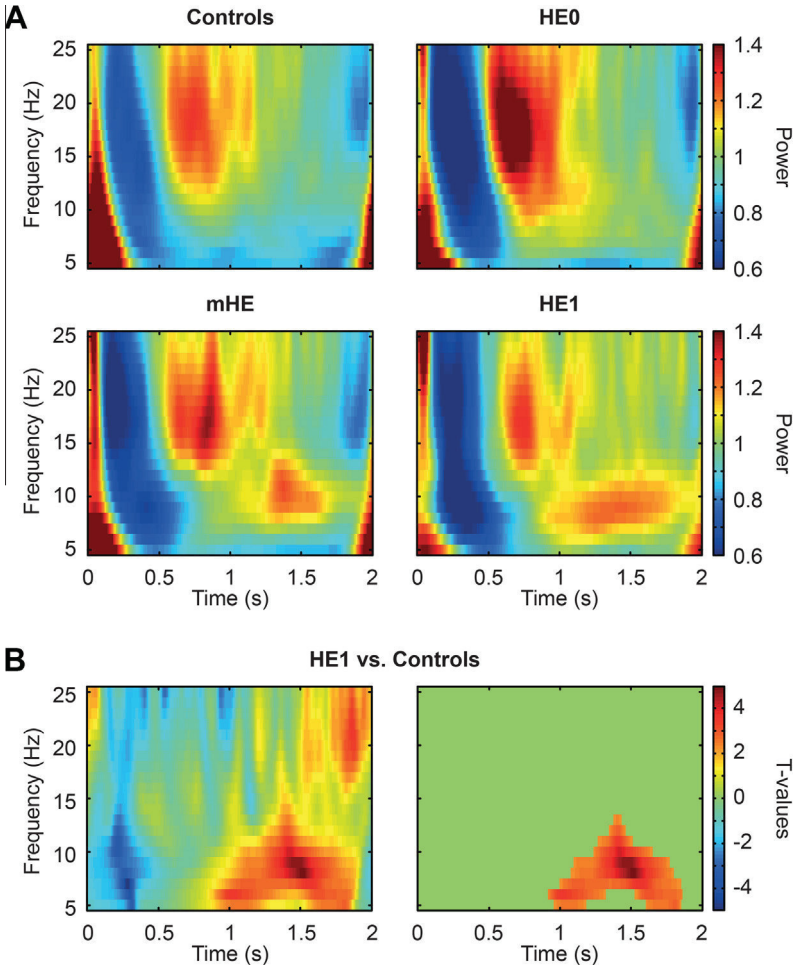

Fig. 2. Time–frequency representations and statistical results. (A) Virtual sensor time–frequency representations (TFRs) averaged across subjects in the four different subject groups (controls, HE0, mHE, HE1). Time point 0 represents the onset of the median nerve stimulus. The subsequent stimulus was administered at 2 s. Color-coded are power values expressed relative to the average power across the complete time interval (0 to 2 s). A value of 1 corresponds to the average power, while values higher than 1 indicate power above and values smaller than 1 power below average. (B) Statistical comparison of TFRs between the groups of HE1 patients and healthy control subjects. Color-coded are *t*-values quantifying the contrast between the two groups. Positive values indicate higher, negative values lower power for HE1 patients. In the left panel, *t*-values are shown for all time–frequency points. In the right panel, non-significant time–frequency points are masked. Statistical analysis revealed a significant cluster ($p < 0.01$) of increased alpha power in HE1 patients compared to healthy controls. This cluster extends from 5 to 15 Hz and between 0.9 and 1.9 s, indicating an increased and/or delayed alpha rebound in HE1 patients. HE0 = cirrhotic patients showing no signs of hepatic encephalopathy, mHE = minimal hepatic encephalopathy, HE1 = hepatic encephalopathy grade 1. (For interpretation of the references to colour in this figure legend, the reader is referred to the web version of this article.)

healthy subjects describing an initial suppression by median nerve stimulation followed by a rebound to or above baseline levels (Salenius et al., 1997; Nikouline et al., 2000; Della Penna et al., 2004). However, the present study revealed distinct pathophysiological modulations of somatosensory alpha activity in HE. Based on the finding of an altered rebound in HE1 patients compared to healthy controls, two features of somatosensory alpha activity were shown to be affected as a function of disease severity. First, the peak frequency of S1 alpha activity was slowed, as demonstrated by both comparisons of the clinical groups and correlations with the CFF. Second, the time of alpha rebound in individually adjusted frequency bands was delayed, as indicated by an inverse correlation to the CFF in all subjects.

The observed slowed peak frequency of S1 alpha activity with increasing HE disease severity tallies with previous findings in HE patients showing slowed neuronal oscillatory activity of spontaneous brain activity (Kullmann et al., 2001; Montagnese et al., 2007; Amodio et al., 2009) and in relation to motor symptoms (Timmermann et al., 2002, 2003, 2008) and visual attention deficits (Kahlbrock et al., 2012). The present findings demonstrate corresponding results for the somatosensory system and provide extra evidence that HE affects oscillatory activity globally, i.e. across different neuronal (sub-)systems, tasks, and frequency bands. Thereby, the hypothesis of slowed oscillatory brain activity as a key hallmark of HE (Timmermann et al., 2005, 2008; Butz et al., 2013) is further substantiated, expanding the understanding of the potential pathophysiological mechanisms of this disease.

The delayed rebound of alpha activity with decreasing CFF reported here is in line with previous somatosensory evoked potential studies, which showed delayed stimulus processing with increasing HE severity (Yang et al., 1985; Chu and Yang, 1987; Davies et al., 1991; Blauenfeldt et al., 2010). These studies focused on immediate stimulus processing measured by evoked responses in the first few hundred milliseconds after median nerve stimulation. Here, we studied modulations of oscillatory alpha activity at a larger time scale and up to 2 s after stimulation, reflecting changes in the overall activation state of the corresponding cortical area rather than immediate stimulus processing. The alpha rebound is part of a typical sequence of alpha modulation in response to simple somatosensory stimuli and follows an initial suppression of oscillatory alpha activity reflecting cortical activation (Salenius et al., 1997; Nikouline et al., 2000; Della Penna et al., 2004).

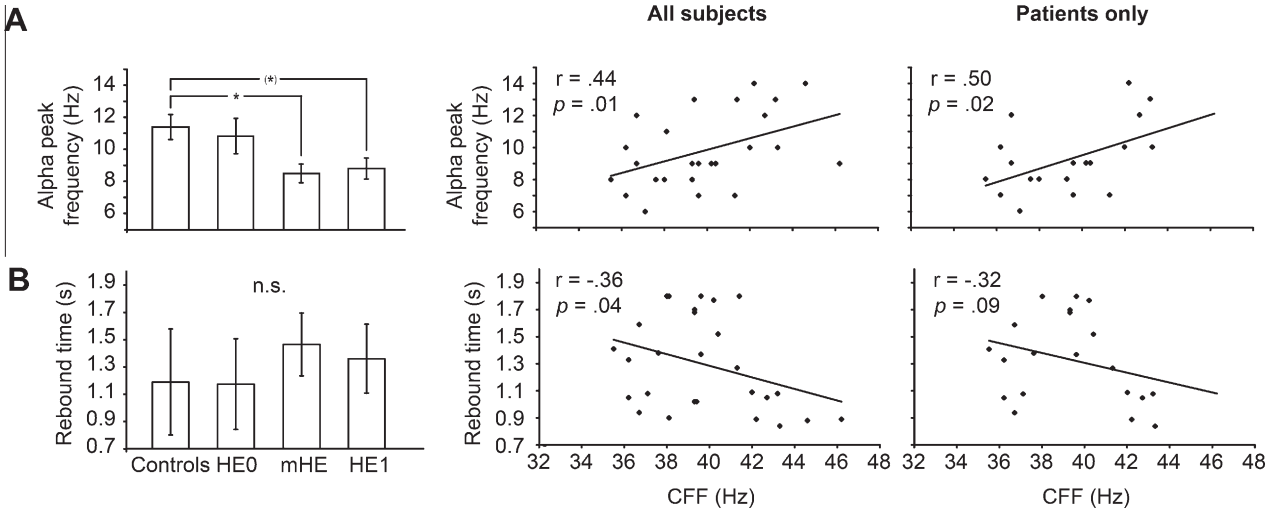

Fig. 3. Analysis of alpha peak frequencies and time of alpha rebound. (A) Left panel: Mean values of alpha peak frequencies for all four subject groups (controls, HE0, mHE, HE1). Error bars indicate the standard error of measurement. Analysis of variance and subsequent post hoc tests were performed to investigate group differences in alpha peak frequencies. Comparisons showing differences between groups are marked ($^{(*)}p < 0.1$, $^{*}p < 0.05$). Compared to healthy controls, statistics revealed lower alpha peak frequencies in mHE patients. Middle and right panel: correlation of the critical flicker frequency (CFF) with the alpha peak frequency for all subjects (middle panel) and patients only (right panel). Correlation coefficients and corresponding *p*-values are given within the figure. All correlation coefficients were corrected for effects of age. Correlations revealed that a lower CFF is associated with a lower alpha peak frequency. (B) Same as (A) but for the time of maximal alpha rebound, i.e. the time point of maximum alpha power between 0.7 and 1.8 s (n.s. = not significant). While no significant group differences were observed, an inverse correlation between the CFF and the time of alpha rebound for all subjects was revealed. Thus, a lower CFF was associated with a later alpha rebound. HE0 = cirrhotic patients showing no signs of hepatic encephalopathy, mHE = minimal hepatic encephalopathy, HE1 = hepatic encephalopathy grade 1.

The observed delay of this rebound in HE might indicate an impaired capability to return to the pre-stimulus or default state of cortical activation and a reduced flexibility of the somatosensory system to adjust activation levels back to baseline levels.

Even in the stages of low-grade HE examined in the present study, the neurophysiological alterations depended on disease severity as quantified by the CFF. Due to both ethical and practical concerns, we did not investigate stages of the disease beyond manifest HE of grade 1 according to the *West-Haven*-Criteria. However, based on previous research, for example on spontaneous brain activity in HE measured with EEG (Davies et al., 1991; Guerit et al., 2009), it can be speculated that the reported alterations of oscillatory alpha activity will progress and become more evident with advanced disease severity.

In general, it is important to note that the present results are based on correlations between features of oscillatory brain activity, the CFF, and the clinical parameters of HE. Thus, they do not prove a direct causal role of alterations of oscillatory brain activity in the emergence of HE and might also present mere associations between oscillatory brain activity and HE disease severity. Nevertheless, they are in good accordance with a growing number of studies arguing for a close link between both (Butz et al., 2013). Importantly, neither the alpha peak frequency nor the time of alpha rebound differed between patients with alcohol-induced cirrhosis and with cirrhosis of other origin, providing evidence that the observed alterations of oscillatory brain activity are most likely related to HE rather than potential alcohol-associated changes of brain function.

4.2. The CFF and oscillatory brain activity

The current results demonstrate a close relationship between the CFF and alterations of oscillatory brain activity, in line with previous studies (Timmermann et al., 2008; Kahlbrock et al., 2012). Ongoing discussions question the usefulness of the commonly used classification scheme of HE and suggest that the neurocognitive changes in HE should be considered as a continuum rather than defining a limited number of distinct stages of the disease (Häussinger et al., 2006; Kircheis et al., 2007; Bajaj et al., 2009). The CFF meets these demands. Our motivation to use the CFF as an additional parameter to assess HE severity was also based on the fact that it has been proven to be a useful tool in several recent HE studies by different clinical and research groups (e.g. Biecker et al., 2011; Lauridsen et al., 2011; Montoliu et al., 2012). A meta-analysis for its use in minimal HE revealed a high specificity and a moderate sensitivity for its diagnosis and emphasized its independence of language and simplicity to perform and interpret (Torlot et al., 2013). The CFF represents a behavioral measure of the processing of an oscillating visual stimulus and is thus particularly interesting in the context of oscillatory brain activity. Our findings strengthen the notion that the CFF as a continuous and fine-graded measure is more sensitive in detecting relationships between neurophysiological measures, behavior, and disease severity.

The CFF quantifies the processing of a flickering, i.e. oscillating, visual stimulus. Flickering visual stimuli are known to drive a frequency-specific brain response of up to 90 Hz in the occipital cortex of healthy subjects (Herrmann, 2001). Thus, they elicit strong oscillatory brain activity resembling the frequency of the incoming stimulation. It is conceivable that alterations in these responses at the cortical level are related to the decreased CFF in HE. As discussed, evidence for a global slowing of oscillatory brain activity in HE in association with a slowing of the CFF and behavioral changes is accumulating (for a review see Butz et al., 2013). This global slowing presumably also affects the processing of an oscillating visual stimulus, making the CFF a potential behavioral parameter of underlying changes of oscillatory brain activity in HE.

Regarding potential pathophysiological mechanisms of HE, a strong role for ammonia has been suggested (Häussinger et al., 2006). However, apart from a correlation with the alpha peak frequency when considering all subjects, high blood ammonia levels did not show significant associations with the neurophysiological alterations reported here. Thus, its potential role in these pathophysiological changes needs to be addressed in future studies. The overall liver function as measured by the Child Pugh score did show similar associations with the changes of oscillatory alpha activity like the CFF. However, due to the unequal distribution of

patients across the four ranks, these results have to be considered with caution.

4.3. Conclusion

The results from the present study demonstrate pathological changes of somatosensory processing as indicated by alterations of oscillatory activity and its stimulus-induced modulation in early stages of HE as a function of disease severity. The finding of slowed oscillatory alpha activity in the somatosensory system tallies with previous results of slowed oscillatory activity in the motor and visual system, deepening the understanding of the pathophysiological processes in HE. The delayed processing of simple somatosensory stimuli in HE patients indicates an impaired capability of the somatosensory system to return to the pre-stimulus or default state of activation. Future studies combining neurophysiological with psychophysical measures of somatosensory processing in HE are needed to reveal the potential consequences of altered oscillatory activity on the behavioral level. Overall, this study strengthens the notion that the slowing of oscillatory brain activity in HE constitutes a common and widespread phenomenon of the disease, which emerges across different brain areas, tasks, and frequency bands.

Acknowledgements

This work was supported by the German Research Foundation (SFB 575, SFB 974). E.S.M. received travel allowances from the Boehringer Ingelheim Fonds (B.I.F.) and the German Academic Exchange Service (DAAD). M.Bu. was supported by a Marie Curie Fellowship of the EU (FP7-PEOPLE-2009-IEF-253965). N.K. received funding by the Studienstiftung des Deutschen Volkes and a travel allowance from the Boehringer Ingelheim Fonds (B.I.F.). G.K. and D.H. belong to a group of patent holders for a bedside device for determination of critical flicker frequency. We are very thankful to Prof. Dr. Joachim Gross from the University of Glasgow and Dr. Tolga Özkurt from the Middle East Technical University Ankara for technical advice regarding data analysis. We furthermore thank Diethelm Plate from the Department of Gastroenterology, Hepatology and Infectious Diseases of the University of Düsseldorf for help in patient recruitment and psychometric testing, Alla Solotuchin and Ulf Zierhut for help with the MEG data collection, and Erika Rädisch for help with MRI acquisitions. We thank Luci Crook (University College London) for skillful language support. Last but not least, we thank all participants who kindly took part in this study.

References

Amodio P, Orsato R, Marchetti P, Schiff S, Poci C, Angeli P, et al. Electroencephalographic analysis for the assessment of hepatic encephalopathy: comparison of non-parametric and parametric spectral estimation techniques. Neurophysiol Clin 2009;39:107–15.

Bajaj JS, Wade JB, Sanyal AJ. Spectrum of neurocognitive impairment in cirrhosis: implications for the assessment of hepatic encephalopathy. Hepatology 2009;50:2014–21.

Biecker E, Hausdörfer I, Grünhage F, Strunk H, Sauerbruch T. Critical flicker frequency as a marker of hepatic encephalopathy in patients before and after transjugular intrahepatic portosystemic shunt. Digestion 2011;83:24–31.

Blauenfeldt RA, Olesen SS, Hansen JB, Graversen C, Drewes AM. Abnormal brain processing in hepatic encephalopathy: evidence of cerebral reorganization? Eur J Gastroenterol Hepatol 2010;22:1323–30.

Butterworth RF. Complications of cirrhosis III. Hepatic encephalopathy. J Hepatol 2000;32:171–80.

Butz M, May ES, Häussinger D, Schnitzler A. The slowed brain: cortical oscillatory activity in hepatic encephalopathy. Arch Biochem Biophys 2013;536:197–203.

Chu NS, Yang SS. Somatosensory and brainstem auditory evoked potentials in alcoholic liver disease with and without encephalopathy. Alcohol 1987;4:225–30.

Davies MG, Rowan MJ, Feely J. EEG and event related potentials in hepatic encephalopathy. Metab Brain Dis 1991;6:175–86.

Della Penna S, Torquati K, Pizzella V, Babiloni C, Franciotti R, Rossini PM, et al. Temporal dynamics of alpha and beta rhythms in human SI and SII after galvanic median nerve stimulation. A MEG study. Neuroimage 2004;22:1438–46.

Ferenci P, Lockwood A, Mullen K, Tarter R, Weissenborn K, Blei AT. Hepatic encephalopathy–definition, nomenclature, diagnosis, and quantification: final report of the working party at the 11th World Congresses of Gastroenterology, Vienna, 1998. Hepatology 2002;35:716–21.

Foxe JJ, Snyder AC. The role of alpha-band brain oscillations as a sensory suppression mechanism during selective attention. Front Psychol 2011;2:154.

Groeneweg M, Quero JC, De Bruijn I, Hartmann IJ, Essink-bot ML, Hop WC, et al. Subclinical hepatic encephalopathy impairs daily functioning. Hepatology 1998;28:45–9.

Guerit J-M, Amantini A, Fischer C, Kaplan PW, Mecarelli O, Schnitzler A, et al. Neurophysiological investigations of hepatic encephalopathy: ISHEN practice guidelines. Liver Int 2009;29:789–96.

Häussinger D, Blei AT. Hepatic encephalopathy. In: Benhamou J-P, Rodes J, Rizzetto M, editors. The textbook of hepatology: from basic science to clinical practice. Oxford: Blackwell Publ; 2007. p. 728–60.

Häussinger D, Kircheis G, Schliess F. Hepatic encephalopathy and nitrogen metabolism. 1st ed. Dordrecht: Springer; 2006.

Herrmann CS. Human EEG responses to 1–100 Hz flicker: resonance phenomena in visual cortex and their potential correlation to cognitive phenomena. Exp Brain Res 2001;137:346–53.

Jensen O, Mazaheri A. Shaping functional architecture by oscillatory alpha activity: gating by inhibition. Front Hum Neurosci 2010;4:186.

Kahlbrock N, Butz M, May ES, Brenner M, Kircheis G, Häussinger D, et al. Lowered frequency and impaired modulation of gamma band oscillations in a bimodal attention task are associated with reduced critical flicker frequency. Neuroimage 2012;61:216–27.

Kircheis G, Fleig WE, Görtelmeyer R, Grafe S, Häussinger D. Assessment of low-grade hepatic encephalopathy: a critical analysis. J Hepatol 2007;47:642–50.

Kircheis G, Wettstein M, Timmermann L, Schnitzler A, Häussinger D. Critical flicker frequency for quantification of low-grade hepatic encephalopathy. Hepatology 2002;35:357–66.

Kullmann F, Hollerbach S, Lock G, Holstege A, Dierks T, Schölmerich J. Brain electrical activity mapping of EEG for the diagnosis of (sub)clinical hepatic encephalopathy in chronic liver disease. Eur J Gastroenterol Hepatol 2001;13:513–22.

Lauridsen MM, Jepsen P, Vilstrup H. Critical flicker frequency and continuous reaction times for the diagnosis of minimal hepatic encephalopathy: a comparative study of 154 patients with liver disease. Metab Brain Dis 2011;26:135–9.

Litvak V, Mattout J, Kiebel S, Phillips C, Henson R, Kilner J, et al. EEG and MEG data analysis in SPM8. Comput Intell Neurosci 2011;2011:852961.

Maris E, Oostenveld R. Nonparametric statistical testing of EEG- and MEG-data. J Neurosci Methods 2007;164:177–90.

Montagnese S, Jackson C, Morgan MY. Spatio-temporal decomposition of the electroencephalogram in patients with cirrhosis. J Hepatol 2007;46:447–58.

Montoliu C, Gonzalez-Escamilla G, Atienza M, Urios A, Gonzalez O, Wassel A, et al. Focal cortical damage parallels cognitive impairment in minimal hepatic encephalopathy. Neuroimage 2012;61:1165–75.

Nichols TE, Holmes AP. Nonparametric permutation tests for functional neuroimaging: a primer with examples. Hum Brain Mapp 2002;15:1–25.

Nikouline VV, Linkenkaer-Hansen K, Wikström H, Kesäniemi M, Antonova EV, Ilmoniemi RJ, et al. Dynamics of mu-rhythm suppression caused by median nerve stimulation: a magnetoencephalographic study in human subjects. Neurosci Lett 2000;294:163–6.

Nolte G. The magnetic lead field theorem in the quasi-static approximation and its use for magnetoencephalography forward calculation in realistic volume conductors. Phys Med Biol 2003;48:3637–52.

Oostenveld R, Fries P, Maris E, Schoffelen J-M. FieldTrip: open source software for advanced analysis of MEG, EEG, and invasive electrophysiological data. Comput Intell Neurosci 2011;2011:156869.

Pfurtscheller G, Stancák Jr A, Neuper C. Event-related synchronization (ERS) in the alpha band–an electrophysiological correlate of cortical idling: a review. Int J Psychophysiol 1996;24:39–46.

Prakash R, Mullen KD. Mechanisms, diagnosis and management of hepatic encephalopathy. Nat Rev Gastroenterol Hepatol 2010;7:515–25.

Pugh RN, Murray-Lyon IM, Dawson JL, Pietroni MC, Williams R. Transection of the oesophagus for bleeding oesophageal varices. Br J Surg 1973;60:646–9.

Romero-Gómez M, Córdoba J, Jover R, del Olmo JA, Ramírez M, Rey R, et al. Value of the critical flicker frequency in patients with minimal hepatic encephalopathy. Hepatology 2007;45:879–85.

Salenius S, Schnitzler A, Salmelin R, Jousmäki V, Hari R. Modulation of human cortical rolandic rhythms during natural sensorimotor tasks. Neuroimage 1997;5:221–8.

Sharma P, Sharma BC, Puri V, Sarin SK. Critical flicker frequency: diagnostic tool for minimal hepatic encephalopathy. J Hepatol 2007;47:67–73.

Timmermann L, Butz M, Gross J, Kircheis G, Häussinger D, Schnitzler A. Neural synchronization in hepatic encephalopathy. Metab Brain Dis 2005;20:337–46.

Timmermann L, Butz M, Gross J, Ploner M, Südmeyer M, Kircheis G, et al. Impaired cerebral oscillatory processing in hepatic encephalopathy. Clin Neurophysiol 2008;119:265–72.

Timmermann L, Gross J, Butz M, Kircheis G, Häussinger D, Schnitzler A. Mini-asterixis in hepatic encephalopathy induced by pathologic thalamo-motor-cortical coupling. Neurology 2003;61:689–92.
Timmermann L, Gross J, Kircheis G, Häussinger D, Schnitzler A. Cortical origin of mini-asterixis in hepatic encephalopathy. Neurology 2002;58:295–8.
Torlot FJ, McPhail MJW, Taylor-Robinson SD. Meta-analysis: the diagnostic accuracy of critical flicker frequency in minimal hepatic encephalopathy. Aliment Pharmacol Ther 2013;37:527–36.
Van Veen BD, van Drongelen W, Yuchtman M, Suzuki A. Localization of brain electrical activity via linearly constrained minimum variance spatial filtering. IEEE Trans Biomed Eng 1997;44:867–80.
Vienna test system, WINWTS, Version 4.50. Mödling, Austria: Dr. G. Schuhfried GmbH, 1999.
Yang SS, Chu NS, Liaw YF. Somatosensory evoked potentials in hepatic encephalopathy. Gastroenterology 1985;89:625–30.

3.)

Butz M[c], Timmermann L, Gross J, Pollok B, Südmeyer M, Kircheis G, Häussinger D, Schnitzler A, *„Cortical activation associated with asterixis in hepatic encephalopathy“,* Acta Neurol Scand 2014 Oct;130(4):260-7.

Impact-Faktor: 2.4

Acta Neurologica Scandinavica

Acta Neurol Scand DOI: 10.1111/ane.12217

ACTA NEUROLOGICA
SCANDINAVICA

Cortical activation associated with asterixis in manifest hepatic encephalopathy

Butz M, Timmermann L, Gross J, Pollok B, Südmeyer M, Kircheis G, Häussinger D, Schnitzler A. Cortical activation associated with asterixis in manifest hepatic encephalopathy.
Acta Neurol Scand: DOI: 10.1111/ane.12217.

Objectives – Severe hepatic encephalopathy gives rise to asterixis, a striking motor symptom also called flapping tremor, which is characterized by a sudden ceasing of muscle tone in all muscles of a limb. In this study, we aimed at scrutinizing the cortical activation associated with asterixis and unraveling the underlying pathophysiological mechanisms. *Material and methods* – We recorded simultaneously neural activity with magnetoencephalography (MEG) and muscle activity with surface EMG in nine patients with manifest hepatic encephalopathy showing asterixis. Asterixis events were detected semiautomatically and served as triggers for averaging MEG signals. Evoked responses averaged time-locked to asterixis events were subjected to equivalent current dipole (ECD) modeling. Additionally, we localized the strongest cortico-muscular coherence in the frequency of the co-occurring tremulousness. *Results* – Evoked fields averaged time-locked to asterixis events were best explained by a single dipolar source in the contralateral primary motor cortex (M1, Talairach coordinates of mean localization: −40, −20, and 64; Brodmann area 4). This dipole showed a twofold field reversal, that is biphasic wave, with frontal dipole orientation at 49 ms before *flap onset* and 99 ms after flap onset. Conversely, two maxima with occipital dipole orientation were observed 2 ms and 160 ms after flap onset. Cortico-muscular coherence for the tremulousness was likewise localized in the contralateral M1 confirming earlier findings in the present patient cohort. *Conclusions* – Our results reveal an involvement of M1 in the generation of asterixis. As also tremulousness, also called mini-asterixis, was shown to originate in M1, asterixis and mini-asterixis may share common pathophysiological mechanisms.

M. Butz[1,2,3], L. Timmermann[4], J. Gross[3], B. Pollok[1], M. Südmeyer[1], G. Kircheis[5], D. Häussinger[5], A. Schnitzler[1]

[1]Medical Faculty, Institute of Clinical Neuroscience and Medical Psychology, Heinrich Heine University Düsseldorf, Düsseldorf, Germany; [2]Sobell Department of Motor Neuroscience and Movement Disorders, UCL Institute of Neurology, London, UK; [3]Centre for Cognitive Neuroimaging (CCNi), Institute of Neuroscience and Psychology, University of Glasgow, Glasgow, UK; [4]Department of Neurology, University of Cologne, Cologne, Germany; [5]Medical Faculty, Department of Gastroenterology, Hepatology and Infectiology, Heinrich Heine University Düsseldorf, Düsseldorf, Germany

Key words: liver cirrhosis; flapping tremor; magnetoencepahlography (MEG); motor symptom; negative myoclonus; oscillations; silent period; synchronization

M. Butz, Medical Faculty, Institute of Clinical Neuroscience and Medical Psychology, Heinrich Heine University Düsseldorf, Universitätsstrasse 1, D-40225 Düsseldorf, Germany
Tel.: +49 211 81 18415
Fax: +49 212 211 81 13015
e-mail: markus.butz@hhu.de

Accepted for publication November 27, 2013

Introduction

Hepatic encephalopathy (HE) is a frequent complication occurring in patients suffering from liver cirrhosis and characterized by a variety of cognitive and motor deficits (1). Manifest HE can be graded into four stages based on the commonly used *West Haven Criteria* (2). Apart from ataxia, the most evident motor symptom in HE 1 is tremulousness called 'metabolic tremor' or mini-asterixis (3–5). This almost rhythmical phenomenon is not thought of as a generic tremor, but appears tremor-like due to its continuous presence. It occurs primarily at 6–12 Hz, is present during maintained posture, and starts after a latent period of about 2–30 s. Previous work demonstrated that mini-asterixis arises from a pathologically slowed drive of the primary motor cortex toward the muscles accompanied by slowed thalamo-motor–cortical coupling (6–8).

In HE 2 and 3, an additional, more striking motor symptom occurs, commonly referred to as asterixis. First described by Adams and Foley in 1949 (9), asterixis is usually characterized by

sudden and irregular lapses of posture at the wrist, metacarpophalangeal, or hip joints (4). According to the nature of this movement, it is also commonly termed flapping tremor and it was suggested to represent a negative myoclonus (4). EMG recordings in asterixis typically reveal a silent period of 50–200 ms in all muscles of a limb resulting in a fall of the hand when the forearm is lifted (4, 10, 11).

Asterixis does not only occur in patients with advanced hepatic encephalopathy, but also in other pathological metabolic conditions such as electrolyte abnormalities or Wilson's disease. Furthermore, it may arise drug-induced or due to focal cortical or subcortical lesions (4, 12–14).

Asterixis and the tremulousness in manifest HE, that is mini-asterixis, were proposed to be activated by the same pathophysiological mechanisms, and therefore, they share the same name (3). Following up our group's previous studies on the origin of mini-asterixis (6–8), the aim of this study was to shed further light on the cortical activation associated with asterixis in HE and to reveal potential common ground in the pathophysiology of both phenomena.

Material and methods

Patients, clinical assessment, and critical flicker frequency

The study was performed in nine patients suffering from manifest hepatic encephalopathy (age, 61.3 ± 5.5 years; mean ± SD) (Table 1). The clinical grading was conducted within 12 h after the MEG recording by a hepatologist (G.K.) and a neurologist (A.S. and L.T.) without knowledge of the MEG findings. According to the *West Haven Criteria,* patients were classified as HE 2 ($n = 6$) and HE 3 ($n = 3$) (2). None of the patients had a history of any other neurological diseases prior to admission. During the observed and documented time span, no neuroleptic drugs were taken by any of the patients. Liver cirrhosis was confirmed in all patients by liver biopsy, if clinically indicated, or by ultrasound of the abdomen, or abdominal CT-scan and laboratory results. Additionally, the critical flicker frequency (CFF) was assessed (15) as the CFF was shown to be a valuable parameter to quantify the gradual brain impairment in HE [for a review see (16)]. In two of the nine patients, the bad general condition disallowed the assessment of the CFF.

All subjects gave their written informed consent prior to the study. The study was approved by the local ethics committee and is in accordance with the Declaration of Helsinki.

Table 1 Clinical characteristics of patients including critical flicker frequency (CFF) and frequency of mini-asterixis. HE grade was determined according to the *West Haven Criteria*

Patient no.	Sex	Age [years]	Genesis of liver cirrhosis	HE grade	CFF [Hz]	Mini-asterixis frequency [Hz]
1	m	67	*Alcohol*	2	34.0	7
2	m	69	*Alcohol*	2	34.4	10
3	m	57	*Alcohol*	2	28.4	7
4	m	65	*Alcohol*	2	25.0	7
5	f	54	*Alcohol*	2	31.2	10
6	m	63	*Alcohol*	3	30.4	9
7	f	59	*Alcohol*	3	ND	5
8	m	53	*Alcohol*	3	ND	6
9	m	65	*Alcohol/ Hepatitis C*	2	30.0	8

M, male; f, female; ND, no data available.

MEG recordings and paradigm

Neuromagnetic activity was recorded using a whole-head Neuromag 122™ MEG system (sample rate: 1000 Hz, band-pass filter: 0.3–330 Hz) in a magnetically shielded room. Muscle activity was recorded simultaneously from three muscles of the right forearm by surface electromyography (EMG): *extensor digitorum communis* (EDC), *flexor digitorum superficalis* (FDL), and *first dorsal interosseus* (FDI). Neural activity was recorded during sustained posture of the right forearm, with the elbow lying on a solid surface and the forearm held in an approximately 45° upright position with fingers splayed. This position was held for 1–3 min, interspersed with pauses for relaxation to avoid fatigue. During pauses, patients rested their arm comfortably on a custom-made arm support. A total of at least 5 min in this holding position was recorded. Additionally, the position and kinematics of the hand were recorded with a 3-D ultrasound system (ZEBRIS, Isny, Germany).

Raw data were carefully inspected offline, and periods contaminated with artifacts (e.g., movement-related artifacts or eye blinks) were excluded from further analysis.

For all patients, T1-weighted high-resolution magnetic resonance images (MRIs) of 1-mm slice thickness were obtained from a 1.5-T Siemens Magnetom™ MRI scanner (Munich/Erlangen, Germany) and realistic head models were generated from these MRIs. The MEG and MRI coordinate systems were aligned by determining the exact position of the head with respect to the MEG sensors using four indicator coils placed on the subject's scalp (two on the forehead and two behind the ears) and three anatomical landmarks (nasion and both preauricular points). These were digitized prior to the MEG recordings with a

three-dimensional digitizer (Polhemus Isotrack, Colchester, VT, USA).

Detection of asterixis events

Asterixis events were identified semiautomatically based on a custom-made MATLAB®-routine (The MathWorks Inc., Natick, MA, USA). This routine was designed to detect the occurrences of silent periods in EMG activity for a defined time period and preceded by an EMG burst, that is representing the characteristic pattern of asterixis described previously (4).

To this end, the routine calculated a convolution of the EMG signal with a 100 ms window consisting of 50 values of 1 (=50 ms) and 50 values of −1. The resulting time series showed local maxima at the beginning of asterixis events, that is flaps. For the positive preselection of an asterixis event, EMG power had to remain at <75% of the mean EMG power in the 50 ms following the local maxima. These points of time were preselected as *flap onset* of asterixis events. In two subjects, EMG power threshold was set to 85% to compensate lower signal-to-noise ratio. We visually examined each preselected event to verify whether the clinically described pattern of asterixis as described by Young and Shahani (4) was present. Each visually confirmed time point was defined as time 0 ms of one asterixis event, that is 0 ms defined the onset of the silent period in the EMG.

Averaging and dipole modeling

Data were analyzed using MATLAB® 7.1 (Mathworks, Natick, MA, USA) and the MATLAB®-based open-source FieldTrip toolbox (17). For each subject, averages for all MEG sensors and EMGs with respect to the onset of asterixis events were calculated. MEG data were band-pass-filtered from 1 to 150 Hz and baseline-corrected with a baseline from −1 to 1 s. EMG data were rectified and filtered with a high pass of 10 Hz. In a separate step, EMG data were band-pass-filtered to specifically survey oscillatory activity in the 4–10 Hz range (see Fig. 2A).

Averaged MEG data were analyzed using the *equivalent current dipole modeling* technique (18). We selected 20 sensors showing strongest activation time-locked to asterixis events and computed one equivalent current dipole (ECD), which best explained the neuromagnetic field. Dipoles were fitted at maximum amplitude of averaged local field power, and a goodness of fit >85% was required. Individual dipole coordinates were normalized to Tailarach space, averaged across the group, and visualized using *Analysis of Functional NeuroImages* (AFNI) (19).

Localization of cortico-muscular coherence for mini-asterixis using DICS

In addition, we localized the cortico-muscular coherence for the co-occurring tremulousness, that is mini-asterixis using *Dynamic Imaging of Coherent Sources* (DICS) (20). To this end, we reran a previously established analysis procedure (6, 8) for the present patient cohort under study. Importantly, this coherence analysis was conducted for the mini-asterixis and not for the asterixis events, which occurred only irregularly.

Results

Patients, critical flicker frequency, and clinical assessment

All patients were diagnosed as having manifest HE and classified as grades 2 and 3 according to West Haven criteria. CFF ranged between 25.0 Hz and 34.4 Hz indicating high-grade HE (Table 1). All patients showed both asterixis and mini-asterixis co-occurring (Fig. 1).

Asterixis-related evoked responses

In all patients, the detection algorithms correctly identified asterixis events adding up to 70.1 ± 35.1

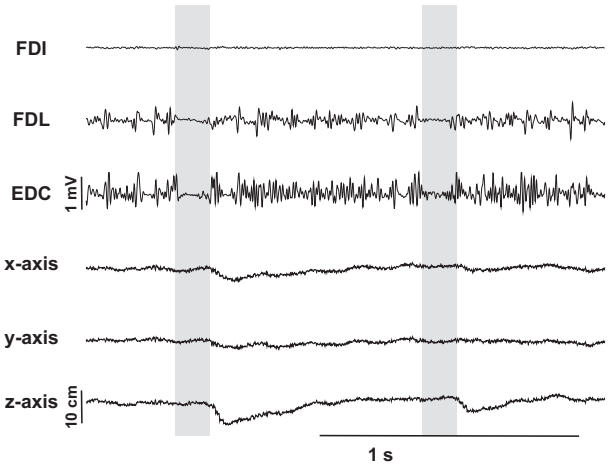

Figure 1. Examples of single asterixis events in one representative subject. Asterixis events are indicated by gray shaded areas. In between asterixis events, a tremor-like pattern can be observed, that is mini-asterixis. Shown are right upper extremity FDI, FDL, and EDC muscle activity (20 Hz high-pass-filtered). In addition, ZEBRIS tracks show movement properties (*x*-axis: right–left, *y*-axis: front–back, z-axis: up–down). A time delay due to the mechanical lag, between EMG silent period and the resulting physical effect, that is falling of the hand, is demonstrated.

(mean and standard deviation) per subject on average.

Averages of EMG activity showed a breakup with flap onset, which usually lasted for 60–100 ms – a result in accordance with the literature (4, 10) (Fig. 2A).

MEG data averaged to asterixis events revealed strongest time-locked activation at sensors over the contralateral primary motor cortex (Fig. 2A). Dipole fitting was successful in 6 of 9 patients. In three patients, no reliable dipole estimation was feasible due to an insufficient signal-to-noise ratio. Dipole fitting was conducted at maximum amplitude at −48.7 ms (±10.1 ms; range −69 ms to −40 ms) and a goodness of fit of 93.2% (±2.7%; range 87.9–96.8%) was obtained.

All dipoles were located within the primary motor cortex (Talairach coordinates of mean localization: x = −40, y = −20, and z = 64; Brodmann area 4) (Fig. 3A).

For all patients, the neuromagnetic field showed a consistent time course characterized by an at least twofold ($n = 4$) in part threefold ($n = 2$) field reversal (Fig. 2A). Around 50 ms before *flap onset,* there was an evident anterior dipole orientation. 2 ms after onset of the silent period in the EMG, a second maximum of activity with reversed dipole orientation was

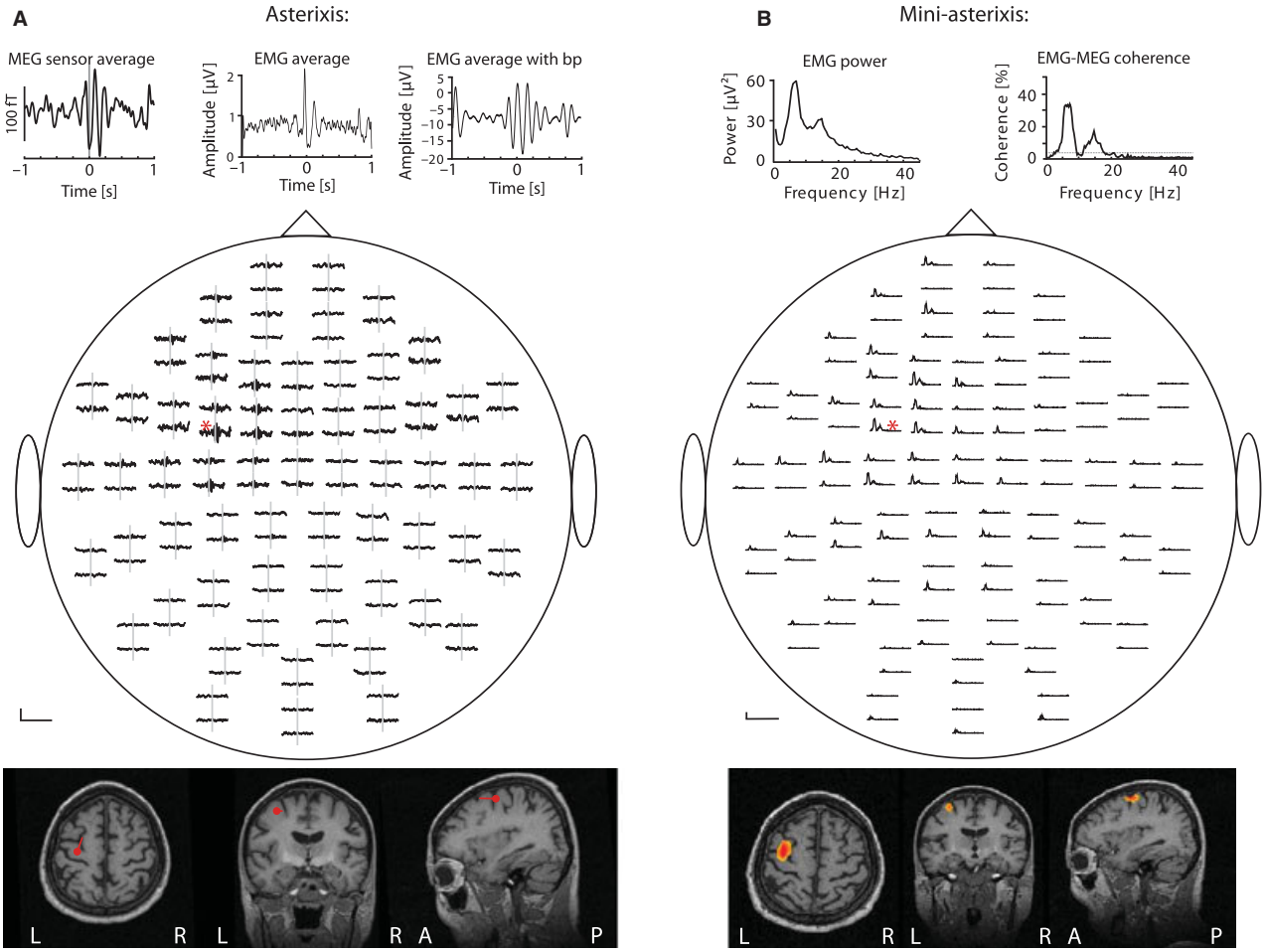

Figure 2. (A) Asterixis: Average of asterixis events for all MEG sensors and EDC muscle in one representative subject. Gray lines indicate time of *flap onset*. Top: Waveform of the sensor showing strongest activity (marked with red asterisk) is magnified in the upper left corner. A ~7 Hz oscillatory activity is evident around *flap onset*. Averaged EMG activity of the right extensor muscle (EDC) is shown at the top centered. A distinct break-up of muscle activity lasting ~80 ms beginning at time 0 ms can be seen preceding and followed by activity peaks. 4–10 Hz band-passed (bp)-averaged EMG activity is shown in the upper right corner. Oscillatory activity is persisting in the frequency of mini-asterixis (~7 Hz). Middle: Strongest activity occurs at the sensors covering the contralateral sensorimotor cortex. Bottom: Dipole estimation revealed a dipole in the contralateral primary motor cortex. (B) Mini-asterixis: Cortico-muscular coherence from EDC muscle to all sensors in one representative subject confirming previous work in the present patients. Top: The coherence spectrum of MEG sensor showing strongest coherence (marked with red asterisk) is magnified in the upper right corner and the frequency spectrum of the EMG activity in the upper left corner. Middle: Strongest coherence occurs at sensors over contralateral sensorimotor cortex at tremor frequency and at double the frequency. Bottom: Tomographic mapping of coherence reveals strongest cortico-muscular coherence to be localized within contralateral primary motor cortex.

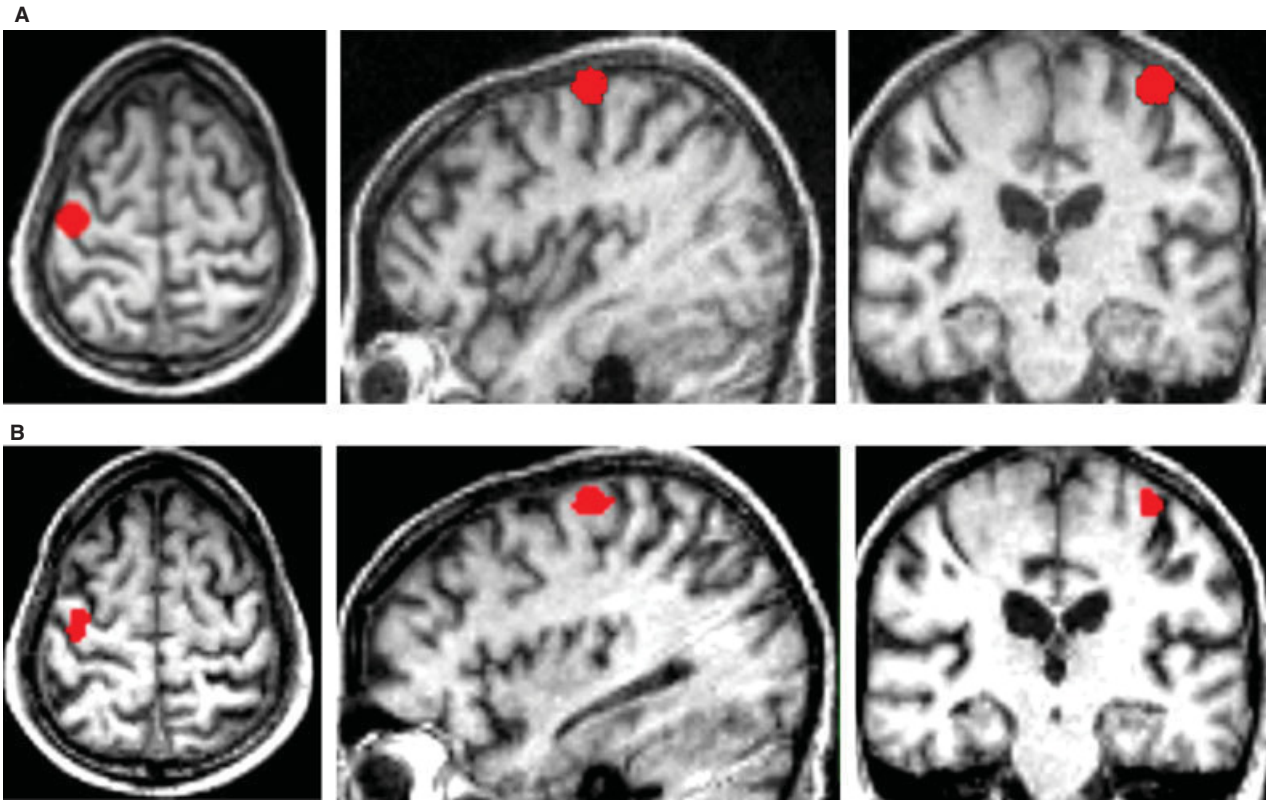

Figure 3. (A) Mean localization of estimated dipoles (n = 6) representing cortical activation associated with asterixis and visualized with AFNI (Talairach coordinates of mean localization: −40, −20, and 64). (B) Mean localization of strongest cortico-muscular coherence at individual frequency of tremulousness, that is mini-asterixis (n = 9) calculated with DICS and visualized with AFNI (Talairach coordinates of mean localization: x = −40, y = −20, and z = 64).

reached. The field turned back and showed a maximum again at around 99 ms with its anterior orientation restored. The next maximum, oriented toward posterior, was reached at around 160 ms. In two patients, a third maximum occurred at around 240 ms with frontal orientation.

Dipole fitting was always performed for the first maximum, which consistently showed the strongest amplitude, but fitting for all maxima consistently revealed a dipole solely within M1 in all six patients.

Cortico-muscular coherence for mini-asterixis

Replicating previous finding, the strongest cortico-muscular coherence for the tremulousness, that is mini-asterixis was localized within the contralateral M1 (Figs 2B and 3B). The Talairach coordinates of mean localization were x = −40, y = −20, and z = 64.

Discussion

The aim of the present study was to reveal the cortical activation associated with asterixis. Findings of this study demonstrate for the first time an involvement of the contralateral primary motor cortex (M1) in the generation of asterixis in a group of patients with high-grade manifest hepatic encephalopathy and suggest a common pathophysiological ground of asterixis and mini-asterixis.

Patients and detection of asterixis events

All patients displayed the characteristics of manifest hepatic encephalopathy including mini-asterixis, asterixis, and low CFF. Our detection algorithm faithfully detected periods of high-EMG power followed by periods of very low EMG power in line with similar approaches used successfully before for the detection of asterixis events (10).

However, one should note that our detection algorithm preferentially detected asterixis events preceded by periods of increased power. In fact, this seems to be primarily the case in times before flap. This observation is also in line with the literature (10), with the description of asterixis (3, 4, 21), and with the visual inspection of the raw data in this study. Previously, Artieda et al.

hypothesized that the cortical motor neuron discharges preceding these EMG bursts are followed by a period of inhibition at the cortical or spinal level (22), an interesting idea, which implies that the cortical discharge triggers the asterixis in a way not understood yet.

Cortical activation associated with asterixis

In the present study, we show for the first time an involvement of the contralateral M1 in the generation of asterixis. Earlier, Ugawa et al. reported in an EEG study scalp potentials with similar field reversals and topographic distribution over the central region in a single patient with liver cirrhosis and suggested this activity to be localized in the M1 contralateral to the muscle demonstrating asterixis (10). Moreover, a case report of a patient suffering from chronic renal failure resulting in myoclonic jerks and asterixis showed that EEG electrodes roughly covering contralateral M1 demonstrate a biphasic wave preceding flaps (22). Also, asterixis caused by thalamic lesions was observed to be associated with activation of the central areas contralateral to the affected hand (23). While these studies already hint at an involvement of the sensorimotor cortex, the present study is the first to precisely localize the cortical activity associated with asterixis in a clinically accurately characterized group of patients. This became feasible by using MEG, which provides a better spatial resolution than EEG. Another important advantage of the present study over previous work is that a group of patients with asterixis was recruited. Considering the rareness and severe general clinical condition of the involved patients, a sample size of nine as in the present study can be regarded as large, exceeding previous studies of asterixis due to liver failure.

The field reversals of the localized dipoles observed here are in accordance with previous findings (10, 22). The exact mechanisms of this phenomenon, however, cannot be finally elucidated. It can be thought of as a pattern of alternating efferent–afferent activity. Along these lines, one might speculate that this represents a reflection of the interruption of the efferent motor command with the onset of the asterixis event, which results into the sudden lapse of posture causing an afferent sensory signal. Then, the motor command is reestablished leading to a rebound movement back to the intended posture after which an additional small correction might be required in case that the actual fall of the hand was 'overcompensated'. This typically observed behavioral pattern might suit interpreting the present phenomenon.

The role of the primary motor cortex

The main cortical activation associated with asterixis was localized in the contralateral M1 in the present work. Interestingly, it is well established that the so-called *cortical silent period* (cSP) can be elicited by transcranial magnetic stimulation of exactly this brain area (24) and that asterixis can also be elicited by percutaneous electrical stimulation of the human motor cortex (25, 26). The cSP describes the pause of EMG activity in tonically activated muscles after contralateral cortical stimulation, a phenomenon similar to asterixis. Importantly, the cSP is believed to be of mainly cortical origin (27, 28). Moreover, the present view is that the cSP is the result of the activation of excitatory and inhibitory GABAergic interneurons of the motor cortex and that the cSP particularly indicates $GABA_B$ transmission (for a review see (29).

Although fairly speculative, following the idea of a similarity between the cSP and asterixis, one might think that asterixis equals a pathologically enhanced cSP. Interestingly, a disturbance in inhibitory GABA-mediated neurotransmission and the GABAergic tone has been suggested as a key factor in the pathogenesis of HE, but the exact underlying mechanisms are not finally clear yet (30). Bringing these findings together, it can be speculated that the disturbed GABAergic tone is one of the key pathophysiological mechanisms for the reported results. Future studies are needed to test this potential link in detail, for example by TMS studies investigating the long- and short-interval intracortical inhibition (LICI/SICI) and cSP in HE patients to examine the postulated enhanced GABAergic tone in this patient population (29, 31, 32). Moreover, it would be interesting to probe, if TMS over the primary motor cortex interferes with mini-asterixis. The use of TMS is also encouraged by previous work which has successfully applied this technique to better assess the pathophysiology of lesion-induced asterixis (23).

The present results confirm that cortical activation in asterixis can be found in the similar brain area as previously reported to be involved in the emergence of mini-asterixis (6, 8). This finding fits nicely to the idea that both symptoms are activated by similar pathophysiological mechanisms (3). Thus, results of this study can be interpreted as evidence for a common pathophysiological ground with the contralateral M1 playing a key

role in both. If this is the case, one might speculate that asterixis constitutes a pronounced occurrence of mini-asterixis, but more work is obviously needed here.

In any case, it is quite likely that M1 represents only one major component in a broader cerebral network, and an involvement of subcortical structures was already shown for mini-asterixis (7). This notion is also supported by findings in other patient populations showing asterixis such as stroke patients and will be discussed in the following.

Asterixis in other pathological entities and potential mechanisms in HE

Studying patients with brain lesions, Young and Shahani postulated that asterixis could be due to a failure of any part of the motor network subserving posture or the arousal system (4). A crucial role of M1 in asterixis was also previously indicated by case reports showing that focal lesions of this part of the cortex may result in asterixis (13). Lesions in the thalamus, however, are more likely to lead to asterixis (12), strengthening the idea that an entire network of brain regions is involved in the generation of asterixis.

The similar phenomenon of negative myoclonus was repeatedly described in patients with epilepsy. Two MEG studies suggest an involvement of M1 in patients with epileptic negative myoclonus (33, 34), but also premotor areas, sensory areas, and supplementary motor areas have been shown to be involved (35). Again, these findings suggest a broad motor network to be involved in the generation of this symptom.

It is not finally clear to what extent our results may also be transferable to healthy subjects. With most people having experienced '*physiological flaps*' in drowsiness, for example lapses in head posture during boring lectures or long train journeys, it can be speculated that asterixis is just a pathologically pronounced and more rapidly iterating form of these *'physiological flaps'* (3, 4). This would be easily imaginable considering drowsiness and the severe general condition present in high-grade HE.

Conclusion

This study is the first to localize the cortical activation associated with asterixis in a series of patients with manifest hepatic encephalopathy. We could show an activation of the M1 contralateral to the limb demonstrating asterixis. As mini-asterixis is also thought to originate in the contralateral M1, the present work provides evidence for a common pathophysiological ground shared between both phenomena. One might speculate that asterixis can be considered as an exaggerated form of mini-asterixis as suggested previously.

Acknowledgments

The authors wish to thank all patients for their cooperation during the measurements. We are thankful to Erika Rädisch and Stefan Ostrowski for technical support and to Dr. Thomas Kramer for support with patient recruitment. In addition, we would like to thank Lucinda Crook (University College London) for skillful language support and Dr. Masashi Hamada (University of Tokyo) for helpful discussions on TMS.

Sources of funding

This work was supported by the German Research Foundation (SFB 575 and SFB 974). Dr. Butz was supported by a Marie Curie Fellowship of the EU (FP7-PEOPLE-2009-IEF-253965).

Conflict of interest

D.H. and G.K. are patent holders for a bedside testing device for assessment of the critical flicker frequency. The authors have no further conflict of interest.

References

1. Häussinger D, Blei AT. Hepatic Encephalopathy. In: Rodes J, Benhamou J-P, Blei AT, Reichen J, Rizzetto M, eds. The textbook of hepatology: from basic science to Clinical practice, 3rd edn. Oxford: Wiley-Blackwell, 2007;728–60.
2. Ferenci P, Lockwood A, Mullen K, Tarter R, Weissenborn K, Blei AT. Hepatic encephalopathy–definition, nomenclature, diagnosis, and quantification: final report of the working party at the 11th World Congresses of Gastroenterology, Vienna, 1998. Hepatology 2002;**35**:716–21.
3. Leavitt S, Tyler HR. Studies in asterixis. Arch Neurol 1964;**10**:360–8.
4. Young RR, Shahani BT. Asterixis: one type of negative myoclonus. Adv Neurol 1986;**43**:137–56.
5. Shahani BT, Young RR. Asterixis - a disorder of the neural mechanisms underlying sustained muscle contraction. In: Shahani M, ed. The motor system: neurophyiology and musle mechanisms. Amsterdam: Elsevier, 1976;301–6.
6. Timmermann L, Butz M, Gross J et al. Impaired cerebral oscillatory processing in hepatic encephalopathy. Clin Neurophysiol 2008;**119**:265–72.
7. Timmermann L, Gross J, Butz M, Kircheis G, Häussinger D, Schnitzler A. Mini-asterixis in hepatic encephalopathy induced by pathologic thalamo-motor-cortical coupling. Neurology 2003;**61**:689–92.
8. Timmermann L, Gross J, Kircheis G, Häussinger D, Schnitzler A. Cortical origin of mini-asterixis in hepatic encephalopathy. Neurology 2002;**58**:295–8.
9. Adams RD, Foley JM. The neurological changes in the more common types of severe liver disease. Trans Am Neurol Assoc 1949;**74**:217–9.

10. Ugawa Y, Shimpo T, Mannen T. Physiological analysis of asterixis: silent period locked averaging. J Neurol Neurosurg Psychiatry 1989;**52**:89–93.
11. Shibasaki H. Pathophysiology of negative myoclonus and asterixis. Adv Neurol 1995;**67**:199–209.
12. Kim JS. Asterixis after unilateral stroke: lesion location of 30 patients. Neurology 2001;**56**:533–6.
13. Nighoghossian N, Trouillas P, Vial C, Froment JC. Unilateral upper limb asterixis related to primary motor cortex infarction. Stroke 1995;**26**:326–8.
14. Rio J, Montalban J, Pujadas F, Alvarez-Sabin J, Rovira A, Codina A. Asterixis associated with anatomic cerebral lesions: a study of 45 cases. Acta Neurol Scand 1995;**91**:377–81.
15. Kircheis G, Wettstein M, Timmermann L, Schnitzler A, Häussinger D. Critical flicker frequency for quantification of low-grade hepatic encephalopathy. Hepatology 2002;**35**:357–66.
16. Butz M, May ES, Häussinger D, Schnitzler A. The slowed brain: cortical oscillatory activity in hepatic encephalopathy. Arch Biochem Biophys 2013;**536**:197–203.
17. Oostenveld R, Fries P, Maris E, Schoffelen JM. FieldTrip: open source software for advanced analysis of MEG, EEG, and invasive electrophysiological data. Comput Intell Neurosci 2011;**2011**:156869.
18. Hämäläinen MHR, Ilmoniemi RJ, Knuutila J, Lounasmaa OV. Magnetoencephalography - theory, instrumentation, and application to noninvasive studies of the working human brain. Rev Mod Phys 1993;**65**:413–97.
19. Cox RW, Hyde JS. Software tools for analysis and visualization of fMRI data. NMR Biomed 1997;**10**:171–8.
20. Gross J, Kujala J, Hämälainen M, Timmermann L, Schnitzler A, Salmelin R. Dynamic imaging of coherent sources: studying neural interactions in the human brain. Proc Natl Acad Sci USA 2001;**98**:694–9.
21. Tyler HR, Leavitt S. Asterixis. J Chronic Dis 1965;**18**:409–11.
22. Artieda J, Muruzabal J, Larumbe R, Garcia de Casasola C, Obeso JA. Cortical mechanisms mediating asterixis. Mov Disord 1992;**7**:209–16.
23. Inoue M, Kojima Y, Mima T et al. Pathophysiology of unilateral asterixis due to thalamic lesion. Clin Neurophysiol 2012;**123**:1858–64.
24. Reid AE, Chiappa KH, Cros D. Motor threshold, facilitation and the silent period in cortical magnetic stimulation. Handbook of transcranial magnetic stimulation. London: Arnold, 2002;97–111.
25. Marsden CD, Merton PA, Morton HB. Direct electrical stimulation of corticospinal pathways through the intact scalp in human subjects. In: Desmedt JE, ed. Motor control mechanisms in health and disease. New York: Raven Press, 1983;387–91.
26. Merton PA, Morton HB. Stimulation of the cerebral cortex in the intact human subject. Nature 1980;**285**:227.
27. Schnitzler A, Benecke R. The silent period after transcranial magnetic stimulation is of exclusive cortical origin: evidence from isolated cortical ischemic lesions in man. Neurosci Lett 1994;**180**:41–5.
28. Hallet M. Transcranial magnetic stimulation: negative effects. In: Fahn S, Hallet M, Lüders HO, Marsden CD, eds. Negative motor phenomena, advances in neurology, Vol. **67**. New York: Raven Press, 1995;107–13.
29. Paulus W, Classen J, Cohen LG et al. State of the art: pharmacologic effects on cortical excitability measures tested by transcranial magnetic stimulation. Brain stimulation 2008;**1**:151–63.
30. Sergeeva OA. GABAergic transmission in hepatic encephalopathy. Arch Biochem Biophys 2013;**536**:122–30.
31. Ilic TV, Meintzschel F, Cleff U, Ruge D, Kessler KR, Ziemann U. Short-interval paired-pulse inhibition and facilitation of human motor cortex: the dimension of stimulus intensity. J Physiol 2002;**545**(Pt 1):153–67.
32. Kujirai T, Caramia MD, Rothwell JC et al. Corticocortical inhibition in human motor cortex. J Physiol 1993;**471**:501–19.
33. Kubota M, Nakura M, Hirose H, Kimura I, Sakakihara Y. A magnetoencephalographic study of negative myoclonus in a patient with atypical benign partial epilepsy. Seizure 2005;**14**:28–32.
34. Shiraishi H, Haginoya K, Nakagawa E et al. Magnetoencephalography localizing spike sources of atypical benign partial epilepsy. Brain Dev 2013;doi: 10.1016/j.braindev.2012.12.011.
35. Rubboli G, Mai R, Meletti S et al. Negative myoclonus induced by cortical electrical stimulation in epileptic patients. Brain 2006;**129**(Pt 1):65–81.

4.)

May ES*, **Butz M*,[c]**, Kahlbrock N, Hoogenboom N, Brenner M, Schnitzler A,

"*Pre- and post-stimulus alpha activity shows differential modulation with spatial attention during the processing of pain*"

Neuroimage 2012 Sep;62(3):1965-74.

Impact-Faktor: 6.3

NeuroImage 62 (2012) 1965–1974

Contents lists available at SciVerse ScienceDirect

NeuroImage

journal homepage: www.elsevier.com/locate/ynimg

Pre- and post-stimulus alpha activity shows differential modulation with spatial attention during the processing of pain

Elisabeth S. May [a,1], Markus Butz [a,b,1,*], Nina Kahlbrock [a], Nienke Hoogenboom [a], Meike Brenner [a], Alfons Schnitzler [a]

[a] Heinrich-Heine-University Düsseldorf, Medical Faculty, Institute of Clinical Neuroscience and Medical Psychology, Universitätsstrasse 1, D-40225 Düsseldorf, Germany
[b] Sobell Department of Motor Neuroscience and Movement Disorders, UCL Institute of Neurology, Queen Square, London, WC1N 3BG, United Kingdom

ARTICLE INFO

Article history:
Accepted 27 May 2012
Available online 1 June 2012

Keywords:
MEG
Oscillations
Lateralization
Gating
Inhibition
Top-down

ABSTRACT

Extensive work using magneto- and electroencephalography (M/EEG) suggests that cortical alpha activity represents a top-down controlled gating mechanism employed by processes like attention across different modalities. However, it is not yet clear to what extent this presumed gating function of alpha activity also applies to the processing of pain.

In the current study, a spatial attention paradigm was employed requiring subjects to attend to painful laser stimuli on one hand while ignoring stimuli on the other hand. Simultaneously, brain activity was recorded with MEG. In order to disentangle pre- and post-stimulus effects of attention, alpha activity was analyzed during time windows in anticipation of and in response to painful laser stimulation.

Painful laser stimuli led to a suppression of alpha activity over both ipsi- and contralateral primary somatosensory areas irrespective if they were attended or ignored. Spatial attention was associated with a lateralization of anticipatory pre-stimulus alpha activity. Alpha activity was lower over primary somatosensory areas when the contralateral hand was attended compared to when the ipsilateral hand was attended, in line with the notion that oscillatory alpha activity regulates the flow of incoming information by engaging and/or disengaging early sensory areas. On the contrary, post-stimulus alpha activity, for stimuli on either hand, was consistently decreased with attention over contralateral areas. Most likely, this finding reflects an increased cortical activation and enhanced alerting if a painful stimulus is attended.

The present results show that spatial attention results in a modulation of both pre- and post-stimulus alpha activity associated with pain. This flexible regulation of alpha activity matches findings from other modalities. We conclude that the assumed functional role of alpha activity as a top-down controlled gating mechanism includes pain processing and most likely represents a unified mechanism used throughout the brain.

Introduction

Rhythmic neuronal alpha oscillations between 8 and 12 Hz are the strongest electrophysiological signal measured from the awake human brain (Berger, 1929; Niedermeyer and Lopes da Silva, 2005). For a long time, alpha activity was thought to merely reflect "cortical idling" (Pfurtscheller et al., 1996). Recently, alpha activity has been assumed to have a more active role in terms of a graded functional inhibition of brain areas not directly involved in a specific task (Jensen and Mazaheri, 2010). In this context, alpha activity has been closely related to selective attention and is understood to actively gate the incoming flow of information (Foxe and Snyder, 2011), enabling us to favor and more efficiently process those of the many incoming stimuli in our environment that are behaviorally relevant. Across different modalities, attention affects oscillatory alpha activity already during anticipatory pre-stimulus periods, i.e. when a stimulus is expected but not yet actually received and processed (Del Percio et al., 2006; Jones et al., 2010; Thorpe et al., 2012; Thut et al., 2006). In the somatosensory system, for example, spatial attention to one hand lateralizes alpha activity in anticipation of a tactile stimulus. Specifically, alpha activity is decreased in the primary somatosensory cortex contralateral to the attended hand, but increased ipsilaterally (Anderson and Ding, 2011; Haegens et al., 2011). Moreover, it has been shown that the degree of pre-stimulus alpha lateralization determines the subsequent behavioral response (Haegens et al., 2011). These findings tally the notion that an increase of alpha activity reflects an active inhibition or disengagement of a cortical area (Foxe and Snyder, 2011; Jensen and Mazaheri, 2010) whereas a decrease of alpha activity is a correlate of an activated or engaged cortical region (Pfurtscheller et al., 1996).

Painful stimuli have been demonstrated to affect oscillatory activity across a range of frequency bands (Hauck et al., 2007, 2008; Schulz et

* Corresponding author at: Sobell Department of Motor Neuroscience and Movement Disorders, UCL Institute of Neurology, Queen Square, London, WC1N 3BG, United Kingdom.
E-mail address: m.butz@ucl.ac.uk (M. Butz).
[1] These two authors contributed equally to this work.

1053-8119/$ – see front matter © 2012 Elsevier Inc. All rights reserved.
doi:10.1016/j.neuroimage.2012.05.071

al., 2012). With respect to lower frequencies, previous work showed that painful laser stimuli, in contrast to stimuli of other modalities (Hari and Salmelin, 1997), globally suppress spontaneous alpha and beta oscillations in somatosensory, motor and visual areas (Ploner et al., 2006a). This finding has been interpreted as a specific alerting function of pain, which is also reflected by an increased excitability of somatosensory cortices to subsequent tactile stimuli (Ploner et al., 2006b). Interestingly, seeing an image of a limb in a painful situation also induces stronger alpha suppression in sensorimotor areas than seeing an image of a non-painful situation (Whitmarsh et al., 2011). Together, these results suggest that the processing of pain and pain-associated stimuli in somatosensory cortices is particularly intense and associated with a strong modulation of oscillatory activity.

The relationship between pain-associated oscillatory alpha activity and attention is not yet fully understood. In a study using subdural electrocorticographic recordings (ECoG) from epilepsy patients, Ohara et al. (2004) found that alpha suppression in response to an attended compared to a non-attended painful laser stimulus is more intense and widespread over primary somatosensory and parasylvian cortices. In contrast, using an oddball paradigm and painful intracutaneous electrical stimulation in healthy subjects, Hauck et al. (2007) did not observe any modulation of pain-associated alpha activity with attention. Both studies, however, did not investigate possible pre-stimulus effects of attention. Previous work addressing pre-stimulus effects showed that anticipation of a painful stimulus already results in a suppression of alpha activity (Babiloni et al., 2003, 2004, 2006; Del Percio et al., 2006). This anticipatory suppression is again stronger for a painful compared to a non-painful stimulus (Babiloni et al., 2003) and less prominent, if the subject is distracted by mentally performing an arithmetical task (Del Percio et al., 2006).

Linking the attentional modulation of pain processing to behavior, previous studies have consistently shown that a stimulus is perceived as less painful if attention is directed away from it (Bushnell et al., 1999; Miron et al., 1989; Petrovic et al., 2000; Schlereth et al., 2003). Yet, even under constant experimental conditions, the pain experience varies substantially both across and within subjects (Babiloni et al., 2006; Gross et al., 2007; Schulz et al., 2011, 2012). These variations covary with alpha activity. For example, the strength of anticipatory pre-stimulus alpha suppression in expectation of a painful stimulus correlates with the intensity of the individual pain perception across subjects (Babiloni et al., 2006). Within subjects, pain ratings across different trials with stimuli of constant intensity vary in close relation to the post-stimulus pain-induced alpha suppression (Schulz et al., 2011). Therefore, the pain sensation seems to be related to the current state of alpha activity. More specifically, pain appears to be perceived more intensely, if alpha activity close to the moment of stimulus onset is low.

The current study intended to shed further light on the role of alpha activity in relation to pain processing. Previous studies indicate both a modulation of pain-related alpha activity by attention and an association between alpha activity and the subjective pain experience. However, concurrent effects of attention on both pre- and post-stimulus pain-associated alpha activity have not yet been addressed. We aimed to test the hypothesis that alpha activity has a similar function for pain processing as for other modalities, representing a gating mechanism employed by top-down processes to streamline information flow in the brain. To this end, we used a spatial attention paradigm requiring subjects to attend to painful laser stimuli on the dorsum of one hand, while at the same time ignoring stimuli on the other hand. Simultaneously, brain activity was recorded using magnetoencephalography (MEG). To disentangle pre- and post-stimulus attention effects, we analyzed alpha activity both in anticipation of and in response to painful laser stimuli. For the anticipatory pre-stimulus period, spatial attention was hypothesized to lateralize alpha activity across left and right somatosensory cortices. In line with an active regulation of the incoming information flow, alpha activity was expected to be lower in primary somatosensory areas when the contralateral hand was attended compared to when the ipsilateral hand was attended. For the post-stimulus period, attention was assumed to decrease alpha activity primarily over contralateral somatosensory areas, in accordance with an increased cortical activation. Lastly, we expected attention-related alpha activity to be predictive of the individual pain perception.

Materials and methods

Subjects

Fifteen healthy subjects (7 female, 14 right-handed, mean age ± standard deviation: 48.33 ± 17.67 years, range: 24–74 years) participated in the study after giving written informed consent. The study was approved by the local ethics committee (study no. 2895) and conducted in conformity with the Declaration of Helsinki.

Experimental paradigm

Subjects performed a spatial attention paradigm as depicted in Fig. 1. Before the experiment, two adjacent rectangles were marked as target areas on the dorsum of each hand within the area innervated by the radial nerve. Each rectangle had a size of 1.5 cm × 4 cm. Both rectangles adjoined along the longer flank with the border between the two following the prolonged course of the index finger. During the experiment, painful laser stimuli of constant intensity were applied to the 4 target areas. In a block design, subjects were instructed to either attend to stimuli on the left hand and rate their localization and intensity while ignoring stimuli on the right hand (left hand attended) or vice versa (right hand attended).

Each trial began with the onset of a visual fixation cross, on which participants were instructed to remain fixated. After a random time interval between 2 and 6 s, a painful laser stimulus was applied to the left or right hand to one of the two designated target areas. In trials where the painful laser stimulus was delivered to the attended hand, a question mark replaced the fixation cross 5 s after the stimulus for 10 s. This cued the subject to verbally rate the last stimulus regarding location on the attended hand (left or right target area) and intensity (from 0 = "not painful" to 10 = "worst imaginable pain"). After the screen turned black for 1 s, the next trial began. In trials where the stimulus was applied to the unattended hand, a black screen appeared instead of the question mark lasting 11 s until the next trial. In these trials, the subject was not asked to give any response to ensure that maximal attention remained on the attended hand. Altogether, interstimulus intervals between two subsequent laser stimuli randomly varied between 18 and 22 s.

Each block (left hand attended or right hand attended) consisted of 40 trials. The combination of the two factors *stimulated hand* (left or right) and *attended hand* (left or right) resulted in four conditions: (i) left hand stimulated and attended; (ii) left hand stimulated, but unattended; (iii) right hand stimulated and attended; and (iv) right hand stimulated, but unattended. In each block, both the respective attended and unattended condition contained 20 trials of which 10 were applied to the left and 10 to the right target area. Within each block, the order of stimulation was randomized. Thus, the probability of a stimulus to occur on a given hand in any given trial was 50%. Each block lasted for about 14 min with a few minutes break in between. The order of blocks was counterbalanced.

The first nine subjects performed one run of each block type (left hand attended/right hand attended) resulting in a total number of 20 trials of each of the four conditions. Six additional subjects underwent a second run of each block type, increasing the total number of trials to 40 trials per condition. The number of trials was aimed to be kept minimal to reduce the risk of potential skin damage associated with laser stimulation at painful intensities, but high enough to obtain a good signal-to-noise ratio.

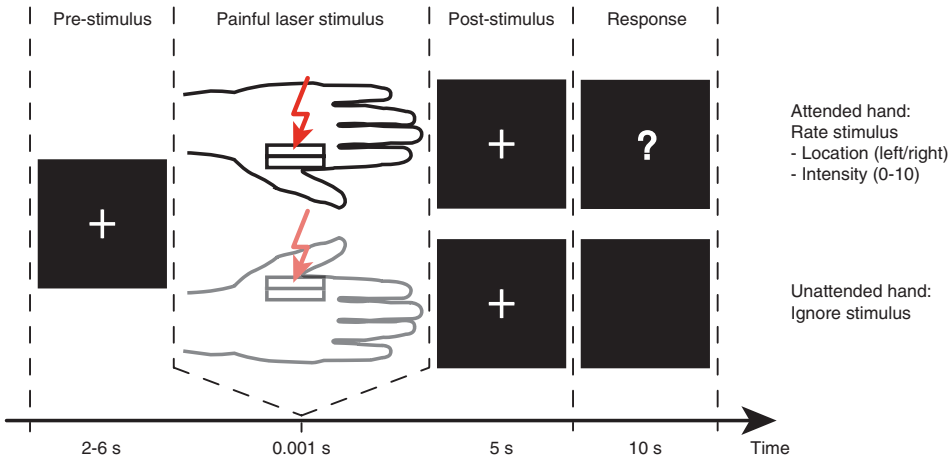

Fig. 1. Experimental paradigm. Subjects performed a spatial attention paradigm where painful laser stimuli were randomly applied to their left or right hand. In a block design, subjects attended to stimuli on the left hand while ignoring stimuli on the right hand or vice versa (left hand attended block shown). Each trial began with the onset of a visual fixation cross. After a random period between 2 and 6 s, a painful laser stimulus was applied to one of the two hands. If the stimulus was delivered to the attended hand, subjects were visually cued by a question mark to rate the stimulus with respect to its location and intensity 5 s after the laser stimulus. The question mark remained on for 10 s followed by 1 s of black screen after which the next trial started (not shown in figure for simplicity). If the stimulus was delivered to the unattended hand, a black screen appeared instead of the question mark and subjects were not asked to give any response but to ignore the stimulus. This black screen was displayed for a total of 11 s after which the next trial began (again, last second not shown in figure for simplicity). The design resulted in four types of trials: (i) left hand stimulated and attended; (ii) left hand stimulated, but unattended; (iii) right hand stimulated and attended; and (iv) right hand stimulated, but unattended.

Stimuli and experimental setup

The administered painful stimuli were cutaneous laser stimuli that selectively activate nociceptive afferents without concomitant activation of tactile afferents (Treede, 2003). Two Tm:YAG-laser devices (Themis, Starmedtec, Starnberg, Germany) with a wavelength of 1960 nm, a pulse duration of 1 ms and a spot diameter of approximately 5 mm were used. Stimulus energy was kept constant at 540 mJ, which evoked slightly to moderately painful, pinprick-like sensations.

Two assistants sat to the left and right of the subject during recordings. Before the experiment, all assistants involved in the data acquisition received detailed instructions on how to perform the stimulation to standardize stimulus application across hands and subjects. Throughout the experiment, each assistant held one laser handle constantly above the subject's left or right hand, respectively, while the actual laser devices were placed outside the MEG room. The assistants were instructed about the target area for the next trial via earphones. Within the marked target areas, stimulation sites were slightly changed after each stimulus. To avoid differences in the exact energy output between the two laser devices leading to unequal stimulation intensities between the hands, assistants exchanged laser handles between subject's left and right hand after half of each block. This ensured that the average stimulation intensity was similar across hands and attentional conditions. For the six subjects who received one additional experimental run of both left and right hand attended blocks, assistants relocated to the other side of the subject after two blocks and performed the stimulation of the other hand for the rest of the experiment.

To prevent subjects from looking at their hands and using visual information rather than the actual somatosensory perception to solve the localization task on the attended hand, their hands were taken as far out of the visual field as possible. Two laser devices were used, of which the two assistants kept the handles constantly above the subject's hands, so that only minimal movements were necessary to target the requested location on each hand. These movements were not detectable by the subject without directly looking at the laser handles. Subjects were instructed to keep central fixation throughout the experiment, which was controlled by the recording of horizontal electrooculograms. Since the probability to receive a stimulus to either hand was 50%, participants could not predict the upcoming hand of stimulation.

Verbal responses of the subjects (left or right target area and pain rating) were collected by the experimenter outside the shielded room, recoded into trigger values and recorded simultaneously with the MEG data. The paradigm was implemented using Presentation (version 13.1, Neurobehavioral Systems, Albany, NY, USA).

MEG recording

Neuromagnetic activity was continuously measured within a magnetically and acoustically shielded room with a 306-channel whole head MEG system (Elekta Oy, Helsinki, Finland) comprising 102 sensor triplets consisting of one magnetometer and two orthogonal planar gradiometers each. Bipolar vertical and horizontal electrooculograms were recorded to later identify epochs containing eye blinks and movements. All data were band-pass filtered by an online filter (0.03 to 330 Hz), digitized at 1000 Hz and stored for offline analysis.

Analysis of behavioral data

Behavioral data were analyzed by means of percentage of correct responses in the localization task and trial-by-trial pain ratings using IBM SPSS Statistics 19 (IBM Corporation, Somers, USA). Results are reported as mean ± standard deviation. Dependent sample *t*-tests were used to compare both the percentage of correct responses and the average pain ratings between the left and right hand.

MEG data analysis

MEG data were analyzed using Matlab 7.1 (Mathworks, Natick, MA, USA) and FieldTrip, an open-source Matlab toolbox (Oostenveld et al., 2011). Unless otherwise stated, all trials of the different conditions were analyzed. Statistical tests were one-tailed.

Preprocessing

MEG data were divided into epochs of interest, starting 2 s before and ending 4 s after the laser stimulus in each trial. Only data recorded by the 204 planar gradiometers were analyzed. For each epoch, power line noise was removed by estimating and subtracting the 50, 100 and 150 Hz components in the MEG data, using a discrete Fourier transform. After visual inspection, epochs and sensors with high variance (containing,

e.g., muscle artifacts or MEG sensor jumps) were removed from the data. This resulted in an average of 19.08 trials ± 0.83 standard deviation (range: 17 to 20 trials) across subjects and conditions for those subjects who completed 20 trials per condition and 38.83 trials ± 1.04 standard deviation (range: 37 to 40 trials) for those who completed 40 trials per condition. Data from all measurement blocks of each subject were then combined. Independent component analysis (ICA) (Jung et al., 2000) was used to identify eye and heart artifacts. The ICA components were visually inspected and those representing eye and heart artifacts were projected out of the data.

Time–frequency analysis

Time–frequency representations (TFRs) of power were estimated using the fast Fourier transform (FFT) for each trial and all channels. An adaptive time window of 7 cycles length was shifted in 50 ms time-steps between −2 and 4 s. After applying a Hanning taper, power was estimated for frequencies between 2 and 30 Hz in steps of 1 Hz. In this type of frequency analysis, alpha power estimates are calculated on the basis of several hundred milliseconds and overlap. This approach allows illustrating and examining the temporal evolution of alpha activity in the different conditions across the complete trial. Since the planar gradiometers of each sensor triplet consist of a horizontal and vertical component, time–frequency analyses were performed separately on each component and afterwards summed to obtain one combined value.

Channel selection

For a selection of channels for further analysis, the obtained TFRs were averaged across subjects and power changes relative to a pre-stimulus baseline interval were computed (percent change relative to a baseline of −1 to 0 s). This was done separately for trials with stimulation of the left and right hand while averaging across attended and unattended trials of each hand. Similar to previous studies investigating the effects of spatial attention on somatosensory alpha activity associated with non-painful tactile stimuli (Haegens et al., 2011; van Ede et al., 2011), channels of interest for the examination of attention effects were chosen according to the strongest stimulus-induced response. Two groups of four adjacent combined sensors, each overlying left and right primary somatosensory areas, were selected according to the strongest post-stimulus alpha and beta suppression to a stimulus on the contralateral hand. For the sake of clarity, these two regions of interest will in the following be termed left and right primary somatosensory (S1) channels with respect to the hemisphere or ipsi- and contralateral S1 channels with respect to the stimulated hand (see highlighted sensors in Fig. 2A). The two groups of channels were symmetrically distributed with respect to the midline of the sensor array.

Individually adjusted alpha activity

For the analysis of pain-associated alpha activity, alpha band power was individually estimated for each subject by averaging power from TFRs across a 4 Hz frequency band comprising each subject's alpha peak frequency ± 2 Hz. To determine the individual peak frequency, segments of data from −1 to 0 s with respect to stimulus onset were extracted and multiplied with a Hanning taper prior to applying an FFT. Power spectra were computed between 2 and 30 Hz, combined for horizontal and vertical gradiometers and averaged across all trials and sensors. Then, the individual peak frequency between 7 and 15 Hz was determined for each subject.

Statistical analysis of attention effects

To analyze attention effects on pain-associated alpha activity, we performed analyses as follows. For each region of interest (left and right S1 channels), individual alpha activity was averaged separately for the 4 conditions (attended left hand stimulation, unattended left hand stimulation, attended right hand stimulation, unattended right hand stimulation). For both attended conditions, only trials in which stimuli were correctly localized were used. To disentangle attention effects in anticipation and in response to painful laser stimuli, the analysis focused on selected pre- (−1 to 0 s) and post-stimulus (0 to 2 s) time windows. The pre-stimulus interval was chosen regarding earlier findings showing that anticipatory attention effects are deployed with temporal specificity and are strongest just before an expected event (Rohenkohl and Nobre, 2011; van Ede et al., 2011). Therefore, in the current experiment, attention effects were expected to build up over the course of the anticipation period and be strongest immediately before each laser pulse. The post-stimulus interval was selected in accordance with earlier work demonstrating that the alpha suppression induced by painful laser stimuli is strongest within this time window (Ploner et al., 2006a).

Each statistical, time-resolved comparison between attended and unattended trials was performed in line with a two-step statistical approach used previously elsewhere (Hoogenboom et al., 2010; Lange et al., 2011). In a first step, individual alpha power was compared between attended and unattended trials by computing *t*-values for each subject and time point. Since *t*-values consist of the difference in mean power between the two attention conditions relative to the variance in power across trials, this step normalizes for inter-individual differences. The outcome was a subject-wise comparison of attended and unattended trials in the form of a *t*-value time course. For a further distributional normalization, all *t*-values were transformed to *z*-values (Mazaheri et al., 2009; van Dijk et al., 2008). In a second step, a group-level statistic used these single-subject *z*-value time courses and determined their consistency across subjects. The statistical significance of the difference between the two conditions was evaluated using a cluster-based randomization test (Maris and Oostenveld, 2007). Pooled *z*-values across subjects were computed for all time points. Neighboring time-bins exceeding an a priori threshold (uncorrected $p<.05$) were combined to clusters. Within every cluster, *z*-values were summed and the maximum of these sums was used as a cluster-level test statistic. Under the hypothesis of no difference between the two conditions, the difference between attended and unattended trials should not significantly differ from zero; i.e. the computed *z*-values should be interchangeable with zero. By randomly interchanging data across the two conditions within each subject (i.e. the individual *z*-scores and 0) and recalculating the cluster-level test statistic 1000 times, a reference distribution of maximum cluster *z*-value sums was obtained. This was then used to evaluate the statistical significance of the observed maximum cluster-level test statistic of the actual data. By clustering neighboring time points showing the same effect and selecting the maximum cluster-level statistic from each randomization for the reference distribution, this method deals with the multiple comparison problem and is not affected by partial dependence in the data (Lange et al., 2011; Maris and Oostenveld, 2007). Using this two-step statistical approach, 4 comparisons of attended vs. unattended trials were performed per hand: left S1 channels, pre-stimulus interval; left S1 channels, post-stimulus interval; right S1 channels, pre-stimulus interval; and right S1 channels, post-stimulus interval. Thereby, time periods showing significant modulation with attention were identified.

A further statistical analysis focused on the time periods with significant attentional modulation and examined the topographical distribution of attention effects beyond the preselected channels of interest. To this end, the same two-step procedure was applied without making an a priori channel selection. Single subject *z*-values were now computed for power averages of individual alpha activity over those time windows that had previously shown significant attentional differences. Clusters showing differences between attended and unattended trials were now formed along the channel instead of the time dimension and then tested for significance.

Pre-stimulus alpha lateralization index

To capture the hypothesized pre-stimulus alpha lateralization over both hemispheres in one value, a lateralization index of alpha power was calculated for each subject, in line with indices used by Haegens et al. (2011) and Thut et al. (2006) in similar spatial attention paradigms.

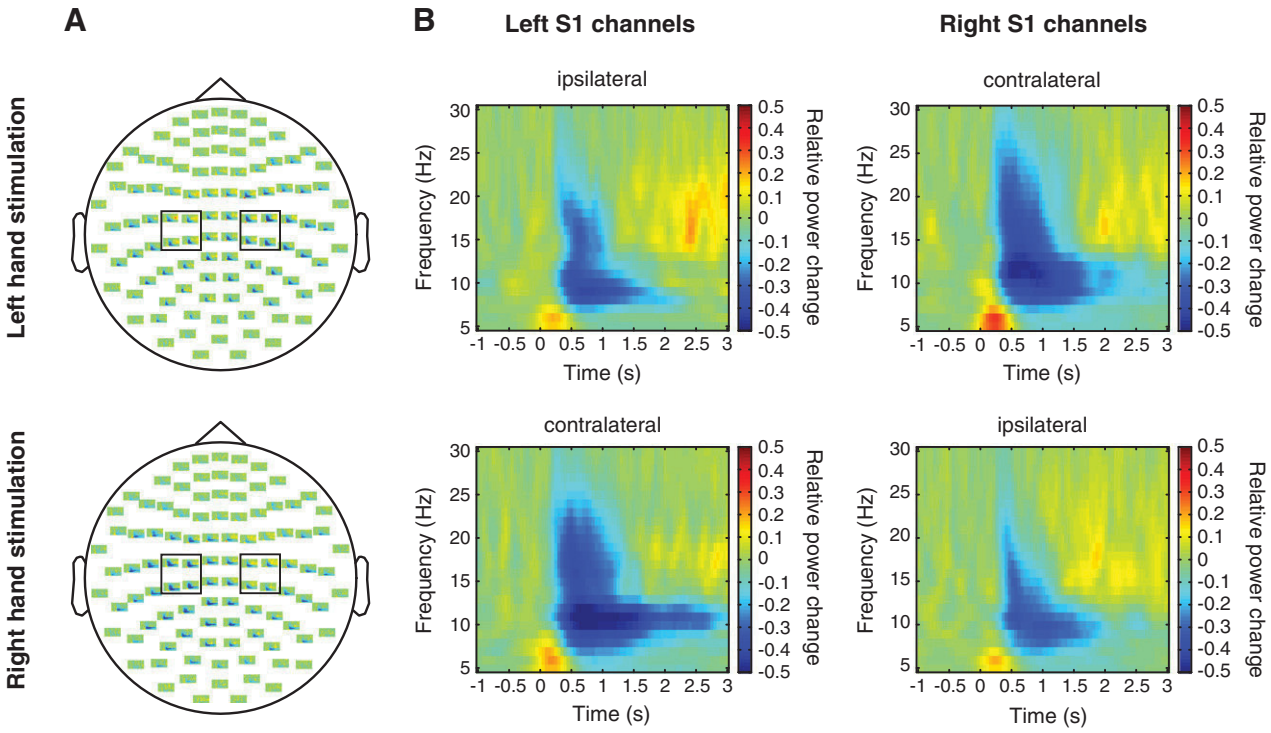

Fig. 2. Stimulus-induced effects used for channel selection. A. Grand average time–frequency representations (TFRs) of all combined MEG sensors across all trials with stimulation of the left (upper row) and right hands (lower row). TFRs were averaged across attended and unattended trials of the respective hand. 2 groups of 4 combined sensors each showing the strongest alpha and beta suppression in response to a laser stimulus on the contralateral hand were chosen for further analysis and denoted as left and right S1 channels. Both sensor groups are highlighted for both left and right hand stimulation trials, respectively. Scale as in B. B. Grand average TFRs across channels marked in A for left (upper row) and right (lower row) hand stimulation trials with time-point 0 representing the onset of the laser stimulus. Power changes relative to a pre-stimulus baseline (−1 to 0 s) are color-coded.

Again, this analysis focused on the last second immediately preceding laser stimulation. Using the previously identified left and right hemispheric S1 channel groups as regions of interest (ROIs), the index was calculated using the following formula:

$$\text{Alpha lateralization index} = \frac{\left(\text{Alpha ROI}_{\text{ipsilateral}} - \text{Alpha ROI}_{\text{contralateral}}\right)}{\left(\text{Alpha ROI}_{\text{ipsilateral}} + \text{Alpha ROI}_{\text{contralateral}}\right)}$$

Ipsi- and contralateral refers to the hemisphere with respect to the alleged spatial attentional orientation to the left or right hand. The calculation was based on the same FFT computation used for determination of the individual alpha peak frequency described in Individually adjusted alpha activity section. This approach was chosen to capture pure pre-stimulus effects and avoid a possible intermixture of pre- and post-stimulus effects close to the time point of laser stimulation caused by the sliding time window approach used for the calculation of TFRs. Power values were averaged across individually adjusted alpha frequency bands and the predefined sensors of interest before the alpha lateralization index were computed. This index gives a positive value when alpha power is lower over contralateral channels and/or higher over ipsilateral channels with respect to the attentional orientation and a negative value for the opposite scenario. The distribution of alpha lateralization indices across subjects was tested against the null hypothesis of zero mean, using a *t*-test. This analysis was performed for both left and right hand stimulation trials.

Trial-by-trial correlation of alpha power and pain ratings

In order to examine the functional relevance of attention-modulated alpha activity for behavior, the relationship between alpha power and pain ratings was investigated in a trial-by-trial analysis. For each trial, alpha power was averaged across those time periods and channels that were significantly modulated with attention in the previous analyses and subsequently log-transformed. Spearman correlation coefficients were calculated between the log-transformed power values and pain ratings for each subject. This analysis was restricted to attended trials since pain ratings were only obtained for trials in which the attended hand was stimulated. Again, the distribution of correlation coefficients across subjects was tested against the null hypothesis of zero mean, using a *t*-test. Bonferroni–Holm correction (Holm, 1979) was applied to all alpha levels to correct for multiple comparisons.

Results

Behavioral results

Laser stimuli on the attended hand were consistently rated as painful, pinprick-like sensations with an average rating of 3.26 ± 1.42 across both hands. Mean pain ratings did not differ between the left and right hand (3.20 ± 1.37 vs. 3.31 ± 1.51, $p > 0.1$). Stimuli on the attended hand were on average correctly localized to the stimulated target area in $84.44\% \pm 9.83$ of the trials. This rate was significantly lower for the left than the right hand ($79.96\% \pm 10.13$ vs. $88.93\% \pm 7.37$, $p = 0.005$).

Stimulus effects

Grand average time–frequency analysis across all left and right hand stimulation trials is illustrated in Fig. 2. Painful laser stimuli to either hand elicited a well-known sequence of a pain-induced power increase between 4 and 8 Hz reflecting the pain-evoked field followed by a pronounced alpha and beta suppression (Ploner et al., 2006a; Schulz et al., 2011). Alpha and beta suppression was widely distributed across bilateral somatosensory and parietal areas. Two groups of channels were selected for further analysis according to the strongest stimulus-induced response, which are supposed to overlay primary sensory cortices (Fig. 2A). Stimulus-induced suppression effects appeared slightly

enhanced over contralateral S1 sensors compared to ipsilateral S1 sensors (Fig. 2B).

Modulation of alpha activity with spatial attention

Across subjects, individual alpha peak frequencies varied between 8 and 11 Hz (mean ± standard deviation: 10.07 ± 0.88 Hz). For one subject, no individual alpha peak frequency could be detected. Instead, a standard value of 10 Hz corresponding to the average peak frequency across subjects was used for subsequent analyses. To reveal time windows during which attention affects pain-associated alpha activity, effects of spatial attention on individual alpha activity were analyzed for both hands on left and right S1 channels and during pre- and post-stimulus time intervals. In Fig. 3A, grand averages of alpha power illustrate the temporal evolution of alpha activity in the different conditions for left and right hand stimuli. Gray boxes mark time windows showing significant differences between attended and unattended trials. Please note that, while raw alpha power is displayed in Fig. 3A, group level statistics were performed on individual *z*-values, quantifying power differences between conditions relative to the variance across trials for each subject. In line with the general stimulus-induced response, alpha power was suppressed on both left and right S1 channels in response to painful laser stimuli, irrespective of whether they were attended or not. Differential attention effects were observed for pre- and post-stimulus time periods.

Pre-stimulus attention effects

For trials with stimulation of the left hand (Fig. 3A, upper row), significant pre-stimulus clusters were found for both ipsi- and contralateral S1 channels. Over ipsilateral S1 channels, a cluster extended from −0.65 to −0.4 s before the laser stimulus and showed increased alpha activity in attended compared to unattended trials (left hand cluster C1: $p = 0.020$). Over contralateral S1 channels, a cluster spanned the time period between −0.2 and 0 s and displayed the opposite pattern showing decreased alpha activity when the left hand was attended compared to when it was unattended (left hand cluster C3: $p = 0.034$). For trials with stimulation of the right hand (Fig. 3A, lower row), a trend for a cluster was observed on contralateral channels. This cluster extended from −0.15 to 0 s and showed decreased alpha activity for attended compared to unattended trials (right hand cluster C5: $p = 0.069$).

After having identified time windows during which attention significantly affects pre-stimulus pain-associated alpha activity, a further statistical analysis examined the topographical distribution of these attention effects over the complete sensor array. Individual alpha activity was averaged over those time windows showing significant differences in the time-resolved analysis and compared between attended and unattended trials for each hand. This analysis resulted in three topographies corresponding to the three time clusters found in the previous analysis (Fig. 3B, left column). The pre-stimulus effects indicated a lateralization of anticipatory alpha activity across hemispheres. For left hand stimulation trials, the topographies showed increased alpha activity over left/ipsilateral primary somatosensory areas (left hand cluster C1: $p = 0.040$) and decreased alpha activity over right/contralateral primary somatosensory areas when the left hand was attended (left hand cluster C3: $p = 0.009$). For right hand stimulation trials, the pre-stimulus cluster showed the corresponding mirroring effect displaying a trend for decreased alpha activity over left/contralateral S1 channels when the right hand was attended (right hand cluster C5: $p = 0.078$).

To capture this anticipatory alpha lateralization over both hemispheres in a single value, pre-stimulus attention effects from −1 to 0 s with respect to the stimulation were additionally quantified by calculating a subject-wise alpha lateralization index. As depicted in Fig. 4,

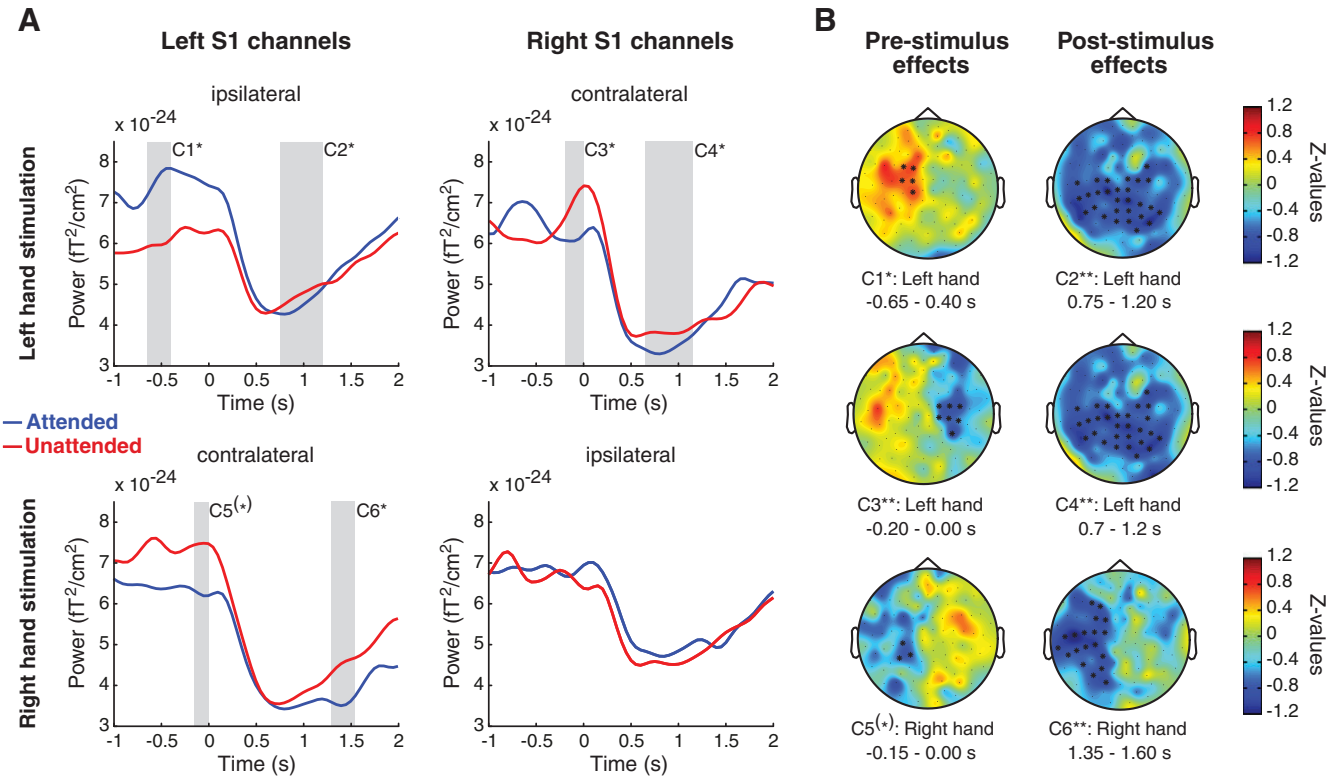

Fig. 3. Attention effects. A. Grand average temporal evolution of individual alpha activity on left and right S1 channels in attended and unattended trials of left (upper row) and right hand (lower row) stimulation trials (please see Fig. 2A for channel selection). Time-point 0 represents the onset of the laser stimulus. Gray boxes mark six time clusters (C1–C6) showing differences between attended and unattended trials ($^{(*)}p<0.1$, $^{*}p<0.05$). B. Topographical distribution of attention effects on alpha activity during time windows showing differences in A (topographical clusters C1–C6 correspond to time clusters C1–C6 in A). Z-values representing the statistical comparison between attended and unattended trials are color-coded. Positive values indicate increased, negative values decreased alpha power with attention. Sensor clusters showing modulation associated with attention are marked ($^{(*)}p<0.1$, $^{*}p<0.05$, $^{**}p<0.01$).

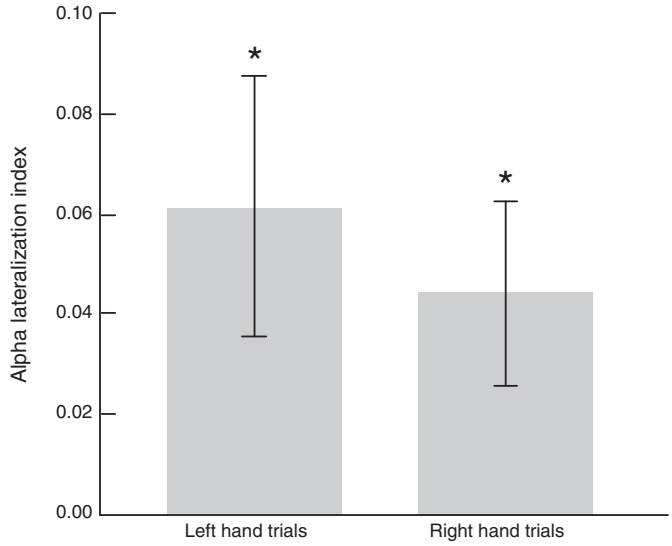

Fig. 4. Pre-stimulus alpha lateralization index. Mean values of alpha lateralization indices across subjects quantifying anticipatory pre-stimulus alpha modulation across both hemispheres. Error bars indicate the standard error of mean. The distribution of alpha lateralization indices across subjects was tested against the hypothesis of zero mean for both left and right hand stimulation trials separately. For both trial types, alpha lateralization indices were significantly higher than zero, indicating decreased contralateral and/or increased ipsilateral alpha power with respect to the attentional orientation to the left or right hand (*$p<0.05$).

pre-stimulus alpha lateralization was significantly higher than zero across subjects for both left and right hand stimulation trials (left hand: $p=0.016$, right hand: $p=0.016$), indicating lower alpha power over contralateral S1 channels and/or higher alpha power over ipsilateral S1 channels during the anticipation of a lateralized painful stimulus.

In summary, these pre-stimulus results indicate a lateralization of alpha activity in anticipation of a painful stimulus to the left or right hand. More specifically, alpha activity in primary somatosensory areas seems to be stronger when the ipsilateral hand is attended compared to when the contralateral hand is attended, indicating increased alpha activity over ipsilateral and/or decreased alpha activity over contralateral channels with respect to the attended hand.

Post-stimulus attention effects

The subsequent post-stimulus period was marked by significant decreases of alpha activity with attention (Fig. 3A). For trials with stimulation of the left hand, significant clusters emerged over both ipsi- (left hand cluster C2: $p=0.018$) and contralateral (left hand cluster C4: $p=0.011$) S1 channels. The significant cluster on ipsilateral S1 channels (C2) covered a time window from 0.75 to 1.2 s, whereas the cluster on contralateral S1 channels (C4) covered a time window from 0.7 to 1.2 s. For trials with stimulation of the right hand, a significant post-stimulus attention effect was found on contralateral S1 channels only (right hand cluster C6: $p=0.045$). This significant time cluster started later and extended from 1.35 to 1.6 s after stimulus onset. Again, alpha activity was decreased in attended trials. Overall, the post-stimulus effects indicate that alpha suppression in response to a painful laser stimulus is stronger and/or prolonged when the stimulated hand is attended.

In accordance with the analysis of pre-stimulus attention effects, a further analysis examined the topographical distribution of post-stimulus attention effects beyond the pre-selected channels of interest (Fig. 3B, right column). For both hands, significant clusters of reduced alpha activity with attention included channels over somatosensory and parietal areas contralaterally to the stimulated hand (left hand cluster C2: $p=0.002$, left hand cluster C4: $p=0.001$, right hand cluster C6: $p=0.002$). For left hand trials, the topographic clusters (C2 and C4) additionally covered ipsilateral somatosensory channels.

To summarize, post-stimulus attention effects of decreased alpha activity with attention were found for both left and right hand stimulation trials covering primarily contralateral somatosensory and parietal areas. The corresponding left hand stimulation post-stimulus clusters appeared both earlier in time and more widely spread including ipsilateral channels.

Correlation between early post-stimulus alpha activity and pain perception

To investigate the functional relevance of attention-related alpha activity for individual pain ratings, single trial correlation analyses were performed. Alpha power was averaged over time windows and channels that had shown modulation associated with attention in the previous analyses (Fig. 3). For each subject and on a trial-by-trial basis, the average alpha power was correlated with individual pain ratings during attended trials.

Trends for inverse correlations between individual pain ratings and alpha power averaged over the two post-stimulus clusters in trials with stimulation of the left hand were found (left hand cluster C2: mean $r=-0.13$; $p=0.027$, uncorrected; left hand cluster C4: mean $r=-0.15$; $p=0.018$, uncorrected). However, these correlations were no longer significant when p-values were corrected for a total of 6 comparisons between alpha power and pain ratings. Pre-stimulus alpha power and post-stimulus alpha power in trials with stimulation of the right hand did not show a correlation or a trend for a correlation with individual pain ratings.

Discussion

The aim of the current study was to investigate pre- and post-stimulus effects of attention on oscillatory alpha activity associated with painful laser stimuli to shed further light on the role of alpha activity during pain processing. We found that spatial attention to one hand differentially modulates alpha activity in anticipation of and in response to a painful stimulus on that hand. As hypothesized, alpha activity during the pre-stimulus period lateralized across the two hemispheres, being lower over primary somatosensory areas when the contralateral hand is attended compared to when the ipsilateral hand is attended. Post-stimulus alpha activity was consistently decreased over contralateral areas when attention was placed on the stimulated hand.

Pre- and post-stimulus alpha activity is differentially modulated with attention

On average, subjects correctly localized attended stimuli to the stimulated target area in 84% of the trials. Thus, performance was well above chance level but below ceiling effects, indicating an appropriate difficulty for a task intended to demand attention. Differential effects of attention on pain-associated alpha activity were observed, supporting a pronounced role of attention for the processing of pain.

Pre-stimulus attention effects

Spatial attention to the left or right hand was associated with a lateralization of pre-stimulus alpha activity. Alpha activity was lower over primary somatosensory areas when the contralateral hand was attended compared to when the ipsilateral hand was attended. This pattern was shown by comparisons of alpha activity in attended and unattended trials over left and right somatosensory areas separately and was additionally confirmed by the calculation of the alpha lateralization index across hemispheres. Interestingly, the alpha lateralization index seems to be most sensitive in detecting this effect. While the alpha lateralization index did reveal significant alpha lateralization for right hand stimulation trials, separate comparisons of alpha activity over left and right S1 channels only displayed a trend for an attention effect over left S1

channels. Together, these pre-stimulus attention effects support previous findings showing a similar anticipatory lateralization of alpha activity in somatosensory (Anderson and Ding, 2011; Haegens et al., 2011), visual (Gould et al., 2011; Thut et al., 2006) and auditory (Müller and Weisz, 2011; Thorpe et al., 2012) tasks. The present study extends these findings to the perception of pain. Our results thereby further substantiate the notion that the level of alpha activity reflects the degree of engagement/disengagement of a cortical region and is actively regulated by top-down processes like attention (Foxe and Snyder, 2011; Jensen and Mazaheri, 2010; Pfurtscheller et al., 1996). Interestingly, pre-stimulus attention effects in the present study appeared more consistently over left primary somatosensory areas, indicating possible hemispheric differences in the strength of modulation of ongoing oscillatory alpha activity in anticipation of a lateralized painful stimulus.

Whether the lateralization of anticipatory alpha activity found here is caused by an ipsilateral increase of alpha activity, a contralateral decrease, or a combination of both cannot be deduced from the current data, since the study used a block design lacking a baseline without an attentional orientation to the left or right hand. Studying anticipatory alpha modulation in the somatosensory system in a similar paradigm using non-painful tactile stimuli, Haegens et al. (2011) found that anticipatory alpha lateralization is mainly driven by a decrease of alpha activity contralateral to the attended hand in combination with a slight ipsilateral increase when the right hand is attended. However, the authors also concluded that the overall lateralization best reflects the attentional bias.

An active inhibition of cortical areas by increased alpha activity has particularly been discussed in the context of inhibiting distracting input presented simultaneously to task-relevant target stimuli (Fu et al., 2001; Haegens et al., 2012; Händel et al., 2011; Kelly et al., 2006). In the present study, painful stimuli were never presented simultaneously to both hands. Our aim was to investigate both pre- and post-stimulus effects of attention on pain-associated alpha activity. A concurrent stimulation of both hands, however, would have caused overlapping neuronal responses to both stimuli in the post-stimulus period. To be able to examine the attentional modulation of a single stimulus, painful stimuli were applied either to the attended or the unattended hand. Previous work showing both stronger anticipatory and stimulus-induced alpha suppression for painful compared to non-painful stimuli already suggested a particularly intense processing of pain and pain-associated stimuli (Babiloni et al., 2003; Ploner et al., 2006a; Whitmarsh et al., 2011). Therefore, one might assume that the inhibition of a distracting painful stimulus by anticipatory alpha modulation requires more resources than the inhibition of a non-painful distracting stimulus. Future studies should examine if anticipatory pre-stimulus alpha lateralization in the context of distracting painful stimuli is also particularly pronounced.

Lastly, anticipatory alpha modulation has been shown to be reduced in older compared to younger subjects in a visual paradigm requiring subjects to anticipate an upcoming target stimulus in time (Zanto et al., 2011). Since the age of subjects in the current study spanned a broad range between 24 and 74 years, age might have had an influence on the size of the effects reported here. However, a correlation analysis between pre-stimulus alpha lateralization as measured by the alpha lateralization index and age did not reveal a significant relation between the two measures (data not reported). Since Zanto et al. (2011) studied temporal attention effects in the visual system, these different results might indicate that age affects attentional processes differently in different modalities and/or regarding different types of attention, which again is a very interesting area of future research.

Post-stimulus attention effects

Attention consistently reduced post-stimulus alpha activity in line with an increased cortical activation following an attended painful stimulus. Since we expected attention to affect both pre- and post-stimulus alpha activity, absolute alpha power values rather than relative power changes with respect to baseline were statistically compared. If attention affects pre-stimulus activity, performing a baseline correction relative to this activity can artificially induce post-stimulus attention effects that in fact originate from baseline differences. Controlling for such a mixture of effects, our data demonstrate that attention can independently influence both pre- and post-stimulus activity. The time courses of alpha activity in the different attention conditions shown in Fig. 3A suggest that spatial attention intensifies and prolongs the stimulus-induced suppression of alpha activity. These findings are consistent with a previous report of increased alpha suppression in response to painful laser stimuli with attention (Ohara et al., 2004). This study analyzed data with respect to a pre-stimulus baseline, which might have biased the size of the attention effect. However, our data revealed a similar effect with an analysis controlling for pre-stimulus effects. Taken together, these results strongly suggest that the widespread pain-induced alpha suppression reflecting the alerting function of pain is increased with attention. Interestingly, attention reduced post-stimulus alpha activity for left hand stimulation trials even on channels overlying ipsilateral somatosensory areas. Thus, the enhancement of the widespread alerting effect of painful stimuli by attention affects large parts of the brain. Again, this hints at the interesting possibility that the left hemisphere is more easily modulated than the right hemisphere during processing of a lateralized painful stimulus.

Relation between attention-modulated alpha activity and individual pain ratings

Under the assumption that the present attention effects are functionally relevant, pain-associated alpha activity should also affect behavioral responses. In the current study, we found trends for an inverse relation between post-stimulus alpha activity and individual pain rating for trials with stimulation of the left hand. In principle, this pattern tallies with previous studies that showed higher pain ratings when alpha activity close the moment of stimulus onset was low (Babiloni et al., 2006; Schulz et al., 2011). In these studies, correlation analyses were performed using selected electrodes of interest, representative of primary somatosensory areas contralateral to the stimulated hand. In the current analysis, alpha activity estimates for the correlation analysis were averaged across all sensors showing significant modulation with spatial attention, which were distributed across broad areas of the brain. Possibly, the level of alpha activity in primary somatosensory areas contralateral to the stimulated hand is most relevant for the actual pain perception while attention affects pain-associated alpha activity in much broader areas. This would have led to relatively small and more variable correlation coefficients between alpha activity and individual pain ratings in the current study.

Regarding pre-stimulus alpha activity, there was no indication of a relation to individual pain ratings. Previously, it has been demonstrated for the visual system that pre-stimulus alpha lateralization across subjects correlates with motion detection performance in the unattended but not in the attended visual hemifield (Händel et al., 2011). The pre-stimulus modulation of alpha might therefore be more related to the successful inhibition of unattended than of the processing of attended stimuli. However, this hypothesis could not be tested in the current study since there was no pain rating given for stimuli applied to the unattended side.

Higher localization rate for right hand than left hand stimuli

As shown by the behavioral results, subjects were more successful in localizing attended stimuli on the right than on the left hand although the subjectively perceived pain intensity did not differ between the two. This finding is unexpected since a previous study by Schlereth et al. (2001) reported no differences in spatial discrimination thresholds for laser stimuli between both hands in a similar task. As the majority of subjects (14 out of 15 subjects) in the current study were right-handed, this might reflect a perceptual superiority of the dominant hand in the specific

task used here. As a consequence, the attentional load due to the localization task might have been higher when the left hand was attended compared to when the right hand was attended, leading to stronger attention effects.

Importantly, such hand differences could not differentially influence pre-stimulus effects for left and right hand stimulation trials since the number of trials where the left hand was attended and the number of trials where the right hand was attended was equal for both, i.e. 50% each. Regarding post-stimulus effects, however, a higher attentional load when the left hand was attended might have contributed to a topographically more widespread reduction of alpha activity with attention for a left hand stimulus. For right hand stimuli, in contrast, the attention effect was confined to the left, i.e. contralateral, hemisphere and we did not find a post-stimulus attention effect over right primary somatosensory areas. Future studies equating performance levels between the two hands are needed to further examine potential effects of attentional load and handedness on the degree of modulation of pain-associated alpha activity with attention.

Conclusions

The present study demonstrated that both pre- and post-stimulus oscillatory alpha activity is modulated, if attention is spatially shifted to one hand during anticipation of a painful laser stimulus to that hand. These effects indicate a pronounced role of attention during the processing of pain, which is at least partially mediated by modulation of alpha activity. Spatial attention was associated with a lateralization of pre-stimulus alpha activity, i.e. alpha activity was decreased over primary somatosensory areas when the contralateral hand was attended compared to when the ipsilateral hand was attended. This modulation of ongoing alpha activity presumably subserves the overall facilitation of processing of stimuli on the attended hand. Post-stimulus alpha activity, in contrast, was reduced with attention over widespread areas, most likely reflecting an increased cortical activation and intensified alerting function of pain. This flexible regulation of alpha activity is in accordance with previous findings in other modalities. Thus, our results further strengthen the notion that oscillatory alpha activity reflects a top-down controlled gating mechanism employed throughout the brain.

Role of the funding source

This study was supported by the German Research Foundation (SFB 575, project C4). M.Bu. was supported by a Marie Curie Fellowship of the EU (FP7-PEOPLE-2009-IEF-253965), N.K. by the German National Academic Foundation and M.Br. by the Integrated Graduate School 575. E.M. and N.K. were supported by travel grants from the Integrated Graduate School 575 and the Boehringer Ingelheim Foundation (B.I.F.).

Acknowledgments

We thank Ms. Alla Solotuchin and Mr. Ulf M. Zierhut for help with the MEG data collection. Furthermore, we are grateful to our colleagues from the University of Düsseldorf Dr. Joachim Lange, Dr. Tolga Özkurt, Dr. Holger Krause, Dr. Hanneke van Dijk and Jan Hirschmann for support with data analysis and for helpful discussions and comments.

References

Anderson, K.L., Ding, M., 2011. Attentional modulation of the somatosensory mu rhythm. Neuroscience 180, 165–180.

Babiloni, C., Brancucci, A., Babiloni, F., Capotosto, P., Carducci, F., Cincotti, F., Arendt-Nielsen, L., Chen, A.C.N., Rossini, P.M., 2003. Anticipatory cortical responses during the expectancy of a predictable painful stimulation. A high-resolution electroencephalography study. Eur. J. Neurosci. 18 (6), 1692–1700.

Babiloni, C., Brancucci, A., Arendt-Nielsen, L., Babiloni, F., Capotosto, P., Carducci, F., Cincotti, F., Del Percio, C., Petrini, L., Rossini, P.M., Chen, A.C.N., 2004. Attentional processes and cognitive performance during expectancy of painful galvanic stimulations: a high-resolution EEG study. Behav. Brain Res. 152 (1), 137–147.

Babiloni, C., Brancucci, A., Del Percio, C., Capotosto, P., Arendt-Nielsen, L., Chen, A.C.N., Rossini, P.M., 2006. Anticipatory electroencephalography alpha rhythm predicts subjective perception of pain intensity. J. Pain 7 (10), 709–717.

Berger, H., 1929. Über das Elektrenkephalogramm des Menschen. Arch. Psychiatr. Nervenkr. 87, 527–570.

Bushnell, M.C., Duncan, G.H., Hofbauer, R.K., Ha, B., Chen, J.I., Carrier, B., 1999. Pain perception: is there a role for primary somatosensory cortex? Proc. Natl. Acad. Sci. U. S. A. 96 (14), 7705–7709.

Del Percio, C., Le Pera, D., Arendt-Nielsen, L., Babiloni, C., Brancucci, A., Chen, A.C.N., De Armas, L., Miliucci, R., Restuccia, D., Valeriani, M., Rossini, P.M., 2006. Distraction affects frontal alpha rhythms related to expectancy of pain: an EEG study. Neuroimage 31 (3), 1268–1277.

Foxe, J.J., Snyder, A.C., 2011. The role of alpha-band brain oscillations as a sensory suppression mechanism during selective attention. Front. Psychol. 2, 154.

Fu, K.M., Foxe, J.J., Murray, M.M., Higgins, B.A., Javitt, D.C., Schroeder, C.E., 2001. Attention-dependent suppression of distracter visual input can be cross-modally cued as indexed by anticipatory parieto-occipital alpha-band oscillations. Brain Res. Cogn. Brain Res. 12 (1), 145–152.

Gould, I.C., Rushworth, M.F., Nobre, A.C., 2011. Indexing the graded allocation of visuospatial attention using anticipatory alpha oscillations. J. Neurophysiol. 105 (3), 1318–1326.

Gross, J., Schnitzler, A., Timmermann, L., Ploner, M., 2007. Gamma oscillations in human primary somatosensory cortex reflect pain perception. PLoS Biol. 5 (5), e133.

Haegens, S., Händel, B.F., Jensen, O., 2011. Top-down controlled alpha band activity in somatosensory areas determines behavioral performance in a discrimination task. J. Neurosci. 31 (14), 5197–5204.

Haegens, S., Luther, L., Jensen, O., 2012. Somatosensory anticipatory alpha activity increases to suppress distracting input. J. Cogn. Neurosci. 24 (3), 677–685.

Händel, B.F., Haarmeier, T., Jensen, O., 2011. Alpha oscillations correlate with the successful inhibition of unattended stimuli. J. Cogn. Neurosci. 23 (9), 2494–2502.

Hari, R., Salmelin, R., 1997. Human cortical oscillations: a neuromagnetic view through the skull. Trends Neurosci. 20 (1), 44–49.

Hauck, M., Lorenz, J., Engel, A.K., 2007. Attention to painful stimulation enhances gamma-band activity and synchronization in human sensorimotor cortex. J. Neurosci. 27 (35), 9270–9277.

Hauck, M., Lorenz, J., Engel, A.K., 2008. Role of synchronized oscillatory brain activity for human pain perception. Rev. Neurosci. 19 (6), 441–450.

Holm, S., 1979. A simple sequentially rejective multiple test procedure. Scand. J. Stat. 6 (2), 65–70.

Hoogenboom, N., Schoffelen, J.-M., Oostenveld, R., Fries, P., 2010. Visually induced gamma-band activity predicts speed of change detection in humans. Neuroimage 51 (3), 1162–1167.

Jensen, O., Mazaheri, A., 2010. Shaping functional architecture by oscillatory alpha activity: gating by inhibition. Front. Hum. Neurosci. 4, 186.

Jones, S.R., Kerr, C.E., Wan, Q., Pritchett, D.L., Hämäläinen, M., Moore, C.I., 2010. Cued spatial attention drives functionally relevant modulation of the mu rhythm in primary somatosensory cortex. J. Neurosci. 30 (41), 13760–13765.

Jung, T.P., Makeig, S., Humphries, C., Lee, T.W., McKeown, M.J., Iragui, V., Sejnowski, T.J., 2000. Removing electroencephalographic artifacts by blind source separation. Psychophysiology 37 (2), 163–178.

Kelly, S.P., Lalor, E.C., Reilly, R.B., Foxe, J.J., 2006. Increases in alpha oscillatory power reflect an active retinotopic mechanism for distracter suppression during sustained visuospatial attention. J. Neurophysiol. 95 (6), 3844–3851.

Lange, J., Oostenveld, R., Fries, P., 2011. Perception of the touch-induced visual double-flash illusion correlates with changes of rhythmic neuronal activity in human visual and somatosensory areas. Neuroimage 54 (2), 1395–1405.

Maris, E., Oostenveld, R., 2007. Nonparametric statistical testing of EEG- and MEG-data. J. Neurosci. Methods 164 (1), 177–190.

Mazaheri, A., Nieuwenhuis, I.L.C., van Dijk, H., Jensen, O., 2009. Prestimulus alpha and mu activity predicts failure to inhibit motor responses. Hum. Brain Mapp. 30 (6), 1791–1800.

Miron, D., Duncan, G.H., Bushnell, M.C., 1989. Effects of attention on the intensity and unpleasantness of thermal pain. Pain 39 (3), 345–352.

Müller, N., Weisz, N., 2011. Lateralized auditory cortical alpha band activity and interregional connectivity pattern reflect anticipation of target sounds. Cereb. Cortex. http://dx.doi.org/10.1093/cercor/bhr232.

Niedermeyer, E., Lopes da Silva, F.H., 2005. Electroencephalography: Basic Principles, Clinical Applications, and Related Fields, fifth ed. Lippincott Williams & Wilkins, Philadelphia.

Ohara, S., Crone, N.E., Weiss, N., Lenz, F.A., 2004. Attention to a painful cutaneous laser stimulus modulates electrocorticographic event-related desynchronization in humans. Clin. Neurophysiol. 115 (7), 1641–1652.

Oostenveld, R., Fries, P., Maris, E., Schoffelen, J.-M., 2011. FieldTrip: open source software for advanced analysis of MEG, EEG, and invasive electrophysiological data. Comput. Intell. Neurosci. 2011, 156869.

Petrovic, P., Petersson, K.M., Ghatan, P.H., Stone-Elander, S., Ingvar, M., 2000. Pain-related cerebral activation is altered by a distracting cognitive task. Pain 85 (1–2), 19–30.

Pfurtscheller, G., Stancák Jr., A., Neuper, C., 1996. Event-related synchronization (ERS) in the alpha band—an electrophysiological correlate of cortical idling: a review. Int. J. Psychophysiol. 24 (1–2), 39–46.

Ploner, M., Gross, J., Timmermann, L., Pollok, B., Schnitzler, A., 2006a. Pain suppresses spontaneous brain rhythms. Cereb. Cortex 16 (4), 537–540.

Ploner, M., Gross, J., Timmermann, L., Pollok, B., Schnitzler, A., 2006b. Oscillatory activity reflects the excitability of the human somatosensory system. Neuroimage 32 (3), 1231–1236.

Rohenkohl, G., Nobre, A.C., 2011. Alpha oscillations related to anticipatory attention follow temporal expectations. J. Neurosci. 31 (40), 14076–14084.
Schlereth, T., Magerl, W., Treede, R., 2001. Spatial discrimination thresholds for pain and touch in human hairy skin. Pain 92 (1–2), 187–194.
Schlereth, T., Baumgärtner, U., Magerl, W., Stoeter, P., Treede, R.-D., 2003. Left-hemisphere dominance in early nociceptive processing in the human parasylvian cortex. Neuroimage 20 (1), 441–454.
Schulz, E., Tiemann, L., Schuster, T., Gross, J., Ploner, M., 2011. Neurophysiological coding of traits and states in the perception of pain. Cereb. Cortex 21 (10), 2408–2414.
Schulz, E., Zherdin, A., Tiemann, L., Plant, C., Ploner, M., 2012. Decoding an individual's sensitivity to pain from the multivariate analysis of EEG data. Cereb. Cortex 22 (5), 1118–1123.
Thorpe, S., D'Zmura, M., Srinivasan, R., 2012. Lateralization of frequency-specific networks for covert spatial attention to auditory stimuli. Brain Topogr. 25 (1), 39–54.
Thut, G., Nietzel, A., Brandt, S.A., Pascual-Leone, A., 2006. Alpha-band electroencephalographic activity over occipital cortex indexes visuospatial attention bias and predicts visual target detection. J. Neurosci. 26 (37), 9494–9502.
Treede, R.-D., 2003. Neurophysiological studies of pain pathways in peripheral and central nervous system disorders. J. Neurol. 250 (10), 1152–1161.
van Dijk, H., Schoffelen, J.-M., Oostenveld, R., Jensen, O., 2008. Prestimulus oscillatory activity in the alpha band predicts visual discrimination ability. J. Neurosci. 28 (8), 1816–1823.
van Ede, F., de Lange, F., Jensen, O., Maris, E., 2011. Orienting attention to an upcoming tactile event involves a spatially and temporally specific modulation of sensorimotor alpha- and beta-band oscillations. J. Neurosci. 31 (6), 2016–2024.
Whitmarsh, S., Nieuwenhuis, I.L.C., Barendregt, H.P., Jensen, O., 2011. Sensorimotor alpha activity is modulated in response to the observation of pain in others. Front. Hum. Neurosci. 5, 91.
Zanto, T.P., Pan, P., Liu, H., Bollinger, J., Nobre, A.C., Gazzaley, A., 2011. Age-related changes in orienting attention in time. J. Neurosci. 31 (35), 12461–12470.

5.)

Kahlbrock N, **Butz M[c]**, May ES, Brenner M, Kircheis G, Häussinger D, Schnitzler A, "*Lowered frequency and impaired modulation of gamma band oscillations in a bimodal attention task are associated with reduced critical flicker frequency*", Neuroimage 2012 Mai 15;61(1):216-27.

Impact-Faktor: 6.3

NeuroImage 61 (2012) 216–227

Contents lists available at SciVerse ScienceDirect

NeuroImage

journal homepage: www.elsevier.com/locate/ynimg

Lowered frequency and impaired modulation of gamma band oscillations in a bimodal attention task are associated with reduced critical flicker frequency

Nina Kahlbrock [a], Markus Butz [a,b,*], Elisabeth S. May [a], Meike Brenner [a], Gerald Kircheis [c], Dieter Häussinger [c], Alfons Schnitzler [a,d]

[a] Heinrich-Heine-University Düsseldorf, Medical Faculty, Institute of Clinical Neuroscience and Medical Psychology, Universitätsstraße 1, D-40225 Düsseldorf, Germany
[b] University College London, Institute of Neurology, 33 Queen Square, London, WC1N 3BG, UK
[c] Heinrich-Heine-University Düsseldorf, Medical Faculty, Department of Gastroenterology, Hepatology and Infectious Disease, Universitätsstraße 1, D-40225 Düsseldorf, Germany
[d] Heinrich-Heine-University Düsseldorf, Medical Faculty, Department of Neurology, Universitätsstraße 1, D-40225 Düsseldorf, Germany

ARTICLE INFO

Article history:
Accepted 21 February 2012
Available online 1 March 2012

Keywords:
MEG
Oscillations
Gamma
CFF
Hepatic encephalopathy
GABA

ABSTRACT

Visual attention is associated with occipital gamma band activity. While gamma band power can be modulated by attention, the frequency of gamma band activity is known to decrease with age. The present study tested the hypothesis that reduced visual attention is associated with a change in induced gamma band activity. To this end, 26 patients with liver cirrhosis and 8 healthy controls were tested. A subset of patients showed symptoms of hepatic encephalopathy (HE), a frequent neuropsychiatric complication in liver disease, which comprises a gradual increase of cognitive dysfunction including attention deficits. All participants completed a behavioral task requiring shifts of attention between simultaneously presented visual and auditory stimuli. Brain activity was recorded using magnetoencephalography (MEG). The individual critical flicker frequency (CFF) was assessed as it is known to reliably reflect the severity of HE.

Results showed correlations of behavioral data and HE severity, as indexed by CFF. Individual visual gamma band peak frequencies correlated positively with the CFF ($r = 0.41$). Only participants with normal, but not with pathological CFF values showed a modulation of gamma band power with attention.

The present results suggest that CFF and attentional performance are related. Moreover, a tight relation between the CFF and occipital gamma band activity both in frequency and power is shown. Thus, the present study provides evidence that a reduced CFF in HE, a disease associated with attention deficits, is closely linked to a slowing of gamma band activity and impaired modulation of gamma band power in a bimodal attention task.

Introduction

Cortical gamma band activity (30–100 Hz) is known as a key correlate of cognition (Fries et al., 2008) and has been associated with various cognitive functions (Gray et al., 1989; Roelfsema et al., 1997; Tallon-Baudry et al., 1998), including attention (Fries et al., 2001; Hoogenboom et al., 2006, 2010; Kaiser et al., 2006; Lachaux et al., 2005; Steinmetz et al., 2000). The power of visually induced gamma band activity can be modulated by attention (Gruber et al., 1999; Kahlbrock et al., 2012; Siegel et al., 2008; Tallon-Baudry et al., 2005; Vidal et al., 2006; Wyart and Tallon-Baudry, 2008). The frequency of visually induced gamma band activity seems to be specific to certain cognitive operations. Vidal et al. (2006) showed in their study that distinct frequencies of gamma band oscillations are related to attention and grouping related activity, respectively. However, when stimuli, cognitive operation, and cognitive demand remain constant, gamma band power and frequency have been demonstrated to be very consistent across measurements within-subjects. Nevertheless, high inter-subject variability in power and frequency of gamma band responses can be observed (Hoogenboom et al., 2006; Muthukumaraswamy et al., 2010). The underlying causes of this variability have not been finally explained so far.

Two recent studies, including participants from first to fifth decade of life, have shown that the frequency of gamma band activity decreases with age (Gaetz et al., 2011b; Muthukumaraswamy et al., 2010). Moreover, in subjects suffering from schizophrenia, it has been shown that the frequency of phase-locked gamma band activity related to gestalt perception is decreased and correlates with specific symptoms of the disease, i.e. visual hallucinations, thought disorder, and disorganization (Spencer et al., 2004). Interestingly, these patients experience multiple cognitive deficits, which can be seen as core pathology of the disorder (Green, 1996).

Distinct oscillation features have been demonstrated in various neurological and psychiatric diseases (Schnitzler and Gross, 2005;

* Corresponding author.
E-mail address: m.butz@ucl.ac.uk (M. Butz).

1053-8119/$ – see front matter © 2012 Elsevier Inc. All rights reserved.
doi:10.1016/j.neuroimage.2012.02.063

Uhlhaas and Singer, 2006). Especially, a slowing of brain activity in lower frequencies, i.e. delta, alpha, and beta band activity has been demonstrated. For example, patients with brain infarct or brain tumor show increased activity in the delta band in perilesional areas (Butz et al., 2004; de Jongh et al., 2003). Patients with Alzheimer's disease show a reduction in resting state gamma band synchronization (Koenig et al., 2005).

Also in hepatic encephalopathy (HE), the neurological entity studied in the present work, spontaneous oscillatory activity and the mean resting activity electroencephalography (EEG) peak frequency have been shown to be progressively slowed (e.g., Amodio et al., 1999, 2009; Bajaj, 2010; Davies et al., 1991; Kullmann et al., 2001; Montagnese et al., 2007, 2011; Olesen et al., 2011; Parson-Smith et al., 1957; Van der Rijt et al., 1984). Alterations in the EEG are associated with the severity of HE (Marchetti et al., 2011). Hence, the EEG can be used to complement the neurological examination for HE, i.e., diagnosis, grading, and prediction (Amodio and Gatta, 2005; Guerit et al., 2009). HE is a frequent, potentially reversible, neuropsychiatric complication of chronic liver disease, involving multiple cognitive and motor symptoms, altered sleep patterns, and changes in vigilance state (for a review see Butterworth, 2000; Häussinger and Schliess, 2008). Of special relevance for the present study is one key symptom of HE — a gradual increase of attention deficits with increasing disease severity (Amodio et al., 2005; Kircheis et al., 2009; Pantiga et al., 2003; Weissenborn et al., 2001, 2005). Previous studies addressing the motor symptoms in HE revealed a pathologically slowed thalamo-cortico-muscular coupling with increasing severity of HE (Timmermann et al., 2002, 2003). Disease severity of HE can be quantified by determining the critical flicker frequency (CFF), which decreases with increasing disease severity (Kircheis et al., 2002; Prakash and Mullen, 2010; Romero-Gómez et al., 2007; Sharma et al., 2007). Accordingly, Timmermann et al. (2008) showed a strong correlation between the slowing of cortico-muscular coupling and the CFF. Based on the findings of slowed coupling in the motor systems of HE patients, Timmermann et al. (2005) hypothesized that a global slowing of oscillatory activity in various human cerebral subsystems could represent a key mechanism in the pathophysiology of HE. Along these lines, the question arises whether certain diseases that involve cognitive deficits are associated with a slowing of gamma band brain activity.

The present study aimed to test the relation of disease severity and the frequency of attention-related visually induced gamma band activity in a population of HE patients. In addition, the subject's capacity to modulate attention and concurrently modulate the power of attention-related occipital gamma band activity was scrutinized. Subjects completed a behavioral task requiring shifts of attention between simultaneously presented visual and auditory stimuli, while brain activity was recorded using magnetoencephalography (MEG). A reduction in attention-related gamma band peak frequencies with increasing disease severity was hypothesized, adhering to the hypothesis of slowed oscillatory brain activity as a key phenomenon in the pathophysiology of HE. Due to the known attentional deficits in this disease, a reduced capacity to modulate gamma band power with attention was expected.

Methods

Participants

Patients and controls

26 patients with liver cirrhosis, confirmed by sonography or fibroscan (>13 kPa) and 8 healthy, age-matched controls underwent a comprehensive clinical assessment including blood tests, neuropsychometric computer tests (Vienna test system, WINWTS, Version 4.50, 1999), assorted subtests of the test battery of Tests of Attentional Performance (TAP; PSYTEST, Herzogenrath, Germany), and CFF measurements (Eberhardt, 1994). As described in Kircheis et al. (2002) and according to *West-Haven* Criteria (Conn and Lieberthal, 1979) and psychometric test results, patients were classified into three groups: (i) HE0, i.e. patients showing no signs of HE, (ii) minimal HE (mHE), i.e., patients showing no clinical signs of HE, but pathological results in at least two psychometric tests, and (iii) HE1, i.e. manifest HE of grade 1, patients showing clinical signs of HE. The fourth group constituted of healthy control participants, i.e., (iv) controls (please see Table 1 for further details about subjects' characteristics). 24 patients performed the tests for grading of HE stage within two days, two patients within a week before or after the MEG measurement. All subjects had normal or corrected to normal vision and normal hearing. All of them gave their written informed consent. The study was approved by the local ethics committee (study no. 2895) and was performed in accordance with the Declaration of Helsinki.

General exclusion criteria were neurological/psychiatric illness, intake of psychoactive drugs, the existence of an HIV infection, Wilson's disease, Korsakoff's syndrome, and chronic pain syndrome. Patients with liver cirrhosis stemming from alcohol abuse had to be abstinent from alcohol for at least 6 months. To further control for this, blood

Table 1
Participant data.

Group	Subj. no.	Age	Sex	CFF	Cirrhosis etiology	Child Pugh Score
Control	1	51	m	44.3	–	–
	2	46	f	41.1	–	–
	3	67	m	39.8	–	–
	4	71	m	–	–	–
	5	69	f	40.8	–	–
	6	58	f	41.4	–	–
	7	61	f	38.4	–	–
	8	73	m	38.1	–	–
	n = 8	**62.0 ± 3.5**		**40.6 ± 0.8**		
HE0	9	55	f	39.4	Ethanol	A
	10	53	m	43.0	Ethanol	B
	11	48	m	41.8	Hepatitis C	C
	12	44	f	41.3	PBC	A
	13	69	f	38.4	Hepatitis C	A
	14	60	m	42.3	Ethanol	A
	15	70	m	39.0	Hepatitis C	A
	16	59	m	39.1	Hepatitis B	A
	n = 8	**52.3 ± 3.3**		**40.5 ± 0.6**		
mHE	17	60	m	38.6	Cryptogenic	B
	18	59	f	39.1	Hepatitis C	A
	19	57	m	38.3	Ethanol	A
	20	65	f	39.0	Ethanol	A
	21	56	m	35.7	Ethanol	B
	22	57	m	37.2	Ethanol	A
	23	62	m	39.9	Cryptogenic	A
	24	52	m	39.4	Hepatitis C	A
	n = 8	**58.5 ± 1.3**		**38.4 ± 0.5**		
HE1	25	69	m	38.6	Ethanol	B
	26	67	m	36.2	Autoimmune	C
	27	70	m	38.3	Hepatitis A/B	B
	28	72	m	35.5	Hepatitis C	B
	29	75	f	38.3	Cryptogenic	B
	30	65	f	37.7	Ethanol	C
	31	45	m	34.8	PSC	C
	32	45	f	32.6	Autoimmune	C
	33	63	m	36.4	Ethanol	A
	34	59	m	32.4	Ethanol	C
	n = 10	**63.0 ± 3.3**		**36.1 ± 0.7**		

Individual participant specific data are shown. For age and CFF, group mean values ± standard errors of the mean are given. Gender is coded as f = female and m = male. Etiology of liver cirrhosis was assessed by each patient's medical history, PSC = Primary sclerosing cholangitis, PBC = Primary biliary cirrhosis. Grading of liver cirrhosis was done according to the European Child-Pugh-classification (Pugh et al., 1973).

ethanol levels and carbohydrate deficient transferrin (CDT) were measured.

Groups of participants sorted by CFF

Due to an ongoing discussion of the validity of the common classification scheme of HE into groups of HE0, mHE, and HE1-HE4 (Häussinger et al., 2006; Kircheis et al., 2007), all analyses were performed on an alternative group classification scheme. According to Kircheis et al. (2002), a critical flicker frequency (CFF, see *Determination of the critical flicker frequency (CFF)* for more information) value of 39 Hz is described as being the critical cut-off frequency separating patients with manifest HE from controls and HE0 patients. Therefore, all participants showing significant gamma band activity in response to the visual stimulus (*visual* condition, *Bimodal reaction time paradigm* and *Individual gamma band peaks and power*) were sorted by CFF into one group of participants with low, i.e. pathological, CFF (<39 Hz, $n=12$) and one group of subjects with high, i.e. normal, CFF (≥ 39 Hz, $n=14$). In a second step, all analyses were repeated, including patients only (low CFF: $n=10$ and high CFF: $n=10$). Henceforth, the groups defined by their CFF values will be referred to as low and high CFF groups respectively.

Data acquisition

Determination of the critical flicker frequency (CFF)

The critical flicker frequency (CFF) is the frequency threshold at which a flickering light is perceived as flickering and no longer as continuous (normally ≥ 39 Hz for healthy people). The CFF has been shown to reliably quantify and monitor the severity of HE, i.e. the lower the CFF the higher the severity of HE (Kircheis et al., 2002; Prakash and Mullen, 2010; Romero-Gómez et al., 2007; Sharma et al., 2007). CFF thresholds were assessed using the Schuhfried Test System (Dr. Schuhfried Inc., Mödling, Austria). In gradual steps of 0.5 to 0.1 Hz/s rectangular light pulses decreased their frequency from 60 Hz downwards until the subjects indicated by a button press that they perceived them as flickering. Details of the recording procedure can be found in Kircheis et al. (2002). Only mean CFF values with a standard deviation below 0.5 Hz were considered for further analyses. All subjects except for one control subject met this criterion. CFF data of this control subject were not used in further analyses.

Bimodal reaction time paradigm

A paradigm adapted and simplified from Kahlbrock et al. (2012) was used, as illustrated in Fig. 1. Subjects worked on three experimental conditions presented in separate blocks. A block design was chosen to make the task accomplishable for all HE patients. Each block was subdivided into smaller blocks of twelve trials separated by self-paced breaks to avoid fatigue.

Before each block, subjects were instructed and trained in the specific task of one of three experimental conditions: (i) *visual*, (ii) *auditory*, or (iii) *divided*. Irrespective of the condition, each trial always started with a 2000 ms fixation period. Then, a visual stimulus (an inwardly contracting grating) and an auditory stimulus (a constant tone) appeared simultaneously. After a randomly assigned period of 500, 1000, 1500, or 2000 ms, either the visual or the auditory stimulus changed its quality (Change 1). 750 or 1000 ms later, the other stimulus also changed (Change 2). In half of the trials, the visual stimulus changed first followed by a change in the auditory stimulus and vice versa. The order of trials was randomized. A change of the visual stimulus was implemented as an increase in speed of the stimulus that either continued to move inwards or changed its direction and then moved outwards (inward/outward). A change in the auditory stimulus was implemented as a change in pitch to a higher or lower pitch (high/low). Please see *Stimuli and stimulus delivery* for a detailed description of the properties and delivery of the stimuli.

Depending on the experimental condition, the change of one of the stimuli became the target. Subjects were required to give a speeded response to the change in the stimulus' quality, i.e. a change in speed of the visual or a change of pitch of the auditory stimulus. In the *visual* condition, subjects had to exclusively react to the change in the visual stimulus (Target), irrespective of its position in the trial (Change 1 or 2) and ignore the change in the auditory stimulus (Non-Target). In the *auditory* condition, accordingly, subjects had to react to the change in the auditory stimulus (Target) only and ignore the change in the visual stimulus (Non-Target). In the *divided* condition, subjects had to respond to the stimulus that changed first (Change 1 = Target) and ignore the change in the other stimulus (Change 2 = Non-Target).

In detail, the subject's task was to react to the target and indicate the quality of this stimulus change by pressing one of two buttons operated with the index fingers of both hands. Thereby, each hand was assigned to one quality change, i.e. in the *visual* condition, the index finger press of one hand indicated inward and the index finger press of the other hand outward movement of the visual stimulus. In the *auditory* condition, the index finger press of one hand indicated a high and the index finger press of the other hand a low tone. In the *divided* condition, the index finger press of one hand indicated a change in the visual and the index finger press of the other hand a change in the auditory stimulus. Feedback was given after each trial. If subjects did not respond within 2000 ms after target appearance, the trial was counted as missed. The assignment of the left or right hand to the target qualities was balanced between subjects.

The paradigm consisted of 540 trials (180 trials of each condition) including 72 catch trials. Catch trials consisted of trials without target appearance and required no response.

As shown in Kahlbrock et al. (2012), three levels of visual attention were sought to be obtained by these conditions; high in the *visual*, medium in the *divided*, and low in the *auditory* condition.

Stimuli and stimulus delivery

The fixation point consisted of a Gaussian (0.56° in diameter), which increased its contrast by 40% after 1000 ms, thereby informing the subject that the stimulation was about to start. The visual stimulus was adapted from Hoogenboom et al. (2006). It consisted of a foveal circular sine wave grating (diameter: 7.13°, spatial frequency: 2 cycles/deg, contrast: 100%) continuously contracting towards the center of the screen (velocity: 2.16°/s). The change in visual stimulus was characterized by an increase in velocity (4.32°/s). The sine wave grating was then either still contracting towards the center of the screen (quality change inward) or changed its direction and expanded outwards (quality change outward).

The auditory stimulus was a binaurally presented 250 Hz sine tone. The change in auditory stimulus consisted of a change in pitch of the tone to either 200 Hz (quality change low) or 300 Hz (quality change high). The auditory stimulus intensity was adjusted to subjectively match the visual stimulus intensity. Thus, auditory stimuli were well audible for all subjects, but at individual volumes.

Stimulus timing was controlled using Presentation® software (version 13.0, www.neurobs.com). Visual stimuli were projected onto a screen with a DLP projector (Panasonic, Osaka, Japan) with 60 Hz refresh rate. Participants were seated approximately 96 cm away from the screen. Auditory stimuli were produced using Audacity® (http://audacity.sourceforge.net/). The analog tonal signal was generated in STIM Audio System (Neuroscan, Abbotsford, Victoria, Australia) and sent into the shielded room. Calibrated earphone transducers (TIP-300 Tubal Insert Phone, Nicolet Biomedical, Inc., Fitchburg, Wisconsin, USA) then converted the electrical to a sonic signal. The earphone transducers had two equal length plastic tubes and earplugs attached, which were inserted into participants' ears.

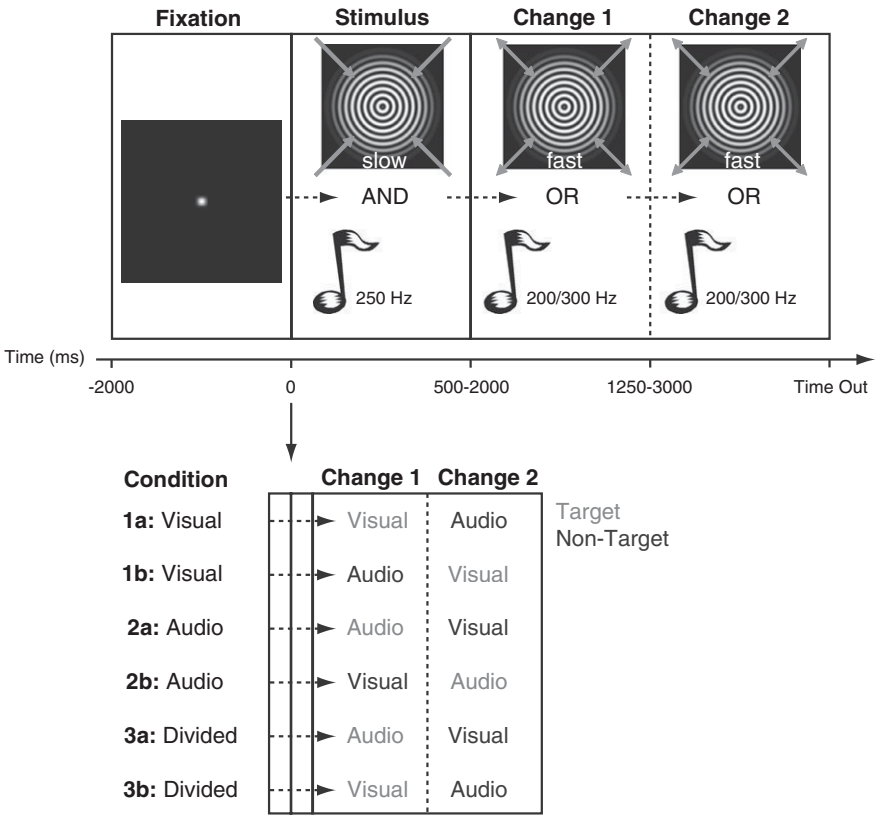

Fig. 1. Paradigm. Upper part: General overview of one trial. Each trial started with the presentation of a fixation dot (Fixation). Thereafter, visual and auditory stimuli were presented simultaneously (Stimulus; t = 0). After a randomly assigned period of 500 to 2000 ms, either the visual or the auditory stimulus changed its quality (Change 1). After another 750 or 1000 ms also the other stimulus changed (Change 2). Depending on the condition, one of the two stimulus changes served as target. Subjects had to give a speeded response indicating the quality of the target as soon as it appeared in the cued modality (see *Bimodal reaction time paradigm* for exact description of target qualities). A response or a reaction time > 2000 ms (Time Out) terminated stimulus presentation. Feedback was given after each trial. Periods used for later analysis were Fixation (baseline) and Stimulus. Lower part: Detailed description of variable parts of each trial. Depending on the condition, the change of either the visual or the auditory stimulus was target. In the *visual* condition (1a/1b), the change in visual stimulus was target and the change in auditory stimulus non-target. In the *auditory* condition (2a/2b), the change in auditory stimulus was target and the change in visual stimulus non-target. Two target positions were possible in these two conditions. In the *divided* condition (3a/3b), exclusively the first changing stimulus was target, irrespective if it occurred in the visual or auditory modality. Targets are depicted in light gray, non-targets in dark gray. Please note that fixation and stimulus periods consisted of the same stimulation in each trial, only duration of stimulus period varied. Thus, these trial periods are depicted as empty boxes in the lower part.

Neurophysiological and anatomical data

Brain activity was recorded using magnetoencephalography (MEG; 306-channel, ELEKTA Oy, Helsinki). Vertical and horizontal electrooculograms were recorded to later indentify epochs with blink artifacts and eye movements. Individual high-resolution standard T1-weighted structural magnetic resonance images (MRIs) were obtained from a 3 T Siemens Magnetom MRI scanner (Munich/Erlangen, Germany). For three participants no MRIs could be obtained. Their data was projected to the single subject T1-weighted template MRI of the Statistical Parametric Mapping 2 software (SPM2; http://www.fil.ion.ucl.ac.uk/spm/).

Data analysis

Behavioral data

Age differences were scrutinized using two-sided Mann–Whitney U test. Behavioral data were analyzed by means of error rates and reaction times. To confirm behavioral effects described previously (Kahlbrock et al., 2012) trials were divided according to the different conditions (*visual*, *auditory*, and *divided*). The *divided* condition was further subdivided into those trials where the visual or the auditory stimulus changed first and therefore became the target (*divided visual* and *divided auditory* respectively). Mean reaction times were calculated for each participant and condition. Only trials with a correct response and reaction times ranging between ±2 standard deviations from the individual mean reaction time of each condition were counted as correct and subjected to further analysis.

Reaction times, percent correct responses, and CFF values were analyzed in two ways. Firstly, a non-parametric Friedman test was employed to determine differences in distributions of reaction times and correctness of responses between selective and divided conditions. Post-hoc one-sided Wilcoxon signed-rank tests were used to test for differences between the single conditions. Secondly, a one-sided Mann–Whitney *U* test was employed to test for differences in distributions of reaction times, correctness of responses and CFF values between groups (low vs. high CFF).

To confirm expected behavioral effects (Kahlbrock et al., 2012), reaction times and correctness of responses of all three behavioral conditions were analyzed in these first steps. As the highest contrast of visual attention was expected between the *visual* and the *auditory* condition, only these two conditions were considered in further analyses.

Partial one-sided correlations, correcting for effects of age, were calculated for reaction times, percent correctness of responses, and CFF. Bonferroni–Holm correction (Holm, 1979) was applied to all alpha levels to correct for multiple comparisons. All statistical analyses of behavioral data were performed using the statistics software package IBM SPSS Statistics 19 for Windows (IBM Corporation, Somers, USA).

MEG data general

MEG data were analyzed using FieldTrip, an open source Matlab toolbox (Oostenveld et al., 2011), and Matlab 7.1 (MathWorks,

Natick, MA). For artifact rejection, continuously recorded MEG data were divided into epochs of interest, starting at time of first fixation point and ending with time of response or time out in case of a catch trial. Semi-automatic routines and visual artifact rejection were applied to remove epochs contaminated with eye blink, muscle, and sensor artifacts. Partial and complete artifact rejection procedures were applied, rejecting either only parts of the trial contaminated by artifacts or the whole trial in case of multiple artifacts. Where necessary, independent component analysis was used to correct for eye blink artifacts. Power line noise was removed by estimating and subtracting the 50- and 100-Hz components in the MEG data, using a discrete Fourier transform. The linear trend was removed from each epoch. Further analyses were performed on the time window from time of first fixation point until the first stimulus change.

Again, analyses were confined to the *visual* and *auditory* conditions, as these two were expected to be most distinctive for effects of visual attention.

Stimulus induced gamma band activity

Oscillatory neuronal activity was estimated by determining time frequency representations of power (TFRs) for frequencies between 30 and 100 Hz using windows of 400 ms moved in steps of 50 ms. Multitaper spectral estimation was used with ±5 Hz smoothing (3 tapers) in steps of 0.5 Hz. For each subject, TFRs were calculated for the *visual* and the *auditory* condition. As previous works showed gamma band activity in response to visual stimuli over occipital areas (Hoogenboom et al., 2006; Kahlbrock et al., 2012), data were averaged over all occipital and the six most caudal parietal sensor pairs (32 sensor pairs in total; Fig. 4A). Group averages were calculated for the two groups under study, i.e., low and high CFF.

Statistical comparison of power between conditions

To determine differences in visual gamma band power between attention conditions, data were first averaged over the above described sensors (Fig. 4A) for each subject. The same number of trials (depending on the condition with the smallest number of trials) was randomly drawn from the available trials for the two conditions. On a single trial basis and using independent samples *t*-tests, *t*-values were calculated for the difference in absolute power between these two conditions from −1500 to 1500 ms (0 being the start of stimulus presentation) and 30 to 100 Hz and resulted in time frequency *t*-maps. Subsequent group level statistics determined time frequency clusters with significant effects at random effects level. To obtain these time frequency clusters, time frequency *t*-maps were thresholded at the *t*-value corresponding to a one-sided *t*-test with an alpha level of 0.05, determined by the values of the permutation distribution. The summed *t*-values per cluster were used as test statistic. Statistical inference was based on a non-parametric randomization test, correcting for multiple comparisons due to a multitude of time- and frequency-points (Maris and Oostenveld, 2007; Nichols and Holmes, 2002). This second step was done for each subject and time frequency points from 500 to 1500 ms (thereby excluding purely stimulus evoked components in the first 500 ms) and 30 to 100 Hz. This analysis was once performed including all participants and repeated separately for each group under study (low and high CFF).

Individual gamma band peaks and power

For frequencies of 30 to 100 Hz, power spectra were calculated for each participant, condition, and all sensors described in *Stimulus induced gamma band activity* (Fig. 4A; ±1 Hz smoothing, Hanning window). To exclude purely stimulus evoked components and to include the strongest gamma band power increase and the maximally possible amount of trials, periods from 500 to 1000 ms were used. Relative changes compared to the pre-stimulus baseline (−1000 to −500 ms) were calculated. For each sensor, the maximal relative gamma band peak frequency and its power were determined. In order to increase the signal-to-noise ratio, the ten sensors showing highest gamma band power and lying in close proximity to each other were identified and averaged for each subject. The average gamma band peak frequency was determined. The power increase relative to baseline was tested for significance using one-sided dependent samples *t*-tests for each frequency point comparing stimulus with pre-stimulus baseline times. Statistical inference was based on a non-parametric randomization test, correcting for multiple comparisons (Maris and Oostenveld, 2007; Nichols and Holmes, 2002). The gamma band peak frequency and its corresponding relative power were only used for further analyses if the power of this peak was significantly different from baseline. This procedure was performed separately for the two conditions.

Statistics gamma band peaks

Non-parametrical one-sided Wilcoxon tests were employed to determine differences in distributions of gamma band peak frequencies between the *visual* and the *auditory* condition. This analysis was done including all participants and repeated for each individual group of participants (low and high CFF). In addition, Mann–Whitney U tests were employed to test for differences in distributions of gamma band peak frequencies between groups for both conditions separately.

To test for effects of age on gamma band peak frequencies, the median age of all participants was calculated. Frequency data were then split at the median age (one half of the subjects being equal/older and the other half being equal/younger than the median age) and compared using a Mann–Whitney *U* test. The same procedure was used to test for effects of age on the modulation of gamma band power between the *visual* and the *auditory* condition averaged in time and space (for details please see *Individual gamma band peaks and power*).

Partial one-sided correlation, correcting for age effects, was calculated for gamma band peak frequencies and CFF using IBM SPSS Statistics 19 for Windows (IBM Corporation, Somers, USA). Bonferroni–Holm correction (Holm, 1979) was applied to the alpha level to correct for multiple comparisons.

Sources of gamma band peaks

Sources of significant gamma band peaks were localized using *Dynamic Imaging of Coherent Sources* (DICS; Gross et al., 2001), an adaptive spatial filtering technique in the frequency domain. To this end, each individual structural MRI was spatially normalized to a smoothed template MRI based on multiple subjects (Statistical Parametric Mapping; SPM2; http://www.fil.ion.ucl.ac.uk/spm/). For the three subjects with missing individual MRI scans the single subject T1-weighted template MRI as given in SPM2 was used. Leadfield matrices were determined for realistically shaped single-shell volume conduction models (Nolte, 2003) derived from the individual normalized structural MRIs. The grid of locations was constructed as a regular 5 mm grid, which was then adjusted to the individuals' head shapes. To obtain the best possible estimate of the location of each subject's strongest gamma band response, cross spectral density matrices between all MEG sensor pairs at individual gamma band peaks ±5 Hz were determined for time frequency windows from −1000 to −500 ms (baseline), and 500 to 1000 ms (stimulus period) averaged over all trials of the *visual* and the *auditory* conditions. These common spatial filters were then used to calculate cross spectral density matrices for the two conditions separately. Finally, relative changes between baseline and stimulus periods were calculated.

Results

Participants

No significant age differences were observed between low and high CFF groups. Details and individual subject dependent data are summarized in Table 1.

Behavioral attention effects

To confirm previously reported effects (Kahlbrock et al., 2012), reaction times and correctness of responses were examined for effects of condition (selective vs. divided) averaged over all subjects (please see Table 2 for individual reaction times).

Median reaction times and standard errors of the median were 714 ± 52 ms for the *visual*, 598 ± 52 ms for the *auditory*, 691 ± 50 ms for the *divided visual*, and 602 ± 52 ms for the *divided auditory* condition. Differences were observed in the distributions of the four conditions ($\chi^2_{(3)} = 26.10$, $p < 0.01$, n = 32). However, post-hoc tests showed no differences between the selective and the divided conditions.

Median percent correct and standard errors of the median were 91.0 ± 0.7% for the *visual*, 94.2 ± 0.9% for the *auditory*, 88.5 ± 1.9% for the *divided visual*, and 90.7 ± 1.4% for the *divided auditory* conditions. Differences in the distributions of the four conditions were observed ($\chi^2_{(3)} = 31.36$, $p < 0.01$, n = 32). Post-hoc analyses showed that the median differences between the *visual* and the *divided visual* condition ($Z = -3.45$, $p < 0.01$, n = 32) and the median difference between the *auditory* and the *divided auditory* condition ($Z = -3.35$, $p < 0.01$, n = 32) were different from zero. Thus, participants reacted more correctly in the selective compared to the divided conditions.

Low and high CFF groups show differential behavioral performance

The comparison of low and high CFF groups showed an overall better performance of the high CFF group (reaction times: *visual*: $U = 35$, $p = 0.02$; *auditory*: $U = 32$, $p = 0.01$; *divided visual*: $U = 41$, $p = 0.05$; *divided auditory*: $p > 0.1$; correctness of responses: *visual*: $U = 44$, $p = 0.04$; *auditory*: $p > 0.1$; *divided visual*: $U = 33$, $p = 0.03$; *divided auditory*: $U = 35$, $p = 0.03$; see Supplementary Table 1 for median values and standard deviations). A similar pattern, however not always reaching significance when corrected for multiple comparisons, was observed when comparing only patients with high and low CFF values (reaction times: *visual*: $U = 18$, $p = 0.03$; *auditory*: $U = 22$, $p = 0.054$; *divided visual*: $U = 24$, $p = 0.09$; *divided auditory*: $p > 0.1$; correctness of responses: *visual*: $p > 0.1$; *auditory*: $p > 0.1$; *divided visual*: $p > 0.1$; *divided auditory*: $U = 19$, $p = 0.06$; see Supplementary Table 1 for median values and standard deviations).

Table 2
Individual behavioral and gamma band data.

Group	Subj. no.	Reaction times		Correctness		Occipital γ frequency		Occipital γ amplitude		
		Visual	Auditory	Visual	Auditory	Visual	Auditory	Visual	Auditory	Visual–Auditory
Control	1	539	451	95	94	–	–	–	–	–
	2	714	672	91	95	56	52	0.64	0.62	0.02
	3	631	602	94	94	46	46	0.30	0.22	0.08
	4	740	489	93	95	–	–	–	–	–
	5	899	774	95	87	52	50	0.92	0.55	0.37
	6	555	489	95	95	52	52	0.43	0.59	−0.16
	7	1049	661	91	92	38	40	0.72	0.83	−0.11
	8	1127	949	90	94	46	–	0.45	–	–
	n = 8	**727 ± 98**	**631 ± 74**	**93 ± 1**	**94 ± 1**	**49 ± 3**	**50 ± 3**	**0.55 ± 0.12**	**0.59 ± 0.12**	**0.02 ± 0.12**
HE0	9	475	459	96	94	52	52	4.52	1.25	3.27
	10	732	556	95	97	52	56	0.82	0.32	0.50
	11	512	371	96	95	48	48	1.15	0.73	0.42
	12	732	522	94	96	62	–	0.20	–	–
	13	945	666	90	95	46	46	0.64	0.84	−0.20
	14	868	594	88	92	42	38	0.76	0.47	0.29
	15	576	524	91	93	–	–	–	–	–
	16	536	538	90	93	48	50	0.78	0.76	0.02
	n = 8	**654 ± 77**	**531 ± 39**	**92 ± 1**	**95 ± 1**	**48 ± 3**	**49 ± 3**	**0.78 ± 0.69**	**0.74 ± 0.16**	**0.36 ± 0.65**
mHE	17	1128	666	82	92	–	–	–	–	–
	18	701	570	92	95	50	50	1.17	0.93	0.24
	19	545	601	93	95	–	54	–	0.16	–
	20	1165	952	90	94	52	50	0.90	0.56	0.34
	21	504	412	92	94	36	40	0.21	0.26	−0.05
	22	706	963	94	76	54	52	1.39	1.45	−0.06
	23	678	522	91	94	52	52	0.70	0.54	0.16
	24	656	568	91	95	52	52	6.44	4.31	2.13
	n = 8	**690 ± 111**	**586 ± 88**	**91 ± 2**	**94 ± 3**	**52 ± 3**	**52 ± 2**	**1.03 ± 1.18**	**0.56 ± 0.69**	**0.20 ± 0.43**
HE1	25	574	530	89	96	–	–	–	–	–
	26	611	552	93	95	–	–	–	–	–
	27	1429	1036	91	87	54	48	0.29	0.31	−0.02
	28	1022	838	91	95	46	–	0.74	–	–
	29	912	864	87	94	44	44	0.30	2.10	−1.80
	30	1098	559	91	95	44	44	0.70	0.64	0.06
	31	786	996	87	86	48	48	1.92	2.05	−0.13
	32	1005	668	87	96	48	50	0.92	0.55	0.37
	33	776	625	94	96	38	–	0.38	–	–
	34	–	1594	–	87	–	–	–	–	–
	n = 10	**912 ± 111**	**753 ± 130**	**91 ± 1**	**95 ± 2**	**46 ± 2**	**48 ± 2**	**0.70 ± 0.27**	**0.64 ± 0.54**	**−0.02 ± 0.48**

Individual behavioral and gamma band data are shown. Reaction times and correctness of responses, gamma band peak frequencies and relative power over occipital sensors are depicted separately for the *visual* and the *auditory* condition. In the last column, individual power differences between the *visual* and the *auditory* condition are displayed. For all parameters, group median values ± standard errors of the median are displayed.

CFF correlates with behavioral performance

Behavioral parameters correlated with the CFF, as a measure of HE disease severity. For the *auditory* condition, a negative correlation of CFF and reaction times was detected ($r = -0.53$, $p<0.01$; Fig. 2A). No correlation of correctness of responses and CFF was found in the *auditory* condition.

In the *visual* condition, the CFF correlated positively with the number of correct responses ($r = 0.40$, $p = 0.02$; Fig. 2B). No correlation of reaction times and CFF was found in the *visual* condition.

Comparing gamma band power between groups and conditions

In all groups, sustained gamma band activity in response to the visual stimulus was observed at sensors overlaying visual cortex (Fig. 3A). Tallying a previous report (Kahlbrock et al., 2012), it was not possible to find any systematic sustained stimulus related gamma band responses in auditory cortex. This is most likely due to stimulus characteristics as discussed elsewhere (Kahlbrock et al., 2012). The analyses were thus confined to the visual system.

The strongest gamma band peaks were localized in visual areas in all groups under study (Fig. 3B). Averaged over individual gamma band peak frequencies and the time of strongest gamma band responses (500 to 1500 ms), no differences in relative gamma band power were observed between any of the compared groups ($p>0.1$). Please see Table 2 for individual changes in gamma band power.

Comparing sensor level gamma band power between the *visual* and the *auditory* condition for each group separately, revealed a significant cluster from 575 to 1500 ms and 44 to 60 Hz ($p = 0.03$; Fig. 4B) for the high CFF group including all participants. A similar cluster was found for the high CFF group of patients only between the two conditions from 500 to 1500 ms and 43 to 58 Hz ($p = 0.02$). For the low CFF groups (either including all participants or patients only), no significant differences were observed ($p>0.1$). This indicates that gamma band power was stronger in the *visual* than in the *auditory* condition for the high CFF groups only.

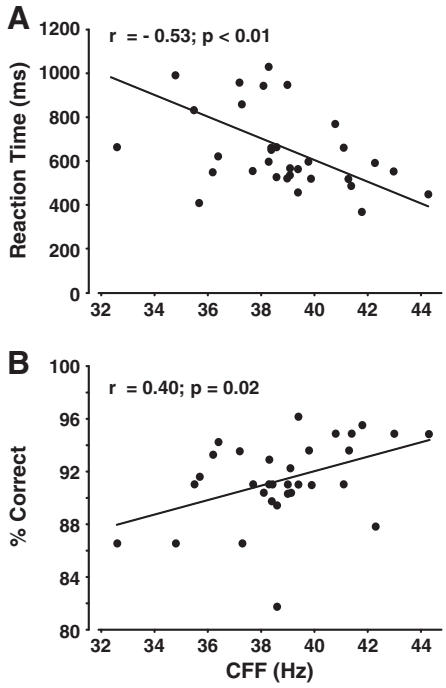

Fig. 2. Disease severity and behavioral performance correlate. A). In the *auditory* condition, the CFF correlated with reaction times ($r = -0.53$, $p<0.01$, corrected). Thus, the lower the CFF, the slower the response given. B). In the *visual* condition, the CFF correlated with the percent of correct responses ($r = 0.40$, $p = 0.02$, corrected). Thus, the lower the CFF, the more incorrect responses were given.

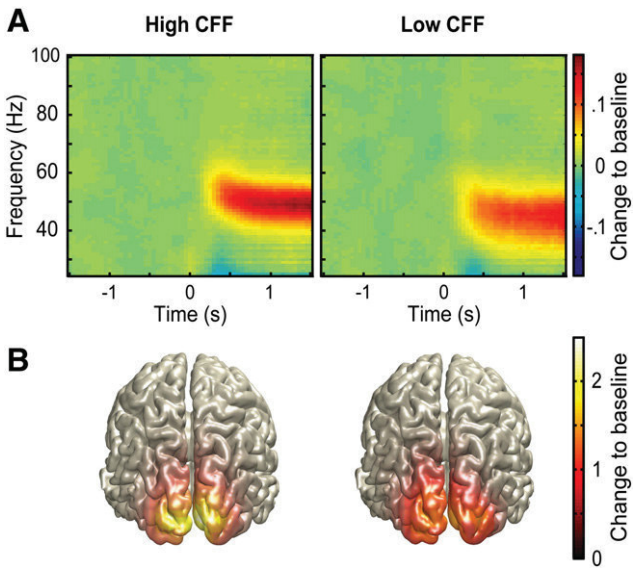

Fig. 3. Patients with HE show visually induced gamma band synchronization. A). For the two groups of participants (left: high CFF, $n = 14$; right: low CFF, $n = 12$) the average relative gamma band response in the *visual* condition is depicted. Only participants with significant gamma band peaks in the *visual* condition were included. Time-point zero constitutes the time of stimulus onset. Color-coding: 0 corresponds to no change, 0.15 to a 15% increase, and −0.15 to a 15% decrease in power relative to baseline (−1000 to −500 ms). B). Localization of strongest relative individual gamma band peaks ±5 Hz from 500 to 1000 ms after start of stimulus for the two groups of participants in the *visual* condition. Color indexes intensity of relative change to the prestimulus baseline as described in A.

Effects of age on gamma band modulation between conditions were scrutinized by calculating a median split for age with the modulation of gamma band power between *visual* and *auditory* condition averaged over time and space. Median difference in gamma band power between *visual* and *auditory* condition for the lower age group (≤59 years, $n = 11$) was 0.02 ± 0.42. For the higher age group (≥59 years, $n = 11$), the median difference in gamma power between the *visual* and *auditory* condition was 0.08 ± 0.23 (for all standard error of the median displayed). The Mann–Whitney *U* test resulted in no significant difference between the two age groups ($U = 48.5$, $p> 0.1$; Fig. 5C).

Gamma band peak frequency differs between groups

Significant differences of gamma band peak frequencies were found between low and high CFF groups (including all participants) for the *visual* ($U = 37.5$, $p = 0.01$; Fig. 5A) and the *auditory* condition ($U = 27$, $p = 0.01$). When looking at patients only, a similar difference for the *visual* and a trend for the *auditory* condition between low and high CFF groups were observed (*visual*: $U = 26.0$, $p = 0.03$; *auditory*: $U = 18.0$, $p = 0.07$). However, individual gamma band peak frequencies were not different between the *auditory* and the *visual* condition (please see Table 2 for individual gamma band peak frequencies).

Gamma band peak frequency is influenced by age

Effects of age on gamma band peak frequencies were examined by calculating a median split for age with the gamma band peak frequency data and comparing the two age groups (*visual* condition: lower age group: ≤59 years, $n = 14$; higher age group: >59 years, $n = 14$). Median *visual* gamma band peak frequency for the lower age group was 52 Hz ± 2 Hz. For the higher age group, the median *visual*

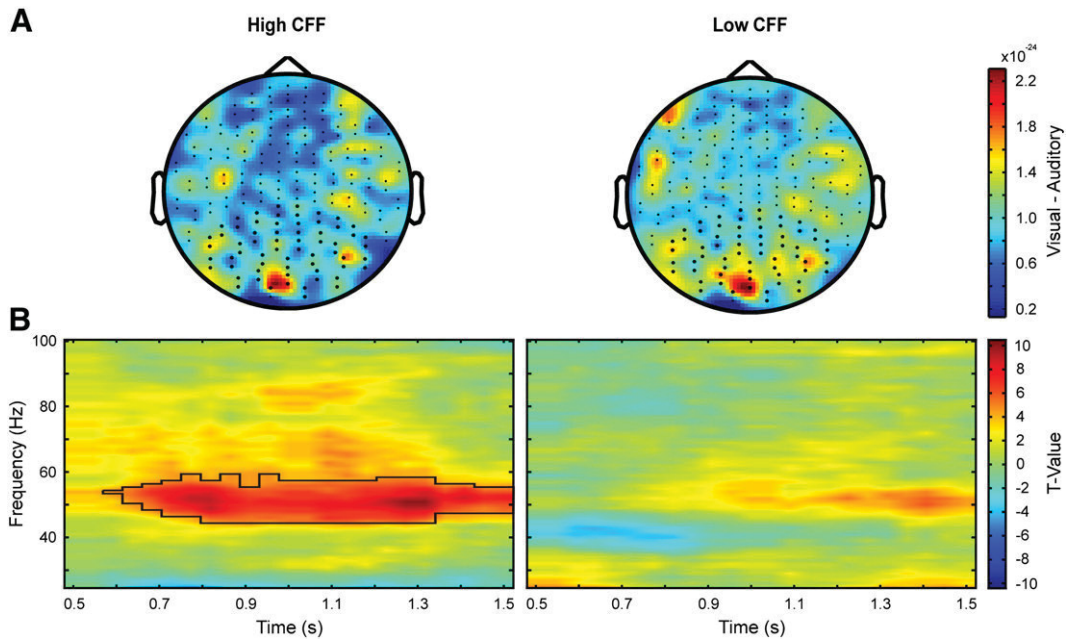

Fig. 4. Modulation of gamma band power with attention in participants with high CFF. A). Grand average difference plot of gamma band power between the *visual* and the *auditory* condition averaged over the period of 500 to 1000 ms at each subject's individual gamma band peak frequency ± 5 Hz. Low (left) and high (right) CFF groups are depicted separately. All sensors used for statistics and used to determine the ten sensors with strongest gamma band peaks are marked by asterisks. B). Statistical comparison of gamma band power in the *visual* and the *auditory* condition for the low (left) and high (right) CFF groups including all participants (n = 12 and n = 14 respectively). Results are shown as *t*-values. Subsequent non-parametric randomization statistics reveal a significant cluster as marked by the black frame. Gamma band power was stronger in the *visual* than in the *auditory* condition ($p = 0.03$, corrected). Please note that similar results were obtained when looking at the high CFF group including patients only ($p = 0.02$, corrected; n = 10).

gamma band peak frequency was 46 Hz ± 2 Hz. The Mann–Whitney *U* test revealed a higher median gamma band peak frequency in the *visual* condition for the lower than the higher age group ($U = 43.5$, $p = 0.02$; Fig. 5B). For the *auditory* condition the median gamma band peak frequency for the lower age group (≤59 years, n = 12) was 52 Hz ± 1 Hz. For the higher age group (≥59 years, n = 11), the median gamma band peak frequency was 46 Hz ± 2 Hz (for all standard error of the median displayed). The Mann–Whitney *U* test showed that the median gamma band peak frequency in the *auditory* condition was higher for the lower than the higher age group ($U = 26.0$, $p = 0.01$). For additional correlations of age with CFF and gamma band parameters see Supplementary Fig. 1.

Gamma band peak frequency correlates with CFF

Individual gamma band peak frequencies correlated with the CFF in the *visual* condition (r = 0.41, $p = 0.04$; Fig. 6, corrected for effects of

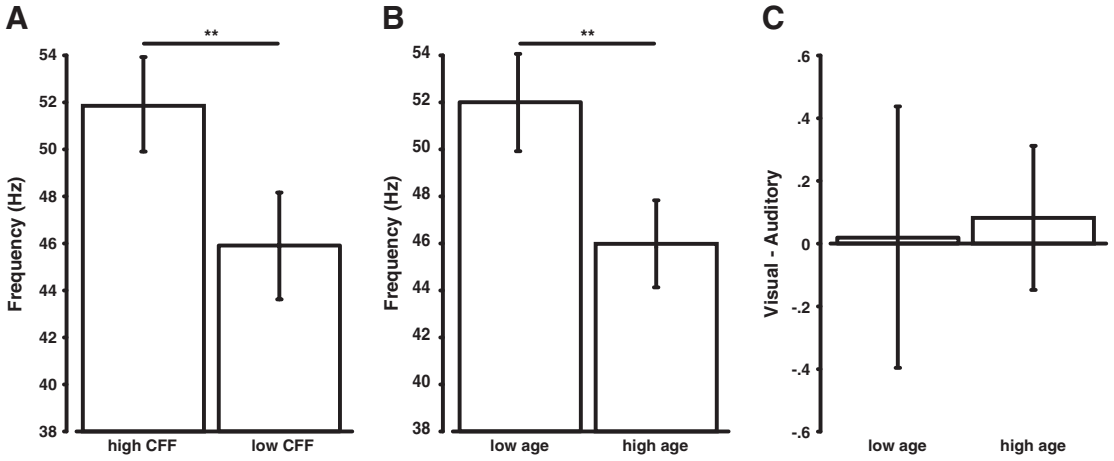

Fig. 5. Differences between high and low CFF and age groups for gamma band peak frequency and gamma band modulation over occipital areas. A). Median values of gamma band peak frequencies in the *visual* condition for high and low CFF groups including all participants (high CFF: n = 14; low CFF: n = 12). Gamma band peak frequencies were different between the two groups ($U = 37.5$, $p = 0.01$, corrected). Please note that when comparing high and low CFF groups including patients only (high CFF: n = 10; low CFF: n = 10), a similar difference was observed between groups ($U = 26.0$, $p = 0.03$, corrected). High CFF group: Median = 51.0 ± 1.5, low CFF group: Median = 45.9 ± 2.1 (standard errors of the median reported). B). Median values of gamma band peak frequencies in the *visual* condition for low and high age groups including all participants (low age: ≤59 years, n = 14; high age: >59 years, n = 14). Median visual gamma band frequency for the low age group was 52 Hz ± 2 Hz. Median visual gamma band frequency for the high age group was 46 Hz ± 2 Hz (standard error of the median). Gamma band peak frequencies were different between groups ($U = 43.5$, $p = 0.02$, corrected). C). Median values of gamma band power modulation (changes in relative gamma band power between the *visual* and *auditory* condition) for low and high age groups including all participants (low age: ≤59 years, n = 11; high age: >59 years, n = 11). The median difference for the lower age group was 0.02 ± 0.42. For the higher age group, the median difference was 0.08 ± 0.23 (standard error of the median). Gamma band modulation was not different between groups ($U = 48.5$, $p > 0.1$, corrected).

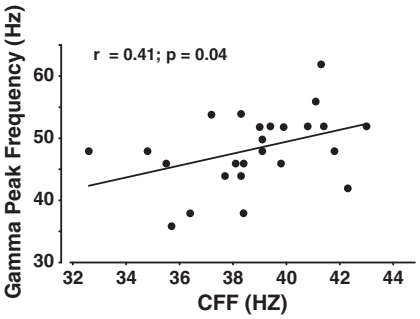

Fig. 6. Gamma band peak frequency over occipital areas correlates with disease severity. Individual peak frequencies of gamma band activity of the *visual* condition and corresponding CFF values are displayed. Gamma band peak frequencies correlated with the CFF ($r = 0.41$, $p = 0.04$, corrected). Thus, the lower the CFF, the lower the gamma band peak frequency.

age). In the *auditory* condition, no correlation of gamma band peak frequency with CFF was observed ($p > 0.1$, corrected for effects of age).

Discussion

Using a bimodal reaction time paradigm requiring modulation of visual attention, this study presents first time evidence of visually induced gamma band activity in HE patients. Moreover, both the frequency of this visual gamma band activity and behavioral performance correlate with the CFF, an indicator of HE disease severity. Thus, the current findings imply that HE disease severity is associated with a decrease of the gamma band peak frequency and a worsening of attentional performance. Furthermore, the current work shows that gamma band power is modulated by the level of visual attention in cirrhotic patients with normal CFF values only, while patients with pathological CFF values are lacking this ability. With these results, conclusions about underlying pathological mechanisms can be drawn, at the same time enhancing our understanding of normal brain functioning.

Behavioral data

Behavioral data, in particular the high percentages of correct responses, show that participants were able to perform all tasks and thereby shift their attention between the visual and the auditory domains. Reaction time differences as expected from a previous study using a similar paradigm (Kahlbrock et al., 2012) could not be reproduced. This is most likely due to the slightly different paradigm, which was simplified to a block design for the present study to make it accomplishable for patients with noticeable attention deficits. Furthermore, the higher age of the current group under study might explain these differences. It has been shown that young adults aim to balance speed and accuracy when working on speeded response tasks. Older adults, on the contrary, aim to minimize errors, irrespective of the time their responses take (Starns and Ratcliff, 2010). Thus, due to a different strategy in the present study, reaction times might not have been as informative as correctness of responses.

A worsening of behavioral performance was associated with a worsening of HE as revealed by correlation analyses with the CFF. Additionally, dividing the data into a high and a low CFF group also revealed that more impaired patients show inferior behavioral performance. This gives further evidence for the notion of a decline of attentional function with increased HE severity and tallies previous findings showing cognitive impairment in patients with HE (Amodio et al., 1998, 2005; Pantiga et al., 2003; Weissenborn et al., 2001, 2003, 2005). It is also in line with a previous study showing performance differences between healthy subjects, patients with mHE and HE1 in tests of attention and short-term memory (Mattarozzi et al., 2005) and studies, already demonstrating the importance of testing for attention in this population (e.g., Amodio et al., 2010).

Gamma band activity in disease

This study is the first to show attention-related visual gamma band brain activity in a cohort of HE patients. This finding is by itself of special relevance as one might predict that due to decreased cognitive abilities in HE (Pantiga et al., 2003; Weissenborn et al., 2001, 2003) and the observed slowing of brain responses in the motor system (Timmermann et al., 2002, 2003, 2008), HE patients, in particular the more impaired ones, would not show substantial cognition related gamma band brain activity at all.

Impaired modulation of attention-related gamma band activity with reduced CFF

Present findings revealed that gamma band power was modulated by the level of visual attention in participants with normal CFF values. This corresponds with previous works in healthy subjects, reporting attentional modulation of induced visual gamma band responses (Gruber et al., 1999; Kahlbrock et al., 2012; Siegel et al., 2008; Tallon-Baudry et al., 2005; Vidal et al., 2006; Wyart and Tallon-Baudry, 2008). Interestingly, patients with low CFF values were lacking this ability. This finding is of high relevance as it shows that with a low CFF and thus higher HE disease severity, gamma band modulation with attention is impaired. This reduced ability to modulate gamma band power with attention could represent an inefficiency in shifting attention between the visual and the auditory modalities. It might be explained by the fact that more impaired HE patients are more easily distracted by irrelevant inputs (Amodio et al., 2005), i.e. the non-target inputs in this study. It could also be partially explained by a deficit in cerebral processing of oscillatory stimuli with reduced CFF, which is discussed in *Slowed oscillatory activity as a key mechanism of HE pathology*.

Slowed oscillatory activity as a key mechanism of HE pathology

The present work shows that the frequency of visually induced gamma band activity correlates with the severity of HE. This was revealed by a correlation of CFF values and individual gamma band frequencies in the *visual* condition and by differences in gamma band frequencies between low and high CFF groups in the *visual* and *auditory* condition.

The reduced frequency of attention-related gamma band activity in more severely impaired patients are in line with earlier findings showing a reduced mean dominant frequency and a general slowing of spontaneous oscillatory brain activity in HE patients (Amodio and Gatta, 2005; Amodio et al., 1999, 2009; Bajaj, 2010; Davies et al., 1991; Kullmann et al., 2001; Montagnese et al., 2007, 2011; Olesen et al., 2011; Parson-Smith et al., 1957; Van der Rijt et al., 1984). A recent study, for example, found a significant association of the alterations in the EEG with the severity of liver disease and HE, i.e. decreased EEG frequency and increased interhemispheric theta coherence (Marchetti et al., 2011). Moreover, these data tally previous reports of slowed oscillatory processes in the motor and visual system (Timmermann et al., 2002, 2003, 2008). Thus, the present results add further evidence to the hypothesis that slowed oscillatory activity is a key mechanism in the pathophysiology of HE (Timmermann et al., 2005). In line with research in patients with schizophrenia showing decreased frequency of phase-locked gamma band activity related to gestalt perception (Spencer et al., 2004), the slowing of gamma band oscillations might represent the pathophysiological mechanism responsible for the diverse cognitive deficits in patients with HE. Thereby the hypothesis of slowed oscillations in HE is extended to the cognitive domain.

The correlation of the gamma band peak frequency with the CFF in the *visual* but not in the *auditory* condition is most likely due to the smaller number of participants showing a significant occipital gamma band peak in the *auditory* condition. This is also supported by the finding that gamma band peak frequencies were not different between the two conditions.

Individual gamma band frequencies varied between 36 and 62 Hz. However, many subjects showed a similar gamma band frequency. This is in line with a previous study where younger subjects were measured with similar visual stimulation (Kahlbrock et al., 2012). From these works it appears that the employed visual stimulation drives, i.e. induces, gamma band oscillations in a specific frequency range. However, within this range, the individual frequency seems to be influenced, i.e. modulated, by other additional and 'stronger' factors, like the HE status here.

The current study focused on the relation between HE disease severity and gamma band oscillations. This focus is firstly due to the finding of a gradual increase of attention deficits with increasing disease severity (Amodio et al., 2005; Kircheis et al., 2009; Pantiga et al., 2003; Weissenborn et al., 2001, 2005). Secondly, cortical gamma band activity has been characterized as a key correlate of attention (Fries et al., 2001; Hoogenboom et al., 2006, 2010; Kaiser et al., 2006; Lachaux et al., 2005; Steinmetz et al., 2000). Attention also changes oscillatory activity in other frequency bands, e.g. the alpha (e.g., Rihs et al., 2009; Thut et al., 2006) and beta bands (Engel and Fries, 2010). In studies of resting state activity in HE patients, all frequency bands under study (usually delta, theta, alpha, and beta) were reported to be affected (e.g., Amodio et al., 2009; Olesen et al., 2011). Thus, during a cognitive task, slowed oscillatory activity in other frequency bands can also be expected. Future studies are needed to address the questions of how other frequency bands are affected by HE disease severity during attentional processing and how different frequencies interact.

Slowed gamma band frequency in disease

As a cognitive task was used, specific inferences can be drawn about the role of gamma band activity in cognitive tasks and its alteration in disease, i.e. with reduced attentional function. Based on the present data, it can be speculated that healthy and reduced attentional performance are encoded by differential mechanisms. Healthy performance seems to be encoded by power only, i.e. the strength of gamma band activity increases with the level of attention given to a stimulus (Gruber et al., 1999; Kahlbrock et al., 2012; Siegel et al., 2008; Tallon-Baudry et al., 2005; Vidal et al., 2006; Wyart and Tallon-Baudry, 2008). The within-subject frequency of gamma band oscillations has been shown to be considerably stable when keeping stimuli, cognitive operation, and cognitive demand constant between recordings (Hoogenboom et al., 2006; Muthukumaraswamy et al., 2010). However, reduced attentional performance seems to be encoded by either power or frequency of gamma band activity. A study in patients with schizophrenia showed for example decreases of gamma band power during visual stimulus processing (e.g., Green et al., 2003). In patients with Alzheimer's disease, decreased resting state gamma band synchronization was found (Koenig et al., 2005). In the current study, no such difference was observed between groups, however, only participants who were least affected by HE showed modulation of gamma band activity by attention. Reduced attentional performance can also be encoded by differences in the frequency of gamma band activity as shown in the current study by the relation of gamma band frequency and HE disease severity. A task for future research is to examine other patient populations with attention deficits and confirm that reduced attentional performance is encoded by gamma band power and frequency. Furthermore, follow-up measurements including patients with changes in HE severity, i.e. patients recovering from severely impaired stages back to mild impairment or vice versa, are likely to substantiate the findings presented here.

An alternative explanation for the decreased gamma band frequency with higher HE severity could be that of a simple deficit in processing of oscillatory stimuli, the further the HE progresses. With higher HE disease severity lower CFF values are measured (Kircheis et al., 2002; Prakash and Mullen, 2010; Romero-Gómez et al., 2007; Sharma et al., 2007). The exact physiological mechanisms of this clinical measure are still unclear. Interestingly, human cortical visual areas are able to process flickering stimuli at frequencies higher than the maximum consciously perceived flicker frequency (Herrmann, 2001). Thus, it is possible that the observed impairment in perception of an oscillatory visual (flicker-) stimulus, i.e. reduced CFF in patients with HE, is due to a dysfunction in the cerebral processing of oscillatory visual stimuli as hypothesized by Timmermann et al. (2008). Hence, the reduced gamma band frequency would be explained by a cerebral processing deficit of oscillatory stimuli. However, in the present study cognitive performance correlates with disease severity. Thus, cognitive dysfunctions cannot be excluded as being involved in the gamma frequency reduction. Furthermore, behavioral performance deficits were shown in the attention task in both the *visual* and the *auditory* condition. Thus, it seems unlikely that pure processing deficits in the visual modality are by themselves responsible for the gamma band frequency reduction. A more global reduction of attentional functioning seems more likely.

The reduced gamma band peak frequency could also have been affected by the age of the participants. Indeed, the current data show an effect of age on gamma band peak frequency, in line with two recent studies showing decreased frequency of gamma band activity with age in a cohort of participants from first to fifth decade of life (Gaetz et al., 2011b; Muthukumaraswamy et al., 2010). Importantly, the reported correlations in the current study were corrected for effects of age by using partial correlation. The correlation between gamma band peak frequency and CFF remained, supporting the conclusion of a relationship between HE disease severity and gamma band peak frequency. However, the two effects cannot be completely disentangled finally.

Interestingly, the frequency of gamma band activity has been shown to positively correlate with resting gamma-Aminobutyric acid (GABA) concentrations measured with magnetic resonance spectroscopy in visual (Muthukumaraswamy et al., 2009) and motor cortices (Gaetz et al., 2011a). Altered inhibitory GABA mediated neurotransmission has been described to contribute to HE (Ahboucha, 2011; Ahboucha et al., 2004; Bassett et al., 1990; Jones et al., 1984). Thus, future research needs to examine the effects of GABA mediated neurotransmission on gamma band frequency in HE patients.

Conclusion

The present work reveals a relation between the attention-related gamma band peak frequency in visual areas and the severity of a disease prominently involving cognitive deficits — HE. Earlier results of slowed oscillatory processes in the motor system of patients with HE are thereby extended to the cognitive domain. The notion that pathologically slowed oscillatory activity is a key mechanism in the pathophysiology of HE is strongly supported. Slowed gamma band oscillations might represent the pathophysiological mechanism responsible for the diverse cognitive deficits in this patient population. Moreover, the present data reveal that only patients with high (normal) CFF values are able to show attention-related gamma band modulation. More impaired patients with low (pathological) CFF values, however, do not show this modulation, in line with previous findings of pronounced attentional deficits in HE. It can be speculated that generally, healthy and reduced cognitive performance are encoded by differential gamma

band modulations: gamma band power encodes healthy performance while reduced performance is encoded by both frequency and power of gamma band activity.

Role of funding source

This study was supported by Deutsche Forschungsgemeinschaft (SFB 575). N.K. was supported by Studienstiftung des deutschen Volkes. NK and EM were supported by a travel allowance of Boehringer Ingelheim Foundation (B.I.F.). M.Bu. was supported by a Marie Curie Fellowship of the EU (FP7-PEOPLE-2009-IEF-253965).

Disclosures

GK and DH belong to a group of patent holders for a portable bedside device for CFF analysis.

Acknowledgments

We thank all participants who kindly participated in this study. We thank Mr. Diethelm Plate for his unfailing support in all patient related issues. We thank Mrs. E. Rädisch and Mrs. A. Solotuchin for technical support with MRI scans, and Mrs. A. Solotuchin and Mr. Ulf Zierhut for assistance in data acquisition.

References

Ahboucha, S., 2011. Neurosteroids and hepatic encephalopathy: an update on possible pathophysiologic mechanisms. Curr. Mol. Pharmacol. 4 (1), 1–13.
Ahboucha, S., Pomier-Layrargues, G., Butterworth, R.F., 2004. Increased brain concentrations of endogenous (non-benzodiazepine) GABA-A receptor ligands in human hepatic encephalopathy. Metab. Brain Dis. 19 (3–4), 241–251.
Amodio, P., Gatta, A., 2005. Neurophysiological investigation of hepatic encephalopathy. Metab. Brain Dis. 20 (4), 369–379.
Amodio, P., Marchetti, P., Del Piccolo, F., Campo, G., Rizzo, C., Iemmolo, R.M., Gerunda, G., Caregaro, L., Merkel, C., Gatta, A., 1998. Visual attention in cirrhotic patients: a study on covert visual attention orienting. Hepatology 27 (6), 1517–1523.
Amodio, P., Marchetti, P., Del Piccolo, F., de Tourtchaninoff, M., Varghese, P., Zuliani, C., Campo, G., Gatta, A., Guérit, J.M., 1999. Spectral versus visual EEG analysis in mild hepatic encephalopathy. Clin. Neurophysiol. 110 (8), 1334–1344.
Amodio, P., Schiff, S., Del Piccolo, F., Mapelli, D., Gatta, A., Umiltà, C., 2005. Attention dysfunction in cirrhotic patients: an inquiry on the role of executive control, attention orienting and focusing. Metab. Brain Dis. 20 (2), 115–127.
Amodio, P., Orsato, R., Marchetti, P., Schiff, S., Poci, C., Angeli, P., Gatta, A., Sparacino, G., Toffolo, G.M., 2009. Electroencephalographic analysis for the assessment of hepatic encephalopathy: comparison of non-parametric and parametric spectral estimation techniques. Neurophysiol. Clin./Clin. Neurophysiol. 39 (2), 107–115.
Amodio, P., Ridola, L., Schiff, S., Montagnese, S., Pasquale, C., Nardelli, S., Pentassuglio, I., Trezza, M., Marzano, C., Flaiban, C., Angeli, P., Cona, G., Bisiacchi, P., Gatta, A., Riggio, O., 2010. Improving the inhibitory control task to detect minimal hepatic encephalopathy. Gastroenterology 139 (2), 510–518 518.e1-2.
Bajaj, J.S., 2010. Current and future diagnosis of hepatic encephalopathy. Metab. Brain Dis. 25 (1), 107–110.
Bassett, M.L., Mullen, K.D., Scholz, B., Fenstermacher, J.D., Jones, E.A., 1990. Increased brain uptake of gamma-aminobutyric acid in a rabbit model of hepatic encephalopathy. Gastroenterology 98 (3), 747–757.
Butterworth, R.F., 2000. Complications of cirrhosis III. Hepatic encephalopathy. J. Hepatol. 32 (1 Suppl), 171–180.
Butz, M., Gross, J., Timmermann, L., Moll, M., Freund, H.-J., Witte, O.W., Schnitzler, A., 2004. Perilesional pathological oscillatory activity in the magnetoencephalogram of patients with cortical brain lesions. Neurosci. Lett. 355 (1–2), 93–96.
Conn, H.O., Lieberthal, M.M., 1979. Hepatic Coma; Lactulose; Disaccharides; Chemotherapy; Therapeutic Use; Drug Therapy. Williams & Wilkins, Baltimore.
Davies, M.G., Rowan, M.J., Feely, J., 1991. EEG and event related potentials in hepatic encephalopathy. Metab. Brain Dis. 6 (4), 175–186.
de Jongh, A., Baayen, J.C., de Munck, J.C., Heethaar, R.M., Vandertop, W.P., Stam, C.J., 2003. The influence of brain tumor treatment on pathological delta activity in MEG. Neuroimage 20 (4), 2291–2301.
Eberhardt, G., 1994. Flimmerfrequenz-Analysator. Automatische Messmethode. Version 3.00. Dr. G. Schuhfried GmbH, Mödling, Austria. .
Engel, A.K., Fries, P., 2010. Beta-band oscillations — signalling the status quo? Curr. Opin. Neurobiol. 20 (2), 156–165.
Fries, P., Reynolds, J.H., Rorie, A.E., Desimone, R., 2001. Modulation of oscillatory neuronal synchronization by selective visual attention. Science 291 (5508), 1560–1563.
Fries, P., Scheeringa, R., Oostenveld, R., 2008. Finding gamma. Neuron 58 (3), 303–305.
Gaetz, W., Edgar, J.C., Wang, D.J., Roberts, T.P.L., 2011a. Relating MEG measured motor cortical oscillations to resting γ-Aminobutyric acid (GABA) concentration. Neuroimage 55 (2), 616–621.
Gaetz, W., Roberts, T.P.L., Singh, K.D., Muthukumaraswamy, S.D., 2011b. Functional and structural correlates of the aging brain: relating visual cortex (V1) gamma band responses to age-related structural change. Hum. Brain Mapp.
Gray, C.M., König, P., Engel, A.K., Singer, W., 1989. Oscillatory responses in cat visual cortex exhibit inter-columnar synchronization which reflects global stimulus properties. Nature 338 (6213), 334–337.
Green, M.F., 1996. What are the functional consequences of neurocognitive deficits in schizophrenia? Am. J. Psychiatry 153 (3), 321–330.
Green, M.F., Mintz, J., Salveson, D., Nuechterlein, K.H., Breitmeyer, B., Light, G.A., Braff, D.L., 2003. Visual masking as a probe for abnormal gamma range activity in schizophrenia. Biol. Psychiatry 53 (12), 1113–1119.
Gross, J., Kujala, J., Hämäläinen, M., Timmermann, L., Schnitzler, A., Salmelin, R., 2001. Dynamic imaging of coherent sources: studying neural interactions in the human brain. Proc. Natl. Acad. Sci. U. S. A. 98 (2), 694–699.
Gruber, T., Müller, M.M., Keil, A., Elbert, T., 1999. Selective visual–spatial attention alters induced gamma band responses in the human EEG. Clin. Neurophysiol. 110 (12), 2074–2085.
Guerit, J.-M., Amantini, A., Fischer, C., Kaplan, P.W., Mecarelli, O., Schnitzler, A., Ubiali, E., Amodio, P., 2009. Neurophysiological investigations of hepatic encephalopathy: ISHEN practice guidelines. Liver Int. 29 (6), 789–796.
Häussinger, D., Schliess, F., 2008. Pathogenetic mechanisms of hepatic encephalopathy. Gut 57 (8), 1156–1165.
Häussinger, D., Kircheis, G., Schliess, F., 2006. Hepatic Encephalopathy and Nitrogen Metabolism, 1st ed. Springer, Netherlands.
Herrmann, C.S., 2001. Human EEG responses to 1–100 Hz flicker: resonance phenomena in visual cortex and their potential correlation to cognitive phenomena. Exp. Brain Res. 137 (3–4), 346–353.
Holm, S., 1979. A simple sequentially rejective multiple test procedure. Scand. J. Stat. 6 (2), 65–70.
Hoogenboom, N., Schoffelen, J.M., Oostenveld, R., Parkes, L.M., Fries, P., 2006. Localizing human visual gamma-band activity in frequency, time and space. Neuroimage 29 (3), 764–773.
Hoogenboom, N., Schoffelen, J.M., Oostenveld, R., Fries, P., 2010. Visually induced gamma-band activity predicts speed of change detection in humans. Neuroimage 51 (3), 1162–1167.
Jones, E.A., Schafer, D.F., Ferenci, P., Pappas, S.C., 1984. The GABA hypothesis of the pathogenesis of hepatic encephalopathy: current status. Yale J. Biol. Med. 57 (3), 301–316.
Kahlbrock, N., Butz, M., May, E.S., Schnitzler, A., 2012. Sustained gamma band synchronization in early visual areas reflects the level of selective attention. Neuroimage 59 (1), 673–681.
Kaiser, J., Hertrich, I., Ackermann, H., Lutzenberger, W., 2006. Gamma-band activity over early sensory areas predicts detection of changes in audiovisual speech stimuli. Neuroimage 30 (4), 1376–1382.
Kircheis, G., Wettstein, M., Timmermann, L., Schnitzler, A., Häussinger, D., 2002. Critical flicker frequency for quantification of low-grade hepatic encephalopathy. Hepatology 35 (2), 357–366.
Kircheis, G., Fleig, W.E., Görtelmeyer, R., Grafe, S., Häussinger, D., 2007. Assessment of low-grade hepatic encephalopathy: a critical analysis. J. Hepatol. 47 (5), 642–650.
Kircheis, G., Knoche, A., Hilger, N., Manhart, F., Schnitzler, A., Schulze, H., Häussinger, D., 2009. Hepatic encephalopathy and fitness to drive. Gastroenterology 137 (5), 1706–1715 e1-9.
Koenig, T., Prichep, L., Dierks, T., Hubl, D., Wahlund, L.O., John, E.R., Jelic, V., 2005. Decreased EEG synchronization in Alzheimer's disease and mild cognitive impairment. Neurobiol. Aging 26 (2), 165–171.
Kullmann, F., Hollerbach, S., Lock, G., Holstege, A., Dierks, T., Schölmerich, J., 2001. Brain electrical activity mapping of EEG for the diagnosis of (sub)clinical hepatic encephalopathy in chronic liver disease. Eur. J. Gastroenterol. Hepatol. 13 (5), 513–522.
Lachaux, J.P., George, N., Tallon-Baudry, C., Martinerie, J., Hugueville, L., Minotti, L., Kahane, P., Renault, B., 2005. The many faces of the gamma band response to complex visual stimuli. Neuroimage 25 (2), 491–501.
Marchetti, P., D'Avanzo, C., Orsato, R., Montagnese, S., Schiff, S., Kaplan, P.W., Piccione, F., Merkel, C., Gatta, A., Sparacino, G., Toffolo, G.M., Amodio, P., 2011. Electroencephalography in patients with cirrhosis. Gastroenterology 141 (5), 1680–1689 e1-2.
Maris, E., Oostenveld, R., 2007. Nonparametric statistical testing of EEG- and MEG-data. J. Neurosci. Methods 164 (1), 177–190.
Mattarozzi, K., Campi, C., Guarino, M., Stracciari, A., 2005. Distinguishing between clinical and minimal hepatic encephalopathy on the basis of specific cognitive impairment. Metab. Brain Dis. 20 (3), 243–249.
Montagnese, S., Jackson, C., Morgan, M.Y., 2007. Spatio-temporal decomposition of the electroencephalogram in patients with cirrhosis. J. Hepatol. 46 (3), 447–458.
Montagnese, S., Biancardi, A., Schiff, S., Carraro, P., Carlà, V., Mannaioni, G., Moroni, F., Tono, N., Angeli, P., Gatta, A., Amodio, P., 2011. Different biochemical correlates for different neuropsychiatric abnormalities in patients with cirrhosis. Hepatology 53 (2), 558–566.
Muthukumaraswamy, S.D., Edden, R.A.E., Jones, D.K., Swettenham, J.B., Singh, K.D., 2009. Resting GABA concentration predicts peak gamma frequency and fMRI amplitude in response to visual stimulation in humans. Proc. Natl. Acad. Sci. U. S. A. 106 (20), 8356–8361.
Muthukumaraswamy, S.D., Singh, K.D., Swettenham, J.B., Jones, D.K., 2010. Visual gamma oscillations and evoked responses: variability, repeatability and structural MRI correlates. Neuroimage 49 (4), 3349–3357.
Nichols, T.E., Holmes, A.P., 2002. Nonparametric permutation tests for functional neuroimaging: a primer with examples. Hum. Brain Mapp. 15 (1), 1–25.

Nolte, G., 2003. The magnetic lead field theorem in the quasi-static approximation and its use for magnetoencephalography forward calculation in realistic volume conductors. Phys. Med. Biol. 48 (22), 3637–3652.
Olesen, S.S., Graversen, C., Hansen, T.M., Blauenfeldt, R.A., Hansen, J.B., Steimle, K., Drewes, A.M., 2011. Spectral and dynamic electroencephalogram abnormalities are correlated to psychometric test performance in hepatic encephalopathy. Scand. J. Gastroenterol. 46 (7–8), 988–996.
Oostenveld, R., Fries, P., Maris, E., Schoffelen, J.-M., 2011. FieldTrip: open source software for advanced analysis of MEG, EEG, and invasive electrophysiological data. Comput. Intell. Neurosci. 2011, 156869.
Pantiga, C., Rodrigo, L.R., Cuesta, M., Lopez, L., Arias, J.L., 2003. Cognitive deficits in patients with hepatic cirrhosis and in liver transplant recipients. J. Neuropsychiatry Clin. Neurosci. 15 (1), 84–89.
Parson-Smith, B.G., Summerskill, W.H., Dawson, A.M., Sherlock, S., 1957. The electroencephalograph in liver disease. Lancet 273 (7001), 867–871.
Prakash, R., Mullen, K.D., 2010. Mechanisms, diagnosis and management of hepatic encephalopathy. Nat. Rev. Gastroenterol. Hepatol. 7 (9), 515–525.
Pugh, R.N.H., Murray-Lyon, I.M., Dawson, J.L., Pietroni, M.C., Williams, R., 1973. Transection of the oesophagus for bleeding oesophageal varices. Br. J. Surg. 60 (8), 646–649.
Rihs, T.A., Michel, C.M., Thut, G., 2009. A bias for posterior α-band power suppression versus enhancement during shifting versus maintenance of spatial attention. Neuroimage 44 (1), 190–199.
Roelfsema, P.R., Engel, A.K., König, P., Singer, W., 1997. Visuomotor integration is associated with zero time-lag synchronization among cortical areas. Nature 385 (6612), 157–161.
Romero-Gómez, M., Córdoba, J., Jover, R., del Olmo, J.A., Ramírez, M., Rey, R., de Madaria, E., Montoliu, C., Nuñez, D., Flavia, M., Compañy, L., Rodrigo, J.M., Felipo, V., 2007. Value of the critical flicker frequency in patients with minimal hepatic encephalopathy. Hepatology 45 (4), 879–885.
Schnitzler, A., Gross, J., 2005. Normal and pathological oscillatory communication in the brain. Nat. Rev. Neurosci. 6 (4), 285–296.
Sharma, P., Sharma, B.C., Puri, V., Sarin, S.K., 2007. Critical flicker frequency: diagnostic tool for minimal hepatic encephalopathy. J. Hepatol. 47 (1), 67–73.
Siegel, M., Donner, T.H., Oostenveld, R., Fries, P., Engel, A.K., 2008. Neuronal synchronization along the dorsal visual pathway reflects the focus of spatial attention. Neuron 60 (4), 709–719.
Spencer, K.M., Nestor, P.G., Perlmutter, R., Niznikiewicz, M.A., Klump, M.C., Frumin, M., Shenton, M.E., McCarley, R.W., 2004. Neural synchrony indexes disordered perception and cognition in schizophrenia. Proc. Natl. Acad. Sci. U. S. A. 101 (49), 17288–17293.
Starns, J.J., Ratcliff, R., 2010. The effects of aging on the speed–accuracy compromise: boundary optimality in the diffusion model. Psychol. Aging 25 (2), 377–390.
Steinmetz, P.N., Roy, A., Fitzgerald, P.J., Hsiao, S.S., Johnson, K.O., Niebur, E., 2000. Attention modulates synchronized neuronal firing in primate somatosensory cortex. Nature 404 (6774), 187–190.
Tallon-Baudry, C., Bertrand, O., Peronnet, F., Pernier, J., 1998. Induced gamma-band activity during the delay of a visual short-term memory task in humans. J. Neurosci. 18 (11), 4244–4254.
Tallon-Baudry, C., Bertrand, O., Henaff, M.A., Isnard, J., Fischer, C., 2005. Attention modulates gamma-band oscillations differently in the human lateral occipital cortex and fusiform gyrus. Cereb. Cortex 15 (5), 654–662.
Thut, G., Nietzel, A., Brandt, S.A., Pascual-Leone, A., 2006. α-band electroencephalographic activity over occipital cortex indexes visuospatial attention bias and predicts visual target detection. J. Neurosci. 26 (37), 9494–9502.
Timmermann, L., Gross, J., Kircheis, G., Häussinger, D., Schnitzler, A., 2002. Cortical origin of mini-asterixis in hepatic encephalopathy. Neurology 58 (2), 295–298.
Timmermann, L., Gross, J., Butz, M., Kircheis, G., Häussinger, D., Schnitzler, A., 2003. Mini-asterixis in hepatic encephalopathy induced by pathologic thalamo-motor-cortical coupling. Neurology 61 (5), 689–692.
Timmermann, L., Butz, M., Gross, J., Kircheis, G., Häussinger, D., Schnitzler, A., 2005. Neural synchronization in hepatic encephalopathy. Metab. Brain Dis. 20 (4), 337–346.
Timmermann, L., Butz, M., Gross, J., Ploner, M., Südmeyer, M., Kircheis, G., Häussinger, D., Schnitzler, A., 2008. Impaired cerebral oscillatory processing in hepatic encephalopathy. Clin. Neurophysiol. 119 (2), 265–272.
Uhlhaas, P.J., Singer, W., 2006. Neural synchrony in brain disorders: relevance for cognitive dysfunctions and pathophysiology. Neuron 52 (1), 155–168.
Van der Rijt, C.C., Schalm, S.W., De Groot, G.H., De Vlieger, M., 1984. Objective measurement of hepatic encephalopathy by means of automated EEG analysis. Electroencephalogr. Clin. Neurophysiol. 57 (5), 423–426.
Vidal, J.R., Chaumon, M., O'Regan, J.K., Tallon-Baudry, C., 2006. Visual grouping and the focusing of attention induce gamma-band oscillations at different frequencies in human magnetoencephalogram signals. J. Cogn. Neurosci. 18 (11), 1850–1862.
Vienna test system, WINWTS, Version 4.50, 1999. Dr. G. Schuhfried GmbH. Mödling, Austria.
Weissenborn, K., Heidenreich, S., Ennen, J., Rückert, N., Hecker, H., 2001. Attention deficits in minimal hepatic encephalopathy. Metab. Brain Dis. 16 (1–2), 13–19.
Weissenborn, K., Heidenreich, S., Giewekemeyer, K., Rückert, N., Hecker, H., 2003. Memory function in early hepatic encephalopathy. J. Hepatol. 39 (3), 320–325.
Weissenborn, K., Giewekemeyer, K., Heidenreich, S., Bokemeyer, M., Berding, G., Ahl, B., 2005. Attention, memory, and cognitive function in hepatic encephalopathy. Metab. Brain Dis. 20 (4), 359–367.
Wyart, V., Tallon-Baudry, C., 2008. Neural dissociation between visual awareness and spatial attention. J. Neurosci. 28 (10), 2667–2679.

6.)

Kahlbrock N*,[c], **Butz M***, May ES, Schnitzler A,

"*Sustained gamma band synchronization in early visual areas reflects the level of selective attention.*"

Neuroimage 2012 Jan 2;59(1):673-81.

Impact-Faktor: 6.3

NeuroImage 59 (2012) 673–681

Contents lists available at ScienceDirect

NeuroImage

journal homepage: www.elsevier.com/locate/ynimg

Sustained gamma band synchronization in early visual areas reflects the level of selective attention

Nina Kahlbrock [a,*,1], Markus Butz [a,b,1], Elisabeth S. May [a], Alfons Schnitzler [a,c]

[a] Heinrich-Heine-University Düsseldorf, Medical Faculty, Institute of Clinical Neuroscience and Medical Psychology, Universitätsstraße 1, D-40225 Düsseldorf, Germany
[b] University College London, Institute of Neurology, 33 Queen Square, WC1N 3BG, London, United Kingdom
[c] Heinrich-Heine-University Düsseldorf, Medical Faculty, Department of Neurology, Universitätsstraße 1, D-40225 Düsseldorf, Germany

ARTICLE INFO

Available online 23 July 2011

Keywords:
Synchronization
Gamma
Attention
Biased competition
MEG
Audiovisual

ABSTRACT

Cortical gamma band synchronization is associated with attention. Accordingly, directing attention to certain visual stimuli modulates gamma band activity in visual cortical areas. However, gradual effects of attention and behavior on gamma band activity in early visual areas have not yet been reported.
In the present study, the degree of selective visual attention was gradually varied in a cued bimodal reaction time paradigm using audio-visual stimuli. Brain activity was recorded with magnetoencephalography (MEG) and analyzed with respect to time, frequency, and location of strongest response.
Reaction times to visual and auditory stimuli reflected three presumed graded levels of visual attention (high, medium, and low). MEG data showed sustained gamma band synchronization in all three conditions in early visual areas (V1 and V2), while the intensity of gamma band synchronization increased with the level of visual attention (from low to high). Differences between conditions were seen for up to 1600 ms.
The current results show that in early visual areas the level of gamma band synchronization is related to the level of attention directed to a visual stimulus. These gradual and long-lasting effects highlight the key role of gamma band synchronization in early visual areas for selective attention.

Introduction

In our complex multisensory environment, it is essential to process relevant information while ignoring the rest. In case of competing input from two different modalities, stimuli in the attended modality receive amplified processing compared to stimuli in the non-attended modality (Gherri and Eimer, 2011; Spence and Driver, 1997). As stimulus processing is believed to be capacity-limited, allocating resources to one attended modality gradually subtracts resources from the available supply of all modalities (Bonnel and Hafter, 1998). Consequently, modulation of attentive processing in one modality can be studied by reallocating available resources between competing modality specific stimuli.

In the brain, attentional modulation of sensory processing has been associated with gamma band (30–100 Hz) synchronization (Fries et al., 2001; Hoogenboom et al., 2006, 2010; Kaiser et al., 2006; Lachaux et al., 2005; Steinmetz et al., 2000). Previous studies reported modulation of visually induced gamma band oscillations by attention in animals (Khayat et al., 2010) and humans (Gruber et al., 1999; Siegel et al., 2008; Tallon-Baudry et al., 2005; Vidal et al., 2006; Wyart and Tallon-Baudry, 2008). In all these studies, states of 'attention' versus 'no attention' were compared. In an EEG study, Simos et al. (2002) provided first evidence that gamma band synchronization gradually increases with task complexity. However, changes remained unspecific and could not be attributed to modality specific regions.

Previous studies on selective visual attention suggest that the attended of two competing visual stimuli gets a competitive advantage over the other by enhancing its gamma band synchronization (Fries et al., 2001, 2008). This effect has been addressed in the hypothesis of biased competition through enhanced synchronization (Fries, 2005), which bases its assumptions on the biased competition hypothesis (Desimone and Duncan, 1995; Reynolds et al., 1999). Nevertheless, the conceptual framework of the biased competition hypothesis has yet to be tested for its application in cross-modal attention designs as for cross-modal designs it has only been addressed on a theoretical level for the visual-tactile domain (Magosso et al., 2010).

While several functional Magnetic Resonance Imaging studies showed that attention modulates processing of sensory information in early visual areas (Gandhi et al., 1999; Munneke et al., 2008), attention dependent modulation of gamma band synchronization has primarily been recorded in mid- and high level stages in the visual processing hierarchy (Fries et al., 2001; Gregoriou et al., 2009;

* Corresponding author at: Heinrich-Heine-University Düsseldorf, Medical Faculty, Institute of Clinical Neuroscience and Medical Psychology, Universitätsstraße 1, D-40225 Düsseldorf, Germany. Fax: +49 211 81 19033.
E-mail address: Nina.Kahlbrock@uni-duesseldorf.de (N. Kahlbrock).
[1] These two authors contributed equally to this work.

1053-8119/$ – see front matter © 2011 Elsevier Inc. All rights reserved.
doi:10.1016/j.neuroimage.2011.07.017

Womelsdorf et al., 2006). One study (Chalk et al., 2010) found decreased local field potential gamma band power and decreased gamma band spike field coherence with attention in monkey primary visual cortex. Previous works in humans using magnetoencephalography (MEG) have shown increased induced gamma band synchronization in visual areas V1–V3 during attention demanding tasks (Hoogenboom et al., 2006, 2010). Nevertheless, these neurophysiological results did not show graded attentional modulation of gamma band synchronization in early visual areas. In fact, up to now, studies on graded attentional modulation of induced gamma band synchronization in early visual areas in humans are lacking.

The present study is the first to systematically manipulate the level of visual attention, relate it to behavioral performance and to the intensity of gamma band synchronization in early visual areas. Subjects were simultaneously presented with visual (Hoogenboom et al., 2006) and auditory stimuli in a cued bimodal reaction time paradigm resulting in a gradual modulation of visual attention.

Materials and methods

Subjects

Sixteen healthy right-handed subjects with normal or corrected to normal vision participated in this study (8 female, mean age: 25.5 ± 4.3 years; SD). All subjects gave their written informed consent. The study was approved by the local ethics committee (study no. 2895) and was performed in accordance with the Declaration of Helsinki.

Paradigm

Fig. 1 provides an overview of the paradigm. Each trial started with a cue presented for 1000 ms indicating the specific task of one of three experimental conditions: (i) *selective visual*, (ii) *selective auditory*, or (iii) *divided*, i.e. visual and auditory. Irrespective of the condition, the cue was followed by a 2000 ms fixation period. Then, a visual stimulus (an inwardly contracting grating) and an auditory stimulus (a constant tone) appeared simultaneously. After a randomly assigned period of 500, 1000, 2000, or 3000 ms, either the visual or the auditory stimulus changed its quality (change 1). 750 or 1000 ms later, the other stimulus also changed (change 2). In half of the trials, the visual stimulus changed first followed by a change in the auditory stimulus and vice versa. The order of these changes was randomized. A change of the visual stimulus was implemented as an increase in speed of the stimulus that either continued to move inwards or changed its direction and then moved outwards (inward/outward). A change in the auditory stimulus was implemented as a change in pitch to a higher or lower pitch (high/low). Please see section on stimuli and stimulus delivery for a detailed description of the properties and delivery of the stimuli.

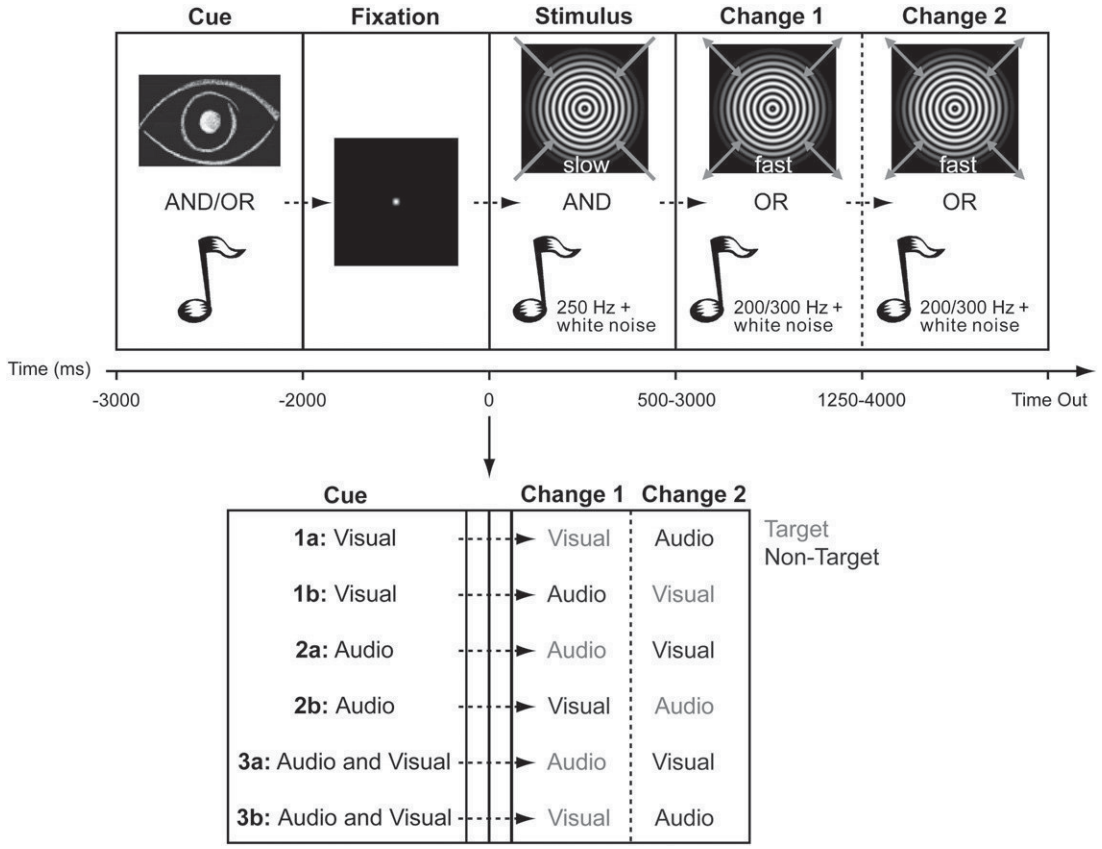

Fig. 1. Paradigm. Upper part: general overview of one trial. Each trial started with a cue indicating the condition (Cue). After presentation of a fixation dot (Fixation), visual and auditory stimuli were presented simultaneously (Stimulus; 0 = start of stimulus). After a randomly assigned period of 500 to 3000 ms, either the visual or the auditory stimulus changed its quality (Change 1). After 750 or 1000 ms also the other stimulus changed (Change 2). Depending on the condition, one of the two stimulus changes served as target. Subjects had to give a speeded response indicating quality of target as soon as it appeared in the cued modality (see section on stimuli and stimulus delivery for exact description of target qualities). A response or a reaction time>2000 ms (Time out) terminated stimulus presentation. Feedback was given after each trial. Periods used for later analysis were Fixation (baseline) and Stimulus. Lower part: detailed description of variable parts of each trial. With a visual cue (1a/1b; condition *selective visual*, n = 108 trials) the change in visual stimulus became target and the change in auditory stimulus non-target. If the cue was auditory (2a/2b; condition *selective auditory*, n = 108 trials) the change in auditory stimulus became target and the change in visual stimulus non-target. Two target positions were possible in the *selective* conditions. When auditory and visual cues were presented together (3a/3b; condition *divided*; 3a: *divided auditory*, n = 108 trials, 3b: *divided visual*, n = 108 trials) the first changing stimulus became target, the second one non-target. Targets are depicted in light grey, non-targets in dark grey. Please note that fixation and stimulus periods consisted of the same stimulation in each trial, only duration of stimulus period varied. Thus, these trial periods are depicted as small empty boxes in the lower part.

Depending on the experimental condition, as indicated by the cue at the beginning of the trial, a change of one of the stimuli became the target. Subjects were required to give a speeded response to the change in the stimulus' quality, i.e. a change in speed of the visual or a change of pitch of the auditory stimulus. In condition *selective visual*, subjects had to exclusively react to the change in the visual stimulus (target), irrespective of its position in the trial (change 1 or 2) and ignore the change in the auditory stimulus (non-target). In condition *selective auditory*, accordingly, subjects had to react to the change in the auditory stimulus (target) only and ignore the change in the visual stimulus (non-target). In the *divided* condition, subjects had to respond to the stimulus that changed first (change 1 = target) and ignore the change in the other stimulus (change 2 = non-target).

The subject's task was thus to react to the target and indicate the quality of this stimulus change by pressing one of four buttons operated with the index and middle fingers of both hands. Thereby, each hand was assigned to one modality (visual and auditory) and each finger to one quality change, i.e. for the visual stimulus an index finger press indicated inward and a middle finger press outward movement, for the auditory stimulus an index finger press indicated a high tone, a middle finger press a low tone. Feedback was given after each trial. If subjects did not respond within 2000 ms after target appearance, the trial was counted as missed. The assignment of the left or right hand to the auditory or visual modality was balanced between subjects, finger assignment was kept fixed.

The paradigm consisted of 432 trials: 108 trials in conditions *selective visual* and *selective auditory* each and 216 in condition *divided* (subdivided into 108 trials where the visual stimulus changed first and thereby became target, *divided visual*; and 108 trials where the auditory stimulus changed first, *divided auditory*). Trials from the different conditions were presented in two blocks in a random order. Each block was subdivided into smaller blocks of twelve trials separated by self-paced breaks to avoid fatigue. Prior to data acquisition, subjects were trained on the paradigm until they thoroughly understood the task.

Three levels of visual attention were sought to be obtained by these conditions; high in condition *selective visual*, medium in condition *divided*, and low in condition *selective auditory*. In analogy to Coull et al. (2004), attentional allocation was obtained by varying the likelihood of whether the motor response was based on changes in the visual or the auditory stimulus (*selective visual*: 100% visual, 0% auditory, *selective auditory*: 0% visual, 100% auditory, *divided*: 50% visual, 50% auditory).

Stimuli and stimulus delivery

The fixation point was of a Gaussian (0.56° in diameter), which increased its contrast by 40% after 1000 ms, thereby informing the subject that the stimulation was about to start. The visual stimulus was adapted from Hoogenboom et al. (2006). It consisted of a foveal circular sine wave grating (diameter: 5.6°, spatial frequency: 2 cycles/°, contrast: 100%) continuously contracting towards the center of the screen (velocity: 1.6°/s). The change in visual stimulus (potential target) was characterized by an increase in velocity (3.38°/s). The sine wave grating was then either still contracting towards the center of the screen or changed its direction and expanded outwards.

The auditory stimulus was a binaurally presented 250 Hz sine tone embedded in white noise (white noise reduced by 9 dB compared to sine tone). The change in auditory stimulus (potential target) consisted of a change in pitch of the tone to either 200 Hz or 300 Hz. The auditory stimulus intensity was adjusted to subjectively match the visual stimulus intensity. Thus, auditory stimuli were well audible for all subjects, but at individual volumes.

Stimulus timing was controlled using Presentation® software (version 13.0, www.neurobs.com). Visual stimuli were projected onto a screen with a dlp projector (PLUS Vision Corp. of America) with 60 Hz refresh rate. Participants were seated approximately 76 cm away from the screen. Auditory stimuli were produced using Audacity® (http://audacity.sourceforge.net/). They were sent into the shielded room via a mixing desk and earphone transducers (E-A-RTONE, Aearo Technologies Inc., Indianapolis, USA), which converted the electrical to a sonic signal. The earphone transducers had two equal lengths plastic tubes and earplugs attached which were inserted into participants' ears.

Data acquisition

Neuromagnetic activity was measured in a magnetically shielded room with a whole-head Neuromag-122 MEG system (Elekta Neuromag Oy, Helsinki, Finland). Vertical and horizontal electrooculograms were recorded to later reject epochs contaminated with blink artifacts and eye movements. Individual high-resolution standard T1-weigthed structural magnetic resonance images (MRIs) were obtained from a 3 T Siemens Magnetom MRI scanner (Munich/Erlangen, Germany).

Data analysis: behavioral data

Behavioral data were analyzed by means of error rates and reaction times. Trials were divided into conditions *selective visual*, *selective auditory*, and *divided*. For analyses of the behavioral data, the divided condition was further split up into two subcategories *divided visual* and *divided auditory*. Only correct trials with reaction times faster than 2000 ms were subjected to further analysis. Reaction times were analyzed using repeated measures analysis of variance (ANOVA) with factors modality (auditory versus visual) and condition (selective versus divided).

Data analysis: MEG data general

MEG data were analyzed using FieldTrip, an open source Matlab toolbox (Oostenveld et al., 2011), and Matlab 7.1 (MathWorks, Natick, MA). Continuously recorded MEG data were divided into epochs of interest, starting at the time of first fixation point and ending with appearance of change in either of the stimuli. Please note that for analyses of neurophysiological data, trials of the condition *divided* were not split up, as only periods prior to stimulus change were analyzed. Semi-automatic routines and visual artifact rejection were applied to discard epochs contaminated with eye, muscle, and sensor artifacts. Partial and complete artifact rejection procedures were applied, rejecting either only parts of the trial contaminated by artifacts or the whole trial in case of multiple artifacts. During partial artifact rejection, for each of the different artifact types (eye, muscle, and sensor artifacts), a z-score with specific sensitivity for the respective artifacts was computed. This was done by selecting either only EOG channels or all MEG sensors. Then, data were band-pass filtered in order to only include frequencies in which the artifacts are known to be most dominant. Subsequently, the envelope of the signal was computed using Hilbert transform and normalized by calculating the z-scores for each sensor. Next, one summed z-value was obtained for each moment in time. For this purpose, the z-scores of all selected sensors were added, and this sum was normalized by dividing it by the root of the number of summed sensors. A rejection threshold was then determined separately for each subject and applied automatically to its entire dataset. This adaptation of z-values between subjects was necessary because of differences in noise levels and in the signal-to-noise ratio. After partial artifact rejection, trials were inspected visually and excluded completely in case of remaining artifacts. Power line noise was removed by estimating and subtracting the 50-, 100- and 150-Hz components in the MEG data, using a discrete Fourier transform. The linear trend was removed from each epoch.

Data analysis: individual gamma band peaks

Rhythmic neuronal activity was estimated determining spectral power of the MEG signals. For the time period of 500 to 1000 ms (0 being the start of stimulus presentation) and frequencies of 30 to 100 Hz power spectra were calculated for each participant averaged over all trials of all conditions and over occipital sensors (±1 Hz smoothing, hanning window). Each participant's absolute maximal gamma band frequency was obtained. Please note that to exclude purely stimulus-evoked components, the first 500 ms were excluded from those analyses steps not involving timely evolution of the signal. To include the strongest gamma band peak and the maximally possible amount of trials, periods from 500 to 1000 ms were used to calculate peak gamma band responses and their localization.

Data analysis: individual gamma sources

The source of the strongest gamma band peak (as obtained from the power spectra), averaged over all trials of all conditions, was localized for each individual using Dynamic Imaging of Coherent Sources (Gross et al., 2001), an adaptive spatial filtering technique in the frequency domain. Leadfield matrices were determined for realistically shaped single-shell volume conduction models (Nolte, 2003) derived from the individual structural MRIs. The grid of locations was constructed as a regular 5 mm grid. In order to account for each subject's strongest gamma band response crossspectral density matrices between all MEG sensor pairs at individual gamma band peaks ±5 Hz were determined separately for time frequency windows from −1000 to −500 ms, i.e. before stimulus start (baseline), and from 500 to 1000 ms after stimulus start (stimulus period). Spatial filters were determined based on the crossspectral density matrices averaged over all trials of all conditions of a given subject. Relative changes between pre-stimulus and stimulus periods were calculated and locations of each subject's strongest relative gamma band peak were retrieved. Each subject's source parameters were displayed on their individual brains. Each structural MRI was spatially normalized to a smoothed template MRI based on multiple subjects (Statistical Parametric Mapping; SPM2; http://www.fil.ion.ucl.ac.uk/spm/). Differences between MNI and Talairach coordinates were adjusted (http://imaging.mrc-cbu.cam.ac.uk/imaging/MniTalairach) and individual virtual sensor locations were identified, Brodmann areas were estimated from Talairach and Tournoux (Talairach and Tournoux, 1988) using 'Talairach Client — Version 2.4.2' (Lancaster et al., 2000).

Data analysis: time course of signal at individual gamma sources

To quantify the time course of the signal at each subject's strongest relative gamma source, virtual sensors were generated by linear constrained minimum variance (LCMV) beamformer reconstructions. The time courses of the source wave forms were obtained using covariance matrices for pre-stimulus (−1000 to −500 ms) and stimulus periods (500 to 1000 ms) separately, band-pass filtered for each subject's strongest gamma band peak. Spatial filters were calculated averaged over all trials of a given subject. For each individual, equal numbers of trials for all three conditions and pre-stimulus and stimulus times, were randomly drawn from the available preprocessed trials. Single trial time courses were then projected through those filters, providing single trial estimates of source power. For further analyses, dipole moments' time courses were projected on the direction of maximal power in the individual gamma band frequency. On the resulting source wave forms, time frequency representations of power (TFRs) were calculated for frequencies between 30 and 100 Hz using windows of 400 ms moved in steps of 50 ms. Multitaper spectral estimation was used with ±5 Hz smoothing (3 tapers) in steps of 0.5 Hz. Relative changes of power in the stimulus period (0 to 2000 ms) to the pre-stimulus baseline (−1000 to −500 ms) were calculated. For each subject, average TFRs were calculated for each of the three conditions. Due to the special tuning of the virtual sensors for the subjects' individual gamma band frequencies, lower frequencies were not subjected to further analyses here.

Data analysis: statistical comparison of conditions

To examine differences between the three conditions, average TFRs were subjected to statistical group analysis. The stimulus period relative to the pre-stimulus baseline and the absolute baseline period were analyzed separately. Dependent samples two-sided t-tests for each time- and frequency-point across epochs were performed for all three comparisons (*selective visual*/*selective auditory*, *selective visual*/*divided*, and *divided*/*selective auditory*). Statistical inference was based on a non-parametric randomization test, correcting for multiple comparisons due to a multitude of time- and frequency-points (Maris and Oostenveld, 2007; Nichols and Holmes, 2002). Bonferroni–Holm correction (Holm, 1979) was applied to the alpha level to correct for multiple comparisons between the three conditions.

Data analysis: signal phase-locked to stimulus onset

In the analysis performed earlier (Data analysis: time course of signal at individual gamma sources and Data analysis: statistical comparison of conditions), trials were averaged after conducting time frequency analysis. This approach significantly favors identification of non-phase-locked (induced) activities. Applying time frequency analysis after averaging mainly provides information on phase-locked (evoked) oscillatory bursts (Tallon-Baudry et al., 1996). To determine whether the here observed statistical effects stem from induced or evoked activity, the analysis was repeated for responses phase-locked to stimulus onset and averaged before performing time frequency analysis. Data were aligned to stimulus onset, baseline corrected with a time window of 200 ms before stimulus onset, projected through the common spatial filters, averaged over trials, and subjected to a time frequency analysis. The same non-parametric randomization test as described earlier was applied.

Data analysis: evoked magnetic fields

The analysis was repeated for modulations in evoked magnetic fields. For a direct comparison with the spectral power analysis, the same source locations (virtual sensors) and trial selections were used. Data were filtered with a band-pass filter from 0.03 to 30 Hz. A baseline of 200 ms prior to stimulus onset was subtracted. The statistical group analysis was repeated (dependent samples two-sided t-tests for all three comparisons).

Results

Behavioral data

In all four behavioral conditions (*selective visual*, *selective auditory*, *divided visual*, and *divided auditory*), error rates were below 10%. Mean reaction times were 586.39 ms ± 14.61 for condition *selective visual*, 669.96 ms ± 22.79 for condition *divided visual*, 299.20 ms ± 21.99 for condition *selective auditory*, and 430.74 ms ± 23.50 for condition *divided auditory* (SEM reported here; Fig. 2). For reaction times a repeated measures analysis of variance (ANOVA) resulted in significant main effects for factors modality ($F_{(1,15)} = 426.57$, $p < 0.001$) and condition ($F_{(1,15)} = 90.61$, $p < 0.001$) and in a significant interaction ($F_{(1,15)} = 10.00$, $p = 0.006$) between both factors. Reaction times were faster in the selective compared to the respective divided attention conditions and in the auditory than in the visual conditions. The

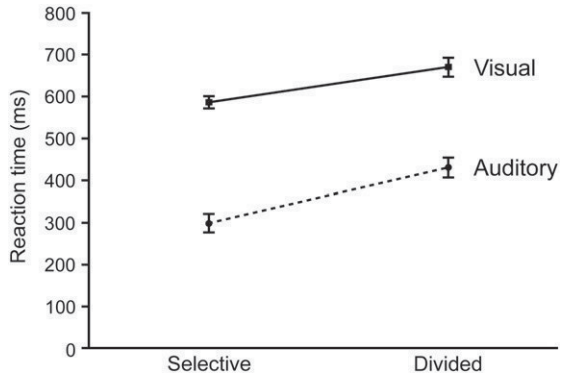

Fig. 2. Reaction times. Reaction times were faster in the selective, compared to the respective divided conditions, in both the visual and the auditory modality ($p<0.001$). Thus, effects of attention between conditions were confirmed. Differences between conditions *selective auditory* and *divided auditory* were more pronounced than differences between conditions *selective visual* and *divided visual* ($p=0.006$). Reaction times were faster in the auditory, than in the visual modality ($p<0.001$; SEM displayed).

difference between selective and divided conditions was more pronounced in the auditory than in the visual modality.

Frequency and location of strongest gamma band source

For MEG data analyses an average of 326 ± 9.48 (SEM reported) trials remained for each subject after rejecting invalid trials and artifacts. Thus, 75% of the previously recorded trials remained. Using only these trials, each subject's strongest gamma band frequency peak was retrieved. Power spectra averaged over each subject's occipital sensors revealed individual peak gamma band frequencies ranging from 54 to 69 Hz (see Table 1 for individual peak frequencies). The maximum gamma band power was localized and a virtual sensor was constructed for each subject. Virtual sensors were mostly localized in early visual cortex. In fourteen of sixteen subjects, the virtual sensor accounting for strongest gamma band activity in response to the visual stimulus was located in Brodmann areas 17 or 18. In one subject, it was located in Brodmann area 19 and in one subject in lingual gyrus, close to the cerebellum (Table 1 and Fig. 3).

Table 1
Characterization of single subject gamma band frequencies and locations. For each subject, individual peak gamma band frequencies and locations of virtual sensors as Brodmann areas and Talairach coordinates are displayed. Please note that for subject 8, the virtual sensor was localized in lingual gyrus, close to the cerebellum, no Brodmann area is specified in this case.

Subject no.	Maximal γ	Brodmann area	Talairach coordinates (x, y, z)		
1	60 Hz	18	−6	−81	20
2	54 Hz	17	14	−82	1
3	66 Hz	18	4	−88	−5
4	65 Hz	18	5	−76	25
5	56 Hz	19	−7	−79	35
6	69 Hz	17	−17	−79	9
7	56 Hz	18	−4	−90	17
8	60 Hz	-	−1	−78	−7
9	58 Hz	18	−17	−95	20
10	54 Hz	18	−6	−98	7
11	58 Hz	17	6	−90	−1
12	66 Hz	17	−8	−84	12
13	64 Hz	18	−21	−99	2
14	54 Hz	17	−11	−84	9
15	60 Hz	17	−2	−84	9
16	56 Hz	18	−19	−95	6

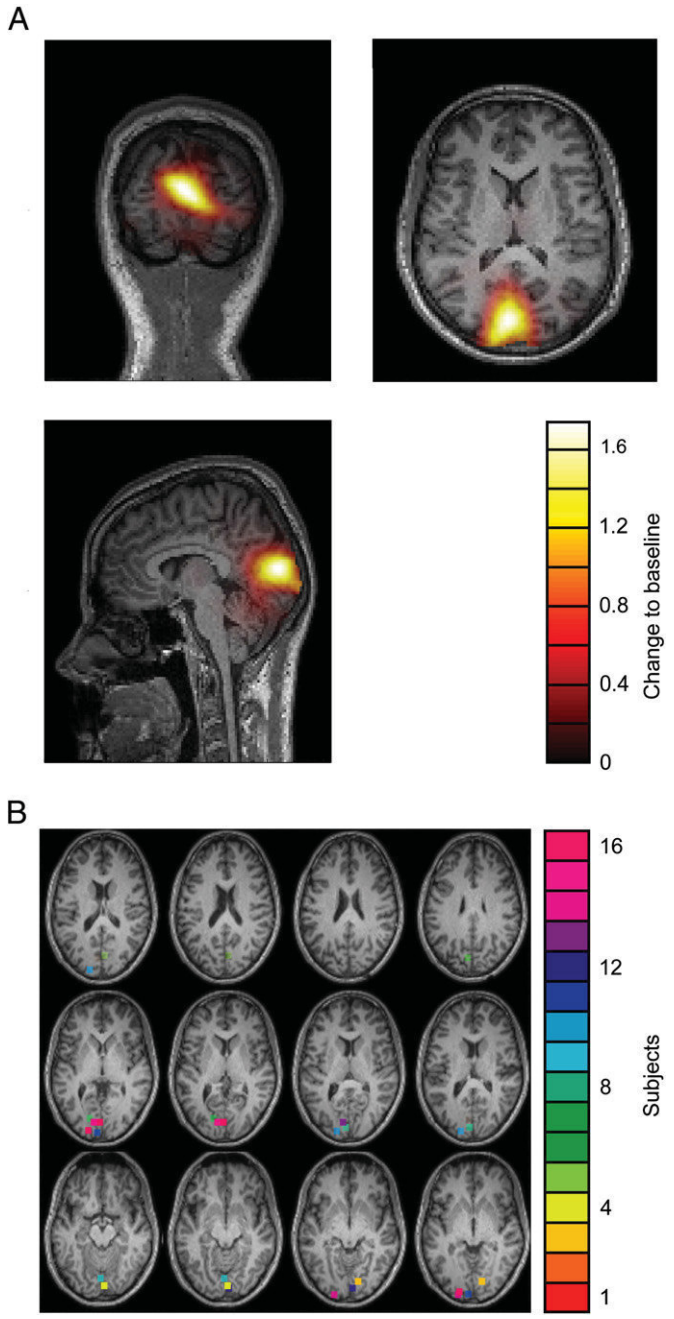

Fig. 3. Localization of gamma band power. A. Gamma band power relative to pre-stimulus baseline activity was localized in early visual areas. Displayed here is the grand average over all correct trials of all conditions for one representative subject (Subject 2). Colors indicate intensity of relative change to the pre-stimulus baseline. Values below 0.5 are masked. B. Virtual sensors were localized in areas V1 and V2 in 14 of 16 subjects. Shown here are virtual sensor locations for all subjects displayed on one individual brain normalized to a smoothed template MRI based on multiple subjects (Statistical Parametric Mapping; SPM2; http://www.fil.ion.ucl.ac.uk/spm/). Each colored point represents the virtual sensor of one subject. Please note that for visualization purposes, the kernels of the virtual sensors were extended to 9 mm. Slice thickness was 3 mm. For that reason, some virtual sensors are present in multiple slices.

Comparing conditions: similar baseline activity between attention conditions

When comparing conditions, the same numbers of trials were retrieved for each of the three conditions (*selective visual*, *selective auditory* and *divided*) and the pre-stimulus baseline and stimulus periods. On average, 79 ± 2.48 (SEM) trials remained per condition.

Between the three conditions no significant differences were found in pre-stimulus baseline activity ($p>0.37$). Thus, further results are based on relative changes in power with respect to a pre-stimulus baseline.

Comparing conditions: differences in gamma band activity between attention conditions

On virtual sensor level, all subjects showed sustained visually induced gamma band synchronization compared to the pre-stimulus baseline in all three conditions (see Fig. 4A for grand averages over all subjects). Pairwise comparisons on group level between all three conditions resulted in significant power differences in the gamma band frequency range. Relative gamma band power was significantly higher in condition *selective visual* than in condition *selective auditory* between 53 and 80 Hz from 400 to 2000 ms ($p<0.001$); it was significantly higher in condition *selective visual* than in condition *divided* between 54 and 74 Hz from 450 to 1550 ms ($p=0.009$); and it was significantly higher in condition *divided* than in condition *selective auditory* between 54 and 75 Hz from 700 to 2000 ms ($p=0.002$; all *p*-values corrected for multiple comparisons). Thus, relative visual gamma band synchronization was highest in condition *selective visual*, medium in condition *divided*, and lowest in condition *selective auditory* (Fig. 4B). Averaged over all subjects, over time (500 to 2000 ms) and individual gamma peak frequencies ±5 Hz mean relative power values were 2.21 ± 0.44 (SEM) for *selective visual*, 2.13 ± 0.41 (SEM) for *divided*, and 1.92 ± 0.38 (SEM) for *selective auditory*. Please note that big standard errors are due to a big variance in overall relative gamma power between subjects (range: 0.16 to 6.91).

Signal phase-locked to stimulus onset and evoked magnetic fields

To examine differences in evoked spectral power between conditions, time frequency representations of power phase-locked to stimulus onset were calculated. No statistically significant differences were observed between the three conditions in gamma band power phase-locked to stimulus onset.

Furthermore, it was investigated, whether attentional modulations were preceded by attentional modulations of evoked magnetic fields. Again, no statistically significant differences were observed between the three conditions.

Discussion

The aim of the present study was to gradually modulate visual attention, thereby examining its relation to gamma band synchronization in visual cortical areas. A bimodal paradigm designed to elicit three levels of visual attention (high, medium, and low) was used and three graded levels of visual attention were confirmed on the behavioral side. In response to the visual stimulus, prominent long lasting local gamma band synchronization in visual cortex was found. Gamma band power was gradually modulated in early visual areas according to the amount of attention directed to the visual stimulus. This gradual modulation suggests that by being precisely adjustable

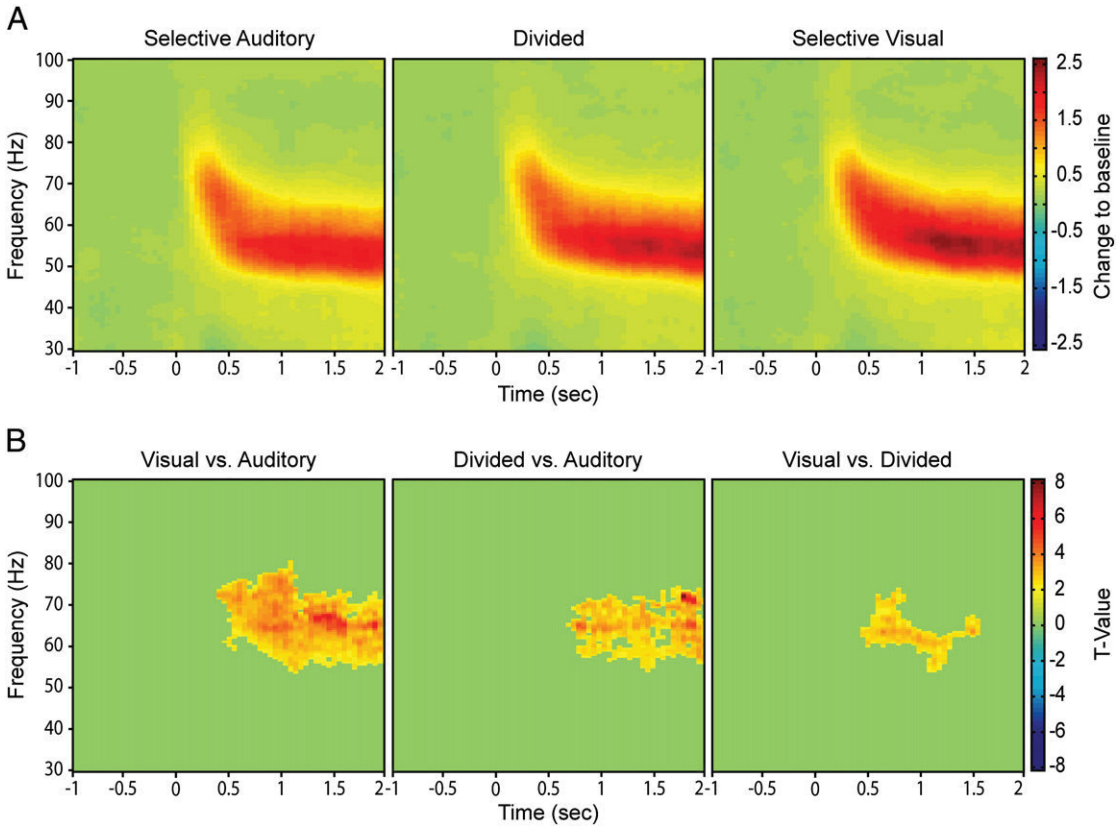

Fig. 4. Virtual sensor time frequency representations and statistics. A. Grand average time frequency representations relative to baseline from each subject's virtual sensor. In all three conditions (*selective auditory*; left, *divided*; middle, and *selective visual*; right) a prominent gamma band response relative to pre-stimulus baseline activity was observed during stimulation (onset of stimulation at t = 0). Color-coding: 0 corresponds to no change and 2.5 to a 250% increase in power relative to baseline. B. Statistical comparisons between all three conditions. Results are shown as t-values; all non-significant frequencies are masked green. Relative gamma band power was stronger in condition *selective visual* compared to condition *selective auditory* ($p<0.001$; left), it was stronger in condition *divided* compared to condition *selective auditory* ($p=0.002$; middle), and stronger in condition *selective visual* compared to condition *divided* ($p=0.009$; right; *p*-values corrected for multiple comparisons).

to current attentional needs gamma band synchronization represents a mechanism enabling an efficient use of cognitive resources.

Behavioral data and induced gamma band synchronization support gradual modulation of attention

Behavioral data confirmed different reaction times for the three attention levels. Thus, one can assume that graded levels of visual attention were reached by the applied bimodal reaction time paradigm and that attention was shifted between the visual and auditory modalities. Extending earlier behavioral work (Posner et al., 1980; Schroeger et al., 2000; Spence and Driver, 1997), a third medium state of visual attention is introduced, thereby enabling measurement of gradually modulated attention.

In line with earlier research (Edden et al., 2009; Fries et al., 2001; Hoogenboom et al., 2006; Muthukumaraswamy et al., 2009), subjects showed prominent long lasting visual gamma band activity in all conditions when presented with the visual stimulus. Underlining the pivotal behavioral relevance of this neurophysiological effect, gamma band activity in early visual cortex was highest in condition *selective visual*, medium in condition *divided*, and lowest in condition *selective auditory*. Thus, three increasing levels of visual attention are associated with a corresponding modulation on the neurophysiological side. While previous works investigated the influence of 'attention' versus 'no attention' on gamma band synchronization (Fries et al., 2001; Gruber et al., 1999; Mueller et al., 2000; Siegel et al., 2008; Wyart and Tallon-Baudry, 2008), the present study extends these findings by establishing gradual attention modulation. Furthermore, attentional effects on gamma band synchronization have never been shown for such long periods of time (lasting up to 1600 ms). Previous studies have provided data either averaged over certain time periods, frequency bands or both (Fries et al., 2001; Gruber et al., 1999; Mueller et al., 2000; Tallon-Baudry et al., 2005; Vidal et al., 2006). Thus, our data provide new insights into long lasting attention modulation and its relation to gamma band synchronization.

Gamma band power phase-locked to stimulus onset and evoked magnetic field strengths were not significantly different between conditions. Tallying with non-existent predictive properties of evoked magnetic fields for reaction times (Hoogenboom et al., 2010) gamma band modulation in this paradigm is assumed to stem from differences in induced and not in evoked gamma band power. These findings oppose animal data, showing attentional modulation of early evoked gamma band responses in primary visual and auditory areas (Lakatos et al., 2009). However, the described work is based on multiunit recordings from macaque primary areas. This different approach and the restriction to primary areas might be an explanation for these dissimilar results. Furthermore, the present restriction to areas of strongest gamma band synchronization, allows no deeper conclusions about the order of processing in visual areas from these data.

The difference in gamma band synchronization between conditions *selective visual* and *divided* was less prominent and shorter lasting than differences between conditions *selective visual* and *selective auditory* and between conditions *divided* and *selective auditory*. In behavioral analogy, we observed a stronger orientation to the visual modality reflected by a greater difference in reaction times between conditions *selective auditory* and *divided auditory* than between conditions *selective visual* and *divided visual*. While emphasizing the relation between behavioral and neurophysiological data, these findings tally with the ventriloquist effect (Alais and Burr, 2004), stating that vision often dominates audition when attentive processes are involved. A very recent study substantiates this by showing that visual dominance is based on less vulnerability of the visual system to competition from auditory stimuli than vice versa (Schmid et al., 2011).

One might speculate that prolonged reaction times in the *divided* compared to the *selective* conditions reflect an effect of task difficulty. Indeed, earlier studies showed that gamma band oscillations can be modulated by overall task difficulty (Posada et al., 2003) and perceptual load (Howard et al., 2003). However, if task difficulty was higher in the *divided* condition, gamma band power would also have been expected to be highest in this condition and similar in the two *selective* conditions. As this is not the case in the current study, we claim to see modulation of gamma band synchronization that is due to modulation of attention by a limited capacity of attention resources (Bonnel and Hafter, 1998) and not due to task difficulty or perceptual load.

The discrepancy in frequencies, observed between highest relative gamma band power and the statistical difference between these two, might firstly be caused by smearing due to frequency smoothing used in time frequency analysis. Secondly, the strong gamma band power peak in the group average is dominated by power values of some subjects. The statistical effects are most likely due to subjects with higher frequency gamma band power peaks showing consistent modulations between conditions.

Gamma band synchronization in the auditory system

The data reported here were also scanned for effects of auditory stimulation (see Supplementary Figs. 1 and 2 for further information). Auditory evoked responses to auditory stimulation were found (see Supplementary Fig. 2). However, most likely due to stimulus characteristics, we were not able to find any systematic sustained stimulus related gamma band responses in auditory cortex. Certainly, intracranial studies have reported evoked short-lasting (Lakatos et al., 2009) and induced auditory gamma band synchronization (Crone et al., 2001). There have also been MEG studies, showing auditory evoked gamma band activity (Joliot et al., 1994; Pantev et al., 1991; Tiitinen et al., 1993). However, to the best of our knowledge, there are no studies using auditory stimuli inducing long-lasting gamma band synchronization in auditory cortex. One possible explanation might be that, MEG sensors are less sensitive to radial sources at the surface of gyri, e.g. superior temporal gyrus (Crone et al., 2001). Thus one might speculate that the signal to noise ratio of a potentially induced auditory gamma band response in our study might have been too low, especially compared to the visual response, to be seen in the MEG recording. Thus, due to the absence of an adequate auditory stimulus, we confined our analysis to the visual system.

The interpretation of the present findings is limited to some degree by the fact that gamma band activity could not be observed in the auditory system. While a shift of attention between the auditory and visual system can be assumed from behavioral data, explicit corresponding evidence from the neurophysiological data is missing. Hence, the proposed shift of attention between modalities remains speculative. Finding stimuli that permit showing mirror effects of modulated gamma band synchronization in auditory cortex, as shown with steady state stimuli at lower frequencies (Saupe et al., 2009) would be a desirable task for future works. This would permit firm conclusions about the relation between gamma band synchronization and resource allocation between modalities.

Modulation of induced gamma band synchronization in early visual areas

Subjects' strongest induced gamma band sources were located in early visual areas (V1 and V2) in fourteen of sixteen subjects. Modulation of gamma band synchronization was also found in these locations. Relative gamma band power in early visual cortical areas increased with the amount of attention directed to the visual stimulus. While some studies showed pronounced gamma band synchronization in visual areas V1–V3 in humans, when attentively

monitoring a visual stimulus (Hoogenboom et al., 2006, 2010), attention dependent modulations of gamma band synchronization have primarily been recorded in mid- and high level stages in the visual processing hierarchy (Fries et al., 2001; Gregoriou et al., 2009). One study (Chalk et al., 2010) however, found decreased local field potential gamma band power and decreased gamma band spike field coherence with attention in V1 of the macaque monkey. The authors suggest that by a reduction of center surround inhibition, gamma band synchronization decreases with attention, which only holds if an experimental design is used where attention is tightly focused at the center of the classical receptive field. The stimuli used in our study were relatively complex gratings, not restricted to the center of one receptive field, but exiting multiple neurons in visual cortex. The here applicable mechanism behind gamma band synchronization has been described in a recent review, which proposes that gamma band synchronization is driven by rhythmically synchronized inhibition through cortical interneurons (Fries, 2009).

Thus, our results substantiate that graded attentional modulation of gamma band synchronization takes place in early visual areas and support the theory that synchronized inhibition of cortical interneurons can serve as a mechanism for gamma band synchronization.

Biased competition model applied gradually

Previous studies on selective visual attention suggest that the attended of two competing visual stimuli gets a competitive advantage over the other by enhancing its gamma band synchronization (Fries et al., 2001, 2008). This effect has been addressed in the hypothesis of biased competition through enhanced synchronization (Fries, 2005), which bases its assumptions on the biased competition hypothesis (Desimone and Duncan, 1995; Reynolds et al., 1999). From the present results one might speculate that the conceptual framework of the biased competition model can also be applied to gradual attention modulation in the visual system. In this respect, enhanced gamma band synchronization could be seen as an adaptive mechanism enhancing the selective processing of a stimulus in a gradual manner, thereby reflecting the amount of selective attention a stimulus receives.

From the current results, one could furthermore speculate on the application of the biased competition model in an intermodal context, as shown in a modeling study for the visual and tactile domains (Magosso et al., 2010). With the attention related increase in gamma band synchronization in visual areas, one could assume a connection of the competitive advantage of the visual over the auditory stimulus to the amount of gamma band synchronization. However, one important aspect of the biased competition model is that responses to the non-preferred stimulus are suppressed, when the other stimulus 'wins' the competition for processing. The current study cannot directly proof suppressive effects of one of the two stimuli over the other. To substantiate the application of the biased competition model in an intermodal context, future studies are needed. These could employ bimodal stimuli, inducing long-lasting gamma band synchronization in visual and auditory areas at the same time and could thereby address suppressive and enhancing effects in modality specific cortical areas. Furthermore, interactions with and between other modalities such as the somatosensory system will be of great interest.

Conclusions

The current study is the first to show gradual and long lasting changes of gamma band synchronization in early visual areas related to the level of attention given to a visual stimulus. These attention effects, potentially achieved by resource allocation between the visual and auditory modality, may extend the biased competition model of selective attention and highlight the key role of gamma band synchronization in visual attention.

Role of the funding source

This study was supported by Deutsche Forschungsgemeinschaft (SFB 575, project C4). N.K. was supported by Studienstiftung des deutschen Volkes and a travel allowance of Boehringer Ingelheim Foundation (B.I.F.).

Supplementary materials related to this article can be found online at doi:10.1016/j.neuroimage.2011.07.017.

Acknowledgments

We thank Mrs. E. Rädisch and Mrs. A. Solotuchin for technical support with MRI scans. We are thankful to Prof. Joachim Gross (CCNi, Glasgow), Dr. Hanneke van Dijk, and Dr. Nienke Hoogenboom (both University Düsseldorf) for helpful suggestions and discussion on data analysis. For critically revising the manuscript we thank Dr. Joachim Lange (University Düsseldorf).

References

Alais, D., Burr, D., 2004. The ventriloquist effect results from near-optimal bimodal integration. Curr. Biol. 14 (3), 257–262.
Bonnel, A.M., Hafter, E.R., 1998. Divided attention between simultaneous auditory and visual signals. Percept. Psychophys. 60 (2), 179–190.
Chalk, M., Herrero, J.L., Gieselmann, M.A., Delicato, L.S., Gotthardt, S., Thiele, A., 2010. Attention reduces stimulus-driven gamma frequency oscillations and spike field coherence in V1. Neuron 66 (1), 114–125.
Coull, J.T., Vidal, F., Nazarian, B., Macar, F., 2004. Functional anatomy of the attentional modulation of time estimation. Science 303 (5663), 1506–1508.
Crone, N.E., Boatman, D., Gordon, B., Hao, L., 2001. Induced electrocorticographic gamma activity during auditory perception. Clin. Neurophysiol. 112 (4), 565–582.
Desimone, R., Duncan, J., 1995. Neural mechanisms of selective visual attention. Annu. Rev. Neurosci. 18 (1), 193–222.
Edden, R.A.E., Muthukumaraswamy, S.D., Freeman, T.C.A., Singh, K.D., 2009. Orientation discrimination performance is predicted by GABA concentration and gamma oscillation frequency in human primary visual cortex. J. Neurosci. 29 (50), 15721–15726.
Fries, P., 2005. A mechanism for cognitive dynamics: neuronal communication through neuronal coherence. Trends Cogn. Sci. 9 (10), 474–480.
Fries, P., 2009. Neuronal gamma-band synchronization as a fundamental process in cortical computation. Annu. Rev. Neurosci. 32, 209–224.
Fries, P., Reynolds, J.H., Rorie, A.E., Desimone, R., 2001. Modulation of oscillatory neuronal synchronization by selective visual attention. Science 291 (5508), 1560–1563.
Fries, P., Womelsdorf, T., Oostenveld, R., Desimone, R., 2008. The effects of visual stimulation and selective visual attention on rhythmic neuronal synchronization in macaque area V4. J. Neurosci. 28 (18), 4823–4835.
Gandhi, S.P., Heeger, D.J., Boynton, G.M., 1999. Spatial attention affects brain activity in human primary visual cortex. Proc. Natl. Acad. Sci. U.S.A. 96 (6), 3314–3319.
Gherri, E., Eimer, M., 2011. Active listening impairs visual perception and selectivity: an ERP study of auditory dual-task costs on visual attention. J. Cogn. Neurosci. 23 (4), 832–844.
Gregoriou, G.G., Gotts, S.J., Zhou, H., Desimone, R., 2009. High-frequency, long-range coupling between prefrontal and visual cortex during attention. Science 324 (5931), 1207–1210.
Gross, J., Kujala, J., Hämäläinen, M., Timmermann, L., Schnitzler, A., Salmelin, R., 2001. Dynamic imaging of coherent sources: studying neural interactions in the human brain. Proc. Natl. Acad. Sci. U.S.A. 98 (2), 694–699.
Gruber, T., Mueller, M.M., Keil, A., Elbert, T., 1999. Selective visual-spatial attention alters induced gamma band responses in the human EEG. Clin. Neurophysiol. 110 (12), 2074–2085.
Holm, S., 1979. A simple sequentially rejective multiple test procedure. Scand. J. Stat. 6 (2), 65–70.
Hoogenboom, N., Schoffelen, J.M., Oostenveld, R., Parkes, L.M., Fries, P., 2006. Localizing human visual gamma-band activity in frequency, time and space. Neuroimage 29 (3), 764–773.
Hoogenboom, N., Schoffelen, J.M., Oostenveld, R., Fries, P., 2010. Visually induced gamma-band activity predicts speed of change detection in humans. Neuroimage 51 (3), 1162–1167.
Howard, M.W., Rizzuto, D.S., Caplan, J.B., Madsen, J.R., Lisman, J., Aschenbrenner-Scheibe, R., Schulze-Bonhage, A., Kahana, M.J., 2003. Gamma oscillations correlate with working memory load in humans. Cereb. Cortex 13 (12), 1369–1374.
Joliot, M., Ribary, U., Llinás, R., 1994. Human oscillatory brain activity near 40 Hz coexists with cognitive temporal binding. Proc. Natl. Acad. Sci. U.S.A. 91 (24), 11748–11751.

Kaiser, J., Hertrich, I., Ackermann, H., Lutzenberger, W., 2006. Gamma-band activity over early sensory areas predicts detection of changes in audiovisual speech stimuli. Neuroimage 30 (4), 1376–1382.
Khayat, P.S., Niebergall, R., Martinez-Trujillo, J.C., 2010. Frequency-dependent attentional modulation of local field potential signals in macaque area MT. J. Neurosci. 30 (20), 7037–7048.
Lachaux, J.P., George, N., Tallon-Baudry, C., Martinerie, J., Hugueville, L., Minotti, L., Kahane, P., Renault, B., 2005. The many faces of the gamma band response to complex visual stimuli. Neuroimage 25 (2), 491–501.
Lakatos, P., O'Connell, M.N., Barczak, A., Mills, A., Javitt, D.C., Schroeder, C.E., 2009. The leading sense: supramodal control of neurophysiological context by attention. Neuron 64 (3), 419–430.
Lancaster, J.L., Woldorff, M.G., Parsons, L.M., Liotti, M., Freitas, C.S., Rainey, L., Kochunov, P.V., Nickerson, D., Mikiten, S.A., Fox, P.T., 2000. Automated Talairach atlas labels for functional brain mapping. Hum. Brain Mapp. 10 (3), 120–131.
Magosso, E., Serino, A., di Pellegrino, G., Ursino, M., 2010. Crossmodal links between vision and touch in spatial attention: a computational modelling study. Comput. Intell. Neurosci. 304941. (Electronic publication ahead of print 2009 Oct 22).
Maris, E., Oostenveld, R., 2007. Nonparametric statistical testing of EEG- and MEG-data. J. Neurosci. Methods 164 (1), 177–190.
Mueller, M.M., Gruber, T., Keil, A., 2000. Modulation of induced gamma band activity in the human EEG by attention and visual information processing. Int. J. Psychophysiol. 38 (3), 283–299.
Munneke, J., Heslenfeld, D.J., Theeuwes, J., 2008. Directing attention to a location in space results in retinotopic activation in primary visual cortex. Brain Res. 1222, 184–191.
Muthukumaraswamy, S.D., Edden, R.A.E., Jones, D.K., Swettenham, J.B., Singh, K.D., 2009. Resting GABA concentration predicts peak gamma frequency and fMRI amplitude in response to visual stimulation in humans. Proc. Natl. Acad. Sci. U.S.A. 106 (20), 8356–8361.
Nichols, T.E., Holmes, A.P., 2002. Nonparametric permutation tests for functional neuroimaging: a primer with examples. Hum. Brain Mapp. 15 (1), 1–25.
Nolte, G., 2003. The magnetic lead field theorem in the quasi-static approximation and its use for magnetoencephalography forward calculation in realistic volume conductors. Phys. Med. Biol. 48 (22), 3637–3652.
Oostenveld, R., Fries, P., Maris, E., Schoffelen, J., 2011. FieldTrip: open source software for advanced analysis of MEG, EEG, and invasive electrophysiological data. Comput. Intell. Neurosci. 2011, 156869.
Pantev, C., Makeig, S., Hoke, M., Galambos, R., Hampson, S., Gallen, C., 1991. Human auditory evoked gamma-band magnetic fields. Proc. Natl. Acad. Sci. 88 (20), 8996–9000.
Posada, A., Hugues, E., Franck, N., Vianin, P., Kilner, J., 2003. Augmentation of induced visual gamma activity by increased task complexity. Eur. J. Neurosci. 18 (8), 2351–2356.
Posner, M.I., Snyder, C.R., Davidson, B.J., 1980. Attention and the detection of signals. J. Exp. Psychol. 109 (2), 160–174.
Reynolds, J.H., Chelazzi, L., Desimone, R., 1999. Competitive mechanisms subserve attention in macaque areas V2 and V4. J. Neurosci. 19 (5), 1736–1753.
Saupe, K., Schröger, E., Andersen, S.K., Müller, M.M., 2009. Neural mechanisms of intermodal sustained selective attention with concurrently presented auditory and visual stimuli. Front. Hum. Neurosci. 3, 58.
Schmid, C., Büchel, C., Rose, M., 2011. The neural basis of visual dominance in the context of audio-visual object processing. Neuroimage 55 (1), 304–311.
Schroeger, E., Giard, M.H., Wolff, C., 2000. Auditory distraction: event-related potential and behavioral indices. Clin. Neurophysiol. 111 (8), 1450–1460.
Siegel, M., Donner, T.H., Oostenveld, R., Fries, P., Engel, A.K., 2008. Neuronal synchronization along the dorsal visual pathway reflects the focus of spatial attention. Neuron 60 (4), 709–719.
Simos, P.G., Papanikolaou, E., Sakkalis, E., Micheloyannis, S., 2002. Modulation of gamma-band spectral power by cognitive task complexity. Brain Topogr. 14 (3), 191–196.
Spence, C., Driver, J., 1997. On measuring selective attention to an expected sensory modality. Percept. Psychophys. 59 (3), 389–403.
Steinmetz, P.N., Roy, A., Fitzgerald, P.J., Hsiao, S.S., Johnson, K.O., Niebur, E., 2000. Attention modulates synchronized neuronal firing in primate somatosensory cortex. Nature 404 (6774), 187–190.
Talairach, J., Tournoux, P., 1988. Co-planar stereotaxic atlas of the human brain: 3-dimensional proportional system: an approach to cerebral imaging. Thieme, Stuttgart.
Tallon-Baudry, C., Bertrand, O., Delpuech, C., Pernier, J., 1996. Stimulus specificity of phase-locked and non-phase-locked 40 Hz visual responses in human. J. Neurosci. 16 (13), 4240–4249.
Tallon-Baudry, C., Bertrand, O., Henaff, M.A., Isnard, J., Fischer, C., 2005. Attention modulates gamma-band oscillations differently in the human lateral occipital cortex and fusiform gyrus. Cereb. Cortex 15 (5), 654–662.
Tiitinen, H., Sinkkonen, J., Reinikainen, K., Alho, K., Lavikainen, J., Naatanen, R., 1993. Selective attention enhances the auditory 40-Hz transient response in humans. Nature 364 (6432), 59–60.
Vidal, J.R., Chaumon, M., O'Regan, J.K., Tallon-Baudry, C., 2006. Visual grouping and the focusing of attention induce gamma-band oscillations at different frequencies in human magnetoencephalogram signals. J. Cogn. Neurosci. 18 (11), 1850–1862.
Womelsdorf, T., Fries, P., Mitra, P.P., Desimone, R., 2006. Gamma-band synchronization in visual cortex predicts speed of change detection. Nature 439 (7077), 733–736.
Wyart, V., Tallon-Baudry, C., 2008. Neural dissociation between visual awareness and spatial attention. J. Neurosci. 28 (10), 2667–2679.

7.)

Butz M[*,c], Timmermann L*, Braun M, Groiss SJ, Wojtecki L, Ostrowski S, Krause H, Pollok B, Gross J, Südmeyer M, Kircheis G, Häussinger D, Schnitzler A,

"*Motor impairment in Liver Cirrhosis without and with Minimal Hepatic Encephalopathy*"

Acta Neurol Scand 2010. Jul;122(1):27-35.

Impact-Faktor: 2.2

Acta Neurol Scand 2010: 122: 27–35 DOI: 10.1111/j.1600-0404.2009.01246.x

ACTA NEUROLOGICA
SCANDINAVICA

Motor impairment in liver cirrhosis without and with minimal hepatic encephalopathy

Butz M, Timmermann L, Braun M, Groiss SJ, Wojtecki L, Ostrowski S, Krause H, Pollok B, Gross J, Südmeyer M, Kircheis G, Häussinger D, Schnitzler A. Motor impairment in liver cirrhosis without and with minimal hepatic encephalopathy.
Acta Neurol Scand: 2010: 122: 27–35.

Aim – Manifest hepatic encephalopathy (HE) goes along with motor symptoms such as ataxia, mini-asterixis, and asterixis. The relevance of motor impairments in cirrhotics without and with minimal HE (mHE) is still a matter of debate. *Patients and methods* – We tested three different groups of patients with liver cirrhosis: no signs of HE (HE 0), mHE, and manifest HE grade 1 according to the *West Haven criteria* (HE 1). All patients ($n = 24$) and 11 healthy control subjects were neuropsychometrically tested including critical flicker frequency (CFF), a reliable measure for HE. Motor abilities were assessed using *Fahn Tremor Scale* and *International Ataxia Rating Scale*. Fastest alternating index finger movements were analyzed for frequency and amplitude. *Results* – Statistical analyses showed an effect of HE grade on tremor and ataxia ($P < 0.01$). Additionally, both ratings yielded strong negative correlation with CFF ($P < 0.01$, $R = -0.5$). Analysis of finger movements revealed an effect of HE grade on movement frequency ($P < 0.03$). Moreover, decreasing movement frequency and increasing movement amplitude parallel decreasing CFF ($P < 0.01$, $R = 0.6$). *Conclusion* – Our results indicate that ataxia, tremor, and slowing of finger movements are early markers for cerebral dysfunction in HE patients even prior to neuropsychometric alterations becoming detectable.

M. Butz[1,2], L. Timmermann[3], M. Braun[1,2], S. J. Groiss[1,2], L. Wojtecki[1,2], S. Ostrowski[1,2], H. Krause[1,2], B. Pollok[1,2], J. Gross[4], M. Südmeyer[1,2], G. Kircheis[5], D. Häussinger[5], A. Schnitzler[1,2]

[1]Institute of Clinical Neuroscience and Medical Psychology, Heinrich-Heine University, Düsseldorf, Germany; [2]Department of Neurology, University Hospital Düsseldorf, Düsseldorf, Germany; [3]Department of Neurology, University Hospital of Cologne, Cologne, Germany; [4]Department of Psychology, University of Glasgow, Glasgow, UK; [5]Department of Gastroenterology and Hepatology, University Hospital Düsseldorf, Düsseldorf, Germany

Key words: ataxia; critical flicker frequency; hepatic encephalopathy; metabolic disorder; neurophysiology; tremor

Markus Butz, Department of Neurology, Heinrich-Heine University, Moorenstr. 5, D-40225 Düsseldorf, Germany
Tel.: +49 211 81 18415
Fax: +49 211 81 19033
e-mail: markus.butz@uni-duesseldorf.de

M. Butz and L. Timmermann have contributed equally to the study.

Accepted for publication June 23, 2009

Introduction

Hepatic encephalopathy (HE) is a complication occurring in patients suffering from liver cirrhosis (1, 2), which is characterized by a variety of neuropsychological, vigilance, and motor deficits (3–6). The current opinion is that in minimal HE (mHE) (3, 4, 6–8), previously known as *subclinical HE*, apparent motor symptoms are lacking, but detailed movement analyses have already revealed slight motor impairments in mHE patients in fine motor control (9, 10). However, extensive neuropsychometric testing has so far been the only way of credibly assessing mHE (11, 12).

Manifest HE can be classified into four stages. In addition to altered sleep patterns, agitation and disorientation, motor symptoms occur already in early stages of HE. Except for ataxia, the most evident motor symptom in HE 1 is mini-asterixis, which is present during maintained posture. Previous studies demonstrated that mini-asterixis in *manifest HE* arises from a pathologically slowed drive of the primary motor cortex towards the muscles (13, 14) that is accompanied by slowed thalamo-motor-cortical coupling (15, 16). In more severe HE (HE 2 and HE 3), an additional, more striking, motor symptom occurs most commonly termed asterixis. It is also referred to as flapping tremor and indicated by a sudden lapse of posture. Moreover, previous findings have suggested the hypothesis that the diverse clinical deficits in HE – in the motor and in the visual system – are the result of a global overall slowing and pathological synchronization of oscillatory cerebral activity (13, 16).

As motor symptoms are an obvious and major symptom in HE, this study tried to determine the degree to which motor impairments can be assessed

in mildly affected patients. We hypothesized that in early stages of HE, motor impairment could already be revealed using sensitive testing. Therefore, HE patients at various stages, patients suffering from liver cirrhosis without signs of HE in evidence, and healthy controls were neuropsychometrically tested including the critical flicker frequency (CFF) and underwent a blinded movement rating. Additionally, we studied fastest index finger movements using a 3D ultrasound motion detection system and a recently developed custom-made automated analysis algorithm determining amplitude and frequency of movements (17).

Our results show motor impairment in cirrhotics without HE. This impairment likely represents earliest signs of HE, even prior to neuropsychometric deficits becoming clinically detectable.

Patients and methods

Patients, clinical assessment and critical flicker frequency

The study was performed in 24 patients with low-grade HE (3) (HE 0, mHE, HE 1). In addition, 11 healthy age-matched controls were recruited by an advert in a local newspaper and included after medical check-up (Table 1).

To reveal the current state of HE, a combination of clinical examination and a neuropsychometric test battery was performed consisting of computer-assisted psychometric measures as described in detail elsewhere (18). Additionally, testing included the CFF determined using an automatic testing device (18). The procedure for assessment of CFF has been extensively described previously and CFF turned out to be a reliable parameter for HE grading (18–20).

All patients suffered from liver cirrhosis and HE was classified according to *West Haven criteria* and neuropsychometric testing (1, 4, 5). Eight patients suffered from HE grade 1 (HE 1). Patients without evidence for manifest HE according to the *West Haven criteria* were classified as having no HE (HE 0; $n = 8$), when none or only one computerized test was abnormal. With two or more pathological tests, patients were classified as mHE ($n = 8$). Clinical grading and assessment of CFF was performed within 12 h, following examination by an experienced hepatologist (G. Kircheis) and a neurologist (L. Timmermann and A. Schnitzler) without knowledge of the findings.

Liver cirrhosis was identified in all patients by liver biopsy, if clinically indicated, or by abdominal ultrasound or CT-scan and laboratory results. Etiology of liver cirrhosis was alcoholic ($n = 10$), hepatitis C virus (HCV) ($n = 9$) or hepatitis B virus ($n = 2$), cryptogenic ($n = 1$), or a combination of HCV and alcoholic ($n = 2$).

None of the patients had a history of other neurological diseases before admission. During the observed and documented time span, no neuroleptic drugs were taken by any of the patients.

Table 1 Patient groups and clinical characteristics

Group	Controls	HE 0	mHE	HE 1
n	11	8	8	8
Age (years)	59.5 ± 7.6	61.0 ± 8.0	68.8 ± 4.8	60.1 ± 8.3
Gender (F/M)	4/7	3/5	2/6	0/8
Child-Pugh score	–	A	5 A/3 B	7 B/1 C
CFF (Hz)	42.0 ± 2.9	40.5 ± 1.0	39.4 ± 4.0	35.7 ± 2.0
Neuropsychometry				
Line tracing test (PR)	58.00 ± 20.75	48.50 ± 13.48	28.75 ± 13.33	12.43 ± 10.46
Reaction time (ms)	440.10 ± 93.42	528.83 ± 94.89	569.50 ± 90.43	733.43 ± 303.51
Cognitrone test (PR)	69.10 ± 14.65	36.67 ± 17.65	32.86 ± 16.75	27.76 ± 19.08
Aiming (duration in s)	8.49 ± 1.36	9.57 ± 1.93	9.54 ± 1.70	15.39 ± 2.90
Steadiness (PR errors)	83.80 ± 17.58	95.33 ± 4.89	84.14 ± 20.40	31.13 ± 19.87
Tapping (PR hits)	68.20 ± 23.82	60.83 ± 22.71	43.57 ± 26.48	25.57 ± 18.13
Movement rating				
Tremor score (%)	1.76 ± 0.40	3.61 ± 0.63	4.25 ± 0.93	8.03 ± 1.52
Ataxia score (%)	2.36 ± 0.58	6.88 ± 0.90	7.94 ± 1.03	12.06 ± 2.07
Movement analysis				
maxFAM (Hz)	6.66 ± 0.96	5.76 ± 0.63	5.64 ± 0.97	5.58 ± 0.64
meanFAM (Hz)	5.06 ± 0.72	4.59 ± 0.52	4.40 ± 0.73	4.25 ± 0.57
maxAMP (°)	32.67 ± 12.29	38.81 ± 10.73	41.94 ± 17.07	43.69 ± 10.43
meanAMP (°)	20.32 ± 5.78	26.69 ± 8.16	28.64 ± 13.48	29.13 ± 8.56

Given are demographics and clinical characteristics, key results of neuropsychometric assessment, movement rating and movement analysis.
PR, percentile rank; F, female; M, male.

The study was approved by the local ethics committee and is in accordance with the Declaration of Helsinki. All subjects gave their written informed consent prior to the study.

Tremor and ataxia rating

Clinical testing was performed by experienced movement disorder specialists (S.J. Groiss or M. Südmeyer) using the *Fahn Tremor Scale* (21) and the *International Ataxia Rating Scale* (22). To ensure interobserver reliability, a second experienced rater (L. Wojtecki) was blinded for severity of HE and performed a second rating based solely on videotapes of the first rating. Mean rating scores of both raters were used for analysis.

Paradigm, measurements and data analysis

Paradigm and measurements had been used previously in a study addressing motor symptoms in Parkinson's disease (17). Handedness in patients and controls was tested using the Annett handedness test (23). Patients and controls were comfortably seated in a chair with bilateral armrests. Fastest alternating index finger movements (FAM) of the right hand were measured. The whole hand was lying with the ulnar side on the armrest. Fingers I and III–V were loosely flexed and the index finger stretched. All subjects were instructed to perform alternating flexion–extension movements of the index finger as 'fast and smoothly as possible' in the metacarpophalangeal joint. Five periods of 10 s of movement alternated with 30 s of rest. Markers (ultrasound transmitters) were positioned on the metacarpophalangeal joint and on the radial end of the index finger.

Movements were recorded using a 3D ultrasound motion detection system (CMS 70P, Zebris, Isny, Germany). This system localizes ultrasound markers within a 1-mm spatial and high-temporal resolution (100 Hz with two markers) by evaluation of transmission times and triangulation of marker position from three microphones integrated into a mobile receiver platform. Using this approach, the system instantaneously calculates the position of all ultrasound-markers in a 3D coordinate system. The receiver panel was positioned about 1 m above the moving hand. Positions of markers and receiver platform were defined to be reliably reproduced in subsequent sessions. Artifacts by reflection from the ultrasound waves were carefully avoided by modifications in the recording setup. Data were stored on the recording PC's hard disk and analyzed offline.

Data analysis was performed using custom-made software based on MATLAB™ 7.1 (The Mathworks Inc., Natick, MA, USA). Each data set was carefully inspected offline for artifacts. Contaminated epochs were excluded from further analysis. From the position of the markers, the maximum and mean values of five movement parameters were determined: maximum frequency (maxFREQ), mean frequency (meanFREQ), maximum amplitude (maxAMP), and mean amplitude (meanAMP). Details of the analysis are provided elsewhere (17).

Statistics

Statistical analyses were done using SPSS 14.0™ software (SPSS Inc., Chicago, IL, USA). Interobserver reliability was tested using Cronbach's alpha. Chi-square tests revealed that all data were normally distributed. CFF, age, mean tremor, and ataxia scores were tested for the four groups by a univariate analysis of variance (ANOVA) (controls vs HE 0 vs mHE vs HE 1). As *post-hoc* test a pairwise multiple comparison was done using least significant difference test (LSD). Correlations between tremor/ataxia scores, neuropsychometric tests, and CFF were determined using one-sided Spearman-Rho correlation.

For group analysis of movement parameters, repeated univariate ANOVA were calculated for each of the four subject groups (controls, HE 0, mHE, and HE 1). Main factors were: (i) maxFREQ, (ii) meanFREQ, (iii) maxAMP, and (iv) meanAMP. Again, a *post-hoc* test using LSD test to reveal intergroup differences was performed.

Correlation between age, CFF, neuropsychometric tests, and movement parameters (maxFREQ, meanFREQ, maxAMP, meanAMP) showed an influence of age on maxFREQ and meanFREQ. Therefore, a partial correlation adjusting for age was calculated.

To reveal the effects of alcohol abuse, a corresponding analysis of data was performed for a subgroup of subjects (non-alcohol group) including non-alcoholic liver cirrhosis patients (HE 0: $n = 6$; mHE: $n = 6$) and healthy controls (23 of 35 subjects). For all repeated measurements, alpha adjustments were performed using the sequential Bonferroni correction (24).

Results

Critical flicker frequency, handedness and age

Testing of handedness using Annett's Handedness Questionnaire revealed pure right-handedness in all subjects. No main effect between groups could be found for age (Table 1).

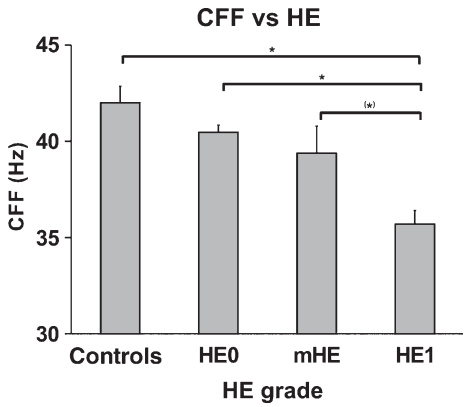

Figure 1. Critical flicker frequency and grade of hepatic encephalopathy. Mean critical flicker frequency (CFF) in the four different subject groups [$^{*}P < 0.05$; $^{(*)}P < 0.1$]. It is evident that CFF decreases as HE worsens. Hence, manifest HE 1 can be distinguished from healthy controls, patients suffering from minimal HE, and cirrhotics without HE. Error bars indicate SE (mHE, minimal HE; HE 0, cirrhotics without HE, HE 1, patients suffering from manifest HE grade 1, following *West Haven criteria*).

Analysis of CFF reproduced results of previous studies (18–20), showing a decrease of CFF with worsening HE ($P < 0.01$; Table 1, Fig. 1). Thereby, significant differences can be shown between HE 1 patients and healthy controls ($P < 0.01$) as well as HE 0 patients ($P = 0.02$). Additionally, a trend can be observed in the comparison of HE 1 patients and mHE patients ($P = 0.08$). Technical problems made CFF testing in two patients and one control subject impossible.

Tremor and ataxia

Interobserver reliability between blinded on-site rating and video-rating was highly significant for both ataxia and tremor ratings (Cronbach's alpha = 0.9).

The ANOVA revealed a strong effect of HE grade on tremor [$P < 0.01$; non-alcohol-group: n.s. ($P = 0.11$)] and ataxia ($P < 0.01$; non-alcohol-group: $P < 0.01$) scores (Table 1, Fig. 2).

Post-hoc analysis for tremor rating showed significant differences between controls and HE 1 patients ($P < 0.01$), HE 1 and HE 0 patients ($P = 0.02$) and between HE 1 and mHE patients ($P = 0.05$) (Fig. 2A).

Post-hoc analysis for ataxia rating yielded significant differences between controls and all other groups (HE 1: $P < 0.01$; mHE: $P < 0.02$, non-alcohol-group: $P < 0.01$; HE 0: $P = 0.04$, non-alcohol-group: $P < 0.02$) and between HE 1 and HE 0 patients ($P = 0.01$). Additionally, a trend was obvious between HE 1 patients and mHE patients ($P = 0.07$; Fig. 2B).

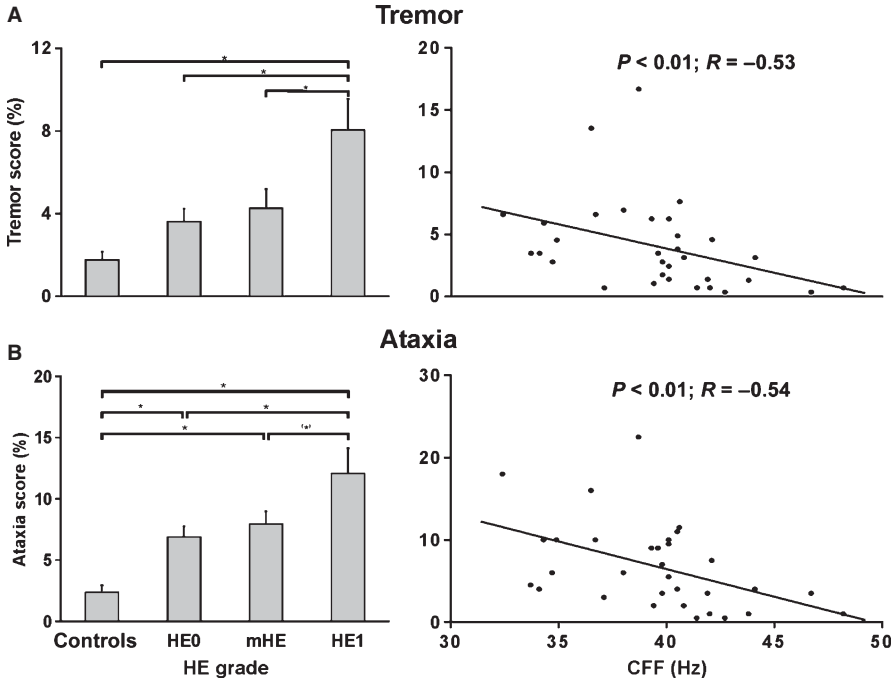

Figure 2. Tremor and ataxia rating. Mean tremor (A) and ataxia (B) rating in the four different subject groups and correlation with the critical flicker frequency (CFF) [$^{(*)}P < 0.1$; $^{*}P < 0.05$]. An increase in tremor and ataxia rating with worsening HE can be seen. Additionally, ratings show a correlation with CFF as a reliable parameter for the severity of HE. Error bars indicate SE (mHE, minimal HE; HE 0, cirrhotics without HE; HE 1, patients suffering from manifest HE grade 1, following *West Haven criteria*).

Correlation with the CFF revealed strong correlations between CFF and tremor rating ($P < 0.01$, $R = -0.53$; non-alcohol group: $P = 0.04$, $R = -0.40$; Fig. 2A) and between CFF and ataxia rating ($P < 0.01$, $R = -0.54$; non-alcohol group: $P = 0.03$, $R = -0.50$; Fig. 2B).

In addition, tremor and ataxia scores correlated with line tracing test (tremor: $P = 0.04$, $R = -0.42$/ataxia: $P = 0.01$, $R = -0.48$); reaction time ($P = 0.02$, $R = -0.46$/$P = 0.08$, $R = -0.36$), Cognitrone Test ($P = 0.02$, $R = 0.46$/$P < 0.01$, $R = 0.53$), aiming ($P = 0.03$, $R = 0.44$/$P = 0.02$, $R = 0.49$), steadiness ($P < 0.01$, $R = -0.58$/$P < 0.01$, $R = -0.59$), line tracking test (errors; $P = 0.03$, $R = -0.44$/$P = 0.03$, $R = -0.50$), and tapping ($P = 0.03$, $R = -0.43$/$P = 0.03$, $R = -0.45$).

Fastest alternating finger movements

Analysis of FAM yielded significant main effects for the maximal movement frequency and a trend for the mean movement frequency (ANOVA: maxFREQ: $P < 0.03$; non-alcohol group: $P = 0.05$, $R = -0.50$, meanFREQ: $P = 0.07$; non-alcohol group: n.s., $P = 0.12$; Table 1 and Fig. 3). Controls performed faster movements than all patient groups, but no significant differences could be observed between patient groups (*Post-hoc* analysis for maxFREQ: controls vs HE 0: $P = 0.04$, controls vs mHE: $P = 0.02$, controls vs HE 1: $P = 0.01$; Fig. 3A; *Post-hoc* analysis for meanFREQ: controls vs mHE: $P = 0.02$; controls vs HE 1: $P = 0.05$; controls vs HE 0: n.s.; Fig. 3B).

By contrast, there were no significant effects evident in the movement amplitude (ANOVA: meanAMP: $P = 0.18$, maxAMP: $P = 0.32$; Fig. 3C–D).

Interestingly, we were able to show strong correlations between CFF as the parameter for the severity of HE and all movements parameters (corrected partial correlation: maxFREQ: $P < 0.01$, $R = 0.64$; non-alcohol group: $P = 0.05$, $R = 0.46$; meanFREQ: $P < 0.01$, $R = 0.57$; non-alcohol group: n.s.; meanAMP: $P = 0.02$, $R = -0.42$; non-alcohol group: n.s.; maxAMP: $P = 0.01$, $R = -0.40$; non-alcohol group: n.s.; Fig. 3A–D).

Additionally, tremor and ataxia scores correlated with line tracing (maxFREQ: $P < 0.01$, $R = 0.63$; meanFREQ: $P < 0.01$, $R = 0.59$/maxAMP: $P = 0.04$, $R = -0.41$; meanAMP: $P = 0.04$, $R = -0.42$); reaction time (maxFREQ: $P < 0.01$, $R = 0.61$; meanFREQ: $P = 0.01$, $R = 0.53$/maxAMP: $P = 0.03$, $R = -0.43$; meanAMP: $P = 0.02$), Cognitrone Test (maxFREQ: $P < 0.01$, $R = 0.66$; meanFREQ: $P < 0.01$; $R = 0.55$/maxAMP: $P = 0.03$, $R = -0.44$; meanAMP: $P < 0.01$, $R = -0.52$), aiming (maxFREQ: $P < 0.01$, $R = 0.53$; meanFREQ: $P < 0.01$, $R = 0.57$), steadiness (maxAMP: $P = 0.04$, $R = -0.43$; meanAMP: $P = 0.8$, $R = -0.036$), and tapping (maxFREQ: $P = 0.02$, $R = -0.43$; meanFREQ: $P < 0.01$, $R = 0.53$).

Discussion

The focus of the present study was to examine motor impairments in patients suffering from liver cirrhosis, but without any signs of HE or with mHE. We were able to demonstrate that HE is accompanied by motor impairments already at the earliest stages.

The present work revealed for the first time that even patients with liver cirrhosis, but without clinical or neuropsychometric signs of HE, show motor impairments. Thus, higher ataxia ratings and a slowing of FAM was evident in HE 0 patients compared with healthy controls. Moreover, strong correlations between CFF as a recently established parameter for severity of HE and both tremor/ataxia ratings and movement kinematics were obvious. These correlations suggest a close relationship between motor impairments and severity of HE. We, therefore, conclude that assessment of these motor deficits may be a sensitive tool to detect first signs of HE, even before neuropsychometric testing allows for the detection of impairments.

Tremor and ataxia

In the present study, we provide evidence that tremor and ataxia rating by specialized physicians can accurately detect motor impairments in cirrhotics without or with mHE and, additionally, can differentiate minimal and manifest stages of HE.

However, ataxia rating seems to be more suitable for differentiation between healthy controls and mHE patients and cirrhotics without HE. Furthermore, correlation with CFF, a reliable parameter for the grading of HE, is stronger with ataxia rating than with tremor rating.

In two studies, Spahr et al. (25, 26) already used the *Unified Parkinson's Disease Rating Scale* to correlate observations with clinical parameters in HE patients. They showed a positive correlation with pallidal hyperintensities and a negative correlation with the choline/creatin ratio in basal ganglia structures and occipital white matter (25, 26). Additionally, they presented a positive correlation between choline/creatin ratio and the Purdue

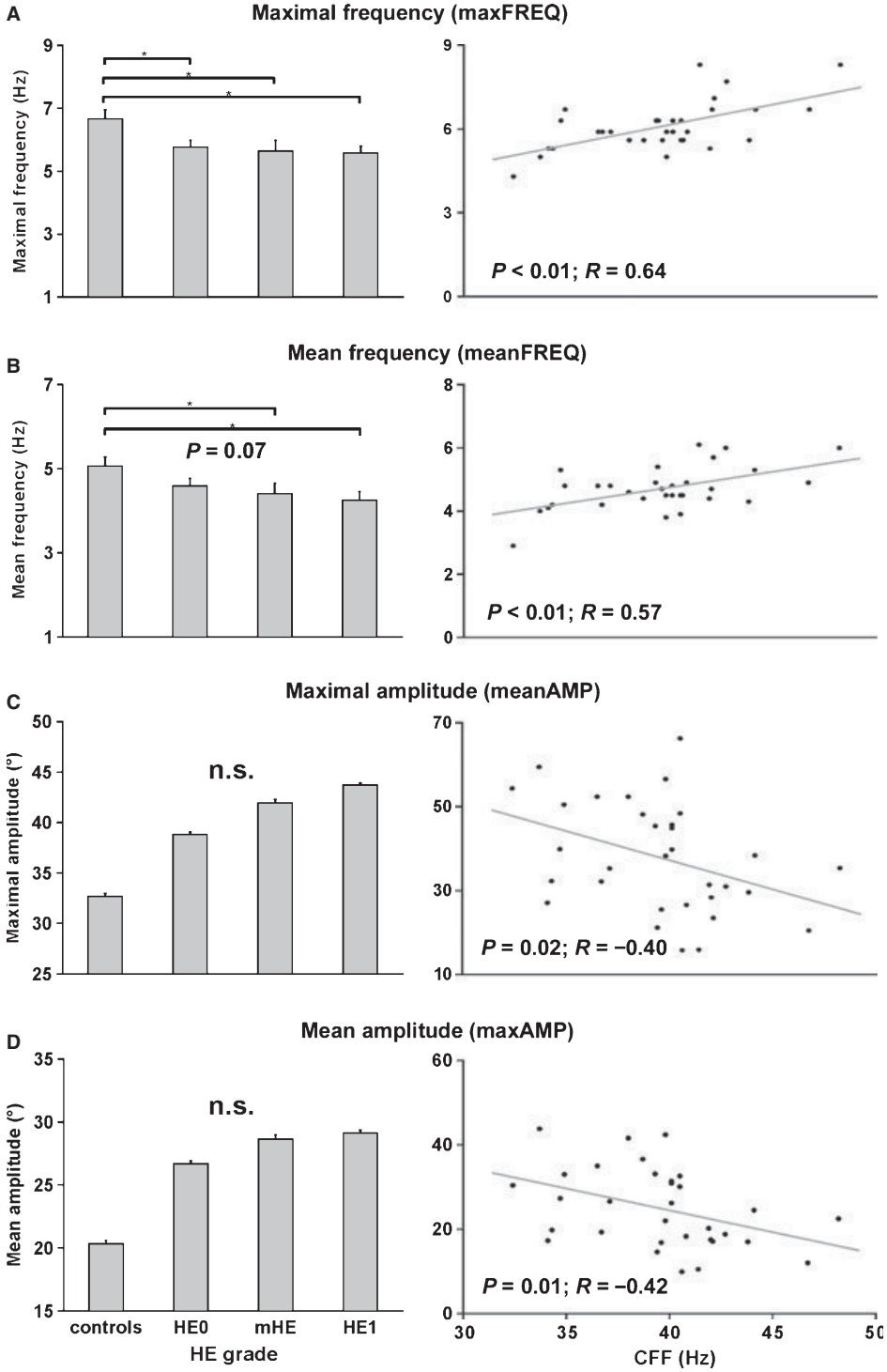

Figure 3. Movement parameters. Mean movement parameters of fastest alternating finger movements (FAM): (A) maximal frequency (maxFREQ), (B) mean frequency (meanFREQ), (C) maximal amplitude (maxAMP), and (D) mean amplitude (meanAMP) in the four different subject groups and correlation with CFF (*$P < 0.05$; n.s., not significant). A slowing of the fastest movement frequency with worsening HE can be observed, whereas the movement amplitude shows no significant changes. Furthermore, with regard to movement frequency and amplitude, there is an evident correlation with CFF as a reliable parameter for the severity of HE. Error bars indicate SE (mHE, minimal HE; HE 0, cirrhotics without HE; HE 1, patients suffering from manifest HE grade 1, following *West Haven criteria*).

Pegboard score, a measurement for mild parkinsonism (25). Along the same line, Kulisevsky et al. gave account of correlations of pallidal hyperintensity with clinical symptoms and functions in HE (27). Moreover, Burkhard et al. (28) referred chronic parkinsonism to be associated with cirrhosis

combined with striking hyperintensities on T1-weigted images typically involving the substantia nigra and the globus pallidus bilaterally. All these studies hint at a key role of basal ganglia alterations for motor impairments in HE.

One might argue that higher ataxia ratings observed here could be, in part, the result of an alcohol-induced cerebellar dysfunction, but the inverse correlation of ataxia rating with CFF clearly points to an HE-related mechanisms. Moreover, only half of studied patients had an ethyltoxic liver cirrhosis (12 of 24), making a primarily alcohol-induced background of results less likely. This is further confirmed by the results of the non-alcohol group, which replicate the key findings of the overall group, although HE 1 patients are lacking in this subgroup.

Fastest alternating finger movements

Our results of the FAM paradigm show that early motor impairments in HE can be established not only through a physician's semi-quantitative rating, but also by a clear technical movement analysis. We have shown that maximal as well as mean movement frequency decrease with worsening HE. Maximal and mean amplitude, vice versa, increase with worsening HE, evident in the correlation with CFF.

Previously, Joebges et al. (10) undertook a detailed view on bradykinesia in cirrhotics. In contrast to the present work, they did not find significant differences between HE 0 patients and healthy controls. But in line with our results, they observed a significant correlation between movement frequency and time period needed to start the subsequent movement cycle in three of four tested movements (hand tapping, finger tapping, hip joint flexion/extension, not in pronation/supination of the forearm) and psychometric HE score, portosystemic encephalopathy index, extrapyramidal symptoms score (*Columbia Rating Scale*), and neurological examination score. Movement frequency, i.e., number of full cycles per time, decreased with increasing grade of HE. However, by contrast to the present study, they did not find an alteration of the average maximal angular velocity of movements. This is most likely because of the difference in the movements investigated or because of the different approaches to analysis.

The presented findings are partly in accordance with results reported by Mechtcheriakov et al. (9, 29). They found handwriting movements performed by HE patients to be markedly slower and less efficiently coordinated than those of healthy controls. Although handwriting is a more complex movement and differs from the simple index finger movements studied here, they already predicted significant alterations for FAM. However, their study did not reveal differences between controls and HE 0 patients and between HE patients of different severity.

One might argue that a slower maximal frequency of FAM as observed in HE 0 patients might not be directly related to HE but to muscle wasting. However, previous studies have shown that muscle wasting does not result in slower maximal movement velocity (30, 31). Hence, muscle wasting is unlikely to explain the present findings.

Interestingly, clinical rating seems to be more sensitive for the classification of patients, whereas correlation with CFF turned out to be stronger with technical movement analysis. However, experienced clinical rating seems to have a sufficient accuracy for day-to-day practice, whereas sophisticated movement analyses may offer the possibility of advanced studies, clinical grading of disease severity and therapy-control. Nevertheless, the results of both approaches in this study support one another.

Motor and neuropsychometric impairments

An interesting outcome of the present study is that dysfunction in the human motor system seems to emerge already at very early stages of HE. Thus, signs of tremor, ataxia, and other motor deficits can be identified in cirrhotics, even before neuropsychometric deficits allow the determination of mHE. This observation may suggest that the motor system is very sensitive to HE.

Furthermore, the usual neuropsychometric tests include a variety of motor tasks and present results show that both tests sensitive for motor impairments and tests sensitive for cognitive impairments show a correlation to the impaired motor performance in cirrhotics. Interestingly, basal ganglia structures play a key role in cortical networks, subserving cognitive as well as motor functions (32) and are altered in HE (25–27, 33). Hence, results indicate that ataxia, tremor, and FAM may serve as significant markers for basal ganglia-cortical dysfunction in general. Therefore, assessment of motor abilities may offer an additional way of detecting earliest signs of HE.

Pathophysiological considerations

Previous studies using magnetoencephalography (MEG) have demonstrated that mini-asterixis, a tremor-like symptom, in HE is associated with slowing of oscillatory cortico-muscular (13, 14) and thalamo-cortical coupling (15) putatively related to

low-grade cerebral edema and neurotransmitter disturbances in HE (3). Furthermore, this oscillatory neuronal slowing in the motor system is paralleled by neuronal slowing in the visual system reflected as reduced CFF (13). These results, thus, suggest that slowing of oscillatory processes represents a common pathophysiological mechanism underlying diverse clinical symptoms in HE (16). It is tempting to speculate, that the same mechanism is also relevant for the motor impairments in cirrhotics without HE. In fact, the reduced frequency of FAM indirectly points to that direction. However, future studies with simultaneous behavioral and MEG recordings are required to provide more direct evidence for the 'oscillatory slowing' hypothesis in cirrhotic without HE.

Conclusions

The present study demonstrates an impairment of motor abilities in cirrhotics without HE. Moreover, this impairment increases with disease severity as assessed by the CFF. Hence, motor impairments may serve as an early indicator for the occurrence of HE, even prior to the appearance of other signs of HE, e.g. pathological neuropsychometric testings. Therefore, including movement analysis in the clinical monitoring of patients with cirrhosis should be considered.

Acknowledgments

The authors wish to thank all patients for their cooperation during the measurements. This work was supported by the Deutsche Forschungsgemeinschaft (DFG) through SFB 575 'Experimentelle Hepatologie'. B. Pollok is grateful for financial support by the Deutsche Forschungsgemeinschaft (PO 806/2-2). L. Timmermann is supported by the 'Manfred-and-Ursula-Mueller Foundation'. M. Butz was supported by two travel allowances of the Boehringer Ingelheim Fonds (B. I. F.). D. Häussinger and G. Kircheis are patent holders for a bedside testing device for assessment of the critical flicker frequency. The authors have no further competing interests.

References

1. Butterworth RF. Complications of cirrhosis III. Hepatic encephalopathy. J Hepatol 2000;**32**(Suppl. 1):171–80.
2. Jones EA, Weissenborn K. Neurology and the liver. J Neurol Neurosurg Psychiatry 1997;**63**:279–93.
3. Häussinger D, Blei AT. Hepatic encephalopathy. In: Rodes J, Benhamou J-P, Blei AT, Reichen J, Rizzetto M, eds. The textbook of hepatology: from basic science to clinical practice, 3rd edn. Oxford: Wiley-Blackwell, 2007,728–60.
4. Ferenci P, Lockwood A, Mullen K, Tarter R, Weissenborn K, Blei AT. Hepatic encephalopathy – definition, nomenclature, diagnosis, and quantification: final report of the working party at the 11th World Congresses of Gastroenterology, Vienna, 1998. Hepatology 2002;**35**:716–21.
5. Conn H, Lieberthal MM. The hepatic coma syndromes and lactulose. Baltimore: Willimas & Wilkins, 1979.
6. Häussinger D, Cordoba J, Kircheis G et al. Definition and assessment of low-grade hepatic encephalopathy. In: Häussinger D, Kircheis G, Schliess F, eds. Hepatic encephalopathy and nitrogen metabolism. Dordrecht: Springer, 2006;423–32.
7. Amodio P, Montagnese S, Gatta A, Morgan MY. Characteristics of minimal hepatic encephalopathy. Metab Brain Dis 2004;**19**:253–67.
8. Ortiz M, Jacas C, Cordoba J. Minimal hepatic encephalopathy: diagnosis, clinical significance and recommendations. J Hepatol 2005;**42**(Suppl. 1):S45–53.
9. Mechtcheriakov S, Graziadei IW, Kugener A et al. Motor dysfunction in patients with liver cirrhosis: impairment of handwriting. J Neurol 2006;**253**:349–56.
10. Joebges EM, Heidemann M, Schimke N, Hecker H, Ennen JC, Weissenborn K. Bradykinesia in minimal hepatic encephalopathy is due to disturbances in movement initiation. J Hepatol 2003;**38**:273–80.
11. Watanabe A. Cerebral changes in hepatic encephalopathy. J Gastroenterol Hepatol 1998;**13**:752–60.
12. Hazell AS, Butterworth RF. Hepatic encephalopathy: an update of pathophysiologic mechanisms. Proc Soc Exp Biol Med 1999;**222**:99–112.
13. Timmermann L, Butz M, Gross J et al. Impaired cerebral oscillatory processing in hepatic encephalopathy. Clin Neurophysiol 2008;**119**:265–72.
14. Timmermann L, Gross J, Kircheis G, Häussinger D, Schnitzler A. Cortical origin of mini-asterixis in hepatic encephalopathy. Neurology 2002;**58**:295–8.
15. Timmermann L, Gross J, Butz M, Kircheis G, Häussinger D, Schnitzler A. Mini-asterixis in hepatic encephalopathy induced by pathologic thalamo-motor-cortical coupling. Neurology 2003;**61**:689–92.
16. Timmermann L, Butz M, Gross J, Kircheis G, Häussinger D, Schnitzler A. Neural synchronization in hepatic encephalopathy. Metab Brain Dis 2005;**20**:337–46.
17. Timmermann L, Braun M, Groiss S et al. Differential effects of levodopa and subthalamic nucleus deep brain stimulation on bradykinesia in Parkinson's disease. Mov Disord 2008;**23**:218–27.
18. Kircheis G, Wettstein M, Timmermann L, Schnitzler A, Häussinger D. Critical flicker frequency for quantification of low-grade hepatic encephalopathy. Hepatology 2002;**35**:357–66.
19. Romero-Gomez M, Cordoba J, Jover R et al. Value of the critical flicker frequency in patients with minimal hepatic encephalopathy. Hepatology 2007;**45**:879–85.
20. Sharma P, Sharma BC, Puri V, Sarin SK. Critical flicker frequency: diagnostic tool for minimal hepatic encephalopathy. J Hepatol 2007;**47**:67–73.
21. Fahn S, Tolosa E, Marin C. Clinical rating scale for tremor. In: Jankovic J, Tolosa E, eds. Parkinson's disease and movement disorders. Baltimore: Williams & Wilkins, 1993;271–80.
22. Trouillas P, Takayanagi T, Hallett M et al. International Cooperative Ataxia Rating Scale for pharmacological assessment of the cerebellar syndrome. The Ataxia Neuropharmacology Committee of the World Federation of Neurology. J Neurol Sci 1997;**145**:205–11.
23. Annett M. The distribution of manual asymmetry. Br J Psychol 1972;**63**:343–58.
24. Holm S. A simple sequentially rejective multiple test procedure. Scand J Statist 1979;**6**:65–70.
25. Spahr L, Vingerhoets F, Lazeyras F et al. Magnetic resonance imaging and proton spectroscopic alterations

correlate with parkinsonian signs in patients with cirrhosis. Gastroenterology 2000;**119**:774–81.
26. Spahr L, Burkhard PR, Grotzsch H, Hadengue A. Clinical significance of basal ganglia alterations at brain MRI and 1H MRS in cirrhosis and role in the pathogenesis of hepatic encephalopathy. Metab Brain Dis 2002;**17**:399–413.
27. Kulisevsky J, Pujol J, Balanzo J et al. Pallidal hyperintensity on magnetic resonance imaging in cirrhotic patients: clinical correlations. Hepatology 1992;**16**:1382–8.
28. Burkhard PR, Delavelle J, Du Pasquier R, Spahr L. Chronic parkinsonism associated with cirrhosis: a distinct subset of acquired hepatocerebral degeneration. Arch Neurol 2003;**60**:521–8.
29. Mechtcheriakov S, Graziadei IW, Rettenbacher M et al. Diagnostic value of fine motor deficits in patients with low-grade hepatic encephalopathy. World J Gastroenterol 2005; **11**:2777–80.
30. Andersen LL, Andersen JL, Magnusson SP et al. Changes in the human muscle force-velocity relationship in response to resistance training and subsequent detraining. J Appl Physiol 2005;**99**:87–94.
31. Mulder ER, Gerrits KH, Rittweger J, Felsenberg D, Stegeman DF, de Haan A. Characteristics of fast voluntary and electrically evoked isometric knee extensions during 56 days of bed rest with and without exercise countermeasure. Eur J Appl Physiol 2008;**103**:431–40.
32. Bhatia KP, Marsden CD. The behavioural and motor consequences of focal lesions of the basal ganglia in man. Brain 1994;**117**(Pt 4):859–76.
33. Spahr L, Butterworth RF, Fontaine S et al. Increased blood manganese in cirrhotic patients: relationship to pallidal magnetic resonance signal hyperintensity and neurological symptoms. Hepatology 1996;**24**:1116–20.

8.)

Timmermann L*,[c], **Butz M*,** Gross J, Ploner M, Südmeyer M, Kircheis G, Häussinger D, Schnitzler A[c],

"Pathological Oscillatory Processing of the human motor and visual system in hepatic encephalopathy",

Clin Neurophysiol 2008 Feb;119(2):265-72.

Impact-Faktor: 3.0

ELSEVIER

Clinical Neurophysiology 119 (2008) 265–272

www.elsevier.com/locate/clinph

Impaired cerebral oscillatory processing in hepatic encephalopathy ☆

L. Timmermann [c,*,1], M. Butz [a,1], J. Gross [d], M. Ploner [f], M. Südmeyer [a], G. Kircheis [b], D. Häussinger [b], A. Schnitzler [a,e,*]

[a] *Department of Neurology, University Hospital Düsseldorf, Germany*
[b] *Department of Gastroenterology and Hepatology, University Hospital Düsseldorf, Germany*
[c] *Department of Neurology, University Hospital Cologne, Germany*
[d] *Department of Psychology, University of Glasgow, United Kingdom*
[e] *Wales Institute of Clinical and Cognitive Neuroscience, University of Wales, Bangor, United Kingdom*
[f] *Department of Neurology, Technical University Munich, Germany*

Accepted 23 September 2007
Available online 4 December 2007

Abstract

Objective: Hepatic encephalopathy (HE) is characterized by neuropsychological and motor deficits. The present study tested the hypothesis that worsening of motor and sensory symptoms of HE results from a common basic deficit in the cerebral oscillatory processing within the human motor and visual system.
Methods: We investigated in 32 patients with liver cirrhosis and HE grades 0–2 critical flicker frequency (CFF) and cortico-muscular (M1–EMG) coherence as a measure of coupling between the surface EMGs of hand muscles and primary motor cortex (M1) activity recorded non-invasively with magnetoencephalography (MEG) during forearm elevation.
Results: Patients with HE-grade 2 developed excessive M1–EMG coherence at low frequencies. In contrast, maximum M1–EMG coherence in patients with no HE showed frequency and amplitude in the physiological range. CFF was continuously reduced with worsening grades of HE. Correlation analysis revealed significant correlation between the frequency of M1–EMG coherence and CFF.
Conclusions: Taken together, we demonstrate that increased grades of HE lead to a pathological M1–EMG drive which is reduced in frequency. These effects are correlated with an impaired perception of oscillatory visual stimuli.
Significance: The results suggest that pathological oscillatory neural processing in different human cerebral systems may represent a basic mechanism for the clinical manifestation of HE.

Keywords: Hepatic encephalopathy; MEG; EMG; Coherence; Tremor; Cirrhosis

1. Introduction

Hepatic encephalopathy (HE) is one of the major complications of liver cirrhosis. Its clinical presentation comprises neuropsychiatric symptoms, altered sleep patterns, changes in the state of vigilance such as somnolence, stupor up to coma and motor deficits (for reviews see (Butterworth, 2000; Conn, 1993)). The broad range of clinical symptoms suggests that HE induces an unspecific, fundamental dysfunction in different systems of the human central nervous system (CNS). However, the pathophysiological mechanism of this CNS-dysfunction has remained unclear.

The irregular tremor at advanced HE is primarily seen during sustained posture while being significantly reduced during movements or rest (Leavitt and Tyler, 1964).

☆ Disclosure: G.K. and D.H. are holding a patent of a CFF-testing device. Otherwise, the authors have reported no conflicts of interest.

* Corresponding authors. Tel.: +49 221 478 4000/7494 (L. Timmermann); +49 211 81 17893/18415; fax: +49 211 81 19033 (A. Schnitzler).
E-mail addresses: lars.timmermann@uk-koeln.de (L. Timmermann), schnitza@uni-duesseldorf.de (A. Schnitzler).

[1] These authors contributed equally to the study.

1388-2457/$32.00
doi:10.1016/j.clinph.2007.09.138

Because of the jerky clinical appearance and the clinical continuum from this "postural tremor" to the "flapping tremor" of asterixis the first was called "mini-asterixis" (Young and Shahani, 1986). A recent study analyzed synchronization between neuronal activity of the primary motor cortex activity (M1) and EMG activity in patients with "mini-asterixis" (Timmermann et al., 2002). The authors could demonstrate that "mini-asterixis" results from a pathologically increased and slowed drive of M1 (Timmermann et al., 2002). In a further study it was shown that this altered cortical drive on the spinal motor neuron pool is probably due to a pathologically slowed and augmented thalamo–cortical oscillatory coupling (Timmermann et al., 2003a). Thus, motor symptoms of HE might be due to a progressive slowing and pathological synchronization of oscillatory activity within the motor system.

Among the broad spectrum of neuropsychological tests, computerized test batteries and paper–pencil tests, the critical flicker frequency (CFF) was identified to be a new tool to access HE severity (Kircheis et al., 2002). This test identifies the lowest frequency at which a patient perceives a flickering light as steady. Interestingly, as HE changes from subclinical to severe grades, this ability to recognize the oscillatory nature of a visual stimulus is declining: Humans without HE reliably recognized stimuli at 39 Hz and more whereas patients with HE declined in the frequency even below 35 Hz depending on their grade of HE (Kircheis et al., 2002). The mechanism of this reversible phenomenon is still unclear. However, the human primary visual areas are able to process flicker-stimuli at frequencies that are higher than the maximum perceived flicker frequency (Herrmann, 2001). Interestingly, this processing involves oscillatory activity at these high frequencies in the involved visual areas (Herrmann, 2001). It is therefore likely that a dysfunction in the cerebral processing of oscillatory visual stimuli leads to the deficits in CFF of HE patients.

The present study tested the recently introduced hypothesis that advanced grades of HE are associated with a basic deficit in oscillatory processing in the visual and motor system (Timmermann et al., 2005). To test this hypothesis, we analyzed M1–EMG coupling in a total number of 32 patients with liver cirrhosis and clinically different stages of HE, ranging from no impairment up to stages with marked motor and neuropsychological deficits. Parallel to the MEG experiments the CFF was determined as a marker for processing of oscillatory information in the human visual system. Our findings provide evidence for a general deceleration and possibly enhanced synchronization of activity in the motor system with changes from low to high-grade HE which are paralleled by deficits in the processing of oscillatory stimuli in the visual system suggesting a principal deficit in cerebral oscillatory processing in HE patients. Preliminary data of this study have been presented in abstract form (Timmermann et al., 2004).

2. Methods

2.1. Patients and clinical assessment

The study was performed in 32 patients with mild to moderate stages of liver cirrhosis (age: mean 56.7 years, range: 32–78 years, 7 female). Etiology of liver cirrhosis was alcoholic, inflammatory (Hepatitis B and C) and, in one patient, an alpha1-antitrypsin-deficiency. Eighteen patients were measured only once without follow-up visits. In 14 patients subsequent measurements were performed at different stages of HE over a time period of up to 6 months (in 6 patients 1 follow up, in 4 patients 2 follow up, in 2 patients 3 follow up, in 1 patient 4 follow up, in 5 patients 5 follow up, together 39 follow up measurements and 32 first measurements). Data of cortico-muscular coherence in a subgroup of 12 patients have been published previously (Timmermann et al., 2003a; Timmermann et al., 2002), data of all other patients only were published in abstract form. Analysis was based primarily on the first measurements of all patients and in a second step repeated measurements were taken into account.

None of the patients had a history of neurological diseases before admission; especially a history of tremor within recent months was not reported by patients or relatives. Patients with alcohol-related cirrhosis had credibly stopped drinking for at least half a year. Therefore an alcoholic tremor could, as far as possible, be excluded (Neiman et al., 1990). During the observed and documented time span no neuroleptic drugs were taken by any of the patients. Liver cirrhosis was approved in all patients by liver biopsy, if clinically indicated, or by ultrasound of the abdomen or abdominal CT-scan and laboratory results. Grading of liver cirrhosis, according to the European Child-Pugh-classification (Pugh et al., 1973), revealed stages of liver cirrhosis between Grade A to C.

Manifest HE (HE 1–2) was diagnosed according to the "West-Haven-criteria" (Conn and Lieberthal, 1979) whereas subclinical HE (SHE) was assessed by computer-psychometry as described elsewhere (Kircheis et al., 2002). Briefly, the computerized test battery accounts for each subject the individual education and age of a large group of healthy controls and has been extensively validated by our group in our testing setting (Kircheis et al., 2002). In the previous study, one pathological test was accepted for patients to be classified as having no HE, two pathological tests were classified as subclinical HE and more than 2 pathological tests were classified as clinically manifest HE. Clinical grading was performed within 12 h after the MEG examination by a hepatologist and a neurologist without knowledge of the MEG findings (G.K., D.H. and A.S). Only one patient with HE grade 3 could be included into the analysis. This was due to the fact that all other patients at this HE grade could not reliably perform the CFF testing anymore. To calculate our results more adequately with a similar number of patients in each group we analyzed the patients by classifying in no HE,

subclinical and mild HE and moderate to severe HE (see Fig. 2).

In each single patient the CFF was tested using an automatic testing device (Kircheis et al., 2002). The testing procedure for assessment of the CFF has been extensively described previously and is extensively described in the appendix (Kircheis et al., 2002).

All patients involved in the study gave their written informed consent. The study was approved by the local Ethics Committee and is in accordance with the Declaration of Helsinki.

2.2. MEG recordings

The MEG recording procedure has been described in detail elsewhere (Timmermann et al., 2002). Briefly, muscle activity was registered with surface EMG electrodes placed on the extensor digitorum communis (EDC) muscle. The EMG was high-pass filtered at 60 Hz and rectified. Simultaneously, cerebral activity was recorded with a whole-head Neuromag 122™ MEG-system (sample rate: 1011 Hz, pass-band-filter: 0.03–330 Hz; for system description, see (Ahonen et al., 1993)). During recordings, subjects kept their forearm elevated with the hand outstretched and fingers slightly abducted. Five ''hold''-periods of 60 s each alternated with 30 s of rest.

Raw data as well as MEG Power spectra of all channels were carefully inspected offline for movement and myogenic artifacts resulting in a typical distribution in the outer and lateral MEG-channels. Analysis was restricted on artifact free recording times.

Coherence between MEG and EMG signals, as a frequently used measure for the interdependence between two signals, was calculated with a resolution of 0.98 Hz. Coherence is the ratio of the magnitude squared cross-spectra of two signals to the product of their individual auto-spectra (for details see (Gross et al., 2000; Schnitzler et al., 2000)). Values can range between 0 indicating independence of two signals and 1 indicating a perfectly linear relationship. All values are in the following shown in percent, i.e. 1 corresponds to 100% coherence and 0 corresponds to 0%.

To identify the brain source that showed maximum coherence to the surface EMG we used the analysis tool DICS (Dynamic Imaging of Coherent Sources, (Gross et al., 2001)) which employs a spatial filter algorithm (Gross and Ioannides, 1999b) on the recorded MEG data. Coherence spectra were calculated between the cerebral source with maximum coherence to the peripheral EMG and EMG activity and the frequency of maximum coherence was determined. Details of this procedure are listed in the Appendix A.

Individual high-resolution MR images were obtained from a 1.5 T Siemens Magnetom™ MRI scanner. From each subject an individual brain boundary element model (BEM) was calculated with respect to anatomical landmarks. The position of the individual BEM was transposed into the MEG-coordinate system by using anatomical landmarks and fiducial point markers used during the MEG measurements. Finally, the cortical sources of the MEG signals were superimposed on the MRI scans.

In patients with subsequent measurements cerebral sources of coupling with the peripheral EMG were introduced into all subsequent measurements with respect to the individual head position in each measurement. Spectra of cortico-muscular coherence were calculated. The most prominent peak of cortico-muscular coherence was detected and its frequency determined using an automated peak-detection algorithm in MATLAB. We decided to focus on the frequency of the maximum peak and not the ''low-frequency boarder'' of significant coherence because the latter was more ambiguous.

For statistical analysis we used the SPSS 11.0™ software and calculated linear correlation (Pearson) and an univariate analysis of variance between HE-grade and CFF as well as peak frequency of M1–EMG coherence. In a second step correlation between peak frequency of M1–EMG coherence and CFF was determined. Level of significance of cortico-muscular coherence, univariate analysis of variance and correlation analysis was taken with an alpha-error $p < 0.05$. All statistical operations were performed in two different steps: First, we included just the very first measurement of all patients thereby excluding the repeated measurements. Since the subjects were measured with at least one week between each testing, the clinical situation changed always slightly, in some patients, however, dramatically e.g. after a severe infection. Therefore, in a second analysis all repeated measurements (taken as independent measurements) were included into the calculations and statistical analysis. In our between-group comparisons and correlation analysis, all significant differences were the same using only the first measurement of each single patient compared to results including all repeated measurements. Therefore, repeated measurements were included in the further data analysis to strengthen the power of the analysis and are shown in Figs. 2 and 3. However, results of statistical analysis are given for first time measurements and including all repeated measurements separately throughout the Results section.

3. Results

HE grading in all 32 patients with liver cirrhosis revealed a broad variety from no HE at all up to manifest stages. In 14 patients subsequent MEG recordings were accompanied by parallel HE grading procedures and testing of CFF.

Patients were classified into three different stages, no HE (HE grade 0), subclinical or mild HE (SHE or HE grade 1) and moderate to severe HE (HE grade 2 and higher).

In the MEG recordings, all patients were able to perform the elevation of the forearm in the EMG. However, patients with a manifest HE showed frequently the previously described irregular ''tremor'' of ''mini-asterixis''

(Timmermann et al., 2003a; Timmermann et al., 2002; Young and Shahani, 1986). As demonstrated previously for HE patients with mini-asterixis the tremor frequency corresponded to the frequency of cortico-muscular coherence (Timmermann et al., 2002). In all patients the cerebral localization of strongest coherence with the peripheral EMG was localized within the "handknob" area of the precentral gyrus, the anatomical correlate of the primary motor cortex (M1) (Yousry et al., 1997).

The alteration of CFF and M1–EMG coherence is illustrated for different patients at different stages of HE (Fig. 1). A patient without clinical or subclinical HE (HE-grade 0, black line) showed a physiological M1–EMG coherence and a CFF of 39.7 Hz. In contrast, in a patient with clinically manifest HE grade 1, M1–EMG coherence increased in amplitude and showed a lower frequency (red line) accompanied by a reduced CFF. In the third patient with clinically severe HE grade 2 a dramatic increase in M1–EMG coherence with a remarkable shift of the peak frequency below 10 Hz (blue line) and a CFF reduction down to 33.1 Hz was observed.

Since we hypothesized that changes in oscillatory processing were altered in the visual and motor system we focus in the following on the peak frequency of cortico-muscular coherence and the CFF. As extensively described before (Kircheis et al., 2002), patients showed during changes from low-grade to high-grade HE a highly significant slowing in CFF (Figs. 1 and 2A, analysis for first measurements only: $F = 29.389$, $df = 2$, $p < 0.001$, analysis including all repeated measurements: $F = 68.02$, $df = 2$, $p < 0.001$). Comparison of the peak frequency of M1–EMG coherence was performed using an univariate analysis of variance (see Fig. 2). The frequency of maximum M1–EMG coherence became significantly lower with higher grades of HE in all first measurements as well as taken into account the repeated measurements (analysis of first measurements only, $F = 5.938$, $df = 2$, $p < 0.007$, analysis including all repeated measurements $F = 7.086$,$df = 2$, $p < 0.002$).

In a further step it was tested whether these differences between no HE, mild HE and moderate to severe HE with respect to M1–EMG coherence were also reflected in linear correlations. Indeed, the frequency of maximum M1–EMG coherence and HE-grade (significant for all first measure-

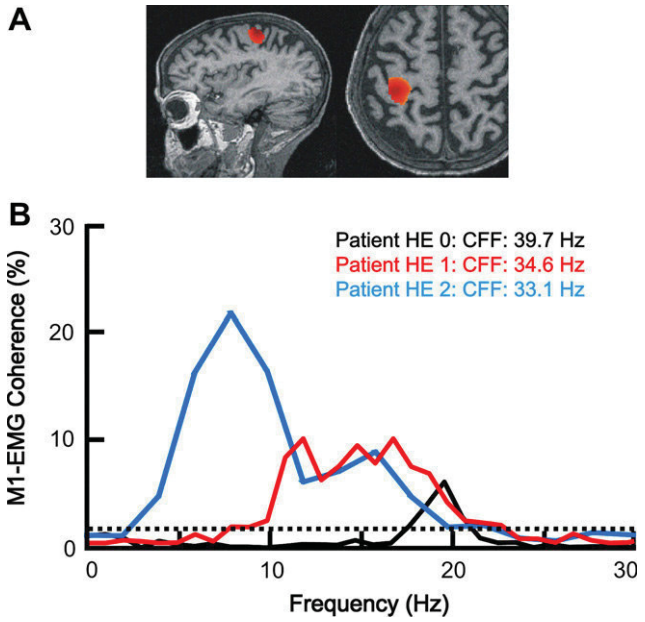

Fig. 1. Changes of CFF and M1–EMG coherence in three different patients at different stages of HE. (A) Localization of strongest cerebro-muscular coherence using DICS in the patient with HE grade 2. The area with highest coherence is the contralateral primary motor cortex (M1). (B) M1–EMG coherence: The patient with liver cirrhosis without HE (black line) shows physiological M1–EMG coherence. In contrast, M1–EMG coherence was remarkably increased at lower frequencies in the patient with clinically manifest HE with a parallel drop in CFF (red line). However, in the patient with HE grade 2 M1–EMG coherence was of high amplitude (blue line) and peak frequency shifted below 10 Hz. The corresponding CFF was below 34 Hz. (Dotted line represents 95% confidence level of coherence, calculated according to (Halliday et al., 1995)). (For interpretation of the references to colour in this figure legend, the reader is referred to the web version of this article.)

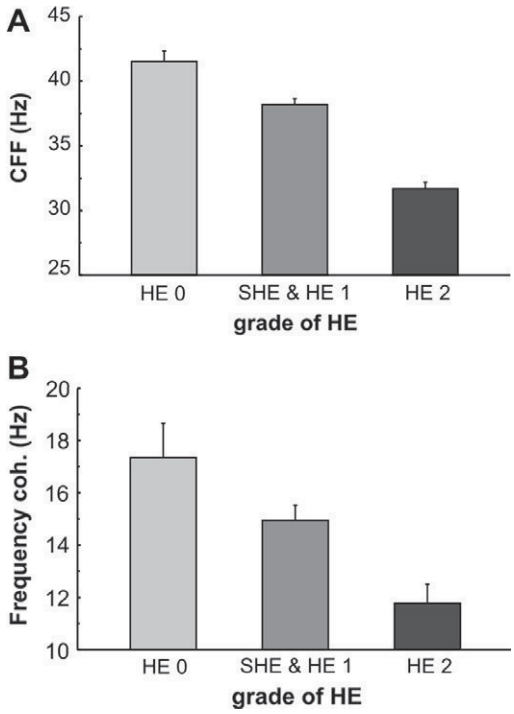

Fig. 2. CFF and peak frequency of M1–EMG coherence in different stages of HE. CFF and peak frequency of M1–EMG coherence in subjects without HE (grade 0), with subclinical or mild HE (SHE & HE 1) and moderate to severe HE (HE 2 and higher, all mean values and SEM, calculated for all 32 subjects including all 32 first time measurements and all 39 repeated measurements). (A) CFF versus HE grade. The CFF reliably reflects the grade of HE and is significantly determined by the severity of HE (all first measurements: $F = 29.389$, $df = 2$, $p < 0.001$, including repeated measurements: $F = 68.028$, $df = 2$, $p < 0.001$, univariate analysis of variance). (B) HE-grade vs. frequency of M1–EMG coherence: higher grades of HE are accompanied by significantly lower peak frequency of M1–EMG coupling (all first measurements: $F = 5.938$, $df = 2$, $p < 0.007$, including repeated measurements $F = 7.086$, $df = 2$, $p < 0.002$, univariate analysis of variance).

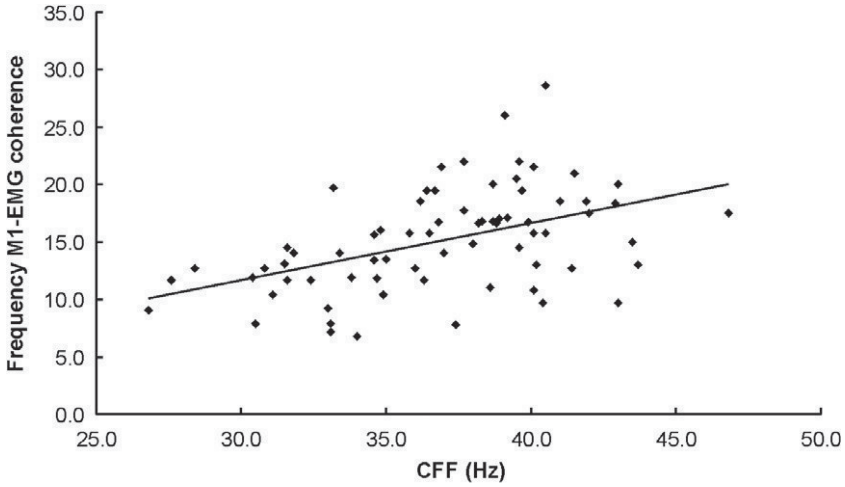

Fig. 3. Correlation between CFF and peak frequency of M1–EMG coherence. The correlation of critical flicker frequency (CFF) and peak frequency of M1–EMG coherence is highly significant (Pearson, $y = 0.498\ x - 3.23$, $R = 0.47$, $p < 0.001$). Shown are all measurements.

ments and all measurements, Pearson, $x = 4.7057 * y + 9.4908$, $R = 0.261$, $p < 0.05$) correlated significantly. Higher HE grades lead to a significantly reduced peak frequency of cortico-muscular coupling. To finally test, whether the dysfunction in the oscillatory processing of the motor system, determined by the frequency of M1–EMG coupling and the visual system, determined by CFF, were similar and simultaneous, CFF was correlated with the peak frequency of M1–EMG coherence. Indeed, lower values of CFF, indicating more severe HE, were significantly correlated with lower peak frequency of M1–EMG coherence (significantly different, $p < 0.001$ in analysis with first measurements only, as well as including all repeated measurements, see Fig. 3).

4. Discussion

The present study demonstrates that clinical worsening of HE is accompanied by reduced peak frequency of coherence between M1 and EMG as a measure for processing within the human motor system. This deterioration is correlated with an aggravating dysfunction of the visual system, namely in the perception of oscillating visual stimuli. These findings corroborate in a large number of patients with liver cirrhosis the hypothesis that severity of HE goes along with a general slowing of coupling within the motor system paralleled by dysfunction and slowing in the processing of oscillatory stimuli in the visual system. This common basic deficit in oscillatory processing could well be the major neurophysiological mechanism of encephalopathic dysfunction in different subsystems of the human central nervous system (Timmermann et al., 2005).

The frequency and the amplitude of cortico-muscular coherence in healthy controls show, even under controlled experimental conditions, a considerable inter-individual variability (Conway et al., 1995; Gross et al., 2000; Salenius et al., 1997). Furthermore, a number of factors can influence cortico-muscular coherence in the same subject. Kristeva-Feige and colleagues demonstrated an enhancing effect of attention on amplitude, but also an increase in peak frequency of EEG–EMG synchronization (Kristeva-Feige et al., 2002). Since patients with HE show deficits in attention this has to be considered as a major factor of influence. In addition, muscular strength used in an isometric contraction task can significantly alter the pattern of cortico-muscular coherence, e.g. by additional involvement of the ~40 Hz Piper rhythm (Brown et al., 1998). Besides these task-related differences pharmacological interventions can also significantly alter cortico-muscular coherence. Diazepam modulates amplitude of sensorimotor ~20 Hz oscillations (Baker and Baker, 2003) and carbamazepine modulates amplitudes of EEG–EMG coherence in the ~20 Hz range (Riddle et al., 2004). Thus, oscillatory coupling in the human motor system can be dose-dependently altered by exogenous pharmacological interventions. It is therefore well conceivable that an intrinsic change in excitatory and inhibitory transmitter systems in patients with HE can ''dose-dependently'' change oscillatory coupling in the human motor system.

Under controlled conditions the amplitude of cerebro-muscular coherence varies to a certain extent whereas the individual frequency band of cortico-muscular coherence remains stable (Gross et al., 2000). In the few patients with repeated measurements at similar severity of HE variation of cerebro-muscular coherence was rarely higher than ±2 Hz. We therefore assume that under controlled conditions the frequency of cerebro-muscular coherence remains stable. Mini-asterixis at higher grades of HE is probably the clinical manifestation of low-frequency M1–EMG coherence. As demonstrated in a previous publication we did not find ''physiological'' 15–30 Hz cerebro-muscular coherence simultaneously with Mini-asterixis at low-frequencies (Timmermann et al., 2002). This observation suggests that the low-frequency M1–EMG coupling in patients

with manifest HE and mini-asterixis corresponds to a pathologically slow M1–EMG drive (Timmermann et al., 2003a; Timmermann et al., 2002). Within the group of manifest HE-patients with mini-asterixis in this study we correlated the frequency of cerebro-muscular coupling and the CFF and could not find a significant correlation ($p > 0.05$). We speculate that this is due to the fact that (i) this subgroup is too small and (ii) the inter-individual differences are too high. Patients with mini-asterixis are difficult to measure repetitively under controlled experimental condition. Therefore, we do not have enough data to show that the intensity of mini-asterixis is increasing with higher grades of HE although one could speculate that this is the case.

A large number of substances are well described to influence excitatory and inhibitory CNS mechanisms in HE including changes in ammonium, excitatory and inhibitory neurotransmitters and cerebral cell hydration (Butterworth, 2000; Haussinger et al., 2000; Haussinger et al., 1994). However, the net effect of these modulations of excitation, inhibition and coupling in the human motor and visual system has so far remained unclear. Based on the present results we cannot decide which of these agents essentially modulates oscillatory processing in HE.

There is growing evidence that changes in excitatory and inhibitory connections between neuronal assemblies can lead to larger or smaller areas of synchronized neuronal activity and can well explain a broad deceleration or acceleration of synchronized oscillatory activity (Herculano-Houzel et al., 1999; Pfurtscheller et al., 2000; Schnitzler and Gross, 2005; Singer, 1993). Previous neurophysiological studies in HE patients have shown deceleration in EEG power spectra (Amodio et al., 1996). Moreover, recent MEG studies could demonstrate that "mini-asterixis" at manifest HE can be attributed to a pathologically increased and slowed M1 drive on spinal motor neurons (Timmermann et al., 2002). This pathological M1-drive is probably due to a pathologically slow thalamo-motor-cortical coupling (Timmermann et al., 2003a). It was therefore hypothesized that motor deficits in HE are a result of pathological synchronization and slowing of oscillatory activity within the human motor system (Timmermann et al., 2003a). Accordingly, the present study showed in a large number of patients that increasing HE severity leads to a continuous slowing in the frequency of M1–EMG coupling. However, since MEG is certainly not a routine examination in HE patients and this study is focusing on *pathophysiological mechanisms* of HE, predictive values, sensitivity and specificity of cortico-muscular coherence have not been assessed.

Certainly our analysis focused on the peak frequency of cerebro-muscular coherence in the physiological range of 15–30 Hz as well below 15 Hz. Therefore, changes in specific other frequency bands cannot be ruled out.

The perception of the "critical flicker frequency" has previously been shown to be a reliable marker for HE-grading (Kircheis et al., 2002). The CFF is a psychophysical measure and not a recording of neuronal activity within the human visual system. However, the cerebral correlate of flicker stimuli, even above the level of perception around 50 Hz, can be non-invasively measured as oscillatory activity at the same frequency of primary visual areas (Herrmann, 2001). Since this cerebral activity shows also oscillatory patterns one can suppose that the physiological processing of flicker stimuli in the sequence of human cerebral visual areas is of oscillatory nature. Therefore, it is likely that the increasing impairment in the perception of an oscillatory visual (flicker-) stimulus by the HE patients is mainly a problem in the processing of visual stimuli in higher cortical (and subcortical) visual pathways. However, future experiments have to test this assumption that the cerebral processing of oscillatory visual stimuli is actually impaired in HE patients.

Interestingly, the dysfunction in the CFF perception showed positive correlation with the alterations of frequency of M1–EMG coherence; a phenomenon clearly generated within the subcortical–cortical loops of the human motor system (Timmermann et al., 2003a). A positive correlation does not indicate a causal relationship. However, this observation demonstrates that different systems (visual and motor) within the human CNS do react to a similar extent with impairment to process oscillatory neuronal activity as the HE is deteriorating. One could therefore speculate whether a slowed oscillatory communication in different subsystems is a key mechanism of encephalopathic brain dysfunction explaining the broad variety of clinical deficits. Future studies should clarify whether this neurophysiological mechanism is limited to changes in HE or whether slowing in oscillatory processing is a basic neurophysiological patho-mechanism to explain changes also in other encephalopathic conditions.

Acknowledgements

The authors wish to thank all patients with hepatic encephalopathy for excellent cooperation during the measurements, Dr. Bettina Pollok for interesting discussions and Mrs. E. Rädisch for technical support with the MRI scans. This work was supported by the VolkswagenStiftung (I/73240) and the Deutsche Forschungsgemeinschaft through SFB 575 "Experimentelle Hepatologie" (Project C4). L.T. had full access to all of the data in the study and takes responsibility for the integrity of the data and the accuracy of the data analysis. L.T. is supported by the "Manfred and Ursula Müller Foundation".

Appendix A

Localization of sources using DICS

Raw data were carefully controlled offline and epochs with eye blinks and other artifacts were rejected from further analysis. Similar to our approach in previous studies (Südmeyer et al., 2004; Timmermann et al., 2003c; Tim-

mermann et al., 2002), we used the analysis tool DICS (dynamic imaging of coherent sources) to calculate coupling between the surface EMG signals and cerebral activity (Gross et al., 2001; Gross et al., 2002). It employs a spatial filter algorithm (Gross and Ioannides, 1999a) and a realistic head model of the individual subject to identify brain areas that are coherent to the surface EMGs. Coherence spectra between the identified areas and EMG were calculated with a resolution of 0.98 Hz. Coherence is a measure applied frequently for the interdependence of two signals in the frequency domain.(Halliday et al., 1995; Schnitzler et al., 2000).

In a first step, we carried out the transition from time to frequency domain by using fast Fourier transform (FFT). FFT was applied to all MEG and EMG signals in segments 1 s long (after applying a Hanning window), and the cross-spectral density C was computed between all combinations of MEG and EMG signals. The complex spectrum C was finally averaged across the entire recording period. One element $C_{i,j}$ of the final cross-spectral matrix consists of the cross spectrum of signals i and j (i.e., signals seen by two different sensors).

In the second step, we extracted the mean cross-spectral density of all sensor combinations in a selected frequency band as a complex N x N matrix, where N is the number of signals (MEG and EMG). Computation of cerebro-muscular coherence used the cross spectrum between the EMG and the MEG signal.

A third step consisted of the application of a spatial filter in the frequency domain (Gross et al., 2001) allowing the estimation of coherence between a point in the brain and an external reference signal (cerebro-muscular coherence). To create tomographic maps, the spatial filter was applied to a large number of voxels (6-mm voxel size) covering the entire brain, assigning to each voxel the coherence value to the EMG signal. Anatomical landmarks were identified in the individual MRI scans, and the MEG and MRI coordinates were aligned. In the final map only voxels with significant coherence were displayed.

Measurements of CFF

Briefly, the CFF was determined using the Schuhfried Test System (Dr. Schuhfried, Inc.). Intrafoveal stimulation with a luminous diode (wave length 650 nm; luminance 270 cd/m2; luminous intensity 5.3 mcd) was achieved through a concave–convex lens system, which allowed eye accommodation to a virtual picture of the light source 12 m in the distance. Rectangle light pulses with a 1:1 ratio between the visual impulse and the interval were used with decreasing (flicker threshold) frequency in gradual steps of 0.5 to 0.1 Hz/s. Stepwise decreasing the frequency of the light pulses from 60 Hz downward allowed determination of the flicker-frequency threshold (CFF), which was the frequency at which the fused light was perceived by the patient as flickering light. After a brief standardized instruction and training period, the CFF was measured 8 times and the mean value was calculated. All HE gradings and assessment of the CFF were performed without knowledge of the MEG findings.

References

Ahonen AI, Hämäläinen MS, Kajola MJ, Knuutila JET, Laine PP, Lounasmaa OV, et al. 122-channel SQUID instrument for investigating the magnetic signals from the human brain. Physica Scripta 1993;T49:198–205.

Amodio P, Quero JC, Del Piccolo F, Gatta A, Schalm SW. Diagnostic tools for the detection of subclinical hepatic encephalopathy: comparison of standard and computerized psychometric tests with spectral-EEG. Metab Brain Dis 1996;11:315–27.

Baker MR, Baker SN. The effect of diazepam on motor cortical oscillations and corticomuscular coherence studied in man. J Physiol 2003;546:931–42.

Brown P, Salenius S, Rothwell JC, Hari R. Cortical correlate of the Piper rhythm in humans. J Neurophysiol 1998;80:2911–7.

Butterworth RF. Complications of cirrhosis III hepatic encephalopathy. J Hepatol 2000;32:171–80.

Conn HO. Hepatic encephalopathy. In: Schiff B, Schiff ER, editors. Diseases of the liver. Philadelphia: Lippincott; 1993. p. 1036–60.

Conn HO, Lieberthal MM. The hepatic coma syndromes and lactulose. Baltimore: Williams and Wilkins; 1979.

Conway BA, Halliday DM, Farmer SF, Shahani U, Maas P, Weir AI, et al. Synchronization between motor cortex and spinal motoneuronal pool during the performance of a maintained motor task in man. J Physiol 1995;489:917–24.

Gross J, Ioannides A. Linear transformations of data space in MEG. Phys Med Biol 1999a;44:2081–97.

Gross J, Ioannides AA. Linear transformations of data space in MEG. Phys Med Biol 1999b;44:2081–97.

Gross J, Kujala J, Hamalainen M, Timmermann L, Schnitzler A, Salmelin R. Dynamic imaging of coherent sources: studying neural interactions in the human brain. Proc Natl Acad Sci USA 2001;98:694–9.

Gross J, Tass PA, Salenius S, Hari R, Freund HJ, Schnitzler A. Cortico-muscular synchronization during isometric muscle contraction in humans as revealed by magnetoencephalography. J Physiol 2000;527 Pt 3:623–31.

Gross J, Timmermann L, Kujala J, Dirks M, Schmitz F, Salmelin R, et al. The neural basis of intermittent motor control in humans. Proc Natl Acad Sci USA 2002;99:2299–302.

Halliday DM, Amjad AM, Conway BA, Farmer SF, Rosenberg JR. A method for comparison of several coherence estimates from independent experiments. J Physiol – London 1995;487P:P76–7.

Haussinger D, Kircheis G, Fischer R, Schliess F, vom Dahl S. Hepatic encephalopathy in chronic liver disease: a clinical manifestation of astrocyte swelling and low-grade cerebral edema? J Hepatol 2000;32:1035–8.

Haussinger D, Laubenberger J, vom Dahl S, Ernst T, Bayer S, Langer M, et al. Proton magnetic resonance spectroscopy studies on human brain myo-inositol in hypo-osmolarity and hepatic encephalopathy. Gastroenterology 1994;107:1475–80.

Herculano-Houzel S, Munk MH, Neuenschwander S, Singer W. Precisely synchronized oscillatory firing patterns require electroencephalographic activation. J Neurosci 1999;19:3992–4010.

Herrmann CS. Human EEG responses to 1–100 Hz flicker: resonance phenomena in visual cortex and their potential correlation to cognitive phenomena. Exp Brain Res 2001;137:346–53.

Kircheis G, Wettstein M, Timmermann L, Schnitzler A, Haussinger D. Critical flicker frequency for quantification of low-grade hepatic encephalopathy. Hepatology 2002;35:357–66.

Kristeva-Feige R, Fritsch C, Timmer J, Lucking CH. Effects of attention and precision of exerted force on beta range EEG–EMG synchronization during a maintained motor contraction task. Clin Neurophysiol 2002;113:124–31.

Leavitt S, Tyler HR. Studies in asterixis. Arch Neurol 1964;10:360–8.

Neiman J, Lang AE, Fornazzari L, Carlen PL. Movement disorders in alcoholism: a review. Neurology 1990;40:741–6.

Pfurtscheller G, Neuper C, Pichler-Zalaudek K, Edlinger G, Lopes da Silva FH. Do brain oscillations of different frequencies indicate interaction between cortical areas in humans? Neurosci Lett 2000;286:66–8.

Pugh RNH, Murray-Lyon IM, Dawson JL, Pietroni MC, Williams R. Transection of the oesophagus for bleeding oesophageal varices. Br J Surg 1973;60:646–9.

Riddle CN, Baker MR, Baker SN. The effect of carbamazepine on human corticomuscular coherence. Neuroimage 2004;22:333–40.

Salenius S, Portin K, Kajola M, Salmelin R, Hari R. Cortical control of human motoneuron firing during isometric contraction. J Neurophysiol 1997;77:3401–5.

Schnitzler A, Gross J. Normal and pathological oscillatory communication in the brain. Nat Rev Neurosci 2005;6:285–96.

Schnitzler A, Gross J, Timmermann L. Synchronised oscillations of the human sensorimotor cortex. Acta Neurobiol Exp 2000;60:271–87.

Singer W. Synchronization of cortical activity and its putative role in information processing and learning. Annu Rev Physiol 1993;55:349–74.

Südmeyer M, Pollok B, Hefter H, Gross J, Wojtecki L, Butz M, et al. Postural tremor in Wilson's disease: a magnetoencephalographic study. Movement Disorders 2004;19:1476–82.

Timmermann L, Butz M, Gross J, Kircheis G, Haussinger D, Schnitzler A. Neural synchronization in hepatic encephalopathy. Metab Brain Dis 2005;20:337–46.

Timmermann L, Gross J, Butz M, Kircheis G, Haussinger D, Schnitzler A. Mini-asterixis in hepatic encephalopathy induced by pathologic thalamo-motor-cortical coupling. Neurology 2003a;61:689–92.

Timmermann L, Gross J, Dirks M, Volkmann J, Freund HJ, Schnitzler A. The cerebral oscillatory network of parkinsonian resting tremor. Brain 2003c;126:199–212.

Timmermann L, Gross J, Kircheis G, Butz M, Haussinger D, Schnitzler A. Influence of hepatic encephalopathy on the motor system. Movement Disorders 2004;Suppl:P1326.

Timmermann L, Gross J, Kircheis G, Haussinger D, Schnitzler A. Cortical origin of mini-asterixis in hepatic encephalopathy. Neurology 2002;58:295–8.

Young RR, Shahani BT. Asterixis: one type of negative myoclonus. Adv Neurol 1986;43:137–56.

Yousry TA, Schmid UD, Alkadhi H, Schmidt D, Peraud A, Buettner A, et al. Localization of the motor hand area to a knob on the precentral gyrus. A new landmark. Brain 1997;120:141–57.